R-08-15

Dose assessments for SFR 1

Ulla Bergström, Svensk Kärnbränslehantering AB

Rodolfo Avila, Per-Anders Ekström, Idalmis de la Cruz
Facilia AB

Maj 2008

Svensk Kärnbränslehantering AB
Swedish Nuclear Fuel
and Waste Management Co
Box 250, SE-101 24 Stockholm
Tel +46 8 459 84 00

ISSN 1402-3091
SKB Rapport R-08-15

Dose assessments for SFR 1

Ulla Bergström, Svensk Kärnbränslehantering AB

Rodolfo Avila, Per-Anders Ekström, Idalmis de la Cruz
Facilia AB

Maj 2008

Keywords: docID 1170619, Dose calculations, Dose assessment, SFR 1 SAR-08.

Preface

This document describes the dose calculations that have been undertaken as part of the safety analysis SFR 1 SAR-08 and the document constitutes one of the references to the safety analysis.

Rodolfo Avila, Per-Anders Ekström, Idalmis de la Cruz and Ulla Bergström have conducted the modelling work and compiled the report.

This document has been reviewed and all comments have been documented in accordance with SKIFS 2004:1.

Stockholm, June 2008

Anna Gordon

Project leader, SFR 1 SAR-08

Abstract

Following a review by the Swedish regulatory authorities of the safety analysis of the SFR 1 disposal facility for low and intermediate level waste /SKB 2001/, SKB has prepared an updated safety analysis, SAR-08.

This report presents estimations of annual doses to the most exposed groups from potential radionuclide releases from the SFR 1 repository for a number of calculation cases, selected using a systematic approach for identifying relevant scenarios for the safety analysis. The dose estimates can be used for demonstrating that the long term safety of the repository is in compliance with the regulatory requirements. In particular, the mean values of the annual doses can be used to estimate the expected risks to the most exposed individuals, which can then be compared with the regulatory risk criteria for human health. The conversion from doses to risks is performed in the main report /SKB 2008a/. For one scenario however, where the effects of an earthquake taking place close to the repository are analysed, risk calculations are presented in this report.

In addition, prediction of concentrations of radionuclides in environmental media, such as water and soil, are compared with concentration limits suggested by the Erica-project /Beresford et al. 2007/ as a base for estimating potential effects on the environment. The assessment of the impact on non-human biota showed that the potential impact is negligible.

Committed collective dose for an integration period of 10,000 years for releases occurring during the first thousand years after closure are also calculated. The collective dose commitment was estimated to be 8 manSv.

The dose calculations were carried out for a period of 100,000 years, which was sufficient to observe peak doses in all scenarios considered. Releases to the landscape and to a well were considered. The peaks of the mean annual doses from releases to the landscape are associated with C-14 releases to a future lake around year 5,000 AD. In the case of releases to a well, the peak annual doses were obtained around year 4,000 AD, when an increase of groundwater discharges occurs in connection with the ongoing shoreline displacement. The peaks for the well are also dominated by C-14, although a few other radionuclides also contribute. This pattern of the peak doses was observed for calculation cases of the main scenario and less probable scenarios. Moreover, the predicted doses, including peak dose values, for calculation cases of the less probable scenarios were very close to the predictions for calculation cases of the main scenario.

Predicted annual doses to the most exposed individuals during the first 1,000 years after the repository closure did not exceed 0.05 μSv per year. Low release rates are predicted for this period, when the recipient for the releases is the sea, and doses per unit release rate are low, as compared to the case with releases to a lake or a mire. Doses from short-lived radionuclides were very low, as these can only be released during the sea period. The doses from actinides were also low, due to effective retention in the engineered barriers and their low inventory. In general, total mean annual individual doses were low during the whole simulation period, with values below 14 μSv per year for the main and less probable scenarios.

Uncertainty analyses were carried out using probabilistic methods. These analyses showed that the parameter uncertainty in the peak doses from releases to the landscape are low due to the dominant role of C-14, for which the dose factors and the biosphere release rates have low uncertainty.

Sensitivity studies were carried out to identify the near field and biosphere parameters that have the highest contribution to the uncertainty of the peak dose estimates. The parameters with the highest contribution to the uncertainties in estimates of release rates from the near field are the

flow uncertainty factors for non-sorbing radionuclides and the distribution coefficients in the construction cement for sorbing radionuclides. The biosphere parameters with the highest effect on the uncertainty of the peak dose estimates for releases to the landscape are the dissolved inorganic carbon content and the net primary production in lakes. In the case of releases to a well, the biosphere parameter with the highest and dominant effect on the uncertainty of dose estimates is the well capacity.

Contents

1	**Introduction**	9
1.1	Background	9
1.2	Regulatory criteria	9
1.3	Purpose and scope	10
1.4	Structure of the report	11
2	**Description of the biosphere and prerequisites for the dose assessment**	13
2.1	The repository	13
2.2	Radionuclide inventory	13
2.3	Biosphere description	13
	2.3.1 Conditions of today	15
	2.3.2 Future conditions	21
2.4	Calculation cases	22
3	**Models for exposure assessment**	27
3.1	Landscape models	27
	3.1.1 Parameter values	28
3.2	Models for aquatic ecosystems	30
	3.2.1 Parameter values	30
3.3	Models for terrestrial ecosystems	30
	3.3.1 Irrigation model	31
	3.3.2 Parameter values	31
3.4	Special models for C-14	32
	3.4.1 Parameter values	32
3.5	Models for dose calculations	32
	3.5.1 Parameter values for dose calculations	33
	3.5.2 Estimation of number of individuals in the exposed group	34
4	**Assessment approaches**	37
4.1	Assessment of doses from releases to the landscape	37
	4.1.1 Derivation of Dose Factors	38
	4.1.2 Dose calculations	38
4.2	Assessment of doses from releases to a well	40
4.3	Assessment of risks from earthquakes	40
	4.3.1 Consequence analysis	41
	4.3.2 Risk calculations	42
4.4	Assessment of doses from an intrusion well	44
4.5	Estimation of the collective dose commitment	44
4.6	Assessment of the impact on non-human biota	44
5	**Results for calculation cases representing the main scenario**	47
5.1	Weichselian variant	47
	5.1.1 Doses from releases to the landscape	47
	5.1.2 Doses from releases to a well	53
5.2	Greenhouse variant	57
	5.2.1 Doses from releases to the landscape	57
	5.2.2 Doses from releases to a well	61
6	**Results for calculation cases representing less probable scenarios**	65
6.1	Earthquake	65
6.2	Earlier freezing (BMA) in the Weichselian variant (CC4) and Earlier freezing (BMA) in the Weichselian variant with talik (CC5)	69

6.2.1 Doses from releases to the landscape 69
6.2.2 Doses from releases to a well 70
6.3 Extreme permafrost (CC7) 72
6.3.1 Doses from releases to the landscape 72
6.3.2 Doses from releases to a well 76
6.4 Extreme permafrost with taliks (CC8) 80
6.4.1 Doses from releases to the landscape 80
6.4.2 Doses from releases to a well 84
6.5 Talik (CC2) 85
6.5.1 Doses from releases to the landscape 85
6.5.2 Doses from releases to a well 89
6.6 High concentrations of complexing agents (CC9) 89
6.6.1 Doses from releases to the landscape 90
6.6.2 Doses from releases to a well 93
6.7 Gas generated advection (CC10) 96
6.7.1 Doses from releases to the landscape 96
6.7.2 Doses from releases to a well 96
6.8 Intrusion well (CC11) 97
6.8.1 Intrusion well with assumptions as in the Weichselian variant 97
6.8.2 Intrusion well with assumptions as in calculation case high concentrations of complexing agents 100

7 Results for calculation cases representing residual scenarios 103
7.1 Alternative inventory 103
7.2 No sorption in the near field 104
7.2.1 Doses from releases to the landscape 104
7.2.2 Doses from releases to a well 107
7.3 Early degradation of technical barriers (CC14) 109
7.3.1 Doses from releases to the landscape 109
7.3.2 Doses from releases to a well 112
7.4 No barrier function in the far-field 113
7.4.1 Doses from releases to the landscape 113

8 Collective dose commitment 117

9 Impact on non-human biota 119

10 Sensitivity and uncertainty analyses 121
10.1 Uncertainty of the dose estimations 121
10.1.1 Releases to the landscape 122
10.1.2 Releases to a well 122
10.2 Sensitivity analyses 123
10.2.1 Releases from the Silo 123
10.2.2 Releases from the BMA 128
10.2.3 Dose Factors for releases to the landscape 133
10.2.4 Dose Factors for releases to a well 135

11 Conclusions 137

12 References 139

Appendix A Model descriptions 145

Appendix B Nuclide and element specific data 151

Appendix C Derivation of aggregated transfer factors for forests 157

Appendix D Dose Factors 159

Appendix E Supporting studies for the dose assessments 165

Appendix F Detailed results for the calculation case earthquake 171

1 Introduction

Following a review by the Swedish regulatory authorities of the safety analysis of the SFR 1 disposal facility for low and intermediate level waste /SKB 2001/, SKB has prepared an updated safety analysis, SAR-08. This report presents the dose assessments of the updated safety analysis.

1.1 Background

Risk analyses shall be performed in order to show compliance with authorities' regulations regarding exposures to man from disposal of nuclear waste /SSI FS1998:1/. This involves an integrated system of calculation steps and models starting from information and knowledge about the waste system, activity content, releases from the waste, transport of radionuclides through the geosphere, turnover in the biosphere and ending up in dose consequences to man. This report covers the last steps of the calculation chain; turnover in the biosphere and dose to man. Effects on biota are also evaluated in the report.

In the dose assessments described in this report, an approach similar to that used in the safety analysis for disposal of spent nuclear fuel, SR-Can /SKB 2006a/, was adopted. This implies that landscape models were used in the assessment, where the potentially affected area was divided into various biosphere objects connected to each other by water flows. The exposure of man was estimated based on maximum individual exploitation of the potentially most affected area. The main differences for SFR 1 with SR-Can are that:

1) all releases of radionuclides occur to the same biosphere object during the whole simulation period, however varying in type with time due to the transformations that occur in the landscape driven by land rise,
2) a new model has been used for C-14,
3) consumption of berries and mushrooms in the forest ecosystem has been included.

In the main report /SKB 2006a/ a reference evolution of the repository system and its environment for the coming 100,000 years is described.

1.2 Regulatory criteria

Human health and the environment should be protected from the harmful effects of ionising radiation from the repository. In SSI:s regulations and guidelines (SSI FS 1998:1 and SSI FS 2005:5) the following risk and dose criteria are given for protection of human health and environment.

Risk criteria for protection of human health

"A repository for spent nuclear fuel or nuclear waste shall be designed so that the annual risk of harmful effects after closure does not exceed 10^{-6} for a representative individual in the group exposed to the greatest risk." /SSI FS 1998:1/

"According to the regulations, the recommendations of the International Commission on Radiological Protection (ICRP) are to be used for calculation of the harmful effects of ionizing radiation. According to ICRP Publication No. 60, 1990, the factor for conversion of effective dose to risk is 7.3% per sievert." /SSI FS 2005:5/

Most exposed group

"One way of defining the most exposed group is to include the individuals that receive a risk in the interval from the highest risk down to a tenth of this risk. If a larger number of individuals can be considered to be included in such a group, the arithmetic average of individual risks in the group can be used for demonstrating compliance with the criterion for individual risk in the regulations. One example of such exposure situation is a release of radioactive substances into a large lake that can be used as a source of drinking water and for fishing." /SSI FS 2005:5/

"If the exposed group only consists of a few individuals, the criterion of the regulations for individual risk can be considered as being complied with if the highest calculated individual risk does not exceed 10^{-5} per year. An example of a situation of this kind might be if consumption of drinking water from a drilled well is the dominant exposure path. In such a calculation example, the choice of individuals with the highest risk load should be justified by information about the spread in calculated individual risks with respect to assumed living habits and places of stay." /SSI FS 2005:5/

Collective dose

"The collective dose, as a result of the expected outflow of radioactive substances during a period of 1,000 years after closure of a repository for spent nuclear fuel or nuclear waste shall be estimated as the sum, over 10,000 years, of the annual collective dose."

Dose corresponding to the risk criteria

Using the recommended factor for conversion of effective dose to risk, the two risk criteria 10^{-6} and 10^{-5}, correspond to a dose of 14 and 140 μSv respectively.

Effects on the environment

For the protection of the environment no risk criteria exists. However, SSI FS 1998:1 states: "The final management of spent nuclear fuel or nuclear waste shall be implemented so that biodiversity and the sustainable use of biological resources are protected against the harmful effects of ionising radiation."

1.3 Purpose and scope

The regulatory criteria have been presented in Section 1.2. The purpose and scope of this report are strongly linked to the regulatory demands. The overall objective of this report is to present results in form of doses to humans from the SFR 1 repository for all calculation cases identified in the safety assessment, see the main report /SKB 2008a/. Doses to man are calculated from release rates of radionuclides to the surface ecosystems and to a well.

The near-field and geosphere transport calculations are presented in /Thomson et al. 2008/. The calculations of doses are presented in this report and the conversion from doses to risks is performed in the main report /SKB 2008a/. The method for scenario selection and quantification of their probabilities are also described in the main report /SKB 2008a/. For one scenario, where the effects of an earthquake taking place close to the repository is analysed, risk calculations are presented in this report.

In addition, concentrations of radionuclides in environmental media, such as water and soil are calculated and compared with concentration limits suggested by the Erica-project /Beresford et al. 2007/ as a base for estimating potential effects on the environment.

Committed collective dose for an integration period of 10,000 years for releases occurring during the first thousand years after closure are also calculated.

1.4 Structure of the report

The report is divided into twelve chapters. The first chapter gives an introduction and present the purpose and scope of the report. In Chapter 2, the starting-points for the dose assessment are briefly described, i.e. the radionuclides considered in the assessments, a description of the biosphere today and its temporal transformation. Chapters 3 and 4 provide a presentation of the models applied and the methods used to assess dose to man and effects on biota. Results from the calculation cases representing the main scenario, less probable scenarios and residual scenarios are presented in Chapters 5, 6 and 7, respectively. Collective dose calculations are presented in Chapter 8 and impact on the biota is presented in Chapter 9. Sensitivity and uncertainties of the results are discussed in Chapter 10. The conclusions from the dose assessments are given in Chapter 11. Finally the references are compiled in Chapter 12.

2 Description of the biosphere and prerequisites for the dose assessment

This chapter gives a description of the current biosphere conditions and an overview of the biosphere and the transformations that have been considered in the dose assessments. Also, some prerequisites for the dose assessment are given such as the radionuclide inventory in the repository and the calculation cases included in the assessment.

2.1 The repository

The SFR 1 repository is constructed about 60 meters down in the crystalline rock. The repository receives operational waste from the Swedish nuclear power plants as well as waste from research and nuclear facilities. In addition, waste from medical use of radioactivity is also deposited in the repository.

The repository consists of four vaults (BMA, 1BTF, 2BTF and BLA) and one Silo, where the major fraction of the activity is deposited. The Silo is constructed in concrete and is surrounded by bentonite. One of the vaults, BMA, has concrete walls that function as technical barriers. The remaining vaults, 1BTF, 2BTF and BLA have no built in technical barriers.

A detailed description of the SFR 1 repository is given in the safety analysis report for SFR 1 /SKB 2008b/.

2.2 Radionuclide inventory

Estimates of the future radionuclide inventory in SFR 1 have been undertaken /Almkvist and Gordon 2007/. Screening calculations have been performed /Thomson et al. 2008/ in order to identify those radionuclides for which complete assessments are necessary. The screening resulted in 25 radionuclides, see Table 2-1 below. Note that C-14 has been divided into organic and inorganic form. The screening study indicates that the potential contribution to the doses of other radionuclides in the inventory is negligible.

The radionuclide inventory in SFR 1 has continuously been improved. The inventory was changed in two steps after the radionuclide transport calculations were completed. In the first step, the inventory of organic and inorganic C-14, Cl-36, Mo-93, Tc-99, I-129 and Cs-135 was altered. The results of the radionuclide transport calculations were corrected for this change both in the radionuclide transport report /Thomson et al. 2008/ and in the dose assessment. In the second step, the inventory for Cs-135 was altered again. This was accounted for only in the dose assessment. The inventory presented in Table 2-1 is the final inventory after these changes.

2.3 Biosphere description

A description of the area in proximity of SFR 1 was performed within the SAFE-project /Kautsky 2001/. However, at present SKB is undertaking site characterisation for location of a future repository for spent fuel at two sites in Sweden. One of them, Forsmark, is in the vicinity of SFR 1. A detailed description of the Forsmark area was carried out for the preliminary safety assessment of high level waste SR-Can /SKB 2006ab/. The description given below of the present biosphere is a summary of the information provided in the main report for SR-Can /SKB 2006a/, which is based on /Lindborg 2005/ and underlying reports.

Table 2-1. Radionuclide inventories (Bq) of SFR 1 calculated for 50 years operation of Swedish nuclear power plants /Almkvist and Gordon 2007/. Only radionuclides which have been judged to be of importance for long term safety are included. Half-lives are also given /Firestone et al. 1999/.

Radionuclide	Half-life (year)	Silo	BMA	1BTF	2BTF	BLA
H-3	$1.23 \cdot 10^{1}$	$3.5 \cdot 10^{10}$	$3.8 \cdot 10^{9}$	$1.6 \cdot 10^{8}$	$4.0 \cdot 10^{8}$	$2.2 \cdot 10^{7}$
C-14 org.[1]	$5.73 \cdot 10^{3}$	$1.4 \cdot 10^{12}$	$3.2 \cdot 10^{11}$	$7.4 \cdot 10^{9}$	$5.5 \cdot 10^{10}$	$1.2 \cdot 10^{9}$
C-14 inorg.[1]	$5.73 \cdot 10^{3}$	$3.2 \cdot 10^{12}$	$7.4 \cdot 10^{11}$	$1.7 \cdot 10^{10}$	$1.3 \cdot 10^{11}$	$2.7 \cdot 10^{9}$
Cl-36	$3.01 \cdot 10^{5}$	$1.1 \cdot 10^{9}$	$2.3 \cdot 10^{8}$	$1.1 \cdot 10^{7}$	$3.1 \cdot 10^{7}$	$1.0 \cdot 10^{6}$
Ni-59	$7.60 \cdot 10^{4}$	$7.3 \cdot 10^{12}$	$2.1 \cdot 10^{12}$	$2.1 \cdot 10^{10}$	$4.2 \cdot 10^{10}$	$5.3 \cdot 10^{9}$
Co-60	5.27	$8.5 \cdot 10^{13}$	$7.0 \cdot 10^{12}$	$2.9 \cdot 10^{11}$	$3.7 \cdot 10^{11}$	$3.6 \cdot 10^{10}$
Ni-63	$1.00 \cdot 10^{2}$	$8.9 \cdot 10^{14}$	$2.6 \cdot 10^{14}$	$2.3 \cdot 10^{12}$	$2.8 \cdot 10^{12}$	$6.6 \cdot 10^{11}$
Se-79	$1.13 \cdot 10^{6}$	$1.0 \cdot 10^{9}$	$2.1 \cdot 10^{8}$	$5.9 \cdot 10^{6}$	$2.4 \cdot 10^{7}$	$4.9 \cdot 10^{5}$
Sr-90	$2.88 \cdot 10^{1}$	$1.1 \cdot 10^{13}$	$1.7 \cdot 10^{12}$	$6.4 \cdot 10^{10}$	$2.1 \cdot 10^{11}$	$4.7 \cdot 10^{9}$
Mo-93	$4.00 \cdot 10^{3}$	$2.9 \cdot 10^{9}$	$6.8 \cdot 10^{8}$	$4.4 \cdot 10^{7}$	$8.9 \cdot 10^{7}$	$2.0 \cdot 10^{7}$
Nb-94	$2.03 \cdot 10^{4}$	$1.6 \cdot 10^{10}$	$3.6 \cdot 10^{9}$	$8.5 \cdot 10^{7}$	$4.2 \cdot 10^{8}$	$1.3 \cdot 10^{7}$
Tc-99	$2.11 \cdot 10^{5}$	$3.6 \cdot 10^{11}$	$3.7 \cdot 10^{10}$	$7.0 \cdot 10^{9}$	$7.6 \cdot 10^{9}$	$5.0 \cdot 10^{8}$
Ag-108m	$4.18 \cdot 10^{2}$	$9.2 \cdot 10^{10}$	$2.0 \cdot 10^{10}$	$4.8 \cdot 10^{8}$	$2.3 \cdot 10^{9}$	$4.2 \cdot 10^{8}$
Sn-126	$1.00 \cdot 10^{5}$	$1.3 \cdot 10^{8}$	$2.7 \cdot 10^{7}$	$7.4 \cdot 10^{5}$	$2.9 \cdot 10^{6}$	$6.2 \cdot 10^{4}$
I-129	$1.57 \cdot 10^{7}$	$8.1 \cdot 10^{8}$	$1.8 \cdot 10^{8}$	$3.1 \cdot 10^{6}$	$1.9 \cdot 10^{7}$	$3.1 \cdot 10^{5}$
Cs-135	$2.30 \cdot 10^{6}$	$4.0 \cdot 10^{9}$	$1.0 \cdot 10^{9}$	$1.6 \cdot 10^{7}$	$1.1 \cdot 10^{8}$	$2.0 \cdot 10^{6}$
Cs-137	$3.01 \cdot 10^{1}$	$1.1 \cdot 10^{14}$	$2.0 \cdot 10^{13}$	$6.7 \cdot 10^{11}$	$1.8 \cdot 10^{12}$	$4.8 \cdot 10^{10}$
Ho-166m	$1.20 \cdot 10^{3}$	$7.0 \cdot 10^{9}$	$1.6 \cdot 10^{9}$	$5.8 \cdot 10^{7}$	$1.9 \cdot 10^{8}$	$1.7 \cdot 10^{7}$
Np-237	$2.14 \cdot 10^{6}$	$1.3 \cdot 10^{8}$	$2.5 \cdot 10^{7}$	$4.1 \cdot 10^{5}$	$1.9 \cdot 10^{6}$	$2.7 \cdot 10^{4}$
Pu-239	$2.41 \cdot 10^{4}$	$8.9 \cdot 10^{9}$	$2.0 \cdot 10^{9}$	$1.5 \cdot 10^{8}$	$2.0 \cdot 10^{8}$	$1.3 \cdot 10^{7}$
Pu-240[2]	$6.56 \cdot 10^{3}$	$1.8 \cdot 10^{10}$	$4.0 \cdot 10^{9}$	$3.0 \cdot 10^{8}$	$4.0 \cdot 10^{8}$	$2.6 \cdot 10^{7}$
Am-241[3]	$4.32 \cdot 10^{2}$	$4.9 \cdot 10^{11}$	$6.9 \cdot 10^{9}$	$8.4 \cdot 10^{8}$	$4.9 \cdot 10^{8}$	$5.0 \cdot 10^{7}$
Pu-241[3]	$1.44 \cdot 10^{1}$	$6.8 \cdot 10^{11}$	$1.3 \cdot 10^{11}$	$6.4 \cdot 10^{9}$	$7.0 \cdot 10^{9}$	$3.6 \cdot 10^{8}$
Pu-242	$3.73 \cdot 10^{5}$	$7.9 \cdot 10^{7}$	$2.3 \cdot 10^{7}$	$1.5 \cdot 10^{6}$	$1.6 \cdot 10^{6}$	$9.0 \cdot 10^{4}$
Am-243	$7.37 \cdot 10^{3}$	$8.4 \cdot 10^{8}$	$2.3 \cdot 10^{8}$	$1.5 \cdot 10^{7}$	$1.6 \cdot 10^{7}$	$9.0 \cdot 10^{5}$
Cm-244[2]	$1.81 \cdot 10^{1}$	$9.2 \cdot 10^{9}$	$1.2 \cdot 10^{9}$	$8.3 \cdot 10^{7}$	$9.0 \cdot 10^{7}$	$1.9 \cdot 10^{7}$

[1] Organic and inorganic C-14 are analysed separately due to different sorption properties.

[2] In the table the inventory of each nuclide is given, but in the calculations the inventory of Cm-244 was added to the inventory of Pu-240.

[3] In the table the inventory of each nuclide is given, but in the calculations the inventory of Pu-241 was added to the inventory of Am-241.

At present, the area above the repository is dominated by the sea. The sea basin just above the repository was selected as local model area in the SAFE-study /Kautsky 2001/ and is hereafter called the SAFE-basin. The ongoing shore-level displacement at the site will lead to substantial changes of the surface ecosystem during the next coming 10,000 years. In a longer time perspective, as considered in this assessment (100,000 years), substantial climate changes will also occur that will influence the biosphere conditions.

The long term development of the area was studied in the context of the SR-Can safety analysis /SKB 2006b/. A description of the past biosphere development at the site was carried out based on an elevation model, a shore-line displacement model, old cadastral maps and site information of the Quarternary deposits. Based on a reconstruction of the landscape succession from 8,000 BC and extrapolation to the future, up-to 10,000 AD /SKB 2006b/, landscape models were constructed and used for dose assessments in the SR-Can safety analysis. Parts of these landscape models were used in the assessments for SFR 1 described in this report.

2.3.1 Conditions of today

The landscape in Forsmark area is a relatively flat peneplain that dips gently towards the east. The whole area is situated below the highest coastline associated with the last deglaciation and today's landscape is strongly influenced by the ongoing shore-line displacement of around 6 mm per year. Most of the area has risen above the sea during the last 1,000 years, which means that processes such as chemical weathering and peat formation have affected the area over a relatively short period of time.

Hydrology

The conceptual and descriptive modelling of the meteorological, surface hydrological and near-surface hydrogeological conditions in the Forsmark area is presented in /Johansson et al. 2005/. The corrected annual mean precipitation is 600–650 mm and the annual mean evapotranspiration can be estimated to be a little more than 400 mm, leaving approximately 200 mm for runoff. Model studies of the area /Bosson and Berglund 2006/ resulted in an annual runoff of 226 mm, a value which has been used in the dose assessments presented in this report.

The SAFE-basin is the recipient for radionuclides released from the repository /Holmén and Stigsson 2001/.

The sea

The marine system in the Forsmark area is the Öregrundsgrepen, a bay in the southern Bothnian Sea. Öregrundsgrepen is shaped as a funnel between the mainland and the islands Gräsö and Örskär to the north-east. The western part is a large shallow water area with many emerging rocks and islands. The bay opens to the Bothnian Sea in the north, but has another more narrow connection at the south-eastern end with the Åland Sea, see Figure 2-1.

Öregrundsgrepen has been divided into seven basins due to present underwater structures leading to distinct catchments areas when terrestrial conditions will prevail (Figure 2-1). This discretisation of the sea was performed for estimation of water exchange times. In Figure 2-1, the SAFE-basin consisting of an 11.6 km^2 area in connection to SFR 1, is indicated. Calculation of groundwater discharges from the repository has shown that groundwater drains to this area at the time of repository closure.

The SAFE-basin is exposed to open sea which implies that the residence time for water is short. The average and maximum depth of the basin are about 10 m and 19 m respectively, see Table 2-2 /Lindborg 2005/. The average age of the water in the SAFE-basin is about 0.7 days. The average age of the water for the entire Öregrundsgrepen is about 6 days.

Table 2-2. Data on the SAFE-basin and Öregrundsgrepen.

Parameter	Value	Reference
SAFE-basin		
Average depth	10 m	/Lindborg 2005/
Maximum depth	19 m	/Lindborg 2005/
Area	11.5 km^2	/Lindborg 2005/
Average age of water	0.66 days	/SKB 2006b/
Öregrundsgrepen		
Average depth	11.2 m	/Kautsky 2001/
Maximum depth	60 m	/Engqvist and Andrejev 1999/
Area	456 km^2	/Kautsky 2001/
Average age of water	6.3 days	/SKB 2006b/

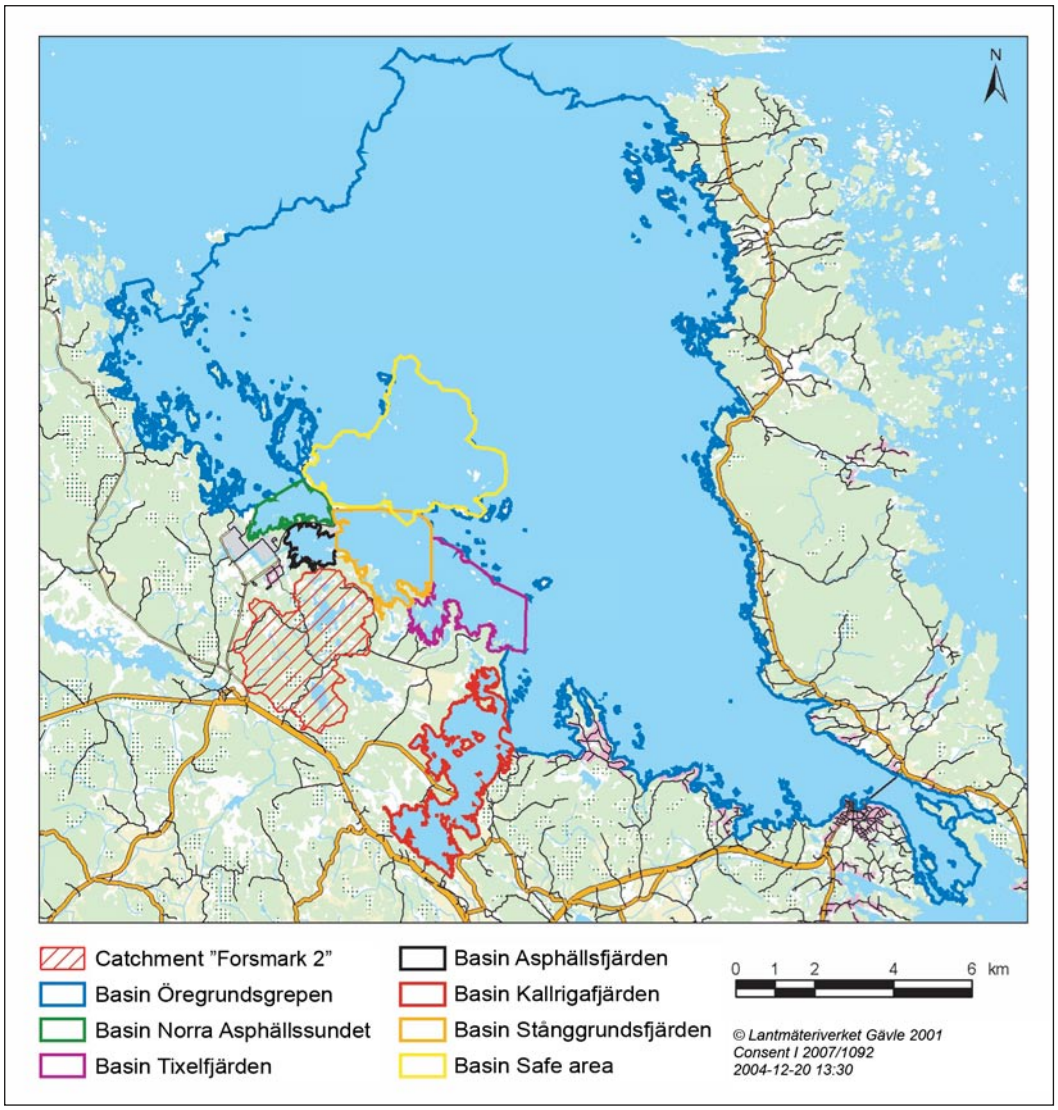

Figure 2-1. *The Öregrundsgrepen including its seven basins with SAFE-basin indicated.*

The water of the SAFE-basin is brackish, with a salinity between 4.5–5.8‰ for the surface water and somewhat higher 5.6–6.4‰ for the deeper water /Gustafsson 2004/. There is no halocline in the area /Persson et al. 1993/.

The marine system in the Forsmark area is a relatively productive coastal area in a region of otherwise fairly low primary production. This is due to up-welling along the mainland /Eriksson et al. 1977/. The surface water has a nutrient concentration ranging from 330 to 790 µg/l tot-N and 12 to 25 µg/L tot-P /Nilsson et al. 2003/. The seabed mainly comprises erosion and transport bottoms with heterogeneous and mobile sediment consisting mainly of sand and gravel, but with varying fractions of glacial clay /Mo and Smith 1988/. The seabed close to the mainland has some areas of rocky bottoms, which are partly covered with coarse till /Sigurdsson 1987/. This has been confirmed from the detailed marine geological survey of the sea bottom outside Forsmark in which the horizontal and vertical distribution of Quaternary deposits on sea bottoms situated at water depths greater than 3 m was studied /Elhammer and Sandkvist 2005/. This information is presented in a map of the Quaternary deposits on the sea bottom /Lindborg 2005/.

Several studies of flora and fauna have been carried out in the Öregrundsgrepen area. In the photic zone (the zone where photosynthesis occur), the seabed is to a large extent covered with a layer of micro algae, mainly diatoms, and is characterised by a relatively high species diversity

and large amount of macrophytes (macroalgae and vascular plants) /Kautsky et al. 1999, Snoeijs 1985, 1986/. The macrophyte species that contribute most to the macrophyte biomass in the benthic community in Öregrundsgrepen are the red algae *Polysiphonia nigrescens*, the brown algae bladderwrack, *Fucus vesiculosus* and *Sphacelaria arctica* and the vascular plant pondweed, *Potamogeton filiformis* /Kautsky et al. 1999/. Herbivorous gastropods together with both herbivore and omnivore crustaceans dominate the grazing macrofauna and the most common filter feeder in the area has been found to be the bivalve clam, *Cardium* spp /Kautsky et al. 1999/. Nematodes, acarins, cladocerans, copepods and ostracods are the major meiofauna taxa present in the area /Snoeijs and Mo 1987/. The most common fish species in Öregrundsgrepen are herring (*Clupea harengus*), roach (*Rutilus rutilus*) and perch (*Perca fluviatilis*) /Neuman 1982/.

The net primary production through photosynthesis was estimated to be 122 g carbon per m^2 /Lindborg 2005/.

Lakes

The characteristics of the limnic system in the Forsmark area are to a great extent determined by the small topographic gradients in combination with the ongoing shore line displacement and a short distance to the sea, and by the occurrence of calcium-rich deposits /Lindborg 2005/.

The investigated lakes in the area can be classified as oligotrophic hardwater lakes /Blomqvist et al. 2002/. This means that they show very unusual chemical conditions, with high alkalinity, conductivity, pH-value and nitrogen concentrations and very high concentrations of slightly coloured dissolved organic carbon (DOC), whereas phosphorus concentrations are very low. Preliminary measurements of primary production in the lakes show that whereas the production in the pelagial zone is always low, the production in the microbial mat may potentially be very high /Andersson and Kumblad 2006/.

The lakes are very shallow, with maximum depths ranging from 0.4 to 2.0 m /Lindborg 2005/.

The dominant habitat in the larger lakes in the area is the littoral with submerged vegetation. In Lake Eckarfjärden, Bolundsfjärden and Fiskarfjärden this habitat makes up at least 50% of the lake area, whereas 20 of the other 22 lakes in the area have a larger percentage of the littoral with emergent and floating-leaved vegetation /Brunberg et al. 2004/. This is not surprising since these lakes are smaller, shallower and at a later successional stage. The extreme is Lake Labboträsket where 96% of the area consists of littoral with emergent and floating-leaved vegetation.

The biomass of dominating fish species was studied in the larger lakes of the Forsmark area in the site investigations (Table 2-3) /Lindborg 2005, Borgiel 2004/.

Land (terrestrial part)

The glacial till and clay in the Forsmark area are characterised by a high content of calcium carbonate. The calcite originates from limestone present at the sea bottom north of the Forsmark area (/Lindborg 2005/ and underlying reports).

The vegetation is affected by the bedrock, the Quaternary deposits and human land use. Pine forest on felsic rocks is scarce, because rock outcrops are not distributed. The Quaternary deposits are mainly wave-washed till, where conifer forests are common. In depressions, a deeper regolith layer is found, with fairly high lime content. The calcareous influence is typical for the north-east part of the county of Uppland and is manifested in the flora. The Forsmark area has a long history of forestry, which is seen today as a fairly high percentage of younger and older clear-cuts in the landscape. The spatial distribution of different vegetation types is presented in a vegetation map /Boresjö Bronge and Wester 2002/.

Table 2-3. Biomass, B (gC/m²), of different fish species in the Forsmark area. Biomass estimates from /Lindborg 2005, Borgiel 2004/.

Species	Size length (mm)	Eckar-fjärden B	Fiskar-fjärden B	Bolunds-fjärden B	Gunnarsbo-Lillfjärden B
Roach (mört) *Rutilus rutilus* L.	200–300	0.23	0.14	0.14	0.00
Tench (sutare) *Tinca tinca* L.	500–600	0.42	0.25	0.29	0.00
Perch (aborre) *Perca fluviatilis* L.	300–400	0.26	0.17	0.19	0.33
Pike (gädda) *Esox lucius* L.	700–1,300	0.13	0.01	0.01	0.00
Ruffe (gärs) *Gymnocephalus cernuus* L.	100–200	0.03	0.00	0.01	0.00
Crucian carp (ruda) *Carassius carassius* L.	250–500	0.00	0.76	0.07	0.59
Total		1.07	1.33	0.70	0.92

The forests are dominated by Scots pine (*Pinus sylvestris*) and Norway spruce (*Picea abies*) situated on till. The spruce becomes more abundant where a deeper soil cover is found along with more mesic-moist conditions. The field layer is here heavily influenced by the calcareous content and is characterised by herbs and broad-leaved grasses along with a number of orchid species. The deciduous tree species are dominated by Birch, *Betula pendula*, Alder, *Alnus glutinosa* and Rowan, *Sorbus acuparia*, but also Maple, *Acer platanoides* and Ash, *Fraxinus excelsior* are fairly common. In particular, Ash may be abundant along sheltered seashores. Oak, *Quercus robur* and Elm, *Ulmus glabra* are close to their northern distribution limit and are very scarce.

Arable land, pastures and clear cuts dominate the open land. Arable land and pastures are found close to settlements. The pastures were earlier intensively used, but are today a part of the abandoned farmland that arose following the nationwide general regression of agricultural activities.

Wetlands are frequent and are characterised by a strong calcareous influence, making them extreme and moderate rich fen types that are common in this area. These fen types lack the dominance of peat moss (*Sphagnum*) species in the ground layer and are instead dominated by brown mosses, e.g. S*corpidium scorpioides*. However, bogs are also present in the more elevated parts of the area, but are rare, partly because of the short time since these areas emerged from the Baltic.

The primary production was estimated to about 250 g carbon per m² and year /SKB 2006b/ and 0.25 g carbon per m² and year due to forest productivity of berries, fungi and game meat. Berries contribute to 70% of this annual production /SKB 2006b/.

Humans and land use

In total, 168 people lived in Forsmark församling (parish) in 2002. The population density of 1.8 inhabitants per square kilometre has been low but fairly stable over the last ten years. It is 24 times lower than in Uppsala Län (County). The dominant employment sector within Forsmark församling is electricity-, gas- and water supply, sewage and refuse disposal and it involves 79% of the employed day-time population (working in the area). In the case of the employed night-time population (living in the area) on the other hand, only 19.7% work in that sector. Thus, there is a major ongoing commuting activity due to presence of the Forsmark nuclear power plant. The net commuting is positive in Forsmark församling, meaning that immigration is larger than emigration /Miliander et al. 2004/.

There are approximately 20 licensed fishermen in Östhammar kommun and they undertake coastal small-scale fishing for consumption, and sell their catch to local grocery stores. None of them seem to live in Forsmark församling.

According to Länstyrelsen of Uppsala (County Administrative Board of Uppsala), moose hunting is currently more intensive in Forsmark församling than in Östhammars kommun and Uppsala län (0.53 individuals/km^2 harvested compared with 0.37 and 0.35, respectively in 2003). The harvest was almost equal in Forsmark församling, Östhammar kommun and Uppsala län in 1999, but since then the harvest has been more intensive in Forsmark församling /Miliander et al. 2004/. Harvest of roe deer was 1.9 individuals/km^2 in average during 1997 to 2001.

The land use in Forsmark församling is assumed to be similar to the land use in Forsmark area. The land use within the Forsmark area differs from the average land use in Uppsala Län, as there is proportionally more forest, wetlands and water in the Forsmark area and the proportional area of agricultural and developed land is smaller.

Wells

A study of the wells in Forsmark area was performed in 2002 /Ludvigson 2002/. The main conclusions from the study are summarised here. In the Forsmark area both excavated and drilled wells exist. Chemical analysis of the water in the wells show that the water quality varies from drinkable to disqualified for use. There are drilled wells with high salinities and relatively high calcium and iron concentrations, giving the water a bad taste. Another common problem is the leakage of surface water, which gives the water a taste of humus. The water quality is mostly poor or disqualified for use in the excavated wells. Many wells have also been disqualified for use due to high levels of bacteria in the water.

In the Forsmark area, the groundwater table is generally very shallow. Groundwater monitoring at the site /Johansson et al. 2005/ shows that the groundwater level in the majority of the groundwater wells is located between the ground surface and a depth of one metre. However, it is not only the groundwater level that is important for the location of a well. The geology has large influence on the capacity of the well. The transmissivity of the bedrock or the Quaternary deposits has to be high enough for the water to flow to the well /Grip and Rodhe 1985/.

The well capacity can be good both in discharge and recharge areas. The topography in Forsmark is very flat, which makes it possible to locate a well even in local high areas. The well creates a local discharge area if it is in use /Grip and Rodhe 1985/. Although the capacity of the well depends more on the geology than of the topography, often the preferred geological and topographic conditions coincide; valleys between high altitude areas are often filled with thick layers of Quaternary deposits.

The overburden in Forsmark is dominated by sandy till. The transmissivity of this fine grained till can be limiting for the water flow to the well and it is necessary to find highly conductive layers of sand or gravel of sufficient extent to ensure the water supply in the well /Grip and Rodhe 1985/. For drilled wells in the bedrock, it is the fracture zones that play an important role for the water supply. The well capacity is limited by the hydraulic conductivity of the fractures close to the well.

Well capacities and depths for wells in the area have been studied in /Gentzschein et al. 2006/. In Table 2-4 well capacities and depths are compiled. Different sets of wells in northern Uppland are shown in Figure 2-2. Green and black dots represent data from drilled wells which are gathered from the national well archive, Brunnsarkivet /SGU 2008/. Red dots represent data from the site investigation at Forsmark /Gentzschein et al. 2006/. The difference between green (arbitrarily named as Guard zone) and black dots (named as Östhammar kommun) is the distance to the potential location of the repository for spend fuel and also to SFR 1. In the candidate area for a deep repository very high capacities are measured, which cannot be found outside the area. For this study the well capacities for wells from the Östhammar set outside the candidate area were used.

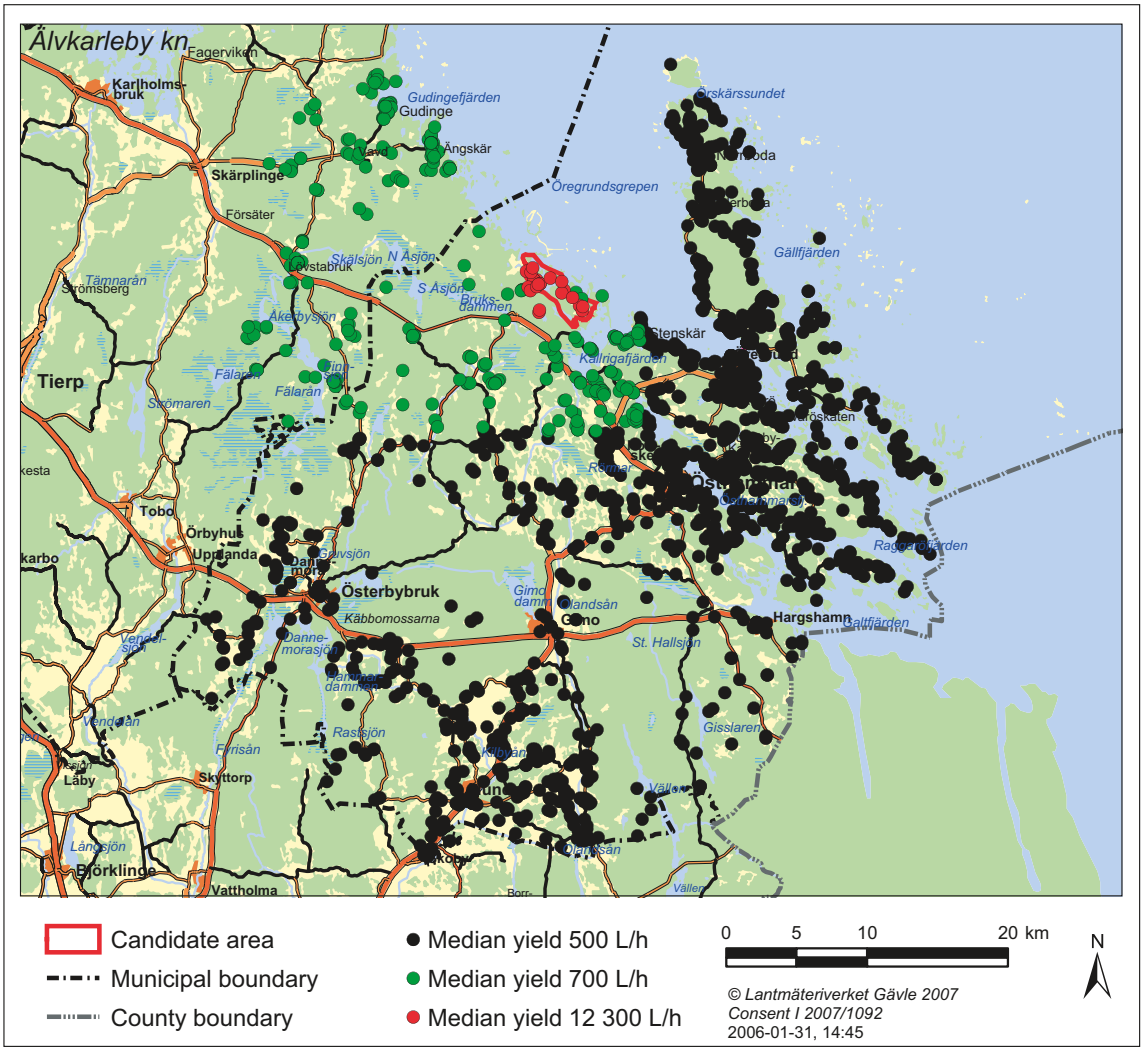

Figure 2-2. *Wells in northern Uppland /Gentzschein et al. 2006/. Östhammar kommun = black dots; Guard zone = green dots; Forsmark area = red dots.*

Table 2-4. Well capacity (Q), depth (D) and specific well capacity (Q/D) for wells in Östhammar municipality /Gentzschein et al. 2006/. OM (Östhammar municipality), GZ (Guard zone), FA (Forsmark area).

Variable	Area	Number of wells	Median	Average	Min	Max
Q (l/h)	ÖM	1,664	500	1,184	1	27,000
	GZ	281	700	1,467	1	10,000
	FA	22	12,300	19,141	216	72,000
D (m)	ÖM	1,664	52	59	7	180
	GZ	281	50	53	7	131
	FA	22	143	144	26	301
Q/D (l/h/m)	ÖM	1,664	9,211	31	0	1,688
	GZ	281	15	46	0	1,143
	FA	22	71	197	2	901

2.3.2 Future conditions

The present coastal condition will change over the next 4,000 years, because the area is strongly influenced of the shore line displacements, which is at present 6 mm per year /Ekman 1996, Hedenström and Risberg 2003/.

The SAFE-basin will successively decrease in size /Brydsten 1999, 2006/ and a semi-enclosed archipelago above and northeast of SFR will emerge. Models accounting for the major processes: shoreline displacement, sediment dynamics, lake formation, and lake choke-up processes have been developed /Brydsten 2006/ and have been used for making prognoses over the future formation of lakes in Öregrundsgrepen and their transformation to mires.

The largest lake is 1.6 km^2 with a mean depth of 1.4 m and a maximum depth of 4.8 m will be formed around year 5,000. This lake is used in the dose assessments presented in this report. It has similar properties with the lake used in the SAFE study. The lake is sufficiently deep that the choke-up processes will go slowly for more than 2,000 years. The water residence time will be about 89 days /Brunberg and Blomqvist 2000/, assuming today's runoff. This lake will probably be an oligotrophic hardwater lake similar to the existing lakes in the Forsmark area,

Figure 2-3. *Present and predicted future lakes formed until year 9,000 in the Forsmark area, based on /Brydsten 2006/.*

with comparable drainage areas and morphometry. Such lakes are characterised by fast sediment growth and clear and hard water, suitable for drinking. Fish production will be limited due to the size of the lake /Brunberg and Blomqvist 2000/ and is assumed to be similar to the fish production in existing lakes.

The lake will gradually be transformed to a mire and at year 7,000 its area will be dominated by a mire ecosystem, which naturally will develop into a moist forest. As an alternative, the lake or mire could be drained to create an agricultural land, as the sediment will have sufficient depth for cultivation. At year 10,000, only some deep lakes at the west coast of Gräsö will remain, while the rest of the former Öregrundsgrepen will be a terrestrial area.

Over a longer time period considerable climate changes will occur. Three different climate variants were indentified in this safety assessment based on the studies performed for SR-Can /SKB 2006c/.

- Weichselian variant – A climate based on a repetition of the last Weichselian glaciation cycle, including temperate, permafrost and glacial conditions.
- Greenhouse variant – A climate where greenhouse effects give a prolonged period of temperate conditions.
- Extreme permafrost – A colder and dryer climate which enhanced permafrost formation.

2.4 Calculation cases

The dose assessment was carried out for a number of scenarios. The method for selection of scenarios and the selected scenarios are described in the main report /SKB 2008a/. For the selected scenarios calculation cases were set up /SKB 2008a/. These calculation cases are summarized in Table 2-5 below, where the main features of the calculation cases are briefly described. A more detailed description is given in /SKB 2008a/ and /Thomson et al. 2008/. The notations used in Table 2-5 coincide with the notations used in /Thomson et al. 2008/. The scenarios, and thus the corresponding calculation cases, have been divided into three categories:

Main scenario	Scenario describing the most probable evolution of external conditions and realistic, or where justified, pessimistic assumptions with respect to internal conditions.
Less probable scenarios	Scenarios with lower probabilities.
Residual scenarios	Hypothetical scenarios, used for system understanding studied independently of probabilities.

The main scenario consists of two calculation cases which describe variations of the future climate change. One of these two calculation cases represents the situation where the future climate is based on a repetition of the last glacial cycle, see Figure 2-4. This calculation case is hereafter called Weichselian variant. The other climate change addresses the consequences of the greenhouse effect with a prolonged period of temperate conditions before a cooler climate appears, see Figure 2-5. This calculation case is hereafter denoted Greenhouse variant.

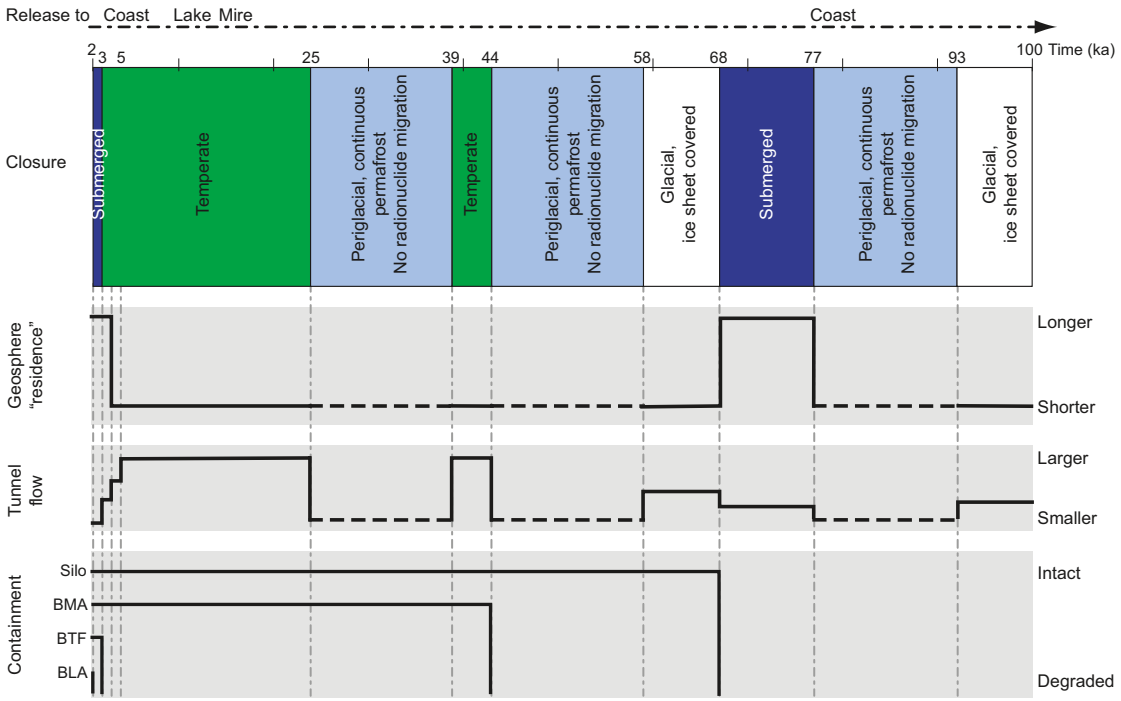

Figure 2-4. *Schematic illustration of calculation case the Weichselian variant.*

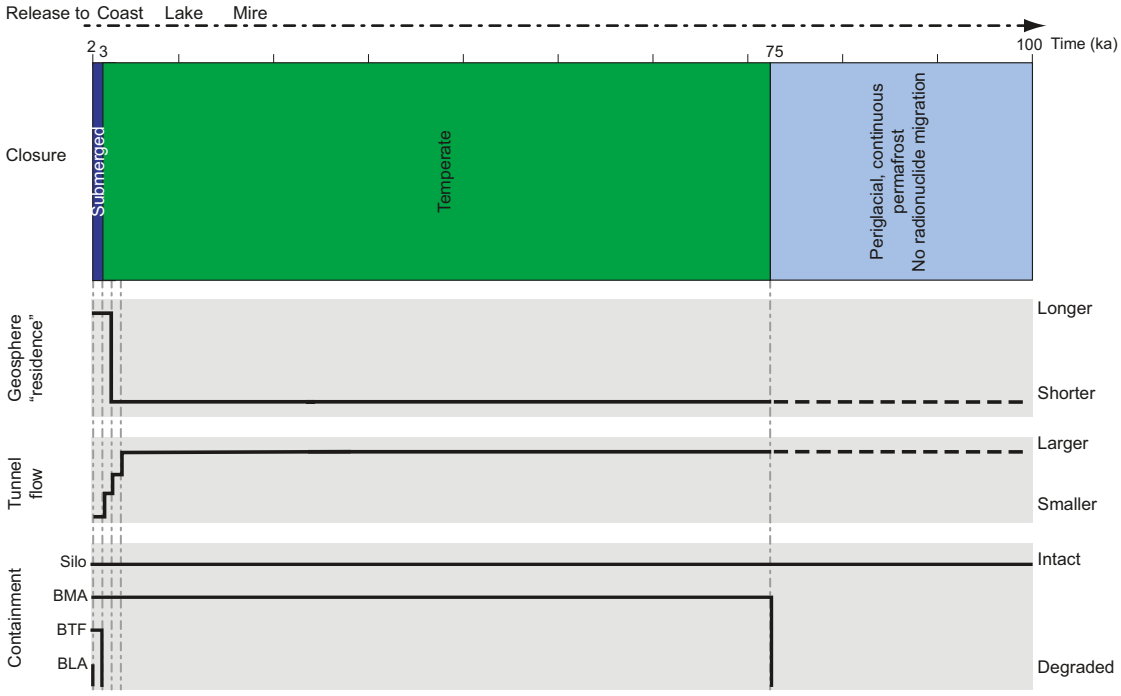

Figure 2-5. *Schematic illustration of calculation case Greenhouse variant.*

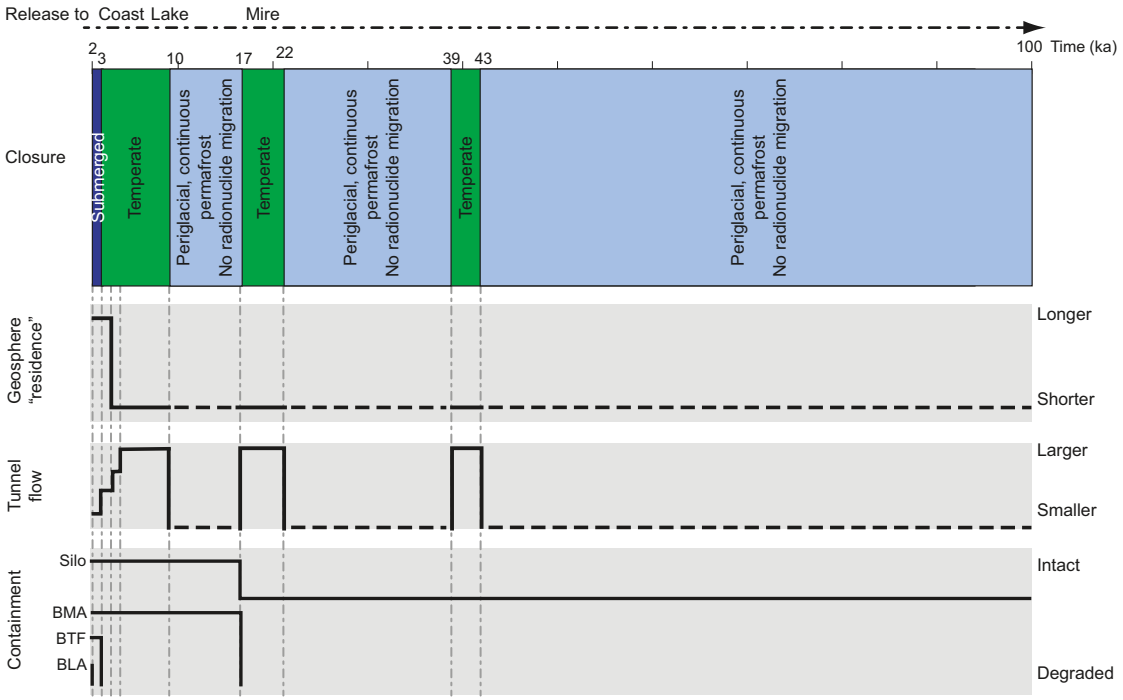

Figure 2-6. *Schematic illustration of the calculation case Extreme permafrost.*

Table 2-5. Calculation cases considered in the dose assessments.

Type of scenario	Calculation case denotation	Calculation case description
Main scenario	CC1	*Weichselian variant* Climate: A repeat of the last Weichselian climate cycle is adopted, see Figure 2-4. Barriers: All technical barriers fulfil their design criteria intially. Concrete barriers degrade at year 44,000 as the repository freezes during a permafrost period. Bentonite barriers degrade at year 68,000 in association with a retreating glacation. Groundwater flow: Variation in groundwater flow due to land rise is simulated using stepwise changes at year 3,000, 4,000 and 5,000, respectively. No migration of groundwater is considered during periods of permafrost. Further changes of the groundwater flow are illustrated in Figure 2-4. Biosphere conditions: The release of radionuclides to the biosphere occurs initially up to year 5,000 to a coastal bay. From year 5,000 to year 7,000 the radionuclides are released to a freshwater lake. Thereafter it is assumed that release occurs to a mire created from the former lake up to year 25,000 when permafrost prevents any migration. From year 39,000 to 44,000 radionuclides once again are released to a mire. From year 58,000 to 77,000 release occurs to a coastal area as a period of glaciation may cause submersion. Between year 77,000 and 93,000 a new period of permafrost prevails before a new glaciation comes, represented by a costal area.
Main scenario	CC6	*Greenhouse variant* Climate: A temperate climate will prevail for a longer time and not before year 75,000 will the repository freeze due to permafrost, see Figure 2-5. Barriers: All technical barriers fulfil their design criteria intially. Concrete barriers degrade year 75,000 as the repository freezes during a permafrost period. Ground water flow: See Figure 2-2. Biosphere conditions: Identical to CC1 up to year 25,000. After 25,000 the mire will receive radionuclides up to year 75,000. After year 75,000 permafrost conditions prevail.

Type of scenario	Calculation case denotation	Calculation case description
Less probable scenario		*Earthquake* Simplified calculation that takes into account the effect of an earthquake.
Less probable scenario	CC2	*Talik* Identical to CC1 except that radionuclide release and transport through taliks is assumed during periods of permafrost. In this case a lake receives the radionuclides during permafrost periods.
Less probable scenario	CC4	*Earlier freezing (BMA) in the Weichsel variant* Identical to CC1 except that the barriers in BMA degrade year 25,000, during an earlier permafrost period.
Less probable scenario	CC5	*Earlier freezing (BMA) in the Weichsel variant with talik* Identical to CC2 except that the barriers in BMA degrade year 25,000, during an earlier permafrost period.
Less probable scenario	CC7	*Extreme permafrost* Climate: Earlier and more intensive periods of permafrost during which no groundwater flow occurs, see Figure 2-6. None climate related conditions equal to CC1. Biosphere conditions: Identical to CC1 until year 10,000 permafrost conditions prevail. A short temperate period occurs again from year 17,000 to year 22,000 after which permafrost appears again. A short temperate period occurs between year 39,000 and 43,000 after which permafrost conditions prevail until the end of the analysed period.
Less probable scenario	CC8	*Extreme permafrost with talik* Identical to CC7 except that radionuclide release and transport through taliks is assumed during periods of permafrost. In this case a lake receives the radionuclides during permafrost periods.
Less probable scenario	CC9	*High concentrations of complexing agents* Identical to CC1 except that higher concenatrations of complexing agents result in reduced sorption of some elements in the near-field.
Less probable scenario	CC10	*Gas generated advection.* Identical to CC1 except that the impact of bulk gas generation on radionuclide transport is considered for the Silo.
Less probable scenario	CC11	*Intrusion well* Illustrates the consequences from a water well drilled directly into the vaults or the Silo.
Residual scenario	CC3	*Alternative inventory* Identical to CC1 except that the total sum of activity contained is considered to be the maximum allowable under licence conditions, i.e. $1\ 10^{16}$ Bq.
Residual scenario	CC12	*No sorption in the near-field* Identical to CC1 except that sorption onto near-field materials is excluded.
Residual scenario	CC13	*No barrier function in the far-field* Identical to CC1 except that the delay of the radionulide transport in the far-field is neglected.
Residual scenario	CC14	*Early degradation of technical barriers* Identical to CC1 except that the barriers in Silo and BMA fail at year 5,000.

3 Models for exposure assessment

Landscape models were used to assess exposures from all radionuclides except for C-14. The landscape models, as well as the ecosystem models included in these, are similar to those that were used in the SR-Can safety assessment /SKB 2006b/. The ecosystem models are basically the same that were used in the previous safety assessment of SFR 1 /Karlsson et al. 2001/, with a few modifications presented in the following sections.

Previous safety assessments of SFR 1 /Lindgren et al. 2001/ have concluded that C-14 is the radionuclide with the highest contribution to the exposure of man due to potential releases from the repository. Estimations of release rates to the biosphere carried out within this safety assessment /Thomson et al. 2008/ have also shown that C-14 dominates the release rates in most calculation cases. Given the importance of this radionuclide, the C-14 biosphere models applied in previous assessments were revised. This resulted in that improved biosphere models for C-14 were developed and applied in this assessment. These models are briefly described in Section 3.4 and a complete description can be found in /Avila and Pröhl 2008/.

3.1 Landscape models

Three landscape models were used, each corresponding to one of the landscape configurations that are projected to develop in the potentially affected area. In the first configuration (Figure 3-1), representing today's situation, all biosphere objects (11, 4, 2, 3 and 1) included are Sea objects, as the repository is under the sea bottom. This landscape configuration will prevail for around 3,000 years after the repository closure, i.e. until around year 5,000, when objects 11 (the SAFE-basin) and 4 have been transformed into lakes due to shore-line displacement. The third landscape configuration starts from year 7,000 when objects 11, 4 and 2 have been transformed into mires. This last configuration prevails during the rest of the temperate period, i.e. for around 18,000 years in the calculation case Weichselian variant.

The assumed sequence of landscape configurations is the same that was used in the SR-Can assessments /SKB 2006b/ for this part of the landscape. Even the numbering of the landscape objects used here is the same that was used in /SKB 2006b/. However, in contrast to SR-Can, the transition between landscape configurations was not modeled dynamically. Rather, the properties of the objects in each landscape configurations were kept constant during the simulations. This has to do with the approach adopted for the assessments, explained in Chapter 4.

The landscape models consists of a series of interconnected ecosystem models, which are compartment type models. Hence, the landscape models can be described as a set of interconnected compartment models, and, in mathematical terms, as a system of ordinary differential equations (ODEs). The fluxes of radionuclides between sea objects were estimated from the residence time of the water in the different sea basins determined from modeling studies /Engqvist and Andrejev 1999/. Fluxes between two sea objects are always in both directions, as illustrated in Figure 3-1, where the connection between objects 1 and 3 is represented with two arrows. The fluxes between terrestrial objects, i.e. lakes and mires, and from terrestrial to sea objects, were assumed to be directly proportional to the fluxes of water through upstream objects. The water fluxes were estimated from the average run-off in the landscape, the areas of the objects and their associated catchment areas. Radionuclides in both dissolved and particulate forms were considered in the transport calculations.

In modelling the transport of radionuclides in the landscape the transformation of mires into forests or agricultural lands was not considered. Such transformations were, however, taken into account for the dose calculations (see Chapter 4). It is considered that this simplification does

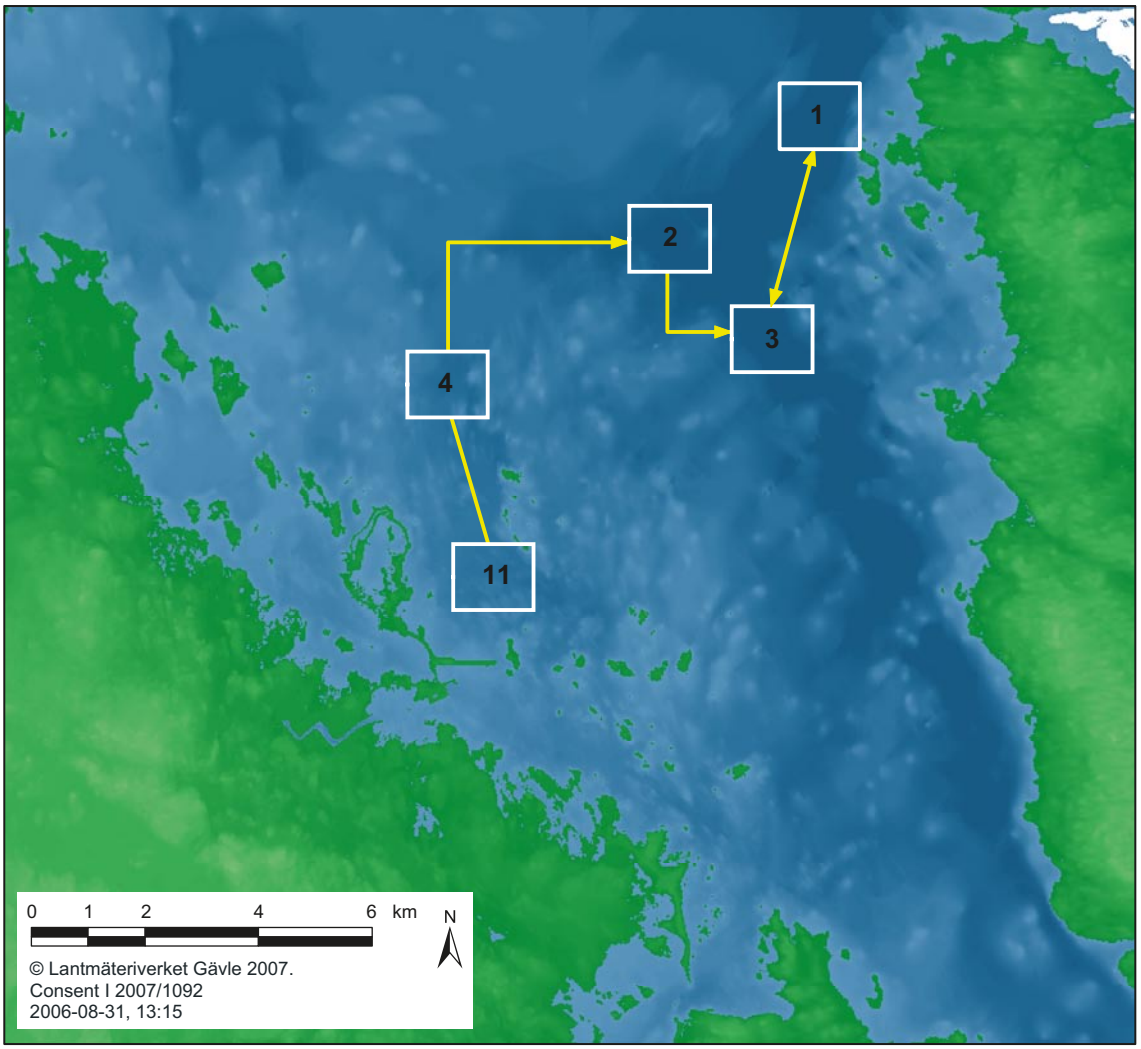

Figure 3-1. *Representation of the landscape model that is used during the first 3,000 years after the repository closure when the repository is under the sea (object 11) and all biosphere objects (numbered squares) are Sea Basins. In the period from 3,000 to 5,000 years after repository closure a second landscape model is used with objects 11 and 4 being Lakes and the rest remaining Sea Basins. Starting from 5,000 years after repository closure a third landscape model is used with objects 11, 4 and 2 being Mires and object 3 and 1 being Sea Basins during the rest of the simulation period. Object 1 represents the Baltic Sea. The arrows represent the direction of downstream water fluxes in the third landscape configuration. Fluxes between objects 3 and 1 are in both directions as these are sea basins. The underlying map shows today's shoreline /SKB 2006b/.*

not underestimate the doses. Previous assessments have shown that radionuclides are retained more in mires than in agricultural lands /Karlsson et al. 2001/. At the same time, the model for the mire is expected to predict at least the same retention as the model for the forest /Avila 2006b/, as in both models the radionuclide retention is modelled basically in the same way and the same values of the distribution coefficients (Kd) are used.

3.1.1 Parameter values

The values of parameters that characterise the dimension of the landscape objects (area) and the transport between objects (water residence time for sea objects and catchment areas for lakes and mires) are presented in Table 3-1. Values assigned to the average runoff at the site are also provided.

Table 3-1. Values assigned to the area of objects, the catchment area of lakes and mires, the water residence time of sea objects and the average runoff in the landscape. For each parameter nominal value and probability density function (PDF) are provided where applicable.

Parameter	Object	Nominal value	PDF[1)]	Reference
Area (km^2)	11 (SAFE-basin)	13.5[2)]		/SKB 2005/
Area (km^2)	4	1.7		/SKB 2005/
Area (km^2)	2	8.3		/SKB 2005/
Area (km^2)	3 (Öregrundsgrepen)	228		/SKB 2006c/
Area (km^2)	1 (Baltic sea)	377		/SKB 2006b/
Water residence time (days)	11 (SAFE-basin)	0.7	T (0.4, 1.5, 0.7)	/Engqvist and Andrejev 1999/
Water residence time (days)	4	14	T (13.5, 16.4, 14)	/SKB 2005/
Water residence time (days)	2	0.4	T (0.36, 0.72, 0.4)	/SKB 2005/
Water residence time (days)	3 (Öregrundsgrepen)	12	T (11, 13, 12)	/Engqvist and Andrejev 1999/
Water residence time (years)	1 (Baltic sea)	22	T (20, 24, 22)	/SKB 2006b/
Runoff (mm/m^2 and year)		226	T (200, 300, 226)	/Bosson and Berglund 2006/
Are of lake (km^2)	11	1.6		/Brydsten 2006/
Catchment area (km^2)	11	14.1	T (11.2, 16.9, 14.1)	/SKB 2005/
Are of lake (km^2)	4	1.7		/Brydsten 2006/
Catchment area (km^2)	4	65		/SKB 2005/
Area of mire (km^2)	11	1.4		/SKB 2005/
Catchment area (km^2)	Mire 11	14.1		/SKB 2005/
Area of mire (km^2)	4	1.2		/SKB 2005/
Catchment area (km^2)	4	65		/SKB 2005/
Area, (km^2)	Large lake[3)]	2.47		/SKB 2005/
Catchment area, (km^2)	Large lake	1,460		/SKB 2005/

[1)] For the lognormal (LN) and normal (N) distributions the first parameter is the Mean and the second the Standard Deviation of the untransformed data. For the triangular distribution (T) and logtriangular (LT) the first parameter is the minimum, the second the Maximum and the third the Mode.

[2)] Slightly changed value compared to SAFE-basin, which was 11.6 km^2.

[3)] This lake was used for releases of activity during permafrost conditions when talik was assumed to be created.

The connection between objects in the landscape model was implemented as follows:

Connection between coast objects: water to water
suspended matter to suspended matter

Connection between lake objects: water to water
suspended matter to suspended matter

Connection between lake and coast objects: water to water
suspended matter to suspended matter

Connection between mire objects: water to water

Connection between mire and coast objects: water to water

The notation of the compartments which are connected is identical to that in Appendix A.

3.2 Models for aquatic ecosystems

The models used for the aquatic ecosystems, marine ecosystems and lakes, are briefly described in Appendix A. These models are the same that were used in the previous safety assessment for SFR 1 /SKB 2001a/, with a modification, introduced for the assessments in SR-Can interim /SKB 2004/ and SR-Can /SKB 2006a/, to represent direct radionuclide discharges to top sediments. As it will be shown in Chapter 4, this modification is not important for the results, given the approach adopted for the dose assessments.

3.2.1 Parameter values

Table 3-2 presents nominal values and PDFs assigned to the radionuclide independent parameters of the ecosystem models for lakes and sea objects. Values of the radionuclide dependent parameters are given in Appendix B.

3.3 Models for terrestrial ecosystems

As mentioned above, in modelling the transport of radionuclides in the landscape the only terrestrial ecosystem considered was the mire. Potential exposures from forests and agricultural lands were assessed (see Chapter 4) by using aggregated transfer factors (see Section 3.5).

Table 3-2. Values assigned to the radionuclide independent parameters of the ecosystem models for SAFE-basin and the lake created in the basin. For each parameter nominal value and probability density function (PDF) are provided.

Parameter	Unit	Nominal value	PDF[1)]	Reference
Mean water depth, coast	M	9.5	T (8.5, 10.5, 9.5)	/Kautsky 2001/
Suspended matter, coast	kg/m^3	$2.8\cdot10^{-4}$	T ($1.3\cdot10^{-4}$, $5.5\cdot10^{-4}$, $2.8\cdot10^{-4}$)	/SKB 2006b/
Sinking velocity, coast	m/year	60	LT (4, 117, 60)	/SKB 2006b/
Depth of upper sediment, sea	M	0.02	T (0.005, 0.05, 0.02)	/SKB 2006b/
Porosity, sea bottom	–	0.39	T (0.14, 0.65, 0.39)	/SKB 2006b/
Density, upper sed, sea	kg/m^3	767	LT (92, 1700, 767)	/SKB 2006b/
Sed growth, sea	m/year	$6.6\cdot10^{-4}$	LT ($3.5\cdot10^{-4}$, $1.4\cdot10^{-3}$, $6.6\cdot10^{-4}$)	/SKB 2005/
Fraction accumulation bottom, sea	–	0.44	T (0.4, 0.5, 0.44)	/SKB 2006b/
Advective flow, upper sediment	m/year	0.016	T (0.013, 0.021, 0.016)	/SKB 2006b/
Mean water depth, lake	m	1.4	T (1.2, 1.6, 1.4)	/Brydsten 2006/
Suspended matter, lake	kg/m^3	$2.8\cdot10^{-4}$	T ($1.3\cdot10^{-4}$, $5.5\cdot10^{-4}$, $2.8\cdot10^{-4}$)	/SKB 2006b/
Sinking velocity, lake	m/year	183	LT (36.5, 3600, 183)	/SKB 2006b/
Depth of upper sediment, lake	m	0.084	–	/SKB 2006b/
Porosity, lake bottom	–	0.93	T (0.81, 0.97, 0.93)	/SKB 2006b/
Density, upper sed, lake	kg/m^3	100	T (50, 200, 100)	/SKB 2006b/
Sed growth, lake	m/year	$6.6\cdot10^{-4}$	LT ($3.5\cdot10^{-4}$, $1.4\cdot10^{-3}$, $6.6\cdot10^{-4}$)	/SKB 2005/
Fraction accumulation bottom, lake	–	0.5	T (0.3, 0.7, 0.5)	/SKB 2006b/
Advective flow, upper sediment, lake	m/year	0.016	T (0.013, 0.021, 0.016)	/SKB 2006b/

[1)] For the lognormal (LN) and normal (N) distributions the first parameter is the Mean and the second the Standard Deviation of the untransformed data. For the triangular distribution (T) and logtriangular (LT) the first parameter is the minimum, the second the Maximum and the third the Mode.

The model used for mires is briefly described in Appendix A. This model is the same that was used in the previous safety assessment of SFR 1 /Karlsson et al. 2001/, with a modification, introduced for the assessments in SR-Can interim /SKB 2004/ and SR-Can /SKB 2006a/, to account for water fluxes from upstream objects.

3.3.1 Irrigation model

The model described in /Bergström and Barkefors 2004/ was applied to assess exposures resulting from the use of contaminated water for irrigation. This model is briefly described in Appendix A.

3.3.2 Parameter values

Table 3-3 presents nominal values and PDFs assigned to the radionuclide independent parameters of the mire. The general parameter values used in the irrigation model are summarised in Table 3-4. Values of the radionuclide dependent parameters are given in Appendix B.

Table 3-3. Values assigned to the radionuclide independent parameters of the mire model. For each parameter nominal value and probability density function (PDF) are provided where applicable.

Parameter	Unit	Nominal value	PDF[1)]	Reference
Density	kg/m^3	1,560	T (1200, 1800, 1560)	/Karlsson et al. 2001/
T_k	year	0.003	T ($1\cdot10^{-4}$, $-1\cdot10^{-2}$, $3\cdot10^{-3}$)	/SKB 2006b/
Mire porosity	–	0.89	T (0.76, 0.95, 0.89)	/SKB 2006b/

[1)] For the lognormal (LN) and normal (N) distributions the first parameter is the Mean and the second the Standard Deviation of the untransformed data. For the triangular distribution (T) and logtriangular (LT) the first parameter is the minimum, the second the Maximum and the third the Mode.

Table 3-4. Values assigned to the radionuclide independent parameters of the irrigation model. For each parameter nominal value and probability density function (PDF) are provided where applicable /Bergström and Barkefors 2004/.

Parameter	Unit	Nominal value	PDF[1)]
Nr of irrigation	–	5	T (3, 7, 5)
Annual amount of water for irrigation	m/(m^{2}year)	0.15	T(0.1, 0.2, 0.15)
Porosity	–	0.5	T (0.4, 0.6, 0.5)
Soil part dens	kg/m^3	2,650	T (2,600, 2,700, 2,650)
Bioturbation	kg/(m^2, year)	2	T (1, 3, 2)
Depth of soil	m	0.25	T (0.2, 0.3, 0.25)
Leaf area index	m^2/m^2	5	T (4, 6, 5)
Water retention per surface area	m^3/m^2	$3\cdot10^{-4}$	T ($2\cdot10^{-4}$, $4\cdot10^{-4}$, $3\cdot10^{-4}$)
Carbon content in vegetables	kg C per kg FW	0.049	LN (0.049, 0.057)
Yield of vegetables	kg FW/m^2	2	T (1.5, 4, 2)

[1)] For the lognormal (LN) and normal (N) distributions the first parameter is the Mean and the second the Standard Deviation of the untransformed data. For the triangular distribution (T) and logtriangular (LT) the first parameter is the minimum, the second the Maximum and the third the Mode.

3.4 Special models for C-14

Special models were developed for assessment of the exposure to releases of C-14 /Avila and Pröhl 2008/. These models are based on the so-called specific activity approach, which has been recommended by /UNSCEAR 2000/ and /IAEA 2001/ for assessment of doses from C-14 releases to the environment from nuclear installations, such as nuclear power plants. The main assumption behind these models is that the long term environmental behaviour of C-14 is modulated by the environmental cycles of stable carbon (C-12) and that isotopic equilibrium between C-14 and C-12 is achieved with a constant isotopic ratio (specific activity), i.e. the same specific activity is observed in all environmental compartments. The specific activity is defined as the activity concentration of C-14 in a media, expressed in Bq/g or Bq/m^3, divided by the stable carbon content in the same media, expressed in g C/g or g C/m^3. Furthermore, several other realistic and cautious assumptions were made for deriving simplified equations for calculating C-14 specific activities. These are documented and justified in /Avila and Pröhl 2008/.

The C-14 specific activity models were applied to assess doses to man resulting from C-14 releases to biosphere objects that may receive direct releases from the geosphere at different time periods after the repository closure: mires, forest ecosystems, agricultural lands, sea basins and lakes. A C-14 specific activity model was also used in assessments of C-14 exposures resulting from the use of waters from an impacted well for drinking and irrigation of vegetables. The exposure to C-14 from biosphere objects located downstream the release object was estimated to be always lower than exposures resulting from the object that receives the releases. This is a direct consequence of the irreversibility of the isotopic dilution, i.e. re-concentration of C-14 will not occur once it has mixed with a certain amount of C-12 /Sheppard et al. 2006/. This means, that using specific activities near the contamination source for dose calculations will result in conservative estimates. The following exposure pathways were considered in calculations of doses from C-14: ingestion of contaminated food and water for both terrestrial and aquatic ecosystems and inhalation of contaminated air for terrestrial ecosystems. The exposure by external irradiation was not considered, as C-14 is a pure low-energy beta emitter.

3.4.1 Parameter values

The parameter values used in calculations with the C-14 models are those given in /Avila and Pröhl 2008, Tables 3-1 and 4-1/. This is the case for all parameters, except for those for which situation specific values are required, as indicated in /Avila and Pröhl 2008/. The values for these parameters are the same as those given for other radionuclides and have been presented in the above sections.

For terrestrial ecosystems (forests and agricultural lands) the area of the biosphere object is given in Table 3-1.

For aquatic ecosystems (lakes and sea basins) the area and catchment area of the lakes are given in Table 3-1, and the area and depth of the sea basins in Table 3-2.

3.5 Models for dose calculations

The dose calculations were carried out using the methods described in /Avila and Bergström 2006/. The methods applied for calculation of doses from water ingestion, inhalation and external exposure are exactly the same as those that were applied in the previous safety assessment of SFR 1 /Karlsson et al. 2001/. However, for estimations of food ingestion doses the approach that was introduced in SR-Can /Avila 2006a/ was applied. In assessments for aquatic ecosystems and agricultural lands the approach described in /Avila 2006a/ was used without modifications. However, a modification, as described in Appendix C, was introduced for estimation of exposures from ingestion of forest products.

In the dose calculations for SR-Can /Avila et al. 2006, Avila and Bergström 2006/, it was assumed that the exposed individuals obtain the whole annual demand of carbon (a value of 110 kg C/yr /Avila and Bergström 2006/ was used) from the ecosystem considered. Hence, the total radionuclide intake with food can be expressed as:

$$Intake^j = IR_C * \sum_k f_k * C_k^j \quad (3.1)$$

where,

IR_C is the annual intake of carbon by an individual [kgC/yr],

f_k is the fraction of the food product "*k*" in the annual intake of carbon [unitless],

$C_k{}^j$ is the *j-th* radionuclide concentration in the food product "k" [Bq/kgC].

The radionuclide concentration in a food product can be obtained by multiplying the radionuclide concentration in soil with the corresponding concentration ratio. The following expression for the total radionuclide intake with food:

$$Intake^j = IR_C * C^j_{media} * \sum_k f_k * CR_k^j \quad (3.2)$$

where,

$C^j{}_{media}$ is the *j-th* radionuclide concentration in the relevant environmental media for example in soil [Bq/kg DW],

$CR_k{}^j$ is the concentration ratio from soil to the food product "*k*" [Bq/kgC per Bq/kg DW].

The sum in Equation 3.2 represents the ratio between the radionuclide concentration in the diet and the radionuclide concentration in the environmental media (soil) and is called in this report "Aggregated Transfer Factor (TF_{agg})". Hence, the TF_{agg} for a given ecosystem type is the sum, over all possible food components of the diet, of the CRs weighted with the fractional contribution of the various food products to the annual carbon intake. A description how values of aggregated transfer factors are obtained for the forest is given in Appendix C. As explained in Appendix C these values have been overestimated by about a factor of 10.

3.5.1 Parameter values for dose calculations

Table 3-5 presents nominal values and PDFs assigned to the radionuclide independent parameters of the dose calculation models. Values of the radionuclide dependent parameters are given in Appendix B, the aggregate transfer factors included.

Table 3-5. Values assigned to the radionuclide independent parameters of the dose calculation models. For each parameter nominal value and probability density function (PDF) are provided where applicable.

Parameter	Nominal value	PDF[1)]	Reference
Dust concentration (kg/m^3)	$5 \cdot 10^{-7}$	T ($1 \cdot 10^{-7}$, $1 \cdot 10^{-6}$, $5 \cdot 10^{-7}$)	/IAEA 2005/
Inhalation rate (m^3/hour)	1	–	/Avila and Bergström 2006/
Annual carbon intake (kg C/year)	110	–	/Avila and Bergström 2006/
Annual consumption rate of water (m^3/year)	0.6	–	/Avila and Bergström 2006/
Annual carbon intake (kg C/year) of irrigated vegetables (only considered for well)	2.1[2)]	–	
Exposure time for external exposure and inhalation (h/year)	2,920	–	/SKB 2006b/

[1)] For the lognormal (LN) and normal (N) distributions the first parameter is the Mean and the second the Standard Deviation of the untransformed data. For the triangular distribution (T) and logtriangular (LT) the first parameter is the minimum, the second the Maximum and the third the Mode.

[2)] The value corresponds to an annual intake of 41.5 kg vegetables according to Swedish food statistics /Jordbruksverket 2007/.

3.5.2 Estimation of number of individuals in the exposed group

The number of individuals that can be supported by a specific ecosystem is calculated using Equation 3.3.

$$N_{eco} = \frac{pty_{eco} * Area_{eco}}{IR_C} \quad (3.3)$$

where,

N_{eco} is the number of individual that can be supported by the ecosystem [unitless],

pty_{eco} is the food production in different ecosystem types [kgC/m^2/yr],

$Area_{eco}$ is the area of the ecosystem [m^2],

IR_C is the annual intake of carbon by an individual [kgC/yr].

The values of the food production of the different ecosystems used are presented in Table 3-6. Food production values were taken from /SKB 2006b/, except for the values for the lake ecosystem. The estimation of the food production in lakes is discussed below. The areas of the ecosystems are given in Table 3-1. A value of 110 kg C/yr /Avila and Bergström 2006/ was used for IR_C (see also discussion below on human food consumption). The number of individuals that can obtain all their food intake for object 11 is indicated for each ecosystem type in Table 3-6.

Food production in lakes

For the safety assessment of SR-Can the production of food was estimated to address the maximum amount that can sustainably be produced by a single object (ecosystem) in the landscape. The food production was categorised as food normally consumed and edible products /SKB 2006b/. Food normally consumed e.g. for a lake is fish, while edible products are everything that has some potential to be consumed by humans. Edible products could be worms, larvae, molluscs as well as fish etc above a certain size that can be handled. In SR-Can this size was set to 1 mm (i.e. macro fauna).

The production was estimated for species or taxa where biomass was quantified in the site investigations in SR-Can. The production for most species was estimated from production per biomass ratios (P/B) reported in the literature. Some estimates (for e.g. fish) were based on calculations of the mass balance from metabolic demands and consumption using literature values /Kautsky 1995, Lindborg 2005/. The production was estimated as the weight of organic carbon (gC/m^2/yr). This partly compensates for the energetic quality of food by that structural components as bones, shells etc which normally are not eaten also contain a low fraction of organic carbon.

The result in SR-Can was that the production of normally eaten products (here fish) was 4 gC/m^2/yr /SKB 2006b/. This estimate was used as the food production in assessments for SR-Can.

Table 3-6. Food production of the different ecosystem types used for estimation of the number of individual that can be sustained by the ecosystem /SKB 2006b/.

Ecosystem	Food production [kgC/m^2/yr]	Number of individuals
Agricultural land	$1.3 \cdot 10^{-1}$	$1.7 \cdot 10^{3}$
Forest	$3.0 \cdot 10^{-4}$	$4.0 \cdot 10^{0}$
Lakes	$9.0 \cdot 10^{-4}$*	$1.3 \cdot 10^{1}$
Sea	$5.3 \cdot 10^{-3}$	$6.5 \cdot 10^{2}$

* For lakes, values estimated here were used.

This value was compared to the estimates of yields of fish as food from lakes, which are about 0.03 to 0.17 gC/m^2/yr (calculated from /Degerman et al. 1998/). This range of values is considerably lower than the value used in SR-Can and cannot be explained by that SR-Can considers all fish, whereas the estimated yields consider only fish normally fished for food.

The fish production was reviewed and the production was estimated using P/B ratios. The P/B ratios are dependent on fish size (weight and length) and an allometric relationship has been established from studies of 79 freshwater species in Canada /Randall and Minns 2000/ Several of the fish species are similar to the Scandinavian species, and as the paper shows the P/B is well correlated to size for most animals /Banse and Mosher 1980, Downing and Plante 1993, Randall and Minns 2000/.

The maximum lengths of the fish species caught in the surveying gillnets were taken from the site study at Forsmark /Borgiel 2004/. These ranges were compared with the data from /Randall and Minns 2000/ and for each species a mean P/B was estimated for this range (Table 3-7). This P/B ratio was multiplied with the estimated biomass per m^2 /Lindborg 2005/ to obtain the area specific fish production for each tabulated species in each of the studied lakes, Eckarfjärden, Fiskarfjärden, Bolundsfjärden and Gunnarsbo-Lillfjärden. The total sum of fish production for each lake was used to obtain an average fish production estimate for the area, which is 0.5 gC/m^2/yr. This estimate is one order of magnitude lower than the estimate in SR-Can and considerably higher than the maximum generic estimates by /Degerman et al. 1998/. Some of the differences can be explained by that our data contains also fish that are not commonly consumed species, which is obvious from Table 3-7. Moreover, the sustainable yield from a lake must be less than the production, to compensate for natural mortality. Thus the production of edible fish is lower than 0.5 gC/m^2/yr.

Additionally, a future potential food item in this area could be crayfish. There are no crayfish in the lakes studied today at the sites, but future lakes could contain these. A generic yield of a good crayfish lake is about 50 kg/ha /Fiskeriverket 2003/ which corresponds to a production of 0.4 gC/m^2/yr. Thus, a maximum total food production from a lake is less than 0.9 gC/m^2/yr.

Table 3-7. Biomass, B (gC/m^2), and production, P (gC/m^2/yr), of different fish species in Forsmark area, based on average P/B ratios (1/yr) of size range from /Randall and Minns 2000/. Biomass and size estimates from /Lindborg 2005/ and /Borgiel 2004/ respectively.

				Eckar-fjärden		Fiskar-fjärden		Bolunds-fjärden		Gunnarsbo-Lillfjärden		Mean
Species	**Name in Swedish**	**Size length (mm)**	**P/B**	**B**	**P**	**B**	**P**	**B**	**P**	**B**	**P**	**P**
Roach *Rutilus rutilus* L.	Mört	200–300	1.0	0.23	0.23	0.14	0.13	0.14	0.13	0.00	0.00	0.12
Tench *Tinca tinca* L.	Sutare	500–600	0.3	0.42	0.14	0.25	0.08	0.29	0.09	0.00	0.00	0.08
Perch *Perca fluviatilis* L.	Aborre	300–400	0.5	0.26	0.14	0.17	0.09	0.19	0.10	0.33	0.17	0.12
Pike *Esox lucius* L.	Gädda	700–1,300	0.2	0.13	0.03	0.01	0.00	0.01	0.00	0.00	0.00	0.01
Ruffe *Gymnocephalus cernuus* L.	Gärs	100–200	1.5	0.03	0.04	0.00	0.00	0.01	0.01	0.00	0.00	0.01
Crucian carp *Carassius carassius* L.	Ruda	250–500	0.5	0.00	0.00	0.76	0.41	0.07	0.04	0.59	0.32	0.19
Total				1.07	0.57	1.33	0.72	0.70	0.38	0.92	0.49	**0.54**

If the range is extended to other theoretical food items, molluscs and insect larvae could be eaten. There is no evidence that insect larvae from aquatic habitats are eaten on regular basis, while molluscs at least are utilised in marine environments. Freshwater mussels of the family of Unionidae (e.g *Anodonta anatina*., Duck mussel, sv. Allmän dammussla) are abundant in the lakes, although there are no biomass estimates for the lakes in Forsmark. Comparing with the production in river Thames, a theoretical upper estimate of production is 132 kg FW/ha/yr /Negus 1966/. The abundance of mussels in Thames is about 100 times higher compared with semi-quantitative estimates from Lake Mälaren in Sweden /Lundberg and Proschwitz 2007/. Thus probably a very high estimate of production of large molluscs is 0.3 gC/m^2/yr. There are no records of humans eating Unionids on regular basis and general discussion about the edibility of Unionids seem to rate them as distasting /Bourquin 2008/.

Thus the maximum production of food from lakes similar to future lakes in the Forsmark area is less than 0.9 gC/m^2/yr.

Humans food consumption

Humans (age > 15 year) need 60–290 kgC/yr to cover their metabolic costs. The range is dependent on sex and physical activity. The lower values are for young females /ICRP 2003/ while the highest are for Olympic athletes /Berglund 2005/. /ICRP 1975/ uses 3,000 kcal/day as the values for reference man, which has been the basis for calculating the dose conversion factors. This corresponds to the energetic content of 110 kgC/yr organic carbon. This is a value close to an adult male working-labour and was the energy intake used in the SR-Can assessment /Avila and Bergström 2006/.

Thus the food needs to contain at least the energetic content balancing the energetic demand, but it also needs to contain essential vitamins, proteins and elements to balance those demands. Moreover, the body is not able to assimilate all nutrients, some are lost through the faeces, although the assimilation efficiency for organic carbon is 98% (calculated from reference man /ICRP 1975/). To obtain this food the additional losses from the preparation, transport as well as detoration of the food from aging, pests and diseases. For e.g. herring it is estimated that 52% of the whole weight is consumed after preparation /Kiljunen et al. 2007/. This means that the catch of food must be larger than the energetic demand to compensate for the losses in handling and assimilation. Thus, the required food production must be larger than 65–110 kgC/yr to supply a human.

The future lake in Forsmark

The future lake above the repository has an initial area of 1.6 km^2. This gives that the food production must be less than 1.2 tonnes C/yr if all fish and crayfish production is used sustainably. This can feed less than 13 humans living entirely on the production from the lake. If the production of large mussels is included, less than 5 additionally persons can obtain their food from the lake. Thus, the total food production from the lake can supply a very small group of humans.

This small group contains also the most exposed individual because they feed entirely on the potentially most contaminated food. The highest doses are obtained if the individuals feed their entire life on the autotonous production from the lake.

In reality, it is likely that humans will take their food intake from various sources, berries, mushrooms, game as well as cultured products, which are all less contaminated than the food from the lake. Even for fisheries the effort for a unit catch will give better value to utilise the Baltic Sea which is in the vicinity of the future lake. Thus the food habits will feed a larger population with a higher diversity of food item which contains considerable less contamination. This means that the dose presented here is the maximum theoretical dose the most exposed individual can obtain and that the size of this group is limited.

4 Assessment approaches

4.1 Assessment of doses from releases to the landscape

The assessments of doses from radionuclide releases to the landscape were carried out using the landscape models described in Section 3.1. The approach adopted for the assessments is similar to that used in SR-Can /Avila et al. 2006/ for derivation of Landscape Dose Factors (LDF). However, whereas in SR-Can a single LDF value was derived for each radionuclide, in this case a Dose Factor was derived for each of the three landscape configurations (see Section 3.1), that are projected will exist in this area from the time of the repository closure until the next permafrost period. Hence, for each time period a Dose Factor was obtained (see Section 4.1.1), which was then used to estimate maximal annual doses by multiplying by the corresponding release rates to the biosphere, as described in Section 4.1.2.

The transformation of the landscape was not modeled dynamically, but instead to obtain the Dose Factors each of the landscape configurations was run for 20,000 years, which is the approximate duration of the temperate period. Supporting studies were carried out (see Appendix E) to investigate whether or not this approach may lead to underestimation of the doses to the most exposed group.

One of the supporting studies (see Appendix E1) aimed at identifying the landscape object with the highest doses to the most exposed group. As mentioned in Chapter 2, it is foreseen that the releases from the geosphere will always be directed to object 11, i.e. the SAFE-basin. Hence, a simulation with each of the landscape models was carried out with constant unit release rates to object 11 during 20,000 years, and the concentrations in different landscape objects were compared. The results of this study (Appendix E1) showed that the highest radionuclide concentrations, and consequently the highest doses, were always obtained for object 11. This is also valid for C-14, as C-14 specific activity reduces as C-14 migrates away from the release source. This is a direct consequence of the irreversibility of the isotopic dilution, i.e. re-concentration of C-14 will not occur once it has mixed with a certain amount of C-12 /Sheppard et al. 2006/. Hence, the dose rates from object 11 were used to obtain the Dose Factors (see Section 4.1.1) that are used to calculate doses to the most exposed group. Equilibrium values of the radionuclide inventories, concentrations and doses were observed in this, and other landscape objects, within the simulation period. This is illustrated in Figure E3-1 in Appendix E3, which shows the time dynamics of the radionuclides inventory in object 11 when this object is a mire, which is the ecosystem where it takes longer time to achieve equilibrium.

For deriving Dose Factors for the Sea period (first 3,000 years after closure) and the Lake period (from 3,000 years to 5,000 years after closure), the releases were directed to the water compartment. As shown from the study presented in Appendix E2, this assumption will maximize the doses while these objects are aquatic, as it gives the highest water concentrations. However, it might potentially give lower doses in the period when the lake has been transformed into mire. This could be the case if the radionuclides' retention in sea or lake sediments was higher than in mires. A substantial role of the radionuclide accumulation in lake or sea sediments is not expected for the context of the present assessment. Indeed, the release rates during the first 5,000 years are dominated by C-14, for which accumulation in sediments is not an important dose contributing process /Avila and Pröhl 2008/. Nevertheless, a comparative study was carried out (see Appendix E3) considering two cases: the first with releases to a mire during 20,000 years and the second with releases to the top sediments of the lake during the first 2,000 years and releases to a mire during the following 18,000 years. The main conclusion from this study was that the second case will give higher inventories, and hence doses, than the first. However, the only radionuclide, apart from C-14, with some, although still relatively low, release rates during the first 5,000 years after closure is Ni-59. For this, and other absorbing

radionuclides, the retained inventory, and the doses, will not be underestimated by more than a factor of about 2–3. This factor can be considered to be small in comparison with other uncertainties, for example Kd values vary by several orders of magnitude.

4.1.1 Derivation of Dose Factors

Probability density functions (PDFs) of the maximal annual effective doses per unit release rate (Dose Factors) for exposures in different time periods were generated by running the C-14 models (see Section 3.4) and the three landscape models (see Section 3.1) probabilistically with constant unit release rates of each radionuclide during the 20,000 years. The maximal dose values obtained for object 11 were used as Dose Factors. An additional Dose Factor was also derived for use in the calculation cases (CC2, CC5, CC8) where releases are directed through taliks to a larger lake (see Section 2.4). This Dose Factor was derived by running the lake model described in Appendix A, and for C-14 in /Avila and Pröhl 2008/, with parameter values, like volume, water retention times, as the last lake formed due to shore displacement in the Forsmark area /SKB 2006b/. The lake that is formed at around year 5,000 has a high probability of being transformed to a mire /Brydsten 2006/, at around year 7,000, and can therefore not be the recipient for releases through taliks during permafrost periods.

The probabilistic simulations were carried out using the software package Eikos /Ekström and Broed 2006/, which is integrated with Pandora /Åstrand et al. 2005/. For assessing exposures to a mire, Dose Factors were derived for the cases when an agricultural land or a forest is established in the contaminated mire. The dose calculations were carried out with the methods described in Section 3.5. The exposure pathways considered in the dose calculations were: food ingestion for all types of biosphere objects, water ingestion for lakes, inhalation and external exposure for forests and agricultural lands. All parameters for which a PDF is given in the Tables in Chapter 3 and Appendix B were sampled using the Latin Hypercube sampling method. For other parameters the nominal values were used in the simulation.

Statistics for each of the PDF of the doses per unit release rates for each time period, hereafter called Dose Factors, are presented in Appendix D. For the period starting at year 7,000 two Dose Factors are provided, corresponding to the use of the mire for forestry or for agriculture.

4.1.2 Dose calculations

From the probabilistic simulations of the transport of radionuclides in the near field and the geosphere /Thomson et al. 2008/ 960 samples were generated. These samples were multiplied by an equal amount of samples of the corresponding Dose Factors, to obtain 960 samples of time dependent annual doses. From the samples of the annual doses different statistic were calculated, including the mean values which are reported for the different calculation cases in Chapters 5, 6 and 7. The generated samples of the annual doses were also used for the uncertainty and sensitivity analyses described in Chapter 10. In periods when the object receiving the releases was a mire the dose calculations were made using the Dose Factors for forest and agricultural lands, and the highest obtained dose values was retained.

The specific Dose Factors that were used for the dose calculations in each period are given in Table 4-1.

Screening study

In addition to the dose assessments, a screening study was carried out to identify radionuclides that have a potentially significant contribution to the doses. The idea with the screening study was to perform a conservative simple dose calculation and compare the results with a screening criterion. If conservatively calculated doses are below the screening criterion, then it can

Table 4-1. Dose Factors used for each time period corresponding to the ecosystem type of object 11, which is the object that receives the direct releases. The time periods and ecosystem types are given for the three different climate evolutions: Weichselian variant, greenhouse variant and extreme permafrost (see Section 2.4).

Time period (thousands of years)	Dose Factor for release to ecosystem
Weichselian variant	
2–5	Coast – Table D-1
5–7	Lake – Table D-2
7–25	Mire (forest – Table D-4 and agricultural land – Table D-5)
25–39	If permafrost, there is no release to the biosphere. In presence of talik, release occurs to a larger lake – Table D-3
39–44	Mire (forest – Table D-4 and agricultural land – Table D-5)
44–58	If permafrost, there is no release to the biosphere. In presence of talik, release occurs to a larger lake – Table D-3
58–77	Coast – Table D-1
77–93	If permafrost, there is no release to the biosphere. In presence of talik, release occurs to a larger lake – Table D-3
93–100	Coast – Table D-1
Greenhouse variant	
2–5	Coast – Table D-1
5–7	Lake – Table D-2
7–75	Mire (forest – Table D-4 and agricultural land – Table D-5)
75–100	If permafrost, there is no release to the biosphere. In presence of talik, release occurs to a larger lake – Table D-3
Extreme permafrost	
2–5	Coast – Table D-1
5–7	Lake – Table D-2
7–10	Mire (forest – Table D-4 and agricultural land – Table D-5)
10–17	If permafrost, there is no release to the biosphere. In presence of talik, release occurs to a larger lake – Table D-3
17–22	Mire (forest – Table D-4 and agricultural land – Table D-5)
22–39	If permafrost, there is no release to the biosphere. In presence of talik, release occurs to a larger lake – Table D-3
39–43	Mire (forest – Table D-4 and agricultural land – Table D-5)
43–100	If permafrost, there is no release to the biosphere. In presence of talik, release occurs to a larger lake – Table D-3

be assured, with a high degree of confidence, that the doses are insignificant. In practice a Screening Quotient (SQ) was calculated, which is defined as the ratio between the conservative dose estimate and the screening criteria. Hence, if the SQ is below one, then it can be assured, with a high degree of confidence, that the doses are insignificant. Conservative estimations of the doses were obtained by multiplying the 95 percentile of the radionuclide release rate, at each time point, taken from /Thomson et al. 2008/ by the 95 percentile of the doses per unit release rate (Dose Factor) for the corresponding time period. This gives a dose estimate that is well above the 95 percentile of the doses that would result from probabilistic dose estimations. As screening criteria a value of 0.1 μSv/y was used, which is 140 times lower than the dose value that corresponds to the lowest of the risk criteria given in the regulations (see Section 1.2). It should be noted that if the SQ are above one this does not mean automatically that the doses are significant. Such situation merely indicates that there is a need for more detailed assessments.

4.2 Assessment of doses from releases to a well

Doses from releases to a well were estimated using the same approach as in SR-Can /Avila et al. 2006/ by assuming that 100 percent of the releases from the geosphere are fully mixed with water from a well, that is used for drinking and irrigation of vegetables. This means that for calculation of the radionuclide concentrations complete capture of the plume was assumed. The radionuclide concentrations in the well water were calculated by dividing the radionuclide release rates by the well capacity. Values of the well capacity were estimated from values measured in existing wells in the Forsmark area /Gentzschein et al. 2006/. The doses resulting from the use of well water for irrigation were calculated with the model described in /Avila and Pröhl 2008/ for C-14 and with the model described in /Bergström and Barkefors 2004/ for other radionuclides. Dose Factors are presented in Table D-6 in Appendix D. These are defined as the annual doses resulting from unit release rates to the well. The exposure pathways considered were: ingestion of water, ingestion of vegetables, inhalation and external exposure. In the calculation of the Dose Factors accumulation of radionuclides in the soil during 20,000 years was taken into account.

This approach assumes that abstraction of radionuclides from the well does not affect substantially the radionuclide releases rate to the receptor object in the landscape. If the well is used by a limited number of individuals, for example 2 families or about 10 individuals, the volume of abstracted water will be only a small percentage of the well capacity. If a larger number of individuals were to use the well, then a larger fraction of radionuclides would be abstracted and would not reach the receptor object in the landscape. The doses to the individuals using the well would be the same, but the size of the group would be larger. At the same time, the doses to individuals exposed to radionuclides discharged into the landscape would be lower, although the same number of individuals would be exposed by this pathway.

In Chapters 5, 6 and 7 the doses from the well are shown starting from year 4,000. The calculated release rates from the geosphere are lower and increasing during the period before year 4,000, except for releases from the BLA /Thomson et al. 2008/. The maximum release rate from the BLA occurs earlier, while the rock above the repository still will be covered by water. Thereafter, the release rate decreases rather fast. Hence, for all repository parts a well drilled before year 4,000 will result in lower doses than at year 4,000.

The first thousand years after closure the rock above the repository will be covered by water. Once the shore-line has passed by the site, it is possible to drill a well at the site. However, the well density is dependent of the time that has elapsed after the shore-line has passed by the site and the probability of a well is low during the first hundreds of years. This is primarily because of the annual sea level variation and that the capacity is limited because of salinity intrusion possibility. The higher density of wells occurs after around thousand years, after the shore-line has passed by the site /Kautsky 2001/.

Screening study

In addition to the dose assessments a screening study was carried out to identify radionuclides that have a potentially significant contribution to the doses. The study was carried out as described above for releases to the landscape, but using 95 percentiles of the Dose Factors for releases to a well.

4.3 Assessment of risks from earthquakes

As a consequence of the more extended time period considered in the SFR 1 SAR-08 safety assessment, even an analysis of the risks associated with damages of the repository due to tectonic effects has been studied. The following are the main steps in the approach adopted for the assessment of radiological risks associated with earthquakes.

1. As no studies of the repositories capability of withstanding earthquake damages have been performed within SAR-08 generic data are used in the present analysis. Based on a previous study of earthquake consequences on underground facilities /Bäckblom and Munier 2002/ and further discussed in the SFR 1 SAR-08 main report /SKB 2008a/ it is assumed that all earthquakes having hypocentre within a 10 km radius from the repository and a magnitude of 5 and above will damage the hydrological concrete barriers so that the integrity of the repository will be breached. The assumption of the critical magnitude is based on references cited by Bäckblom and Munier likely to be pessimistic and will most likely overestimate the radiological risk from earthquakes.
2. Based on probabilities that an earthquake of the critical magnitude and above will take place within the area considered /Böðvarsson et al. 2006/ the probability of earthquakes damaging the repository may hence be estimated.
3. Within the SAFE Project, the hydrogeological consequences of damaged barriers were studied /Holmén and Stigsson 2001/ and the resulting flow, in the case of damaged barriers were calculated. These results are used to estimate the radionuclide release rate from the repository.
4. In addition to the assumption above, that an earthquake of magnitude 5 and above will damage the repository, studies have also been made where the sensitivity on the radiological risk of this assumption is investigated by assuming that the repository will be damaged by earthquakes of magnitude 3 and 4.

A more detailed description of the risk assessment steps is provided in the following text. The risk analysis presented here does not cover the effects of glacially induced earthquakes (the probability of having large earthquakes will increase due to mechanical effects of the advancing/retreating ice). The reason for this is that, in the reference evolution of the repository system, it is assumed that the barriers will be damaged during glaciations to such large extent, that they cannot longer be credited as a safety function. Hence, the effects of glacially induced earthquakes are already included in the reference evolution.

4.3.1 Consequence analysis

For assessing the radiological consequences of earthquakes, it is necessary to estimate the release rates from the repository (the Silo and the BMA), the transport in the geosphere to the discharge points in the biosphere and the doses to man resulting from releases to the biosphere. Estimations of the release rates from the Silo and the BMA were carried out on the basis of hydro-geological simulations that were carried out within the SAFE project /Holmén and Stigsson 2001/. As changes in the geosphere caused by earthquakes have not been studied, it is in the present study conservatively assumed that the whole radionuclide inventory that is released from the repository will reach the biosphere without retardation.

The yearly release rate from the repository components to the biosphere were obtained from the turnover times of the water in repository pores as described below.

Releases from the Silo

In the hydrological simulations that were carried out within the SAFE project /Holmén and Stigsson 2001, Section 14.3/, it was assumed that the low permeability of Silo components, for some reason, will be damaged. It is, however, likely that the bentonite layers will still act, at least partly, as hydrological barriers. The resulting water fluxes through different components of the repository were estimated and a total water flux through the Silo of around 1 m^3/y was obtained. The total volume of the radioactive waste in the Silo is 13,700 m^3 /Almkvist and Gordon 2007/ and the porosity of the conditioning cement is 0.2 /Lindgren et al 2001/. Hence, the total pore volume in the Silo can be estimated as 2,740 m^3 and the turnover time of the water storage in the Silo pores is about 2,500 years. If one assumes that the whole Silo is sheared and

defines a concentration boundary condition at the open surface then, assuming that the diffusivity in the backfill is about 0.003 m^2/y, the affected area will have a thickness of a few meters. In this case, the time needed for releasing the radionuclides will be more than 2,500 years.

For estimating the release rate from the Silo, it was conservatively assumed that the whole radionuclide inventory in the waste will be dissolved in the pore water. The radionuclide release rate (in Bq/y), for an earthquake occurring at a given time point, was then obtained by dividing the radionuclide inventory (in Bq) by the turnover time of the pore water (in years). The radionuclide inventory in the Silo, as a function of time, was estimated by subtracting from the initial inventory the amount released in the main scenario with base variant climate evolution /Thomson et al. 2008/ and making proper correction for radioactive decay and ingrowths.

Releases from the BMA

In the hydrological simulations that were carried out within the SAFE project /Holmén and Stigsson 2001, Section 14.4/, it was assumed that the concrete structures of the BMA, for some reason, will be damaged. From this study, the total water flux through the BMA was estimated at 10 m^3/y. The total volume of the concrete structures of the BMA is 1,400 m^3 /Almkvist and Gordon 2007/ and the porosity of the concrete is 0.2 /Lindgren et al. 2001/. Hence, the total pore volume of the BMA repository is around 2,800 m^3. In the case the turnover time of the water in the BMA pores is around 300 years.

The release rates from the BMA were estimated in the same way described above for the Silo, using a value of 300 years as turnover time of the water in the BMA pores.

Dose estimations

To assess risks associated with earthquakes, it is necessary to estimate doses to the potentially most exposed group to the releases. Release rates were assumed to be independent on the magnitude of earthquake and the associated doses were estimated by multiplying the release rates (Bq/y), estimated as discussed above, by a Dose Factor (Sv/y per Bq/y). The Dose Factors in this context are defined as the maximum doses, over a time period of 10^5 years, resulting from a constant unit release rate to the biosphere during a period equal to the turnover time of the pore water in the repository, that is 2,500 years for the Silo and 300 years for the BMA (see above).

It is assumed that the surface ecosystem will undergo changes with time due to land rise and ecosystem succession processes. Hence, radionuclides released from the repository following an earthquake when reaching the biosphere will encounter different landscape configurations, depending on when the release occurs. To take this into account, different Dose Factors were derived for different time periods (see Tables D-7 and D-8 in Appendix D), using the same models and parameter values that were applied for the dose calculations due to releases to the landscape (see Chapter 3 and Section 3.1).

4.3.2 Risk calculations

The dose values, calculated as described above, should be interpreted as the maximum value that an individual could receive, at any time after the time of occurrence of an earthquake. For estimating the risk to an individual living at a certain time "*T*" the probabilities and consequences (associated doses) of earthquakes occurring before that time should be considered. For discrete events the following equation is commonly applied for the risk calculation:

$$Risk(T) = RiskFactor * \sum_{t=0}^{T} p(t) * D(T,t) \qquad (4.1)$$

where,

Risk (T) is the risk at time T [1/y],

D(T,t) is the annual dose at time T associated with an event at time t [Sv/y],

p(t) is the probability of occurrence at time t [unit less],

RiskFactor is the risk factor [1/y].

The probability of occurrence at time t can be estimated with an exponential distribution using the Mean Interval Between Earthquakes (MIBE) as distribution parameter. Values of the cumulative probabilities of occurrence of earthquake of different magnitude calculating using MIBE values obtained for the study area /Böðvarsson et al. 2006/ are presented in Table 4-2 and Figure 4-1.

Considering time as a continuous variable and using an exponential distribution for the probability of occurrence, Equation 4.1 can be reformulated as:

$$Risk(T) = RiskFactor\int_0^T p(t)D(T,t)dt = Riskfaktor\int_0^T \frac{e^{-t/MIBE}}{MIBE} D(T,t)dt \quad (4.2)$$

where,

Risk (T) is the risk at time *T* [1/y],

D(T,t) is the annual dose at time *T* associated with an event at time *t* [Sv/y],

RiskFactor is the risk factor [1/y].

Table 4-2. Probabilities (in percent) of earthquakes of different magnitudes within a distance of 100 km from the repository corresponding to different observation times in years. MIBE is the mean interval between earthquakes /Böðvarsson et al. 2006/.

Magnitude	MIBE	10	20	30	50	100	1,000	100,000
3	2,666	0.37	0.75	1.12	1.86	3.68	31.28	100.00
4	16,820	0.06	0.12	0.18	0.30	0.59	5.77	99.74
5	106,127	0.01	0.02	0.03	0.05	0.09	0.94	61.03
6	669,617	0.00	0.0	0.0	0.01	0.01	0.15	13.87

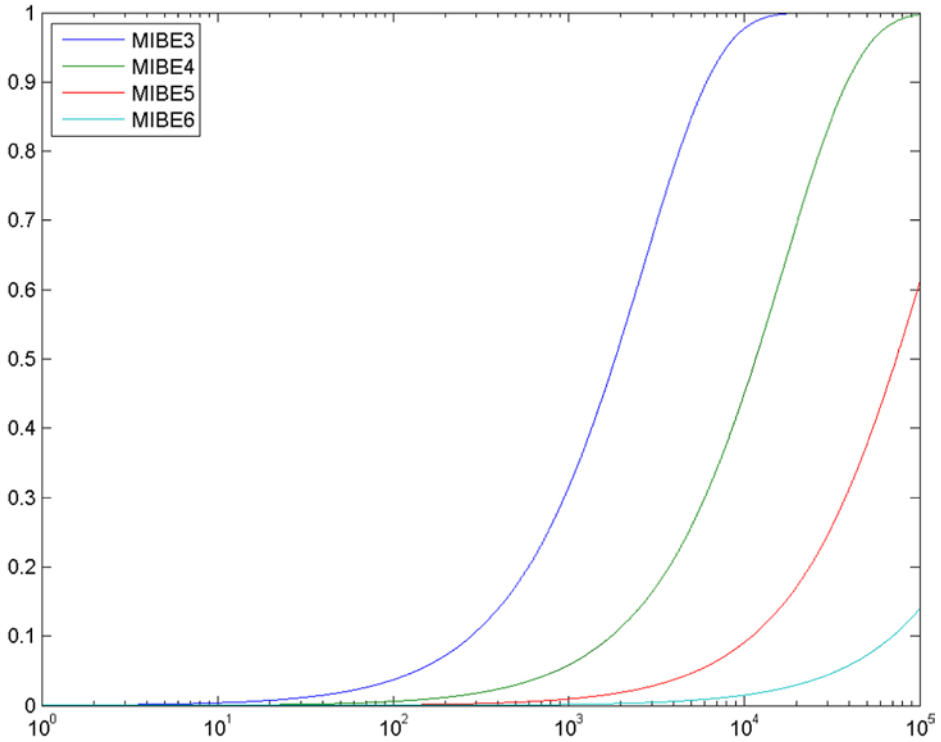

Figure 4-1. *Cumulative probability of earthquakes of different magnitudes (3, 4, 5 and 6), with different values of the Mean Interval Between Earthquakes (MIBE) at different times after the repository closure.*

4.4 Assessment of doses from an intrusion well

Time dependent values of the concentration of radionuclides in the water of the gravel backfill were calculated in /Thomson et al. 2008/, according to the assumptions in calculation cases Weichselian variant (CC1) and high concentrations of complexing agents.(CC9). For the dose calculations it was assumed that 0.6 m^3 per year of the water in the gravel backfill was consumed by an individual (normal annual drinking water consumption) using the dose coefficients presented in Table B-1 in Appendix B.

4.5 Estimation of the collective dose commitment

Collective dose should, according to the regulatory criteria (see Section 1.2), be calculated as the collective dose commitment, integrated over 10,000 years, from releases of radionuclides during the first thousand years after closure. There are a limited number of radionuclides released to the sea during the first 1,000 years, when the releases are dominated by C-14 / Thomson et al. 2008/. The most important contributor to the collective dose is C-14. This was already shown in the first safety analysis of SFR 1 /Bergström and Puigdomenech 1987/.

The complete, i.e. integrated over 50,000 years, collective dose commitment from C-14 releases during the first thousand years was estimated by multiplying the total releases of C-14 (both organic and inorganic C-14) from all repository parts during this period in the Weichselian variant by a conversion factor of 109,000 manSv per PBq. This conversion factor has been used by the UNSCEAR /UNSCEAR 2000/ for estimating the complete collective dose commitment to the global population from releases of C-14 to the atmosphere. It has been calculated under the assumption that the future world population stabilises at 10^{10} people, and that the global inventory of stable carbon does not increase from its present value. Further, according to the UNSCEAR /UNSCEAR 2000/ collective doses following releases to soils or to surface oceans are about the same as those for atmospheric releases. To estimate the incomplete collective dose commitment, i.e. the collective dose integrated over 10,000 years, the complete collective dose commitment was multiplied by 0.75. This is because, according to /UNSCEAR 2000/, 75% of the complete dose commitment from a single release is delivered within 10,000 years. Estimations of collective dose commitments from C-14 releases made with several different models have given very similar results /UNSCEAR 2000/. This consistency between model predictions has been attributed to the long half-life of C-14, relative to its rate of environmental transport, which makes the estimated dose commitments insensitive to the detailed structure of the models or to the values of the parameters used in them (see /UNSCEAR 2000/ and references therein).

4.6 Assessment of the impact on non-human biota

The assessment of the impact on non-human biota was carried out using the integrated approach developed with the EC project ERICA /Erica 2008, Beresford et al. 2007/. The assessment element of the ERICA Integrated Approach is organised in three separate *tiers*, where satisfying certain criteria in Tiers 1 and 2 allows the user to exit the assessment process while being confident that the effects on biota are low or negligible, and that the situation requires no further action. Where the effects are not shown to be negligible, the assessment should continue to Tiers 2 and 3. Situations of concern should be assessed further in Tier 3, by making full use of all relevant information available through the ERICA Integrated Approach or elsewhere. In principle, the user can choose to start the assessment at any Tier.

In this study, the assessments were started at Tier 1, which is designed to be simple and conservative. The default screening criterion proposed in the ERICA integrated approach was used, which consists of an incremental dose rate of 10 μGy h^{-1}, to be used for all ecosystems and organisms. This value was derived from a species sensitivity distribution analysis performed on

chronic exposure data in the FREDERICA database /FREDERICA 2005/ and is supported by other methods for determining predicted no effect values. For Tier 1, the predefined screening dose rate is back-calculated to yield Environmental Media Concentration Limits (EMCLs) for all reference organism/radionuclide combinations and the most restrictive is selected for comparison with environmental media concentrations, i.e. concentrations in soil, air, water and sediments. In practice, for each radionuclide a Risk Quotient (RQ) is calculated defined as the ratio between the environmental media concentrations and the most restrictive EMCL. If the sum of the RQs across all radionuclides is less than one, then it is possible to exit the assessment process, while being confident that the effects on biota are negligible. If the sum of the RQ is greater than one, then it is necessary to continue with the assessment.

To following procedure was carried out to obtain conservative estimates of the RQs:

1. Each of the three landscape models, and the C-14 models, described in Chapter 3 was run probabilistically with a constant unit release rate of each radionuclide. The simulations were carried out during 20,000 years, to ensure that equilibrium in the different environmental media was achieved. The peak value of the 95 percentiles of the concentrations in soil, air (for C-14), fresh water and marine water were selected as a conservative estimates of the concentrations per unit release rate, expressed in Bq/m^3 per Bq/y for water and air and in Bq/kg DW per Bq/y for soils.
2. The concentrations per unit release rate obtained in step 1 were multiplied by the highest peak value of the release rates to the biosphere obtained from the probabilistic simulations reported in /Thomson et al. 2008/ for the main scenario with base variant climate evolution. This yielded conservative estimates of the radionuclide concentrations in environmental media: fresh waters, marine waters, soil and air (for C-14).
3. The concentrations in environmental media obtained in step 2 were divided by the corresponding EMCL, taken from the ERICA tool /Erica 2008/, to obtain conservative estimates of the RQs.

RQs for lake and marine sediments were not calculated. The reasons for this are twofold: i) in the EMCL for the fresh and marine water, the biota exposure from sediments is also considered and ii) the approach adopted in this assessment maximizes concentrations in water (see Section 4.1). When applying the Tier 1 of the ERICA approach to aquatic ecosystems it is sufficient to calculate RQs either from the concentrations in water or from the concentrations in sediments. In both cases the biota exposure from water and sediments is taken into account.

5 Results for calculation cases representing the main scenario

This chapter presents the dose calculation results from the two calculation cases (CC1 and CC6) undertaken as part of the main scenario using values of release rates to the biosphere from /Thomson et al. 2008/. The results of the screening study are presented and figures are provided showing time series of radionuclide specific and total mean annual doses to individuals from the most exposed group. In this context, the mean value is defined as the arithmetic mean of the dose values obtained at given time points from the probabilistic simulations. Releases from each repository part to the landscape and to a well are considered.

It was assumed that during permafrost periods there is no groundwater migration and consequently there is no radionuclide releases to the biosphere /Thomson et al. 2008/. Although some activity from previous releases may remain in the biosphere objects, annual doses for these periods are not calculated, but it is expected that these will not exceed dose values obtained for temperate periods.

For releases to a well, 50-years moving averages of the calculated mean values of the annual doses are presented, whereas for releases to the landscape the calculated mean values are given directly, i.e. without taking a moving average. Hence, the doses from releases to the landscape may overestimate the average life time doses, especially in periods with pronounced short time variations in the annual doses.

The doses from the wells are shown starting from year 4,000 as described in Section 4.2.

5.1 Weichselian variant

The climate evolution considered in this calculation case is based on a repeat of the previous glacial cycle, including the Weichselian glaciation /Vidstrand et al. 2007/, see Figure 2-4. The anticipated climate evolution is a period of temperate conditions at the Forsmark site for approximately 23,000 years. Following this the temperate conditions are gradually replaced by permafrost conditions between year 25,000 and 39,000 and from year 44,000 to 58,000. The period between years 39,000 and 44,000 is characterized by a temperate period. From year 58,000 glacial conditions exist until the retreat of the ice at year 68,000 at which time the area of the site is considered to be submerged and remains below sea-level, most likely under cold climate conditions, until year 77,000. Cold climate conditions continue and permafrost returns from year 77,000 to 93,000 and glacial conditions are re-established from year 93,000 to the end of the assessment period (year 100,000).

In this calculation case it is assumed that the initial properties of the engineered barrier system are at least equivalent to its design specification. This implies that concrete floor, walls and lids in the different repository facilities do not contain large intersecting fractures. The same assumption is made of the porous concrete or concrete grout surrounding the waste packages. It should be noted that in the case of the BLA no credit is given to any engineered barrier for retaining or retarding radionuclides. More details on assumptions made for this calculation case can be found in /Thomson et al. 2008/.

5.1.1 Doses from releases to the landscape

As explained in Section 4.1.4, for screening out unimportant radionuclides a Screening Quotient (SQ) was calculated, which is defined as the ratio between the conservative dose estimate and a screening criteria. If the SQ for a given radionuclide is below one then it can be assured with a

high degree of confidence that the doses from this radionuclide are insignificant in this assessment context. The Screening Quotients (SQs) obtained from the screening study of doses from releases to the landscape, are presented in Table 5-1. Only the peak values of SQs that are above one are presented. The results indicate that radionuclides with short half lives (H-3, Co-60, Ni-63, Sr-90, Cs-137, Pu-238 and Pu-241) do not have any important contribution to the doses. This is because most of their inventory decays before they can be released to the biosphere and the releases will end up in sea basins, where the water residence time is short. It appears that C-14 has the largest contribution to the doses for all repository parts. Other radionuclides with some contribution to the doses (Ni-59, Se-79, Mo-93, I-129 and Cs-135) have long half lives and are relatively mobile. The repository barriers effectively prevent releases to the biosphere of non-mobile radionuclides such as Pu-isotopes, Np-237 and Am-isotopes /Thomson et al. 2008/, which together with their low inventory explains why very low SQs were obtained for these radionuclides. For the BLA all SQs were below one, which reflects the lower radionuclides inventory in this repository part and the absence of barriers, which results in that most of the releases go to the sea basins, where the doses are lower (see Chapter 4).

Time series of the mean values of the annual doses to the most exposed group resulting from radionuclide releases to the landscape from the different repository parts are presented in Figures 5-1 to 5-5. Both the total dose from all radionuclides and the doses from the radionuclides with the highest contribution are presented in these figures.

The peak of the mean annual doses from all repository parts is observed around year 5,000. This is due to an increased release rate of C-14 as result of the stepwise increase in groundwater flow that is caused by shoreline displacement /Thomson et al. 2008/. The maximum dose is associated with the lake, which receives the releases from the geosphere at the time of the peak dose. The doses from releases of C-14 to the lake are dominated by fish ingestion pathway /Avila and Pröhl 2008/, being the contribution of water intake negligible. Thereafter, the doses from C-14 decrease, as the release rates to the biosphere decrease and the lake is successively transformed into mire. Note that C-14 releases to terrestrial objects (forest and agricultural lands) generally result in lower doses than releases to lakes of the same size /Avila and Pröhl 2008/.

Table 5-1. Results of the screening study for the Weichselian variant for the case of releases to the landscape. The peak values of the Screening Quotients (SQs) and the time (in years AD) at which the peak SQs are observed are presented for each repository part. Values are given only for radionuclides for which SQs above 1 were obtained.

Radionuclide		Silo	BMA	BLA	1BTF	2BTF
C-14-in	Peak SQ		2		10	70
	Time		6,640		5,090	5,060
C-14-org	Peak SQ	85	67			6
	Time	5,540	5,060			5,039
Ni-59	Peak SQ		12		2	4
	Time		17,040		7,240	7,240
Se-79	Peak SQ		4			
	Time		7,240			
Mo-93	Peak SQ		3			
	Time		7,240			
I-129	Peak SQ	4	9			
	Time	14,540	7,240			
Cs-135	Peak SQ	6	197		4	28
	Time	43,540	7,240		7,240	7,240

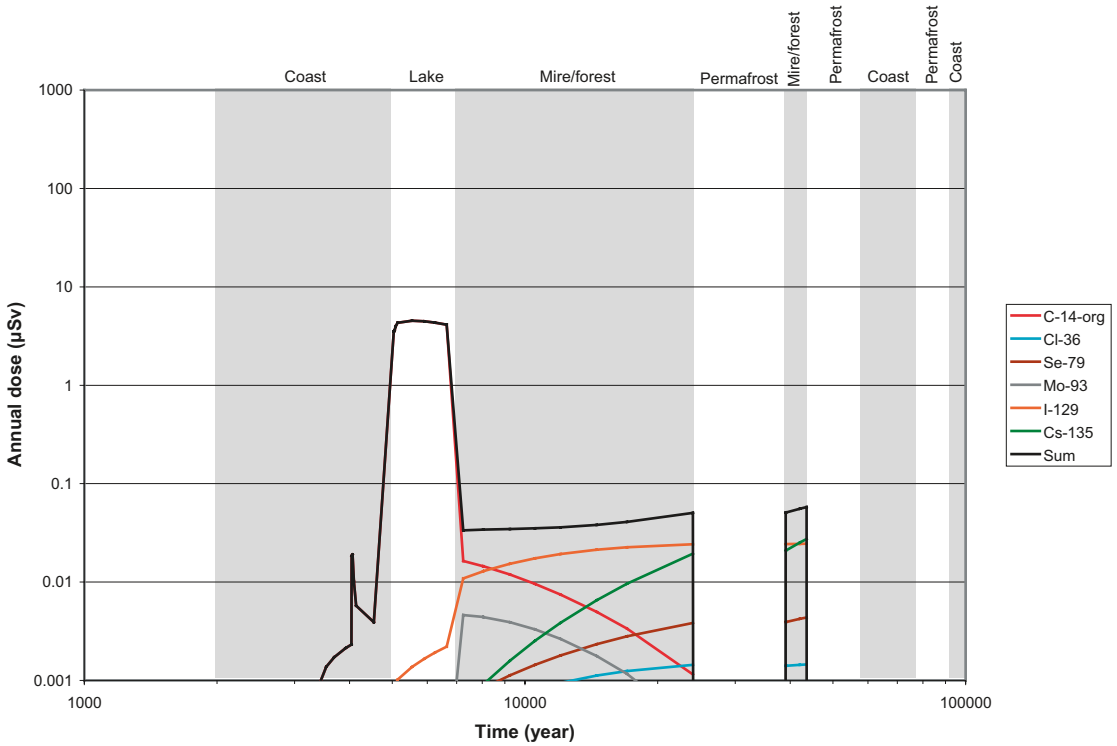

Figure 5-1. *Mean values of the annual individual dose from radionuclide releases to the landscape from the Silo for the Weichselian variant (CC1). The sum corresponds to the total dose considering all released radionuclides.*

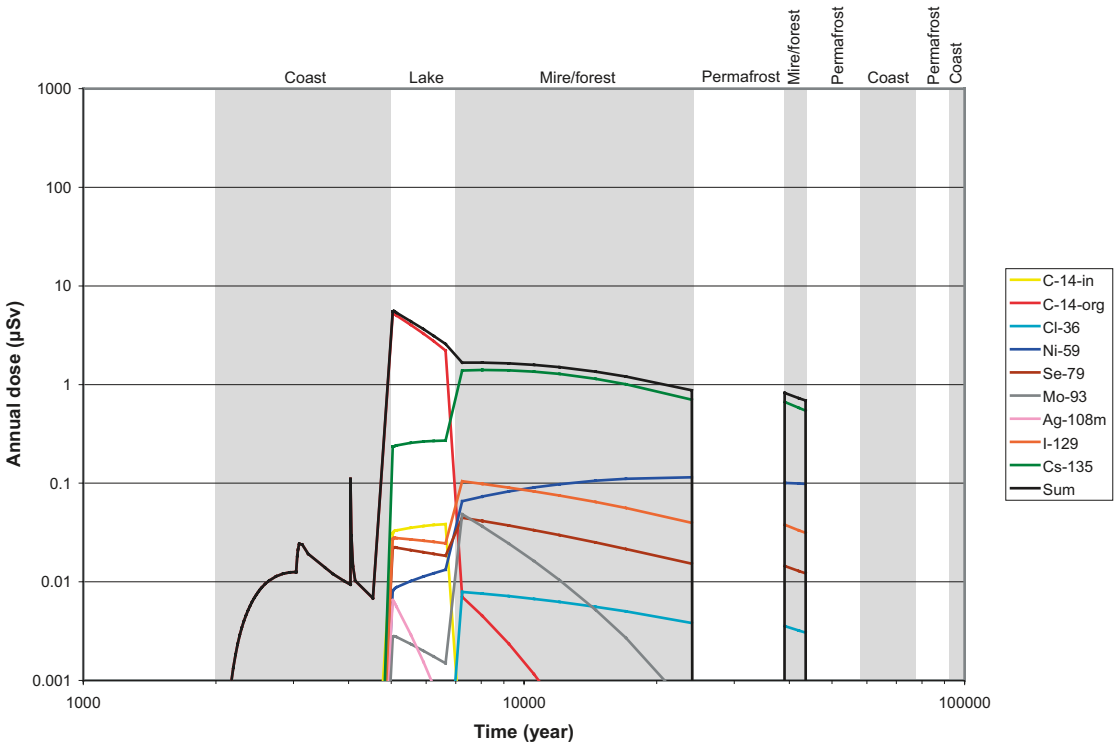

Figure 5-2. *Mean values of the annual individual dose from radionuclide releases to the landscape from the BMA for the Weichselian variant (CC1). The sum corresponds to the total dose considering all released radionuclides.*

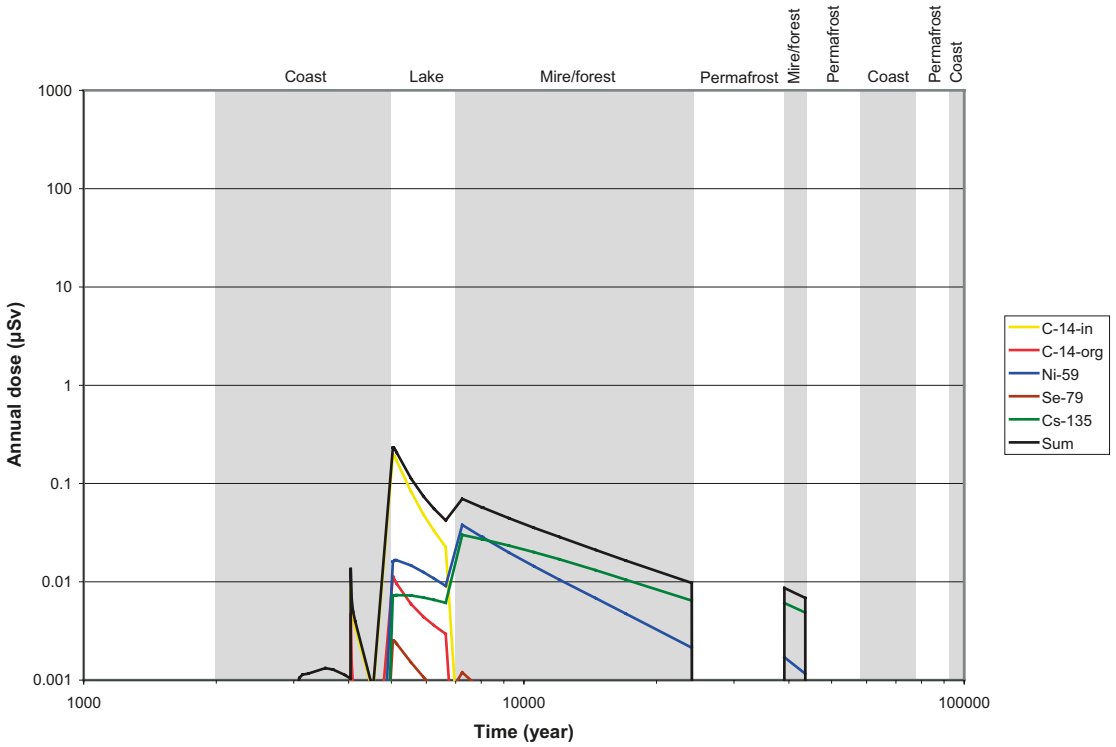

Figure 5-3. *Mean values of the annual individual dose from radionuclide releases to the landscape from the 1BTF for the Weichselian variant (CC1). The sum corresponds to the total dose considering all released radionuclides.*

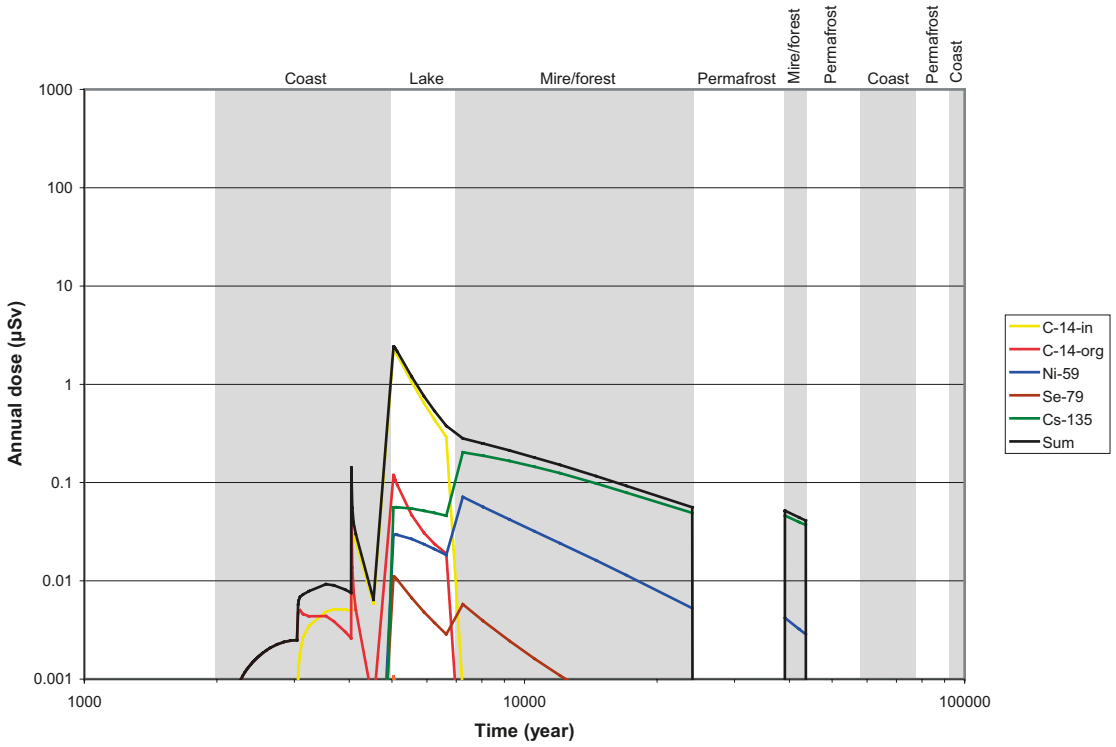

Figure 5-4. *Mean values of the annual individual dose from radionuclide releases to the landscape from the 2BTF for the Weichselian variant (CC1). The sum corresponds to the total dose considering all released radionuclides.*

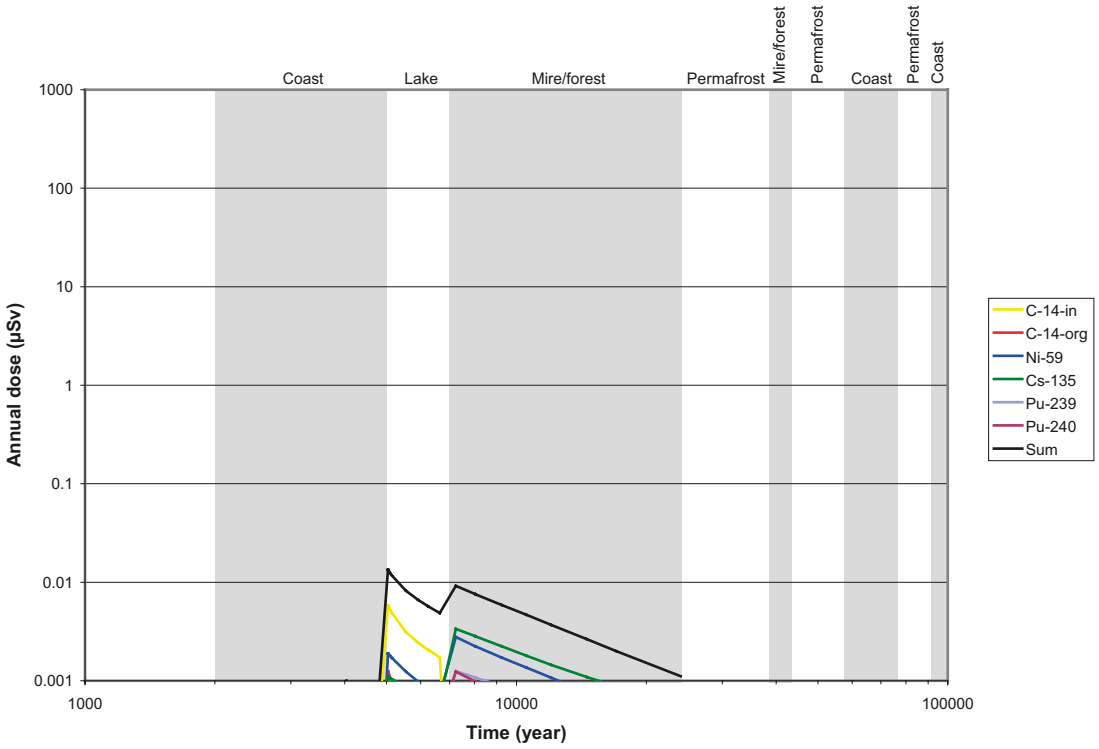

Figure 5-5. *Mean values of the annual individual dose from radionuclide releases to the landscape from the BLA for the Weichselian variant (CC1). The sum corresponds to the total dose considering all released radionuclides.*

Starting from year 7,000, a few other radionuclides, Ni-59, I-129 and Cs-135, have a higher contribution to mean annual doses than C-14. However, during this period the total doses from all repository parts, except for the BMA, are one order of magnitude or more below the peak values at year 5,000. In the case of the BMA, dose values of the same order of magnitude as the peak doses are observed after year 7,000. These relatively higher values are due to exposures to Cs-135 which is accumulated in the mire formed from the lake. When assessing the exposure to contamination in mires two cases were considered: i) the mire is used for agricultural purposes and ii) the mire develops into a forest. The highest dose value was obtained for the case of a forest growing in the contaminated mire, due to higher aggregated transfer factors for the forest than for the agricultural land (see Chapter 4).

After year 7,000 the time dynamics of the mean annual doses resembles the time dynamics of the release rates to the biosphere (see /Thomson et al. 2008/). This should be expected as during this period the mire is the receiving object of the landscape most of the time. During this period, the annual doses due to releases from the BMA, BLA, 1BTF and 2BTF show a similar time dependency characterised by two peak values followed by a decrease. For the Silo a slower and more monotonic increase of the doses is observed. The releases to the biosphere of Ni-59, I-129 and Cs-135 from the BMA, BLA, 1BTF and 2BTF start earlier (at year 6,000) than the releases from the Silo as these vaults lack bentonite barriers which prevent water inflow. At year 6,000, the receptor of the releases is a lake, which is then converted into mire where the doses per unit release rate are higher for these radionuclides. This explains the second dose peak obtained for the vaults. The receptor of the releases of these radionuclides from the Silo is always the mire, and therefore a monotonic increase is obtained, which follows the dynamics of the release rates.

Figure 5-6 presents the total mean annual doses from the whole repository, and for each repository part, taking into account all released radionuclides. The Silo and the BMA have the highest contribution to the peak doses due to their larger inventory of C-14. The BLA gives the lowest contribution during the whole simulation period due to lower radionuclide inventory and because releases from this repository part occur early in the sea period, when the dilution is higher, which leads to lower doses per unit release rate.

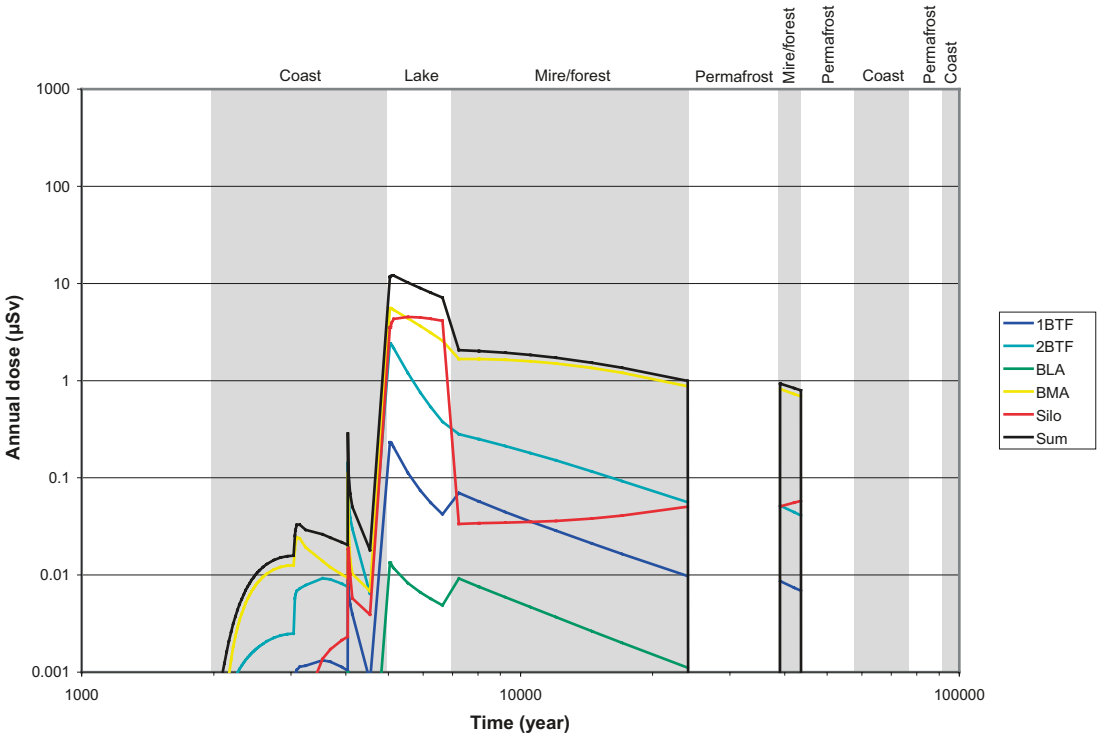

Figure 5-6. *Mean values of the total annual individual dose from radionuclide releases to the landscape from each repository part and from the whole repository (Sum) for the Weichselian variant (CC1).*

Figure 5-7 presents the total mean annual doses from each radionuclide taking into account all repository parts. During the period from year 5,000 to 7,000 the doses are dominated by C-14 in organic form and to a lesser extent by C-14 in inorganic form. As explained above, the doses during this period are associated to exposures from the lake that receives direct releases, which as shown in Chapter 4 has the highest dose rate per unit release rate of C-14 among all ecosystem objects in the landscape. After year 7,000 the total annual doses are dominated by Cs-135 and the next most contributing radionuclides are Ni-59 and I-129. In this case, the doses are associated with exposure from a forest growing in the object that receives the releases, i.e. the mire that is formed from the lake. Assuming that the mire is used for agricultural purposes would have resulted in lower doses (see Chapter 4).

A summary of peak values of the mean annual doses for each repository part and the whole repository is presented in Table 5-2.

Table 5-2. Peak values of the mean annual doses and time at which the peak value is observed for releases to the landscape from each repository part and from the whole repository in the Weichselian variant (CC1). The value given for each repository part is the sum of values obtained for all released radionuclides. The radionuclides with the highest contribution to the peak doses are indicated.

Repository part	Peak annual mean dose µSv/year	Time of the peak years AD	Most contributing radionuclide
Silo	4.5	around 5,000	Organic C-14
BMA	5.6	around 5,000	Organic C-14
1BTF	0.2	around 5,000	Inorganic C-14
2BTF	2.4	around 5,000	Inorganic C-14
BLA	0.01	around 5,000	Inorganic C-14
Total SFR 1	12	around 5,000	Organic C-14

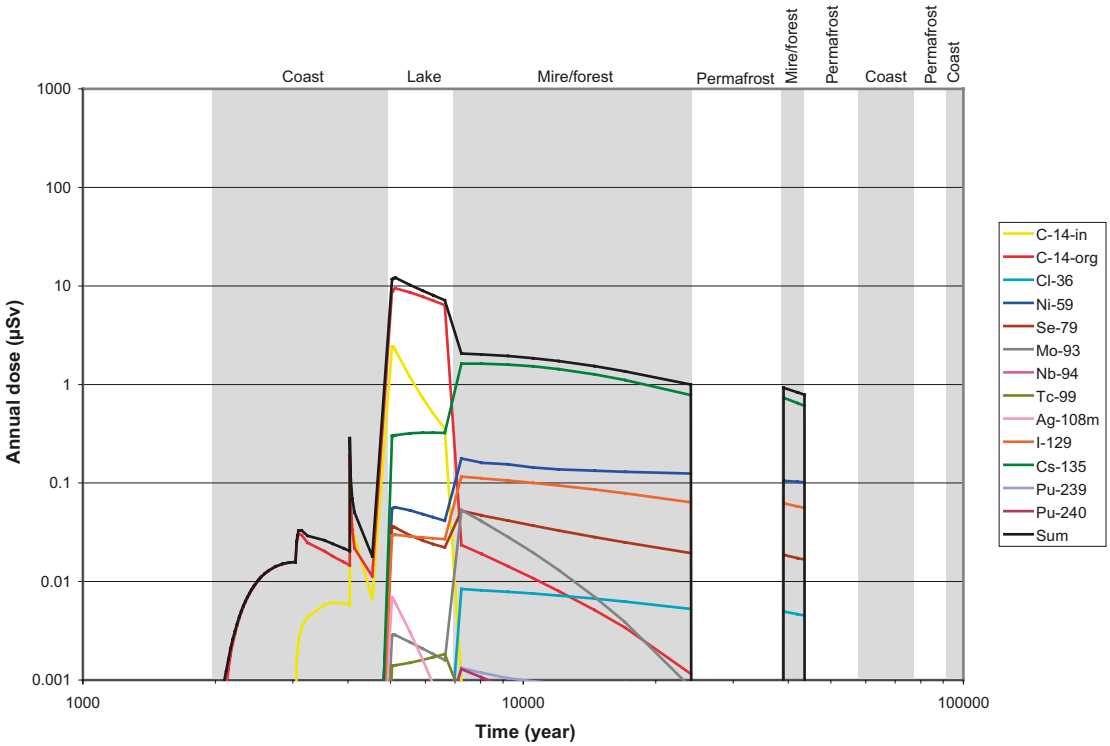

Figure 5-7. *Mean values of the total annual individual dose from radionuclide releases to the landscape from all repository parts for the Weichselian variant (CC1). The sum corresponds to the total dose considering all released radionuclides.*

5.1.2 Doses from releases to a well

The results of the screening study for the doses resulting from releases to a well are presented in Table 5-3. It can be assumed that a larger number of radionuclides are potential important contributors to the doses, as compared to the case with releases to the landscape. At the same time, for most of these radionuclides the maximum values of the SQ were observed around 4,000, when the releases to the landscape are directed to the sea basin, which results in low doses, as compared to releases to the lake or the mire at a later stage. From the results it appears that C-14, Mo-93 and I-129 have the highest contribution to the doses.

Times series of the mean annual doses from releases to a well are presented in Figures 5-8 to 5-12. For all repository parts a peak value of the doses is observed around year 4,000. This is followed by a decreasing trend of the sum of doses across all radionuclides, although an increasing trend is observed for some radionuclides, like Se-79 and I-129 for the Silo and Ni-59 for the BMA. A summary of the peak values for the well doses and the most contributing radionuclides is presented in Table 5-4. The relatively high contribution of Pu-240 for the BLA is explained by the lower radionuclide inventory and lack of sorption barriers in this repository part. Most part of the inventory of potentially dose contributing radionuclides has been released from BLA before a well can be drilled in this area.

Table 5-3. Results of the screening study for the Weichselian variant (CC1) with releases to a well. The peak value of the Screening Quotient (SQ) and the time (in years AD) at which the peak SQ is observed are presented for each repository part. Values are given only for radionuclides for which SQ above 1 were obtained.

Radionuclide		Silo	BMA	BLA	1BTF	2BTF
C-14-in	Peak SQ		1	10	84	628
	Time		4,041	4,041	4,041	4,041
C-14-org	Peak SQ	100	943	4	43	411
	Time	4,041	4,041	4,041	4,041	4,041
Cl-36	Peak SQ				8	28
	Time				4,041	4,041
Ni-59	Peak SQ		22	15	20	34
	Time		17,040	4,060	4,540	4,540
Se-79	Peak SQ		19		5	23
	Time		4,041		4,041	4,041
Mo-93	Peak SQ	9	765	19	92	222
	Time	4,060	4,041	4,041	4,041	4,041
Tc-99	Peak SQ			6.1	5	4
	Time			4,140	10,540	12,040
Ag-108m	Peak SQ		52			3
	Time		4,090			4,140
I-129	Peak SQ	10	580	9	216	1,549
	Time	14,540	4,041	4,041	4,041	4,041
Cs-135	Peak SQ					
	Time					
Pu-239	Peak SQ			22	3	4
	Time			4,140	24,040	24,040
Pu-240	Peak SQ			36	1	2
	Time			4,540	17,040	17,040

Table 5-4. Peak values of the 50-years moving average of the mean annual dose and time at which the peak value is observed for releases to a well from each repository part and summed over the vaults in the Weichselian variant. The value given for each repository part is the sum of values obtained for all released radionuclides. The radionuclides with the highest contribution to the peak doses are indicated.

Repository part	Peak annual mean dose µSv/year	Time of the peak years AD	Most contributing radionuclide
Silo	0.9	around 5,000	Organic C-14
BMA	5.7	around 4,000	Organic C-14
1BTF	1.4	around 4,000	I-129
2BTF	8.0	around 4,000	I-129
BLA	0.5	around 4,000	Pu-240
Total SFR 1	16	around 4,000	I-129

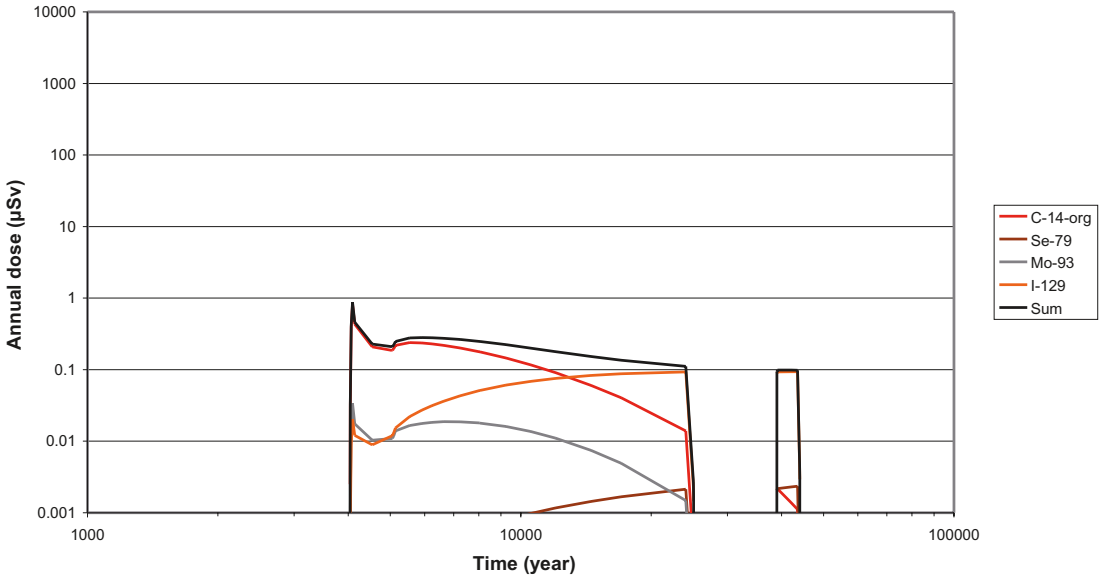

Figure 5-8. *Moving average (50 years) of the mean annual doses from radionuclide releases to a well from the Silo for the Weichselian variant (CC1). The sum corresponds to the total dose considering all released radionuclides.*

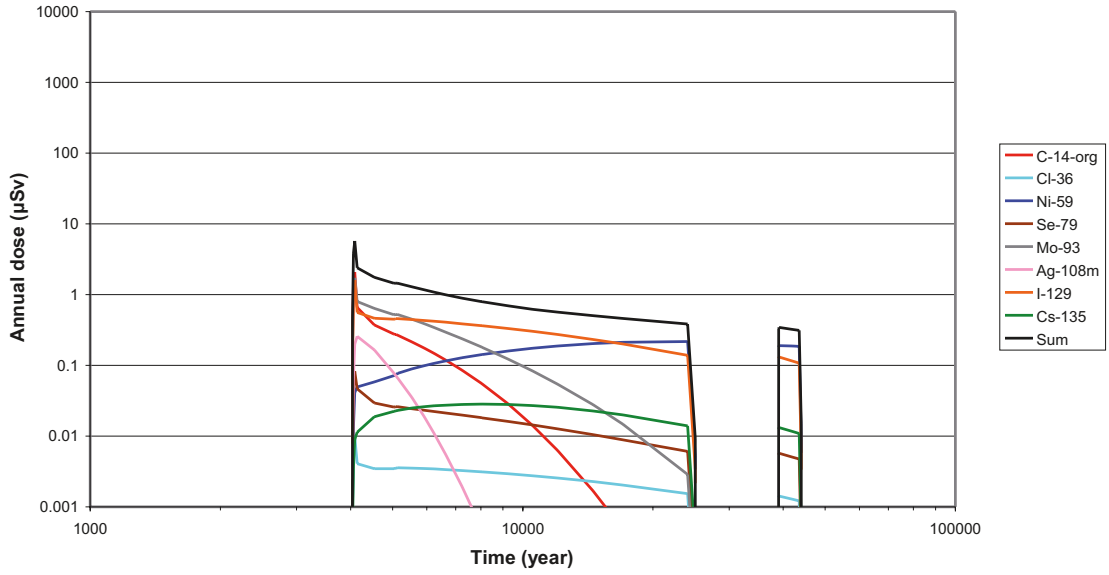

Figure 5-9. *Moving average (50 years) of the mean annual doses from radionuclide releases to a well from the BMA for the Weichselian variant (CC1). The sum corresponds to the total dose considering all released radionuclides.*

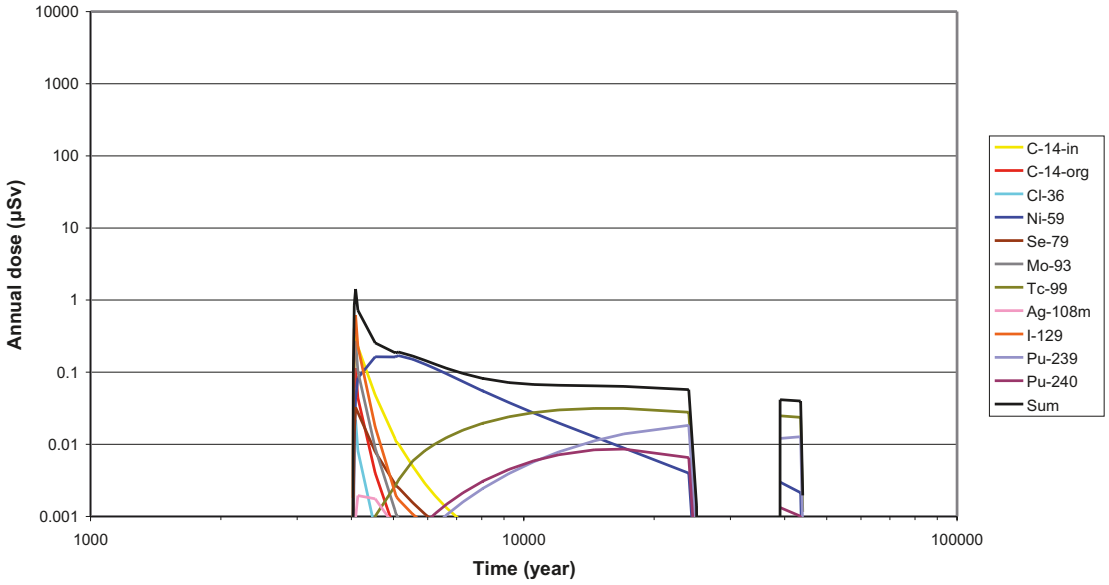

Figure 5-10. *Moving average (50 years) of the mean annual doses from radionuclide releases to a well from the 1BTF for the Weichselian variant (CC1). The sum corresponds to the total dose considering all released radionuclides.*

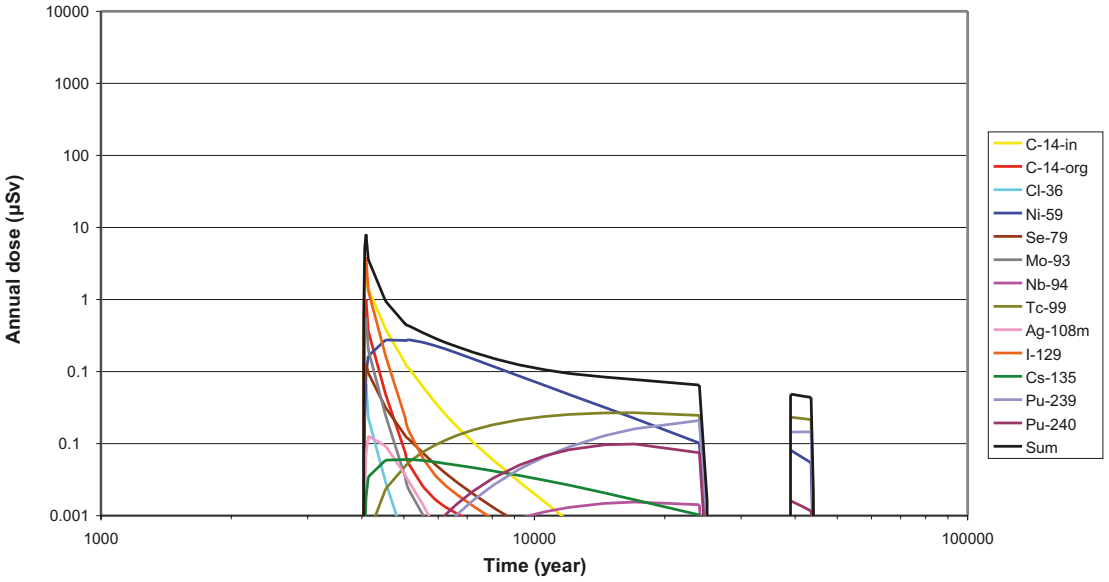

Figure 5-11. *Moving average (50 years) of the mean annual doses from radionuclide releases to a well from the 2BTF for the Weichselian variant (CC1). The sum corresponds to the total dose considering all released radionuclides.*

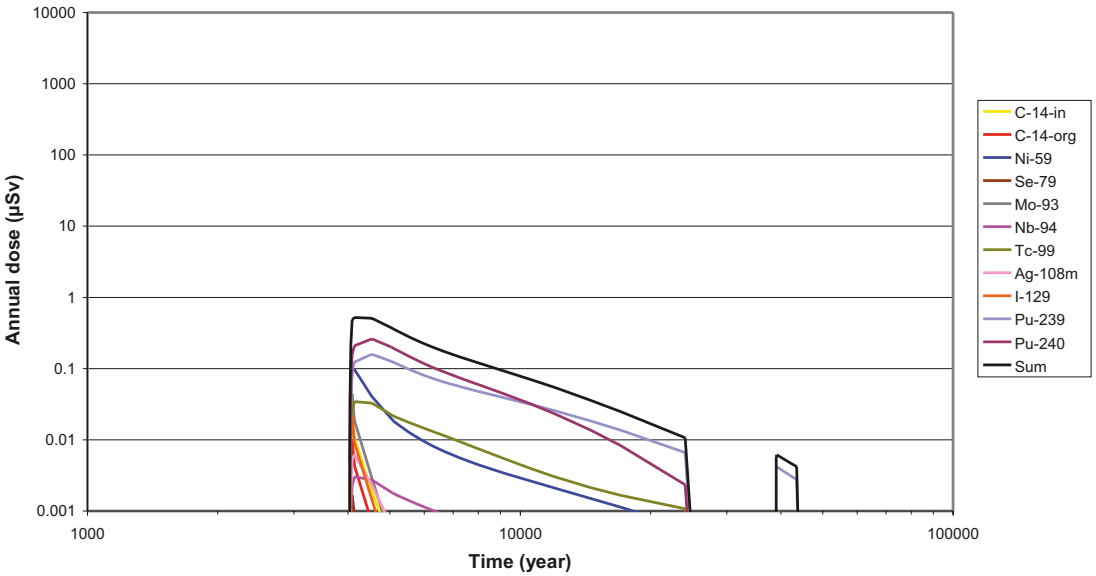

Figure 5-12. *Moving average (50 years) of the mean annual doses from radionuclide releases to a well from the BLA for the Weichselian variant (CC1). The sum corresponds to the total dose considering all released radionuclides.*

5.2 Greenhouse variant

This calculation case adopts the Greenhouse variant climate evolution, where the anticipated climate evolution is a significant period of temperate conditions at the site until approximately year 75,000 and thereafter a period of continuous permafrost. Most other features of the calculation case follow those for the Weichselian variant. However, the following differences exist /Thomson et al. 2008/:

- Degradation of the BMA is assumed to take place at 73,000 years post-closure (i.e. at year 75,000), the Silo remains intact through the assessment timescale.
- The tunnel plugs are assumed to remain intact throughout the assessment timescale.
- The geosphere changes from saline to non-saline at 1,000 years post-closure as in the Weichselian variant and remains non-saline from here on.

5.2.1 Doses from releases to the landscape

The results of the screening study for this calculation case were practically identical with the results obtained for the Weichselian variant presented in Table 5-1 (Section 5.1). Time series of the mean annual doses are shown in Figures 5-13 to 5-17. Until year 25,000, the release rates and biosphere conditions in this calculation case are the same as in the Weichselian variant. This explains why the time dependencies of the doses until 25,000 are identical for these two calculation cases. The main difference between these two calculation cases is in the duration of exposure conditions, as in the calculation case Weichselian variant it is assumed that there is no exposure during permafrost periods.

A summary of the annual doses obtained from the different repository parts is presented in Figure 5-18 and Table 5-4. The total doses from the different repository parts have practically the same values as for the Weichselian variant.

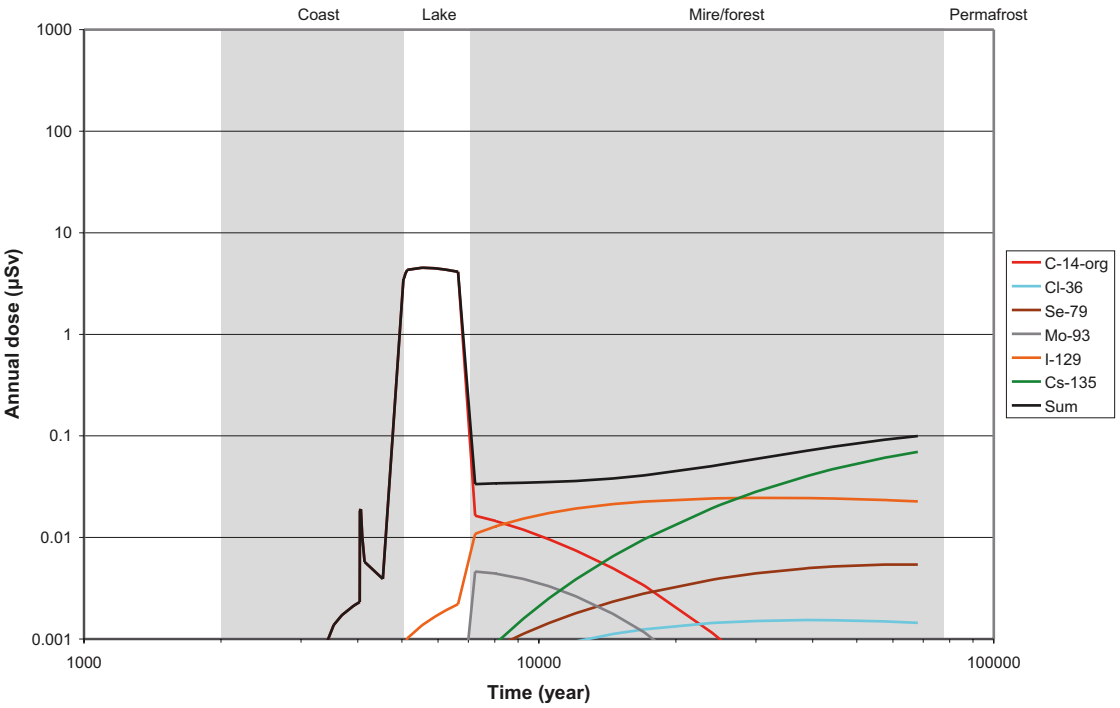

Figure 5-13. *Mean values of the annual individual dose from radionuclide releases to the landscape from the Silo for the Greenhouse variant (CC6). The sum corresponds to the total dose considering all released radionuclides.*

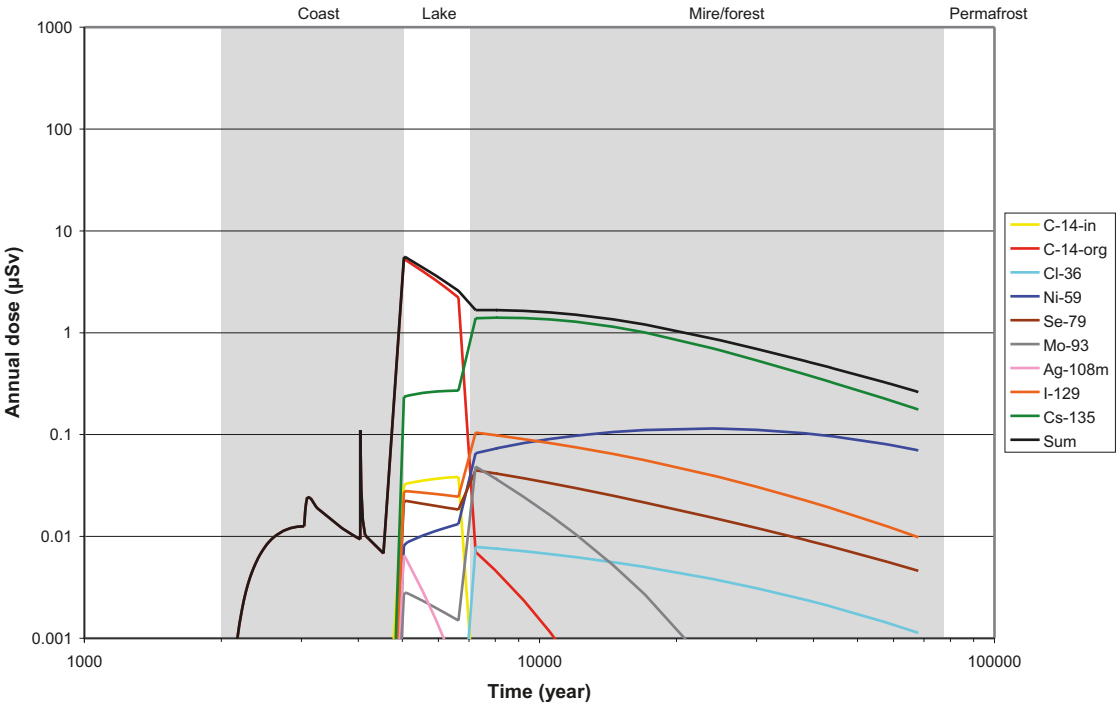

Figure 5-14. *Mean values of the annual individual dose from radionuclide releases to the landscape from the BMA for the Greenhouse variant (CC6). The sum corresponds to the total dose considering all released radionuclides.*

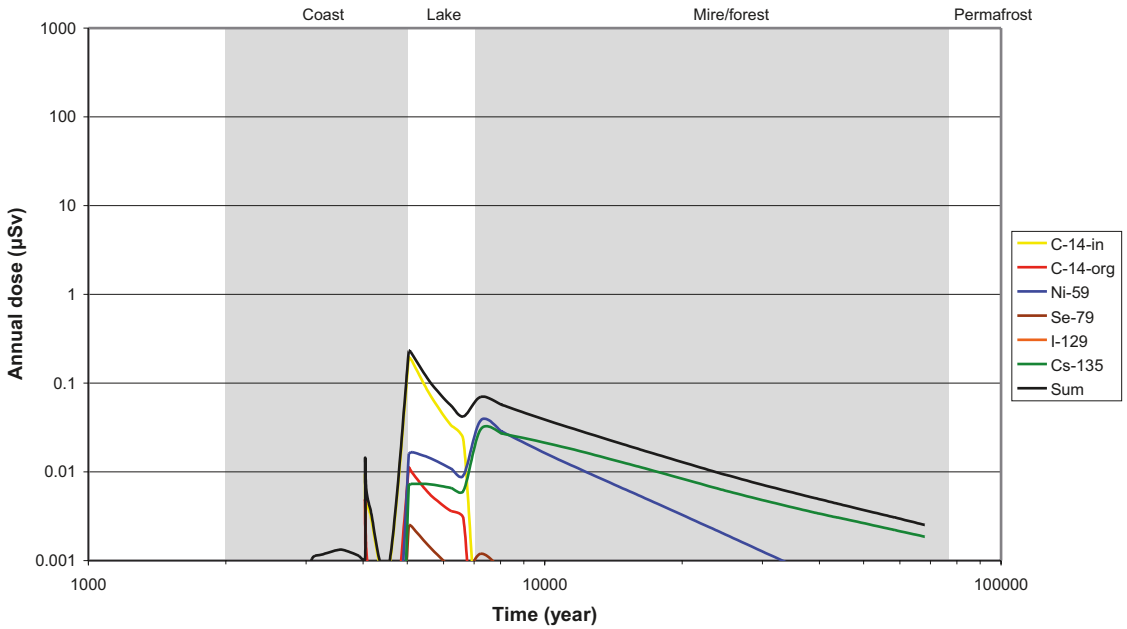

Figure 5-15. *Mean values of the annual individual dose from radionuclide releases to the landscape from the 1BTF for the Greenhouse variant (CC6). The sum corresponds to the total dose considering all released radionuclides.*

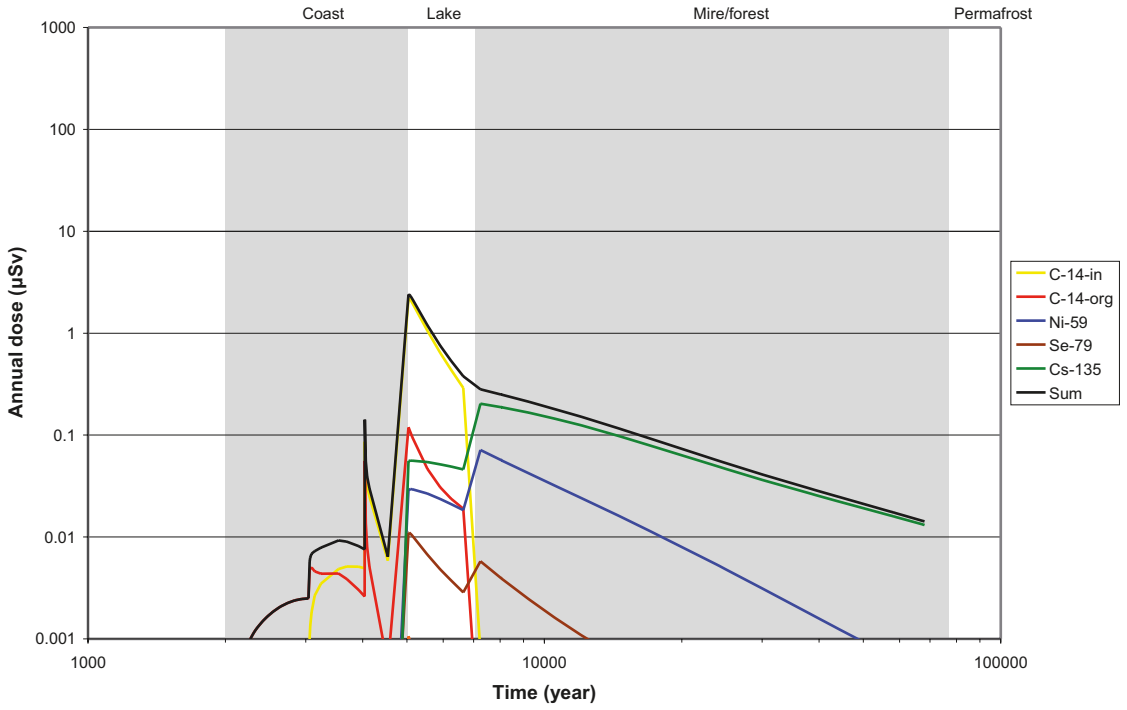

Figure 5-16. *Mean values of the annual individual dose from radionuclide releases to the landscape from the 2BTF for the Greenhouse variant (CC6). The sum corresponds to the total dose considering all released radionuclides.*

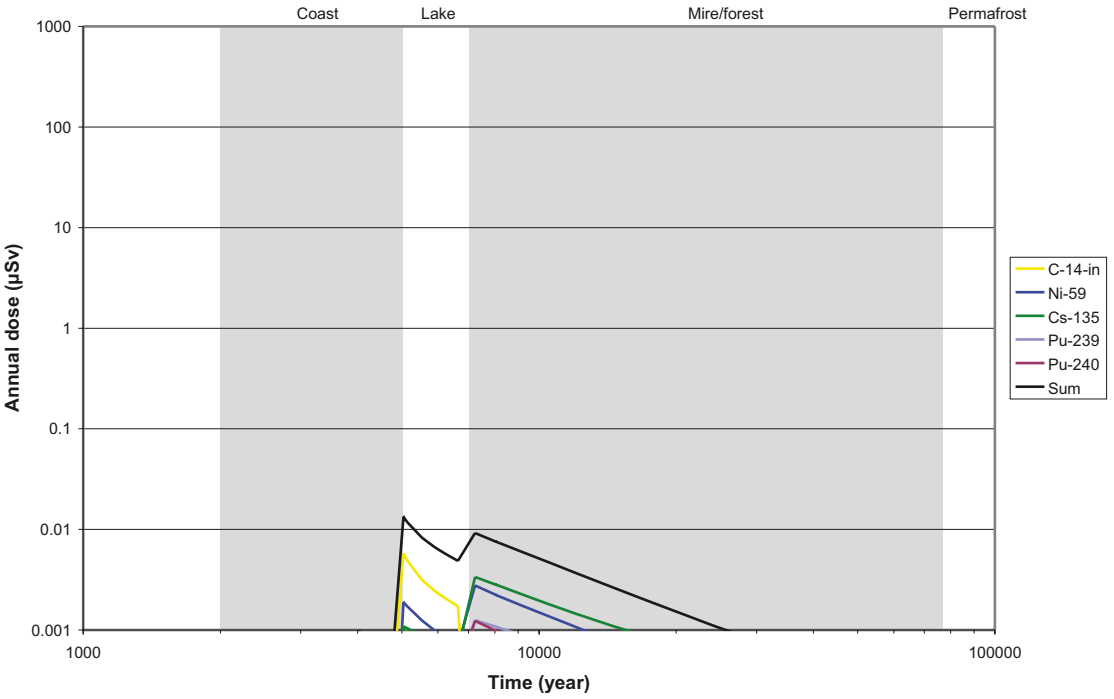

Figure 5-17. *Mean values of the annual individual dose from radionuclide releases to the landscape from the BLA for the Greenhouse variant (CC6). The sum corresponds to the total dose considering all released radionuclides.*

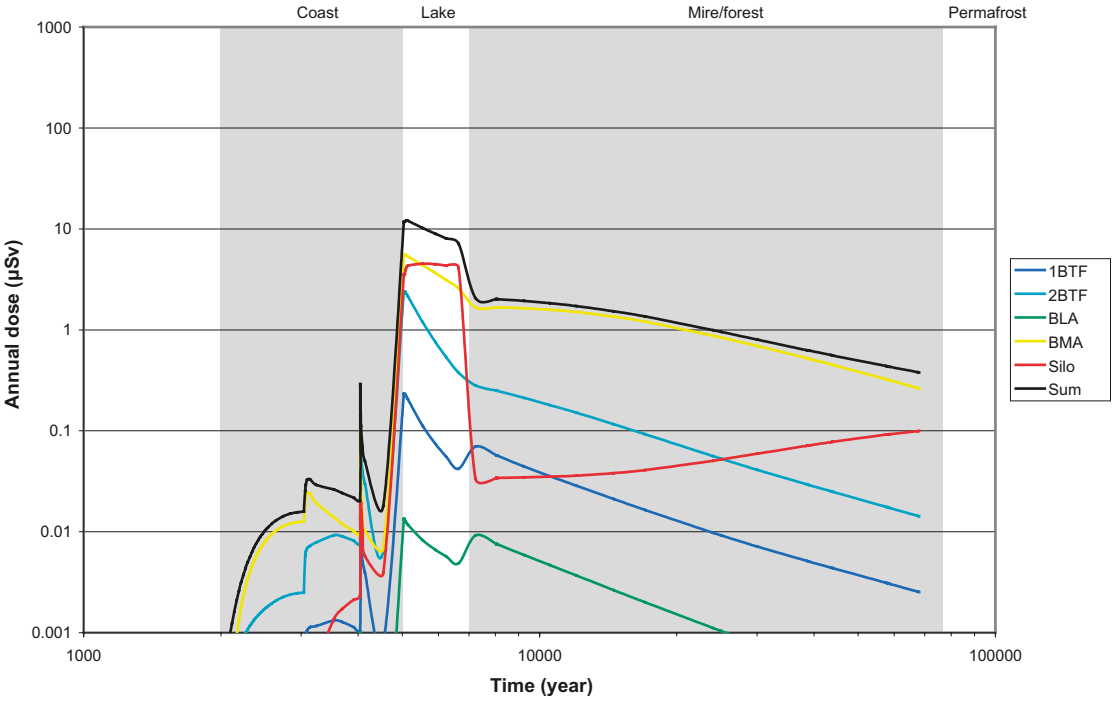

Figure 5-18. *Mean values of the total annual individual dose from radionuclide releases to the landscape from each repository part and from the whole repository (Sum) for the Greenhouse variant (CC6).*

Table 5-4. Peak values of the mean annual doses and time at which the peak value is observed for releases to the landscape from each repository part and from the whole repository in the Greenhouse variant. The value given for each repository part is the sum of values obtained for all released radionuclides. The radionuclides with the highest contribution to the peak doses are indicated.

Repository part	Peak annual dose µSv/year	Time of the peak years AD	Most contributing radionuclide
Silo	4.5	around 5,000	Organic C-14
BMA	5.6	around 5,000	Organic C-14
1BTF	0.2	around 5,000	Inorganic C-14
2BTF	2.4	around 5,000	Inorganic C-14
BLA	0.01	around 5,000	Inorganic C-14
Total SFR 1	12	around 5,000	Organic C-14

5.2.2 Doses from releases to a well

The results of the screening study for the releases to the well were practically the same as those obtained for the calculation case Weichselian variant. The predicted time series of the mean annual doses for this calculation case are presented in Figures 5-19 to 5-23. The peak values of the doses in the two calculation cases of the main scenario were exactly the same.

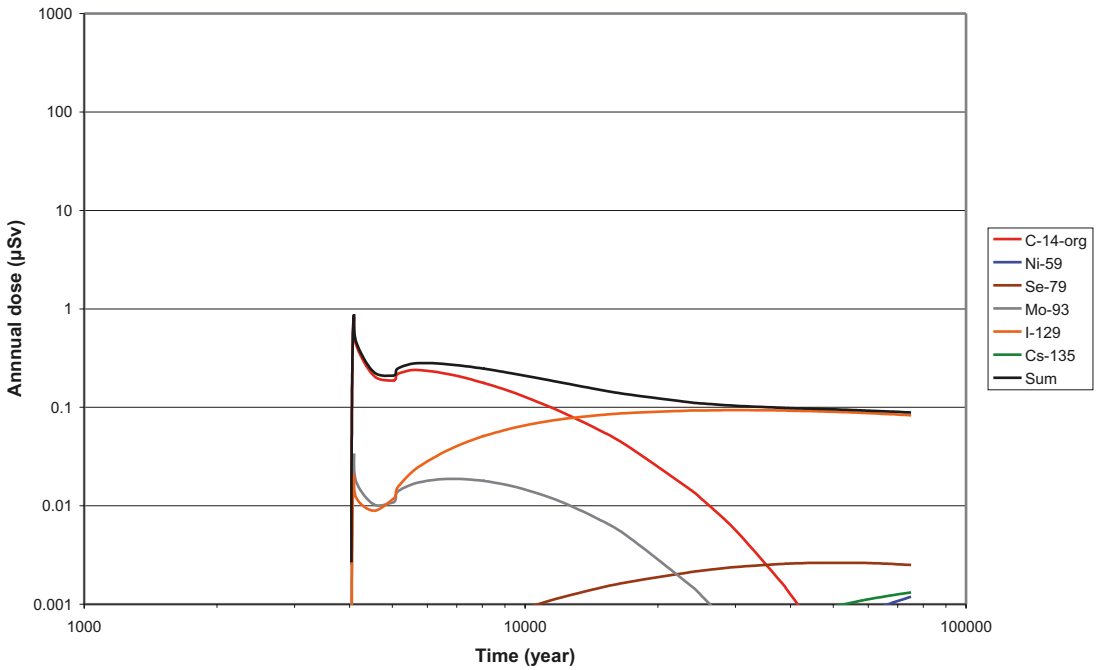

Figure 5-19. *Moving average (50 years) of the mean annual doses from radionuclide releases to a well from the Silo for the Greenhouse variant (CC6). The sum corresponds to the total dose considering all released radionuclides.*

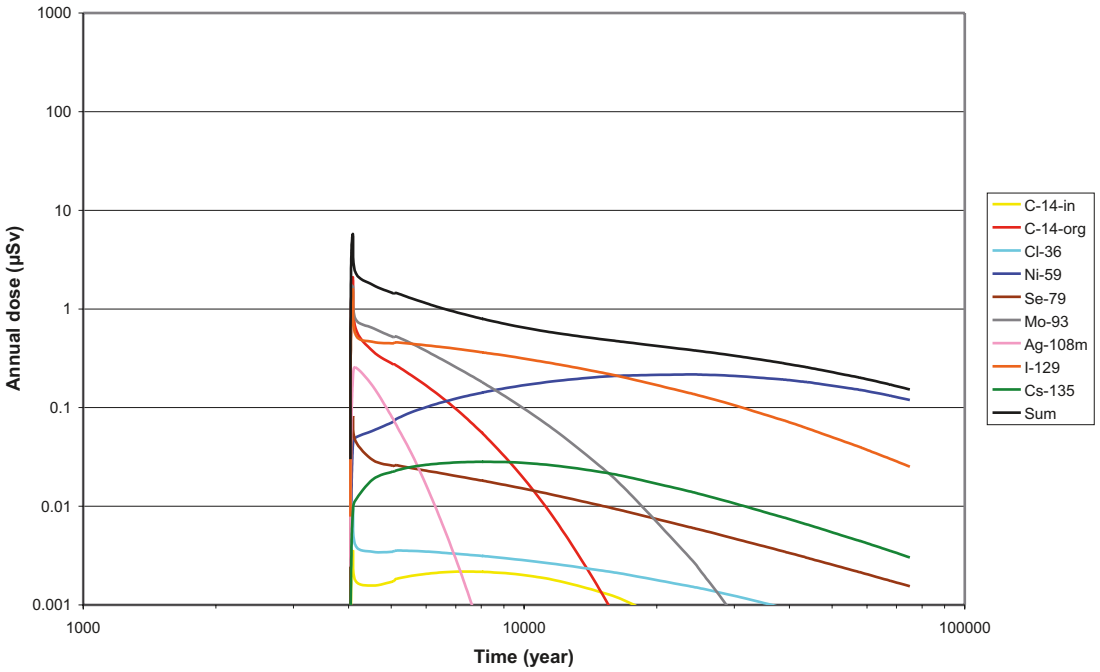

Figure 5-20. *Moving average (50 years) of the mean annual doses from radionuclide releases to a well from the BMA for the Greenhouse variant (CC6). The sum corresponds to the total dose considering all released radionuclides.*

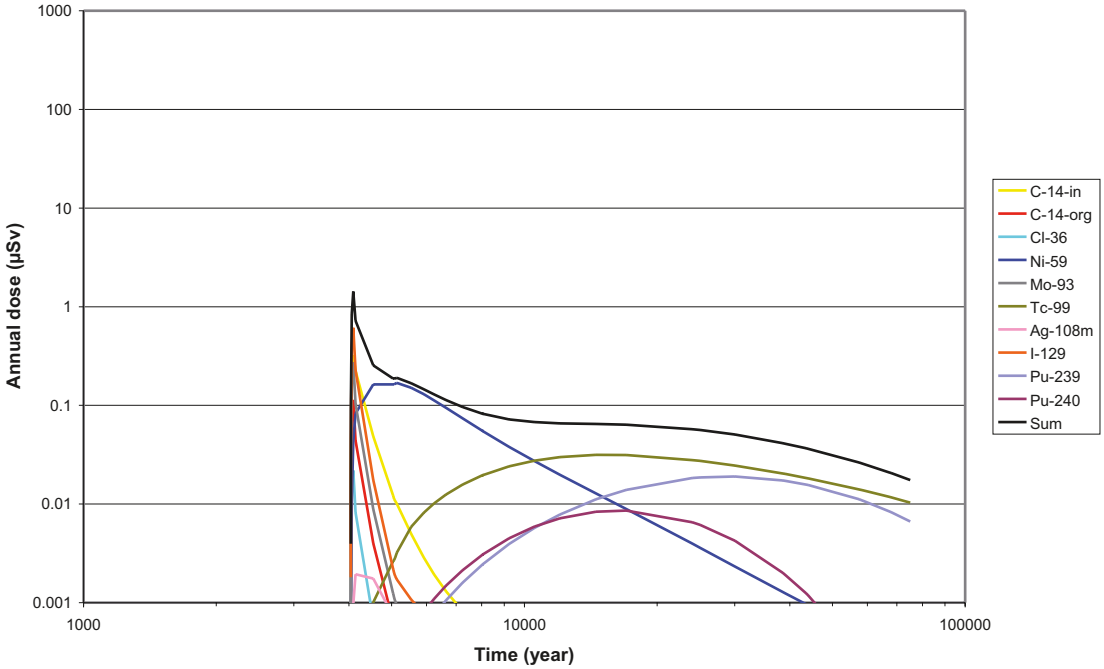

Figure 5-21. *Moving average (50 years) of the mean annual doses from radionuclide releases to a well from the 1BTF for the Greenhouse variant (CC6). The sum corresponds to the total dose considering all released radionuclides.*

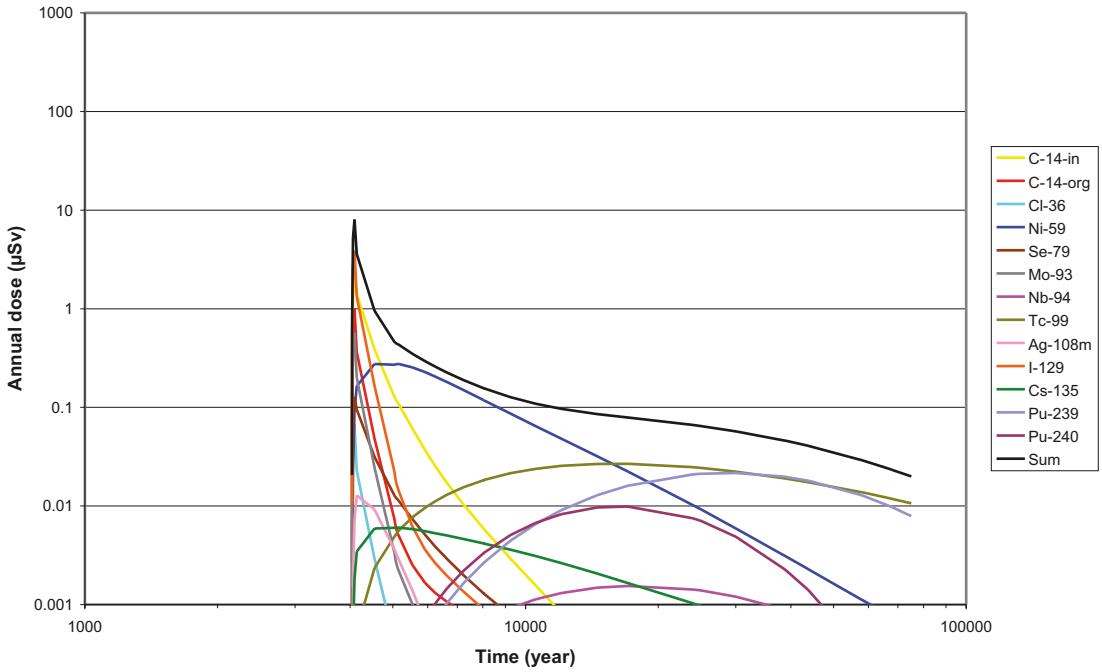

Figure 5-22. *Moving average (50 years) of the mean annual doses from radionuclide releases to a well from the 2BTF for the Greenhouse variant (CC6). The sum corresponds to the total dose considering all released radionuclides.*

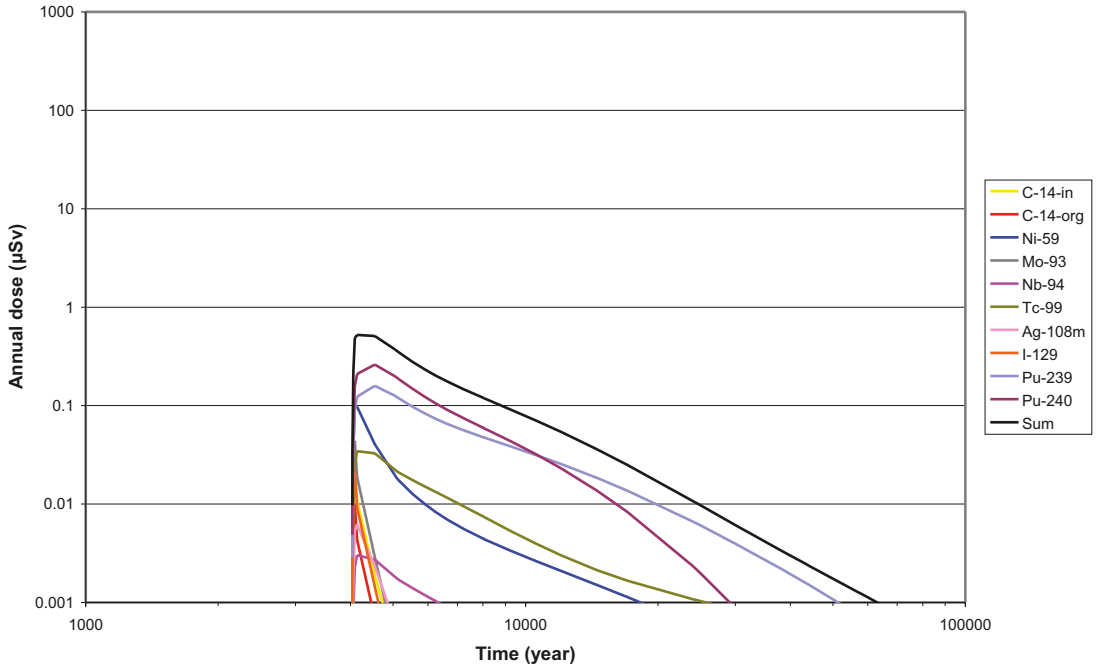

Figure 5-23. *Moving average (50 years) of the mean annual doses from radionuclide releases to a well from the BLA for the Greenhouse variant (CC6). The sum corresponds to the total dose considering all released radionuclides.*

6 Results for calculation cases representing less probable scenarios

This chapter presents the results for calculation cases representing less probable scenarios:

- A calculation case which considers the effect of earthquakes.
- Calculation cases that consider uncertainty in the behaviour of the concrete barriers in BMA during periods of continuous permafrost (CC4 and CC5).
- Calculation cases that consider a more extensive development of permafrost (CC7 and CC8).
- A calculation case that considers formation of taliks (CC2).
- A calculation case that considers the potential consequences for radionuclide releases from the repository under conditions with high levels of complexing agents in the near-field (CC9).
- A calculation case that considers the potential consequences for radionuclide release from the Silo when taking into account bulk gas generation (CC10).
- Calculation cases that consider the consequences from a water well drilled directly into the vaults or the Silo (CC11).

A more detailed description of the calculation cases is given in Table 2-5.

For each calculation case the results of the screening study are presented and figures are provided showing time series of radionuclide specific and total mean annual doses to the most exposed group. Releases from each repository part and from the whole SFR 1 to the landscape and to a well are considered.

As for the calculation cases of the main scenario, for the dose calculations it was assumed that during permafrost periods without taliks, there is no groundwater migration and consequently there is no radionuclide release to the biosphere /Thomson et al. 2008/. The doses from releases to a well shown in the figures are, in most cases, 50-years moving averages of the simulated mean values of the annual doses, whereas in the case of releases to the landscape the simulated mean values are plotted without taking a moving average. Hence, in the case of releases to the landscape the presented doses may overestimate the average life time doses, especially in periods with pronounced short time variations in the annual doses.

The doses from the well are shown starting from year 4,000 as described in Section 4.2.

6.1 Earthquake

Values of calculated inventories in the Silo and the BMA as a function of time are presented in Figures 6-1 and 6-2, respectively. These values have been derived from the initial radionuclide inventories taking into account decay/ingrowth of radionuclides and their inventory reduction as result of projected releases in the Weichselian variant (see Section 5.1). These calculated inventories were used to obtain release rates in case of an earthquake, by dividing with the release duration (see Section 4.3).

Calculated maximum values of the total annual doses that may be received by the most exposed individual, had an earthquake occurred at a given time point, are presented in Figure 6-3 for the Silo and Figure 6-4 for the BMA. Peak values of the maximal annual doses are given in Table F-1 in Appendix F for the Silo and Table F-2 in Appendix F for the BMA. The peak doses are obtained around year 5,000 in connection with releases to the lake that will be formed in the area above the repository.

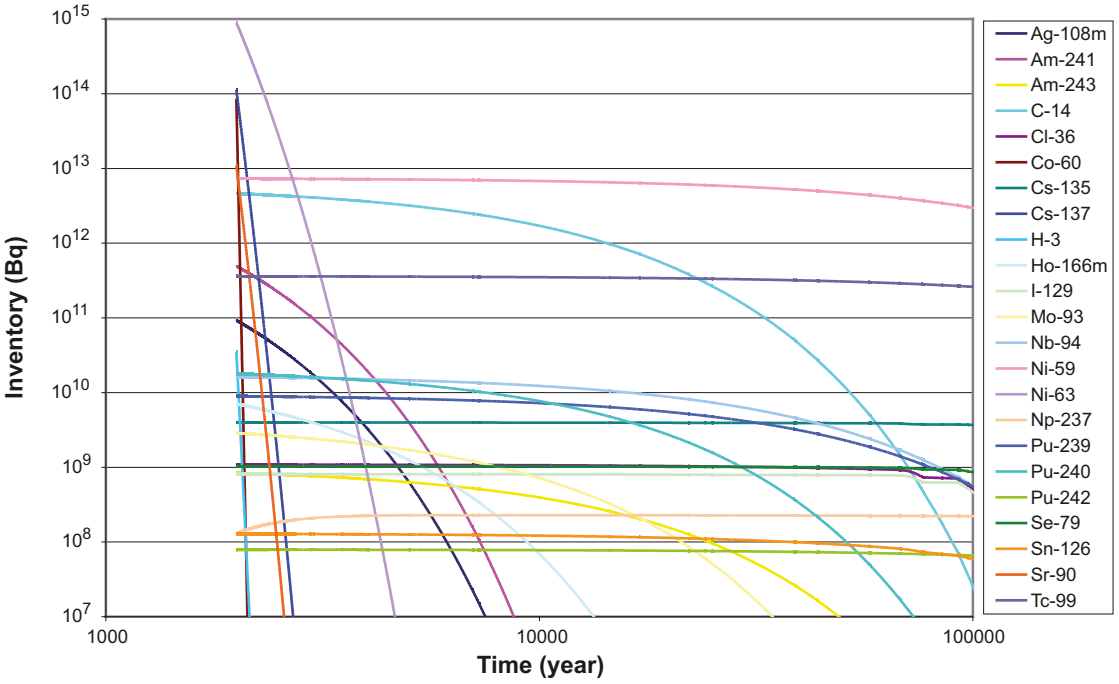

Figure 6-1. *Inventory (Bq) of radionuclides in the Silo as a function of time taking into account reductions due to releases predicted for the Weichselian variant and the radioactive decay/ingrowth.*

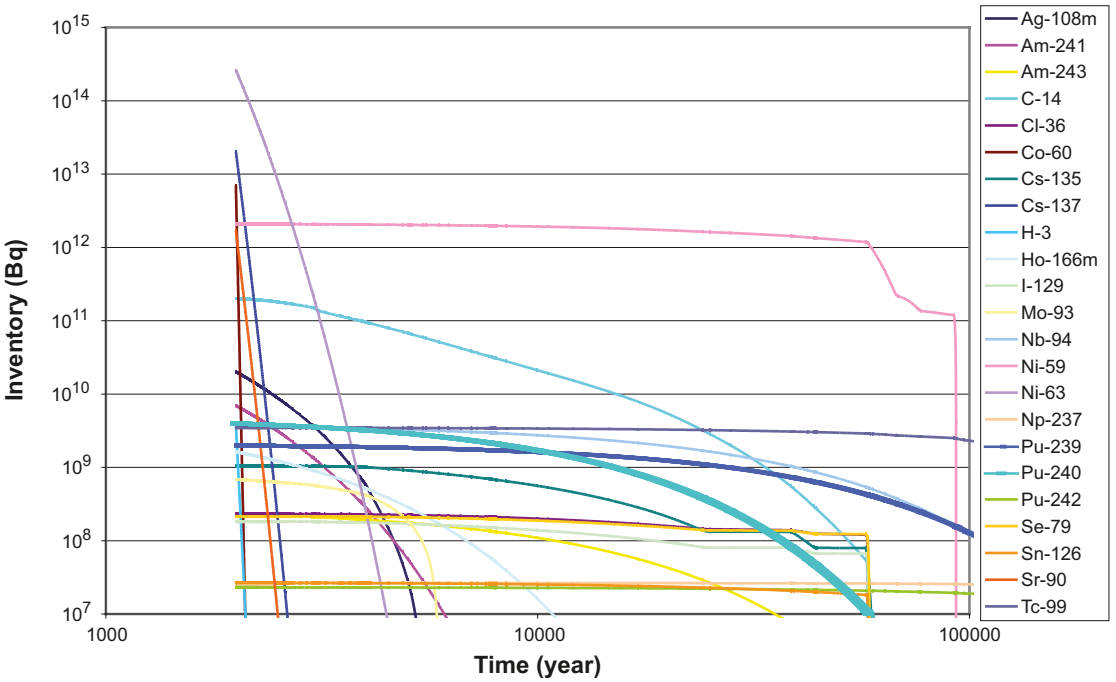

Figure 6-2. *Inventory (Bq) of radionuclides in the BMA as a function of time taking into account reductions due to releases predicted for the Weichselian variant and the radioactive decay/ingrowth.*

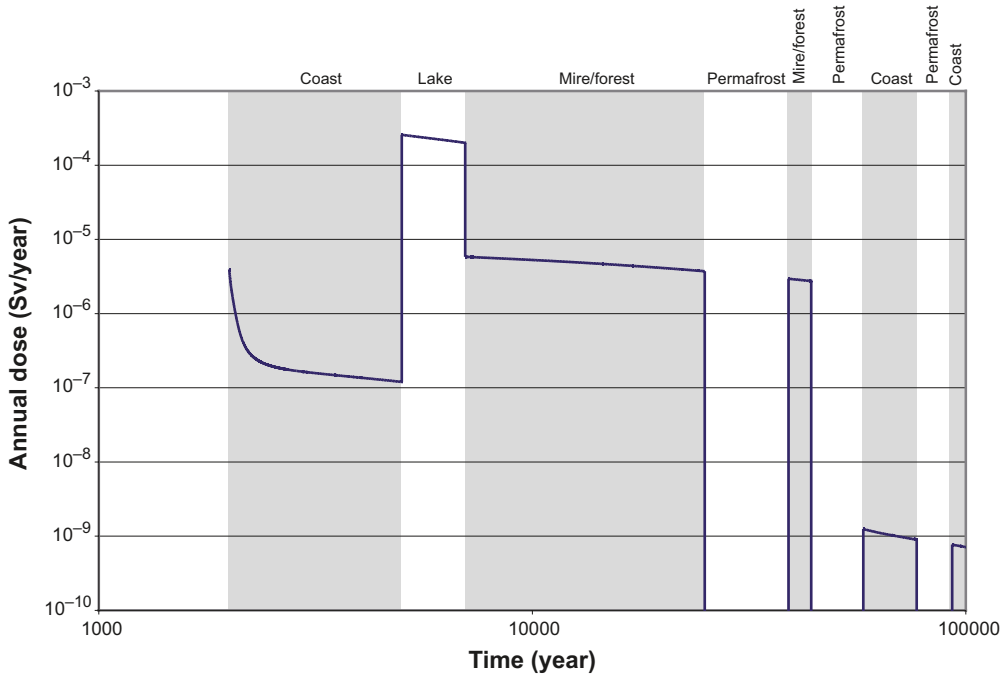

Figure 6-3. *Earthquake, Silo. Maximum values of the total annual dose (Sv/y) resulting from damages of the Silo associated with an earthquake occurring at different time points.*

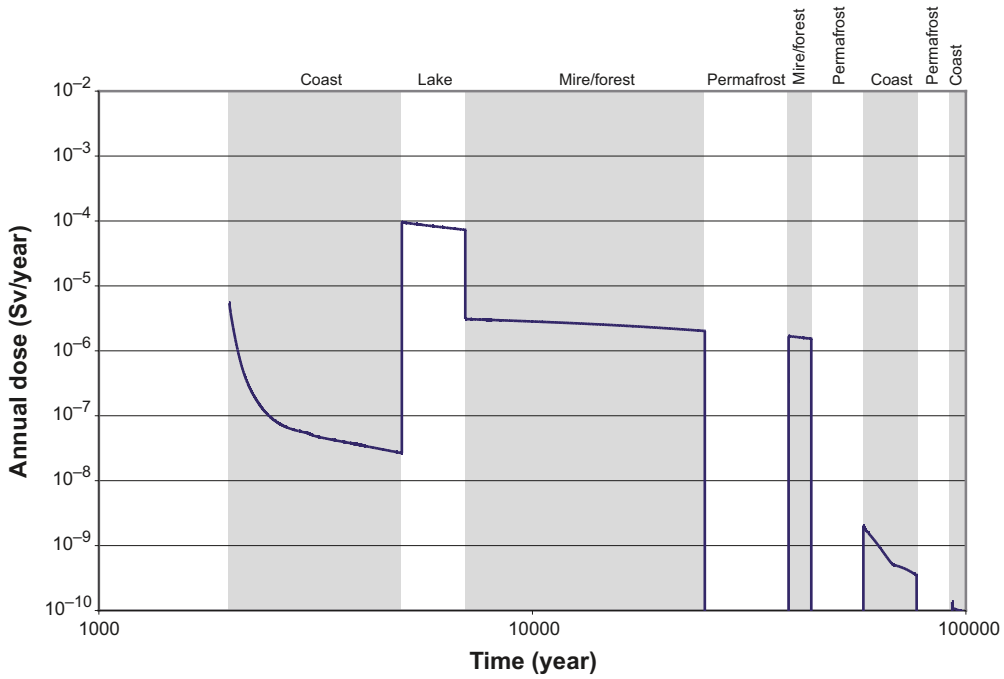

Figure 6-4. *Earthquake, BMA. Maximum values of the total annual dose (Sv/y) resulting from damages of the BMA associated with an earthquake occurring at different time points.*

The maximum values of the risks obtained from simulations for earthquakes of magnitude 5 and 6 are given in Tables F-3 and F-4 in Appendix F for the Silo and Tables F-5 and F-6 in Appendix F for the BMA. In these tables, the time at which the maximum occurs is also indicated. For the calculations, maximum dose values (see Figures 6-3, 6-4 and Tables F-1 and F-2 in Appendix F) were used and therefore the risk estimates can considered as being conservative.

For both repository parts, the maximum risk values are observed around year 5,000 and are associated with potential releases of C-14 to a lake.

Risk values at different times after the repository closure obtained for earthquakes of different magnitude are presented in Figure 6-5 for the Silo and in Figure 6-6 for the BMA. The peak values of the risks are observed around year 5,000 independently of the magnitude of the earthquake. Thereafter the risk remains at nearly the same level for a period of 2,000 years, while the lake receiving the releases still exists, and reduces rapidly to much lower values when the lake is transformed into a mire. This pattern in the time dependency of the risk is dictated by the dominant contribution to the risk from C-14, which gives much higher doses if the receptor of the releases is a lake, than if it is a terrestrial object of the same size /Avila and Pröhl 2008/.

As it was mentioned in Section 4.3, earthquakes with a magnitude lower than 5 are not expected to affect the repository. Nevertheless, in Figures 6-5 and 6-6 values for earthquakes of lower magnitude are also provided to illustrate the effect of the probabilities on the risks. Initially, the lower the magnitude of the earthquake the higher the predicted risk. This is because the consequences of the earthquakes are assumed not to depend on the magnitude, whereas the frequency of earthquakes decreases with their magnitude. At the same time, the probability that an earthquake had taken place will approach 1 faster for earthquakes of lower magnitude (see Figure 4-1), which explains why the risk at longer time periods tends to be higher for earthquakes of higher magnitude.

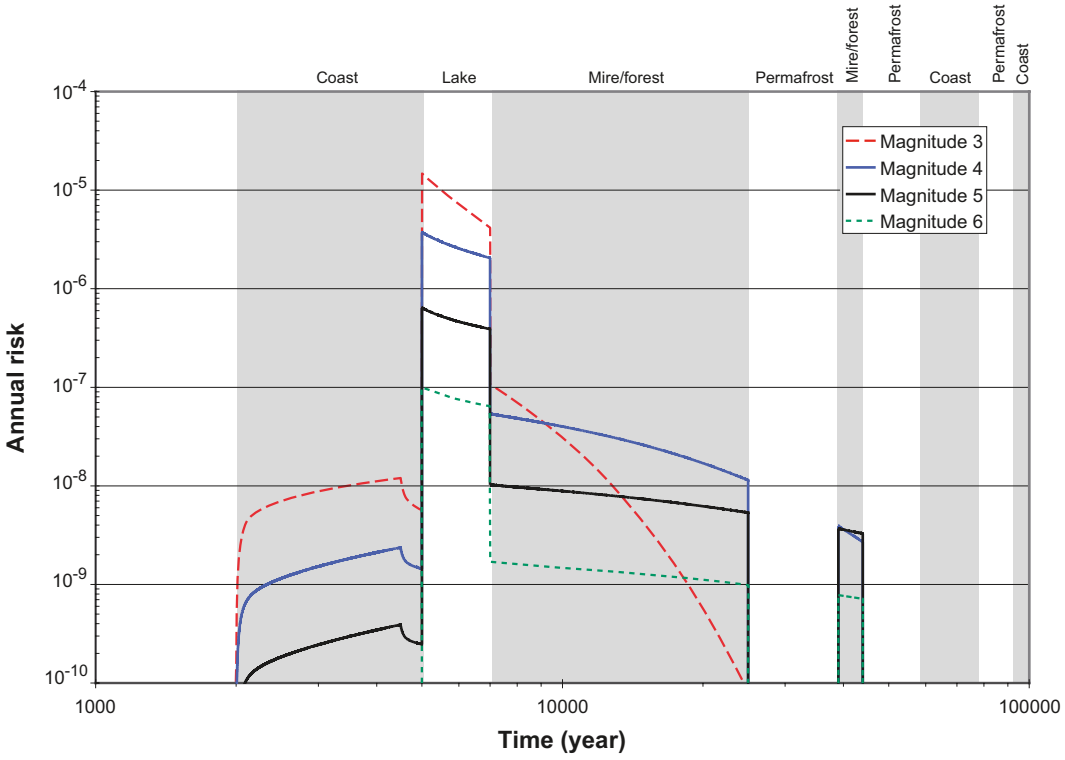

Figure 6-5. *Earthquake, Silo. Estimates of the annual risk (1/y) associated with damages of the Silo caused by earthquakes of different magnitudes at different times after the repository closure. The legends indicate the magnitude of the earthquake.*

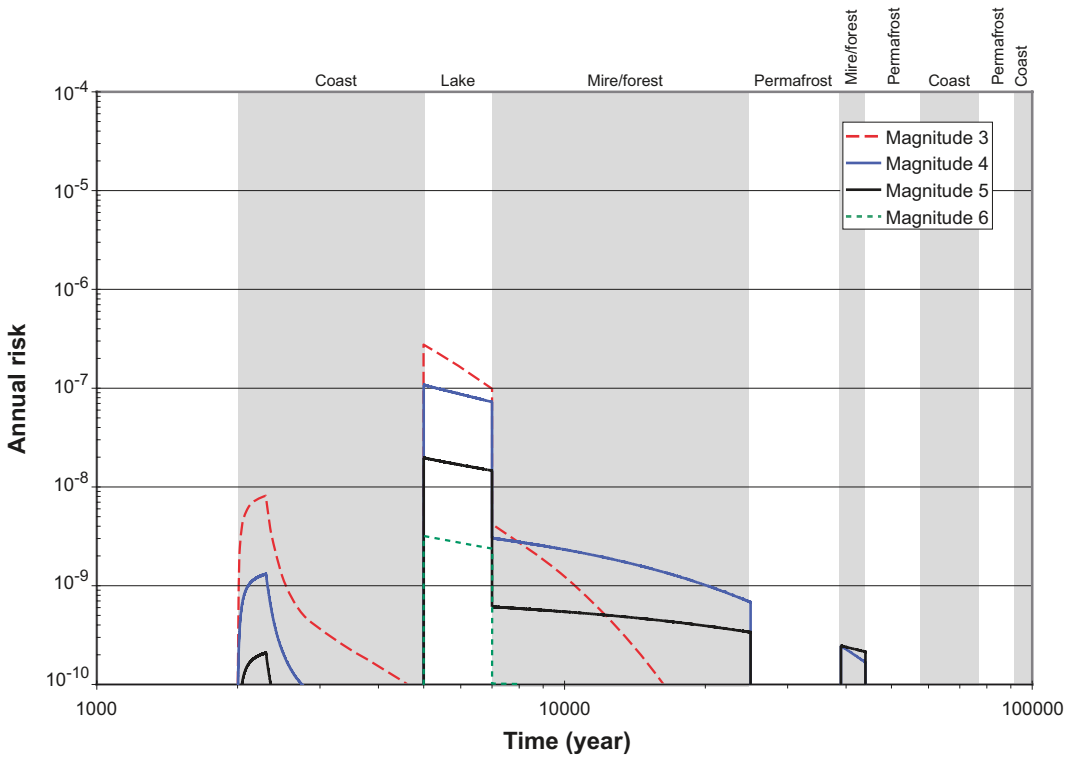

Figure 6-6. *Earthquake, BMA. Estimates of the annual risk (1/y) associated with damages of the BMA caused by earthquakes of different magnitudes at different times after the repository closure. The legends indicate the magnitude of the earthquake.*

6.2 Earlier freezing (BMA) in the Weichselian variant (CC4) and Earlier freezing (BMA) in the Weichselian variant with talik (CC5)

These calculation cases address the consequences if the BMA barriers are insufficient to withstand the consequences of the first period of permafrost and the encapsulation may fail at the start of the first period of continuous permafrost, i.e. at year 25,000. At this point, the BMA barriers are considered to fail in a similar manner as in the Weichselian variant with increases in groundwater flow rates and the effective diffusivity of concrete and reductions in the sorption capacity of concrete and cement. Two calculation cases are considered with different assumptions regarding fluxes to the biosphere during permafrost periods: one without talik (CC4) with no groundwater flux and no radionuclide releases and one with talik (CC5) with increased groundwater flows and radionuclide releases.

6.2.1 Doses from releases to the landscape

The results of the screening study for both calculation cases are presented in Table 6-1. The same radionuclides, as for the Weichselian variant, are identified as potential important dose contributors in both calculation cases (CC4 and CC5).

Table 6-1. Results of the screening study for the calculation cases with earlier freezing of the BMA (CC4 and CC5) with releases to the landscape. The peak value of the Screening Quotient (SQ) and the time (in years AD) at which the peak SQ is observed are presented. Values are only given for radionuclides for which SQ above 1 were obtained. Note that in this calculation case only the BMA is affected.

Radionuclide		Without talik CC4	With talik CC5
C-14-in	Peak SQ	2	306
	Time	6,640	25,050
C-14-org	Peak SQ	67	67
	Time	5,060	5,060
Cl-36	Peak SQ	49	
	Time	39,140	
Ni-59	Peak SQ	325	12
	Time	39,140	17,040
Se-79	Peak SQ	138	4
	Time	39,140	7,240
Mo-93	Peak SQ	3	3
	Time	7,240	7,240
I-129	Peak SQ	419	9
	Time	39,140	7,240
Cs-135	Peak SQ	197	197
	Time	7,240	7,240

The results until the start of the first permafrost period are the same as for the Weichselian variant. However, at later time periods higher values, than in the Weichselian variant, are observed for some radionuclides, e.g. inorganic C-14 and I-129. The time dynamics of the mean annual doses obtained for the two calculation cases are shown in Figures 6-7 and 6-8. The peak observed at around year 5,000 is caused by C-14 releases, as for the Weichselian variant. The second peak is observed at later time periods, at around year 39,000 for the calculation case without talik and around year 25,000 for the calculation case with talik. These peaks are associated with transient changes in the groundwater fluxes. Thereafter, follows a fast decrease of the doses. Note that if a smother increase of the groundwater fluxes had been assumed, lower values of the peak doses had been obtained.

A summary of the peak values of the mean annual doses is shown in Table 6-2. The values obtained for the BMA are higher than the values obtained for the Weichselian variant (see Table 5-1) for this repository part. However, the peak values from the whole SFR 1 in this calculation case are nearly the same as in the Weichselian variant. This is because the peak values for the BMA in this calculation case are observed at later times, when the doses from other repository parts are smaller.

6.2.2 Doses from releases to a well

The peak dose from BMA due to exposure from a well is 17 μSv per year for the case without talik. It is mainly caused by I-129 around year 39,000, when the first temperate period after the concrete barriers have degraded occurs. The case with talik does not give a high dose at year 39,000 since a continuous release of radionuclides through the talik has reduced the inventory in the repository. The peak dose for the case with talik occurs during the time period when this calculation case is identical to the Weichselian variant, i.e. at year 4,000.

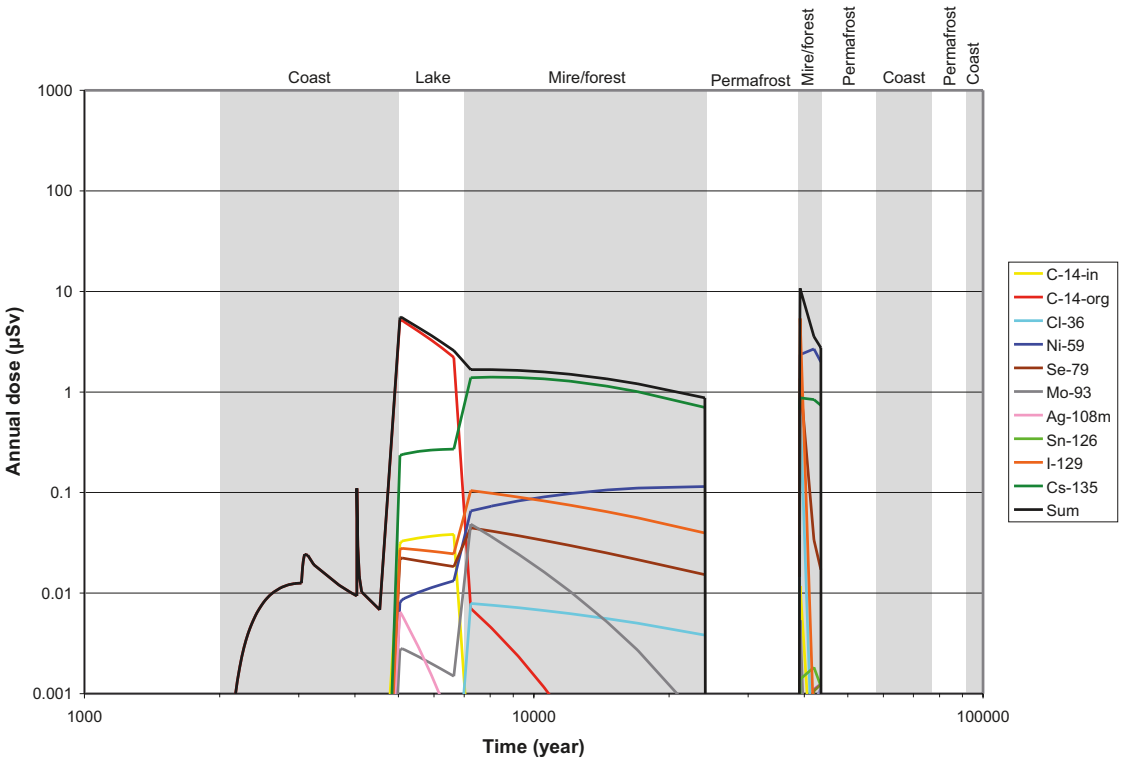

Figure 6-7. *Earlier freezing (BMA) in the Weichselian variant (CC4), BMA. Mean values of the annual individual dose from radionuclide releases to the landscape. The sum corresponds to the total dose considering all released radionuclides. This calculation case considers degraded BMA barriers at year 25,000.*

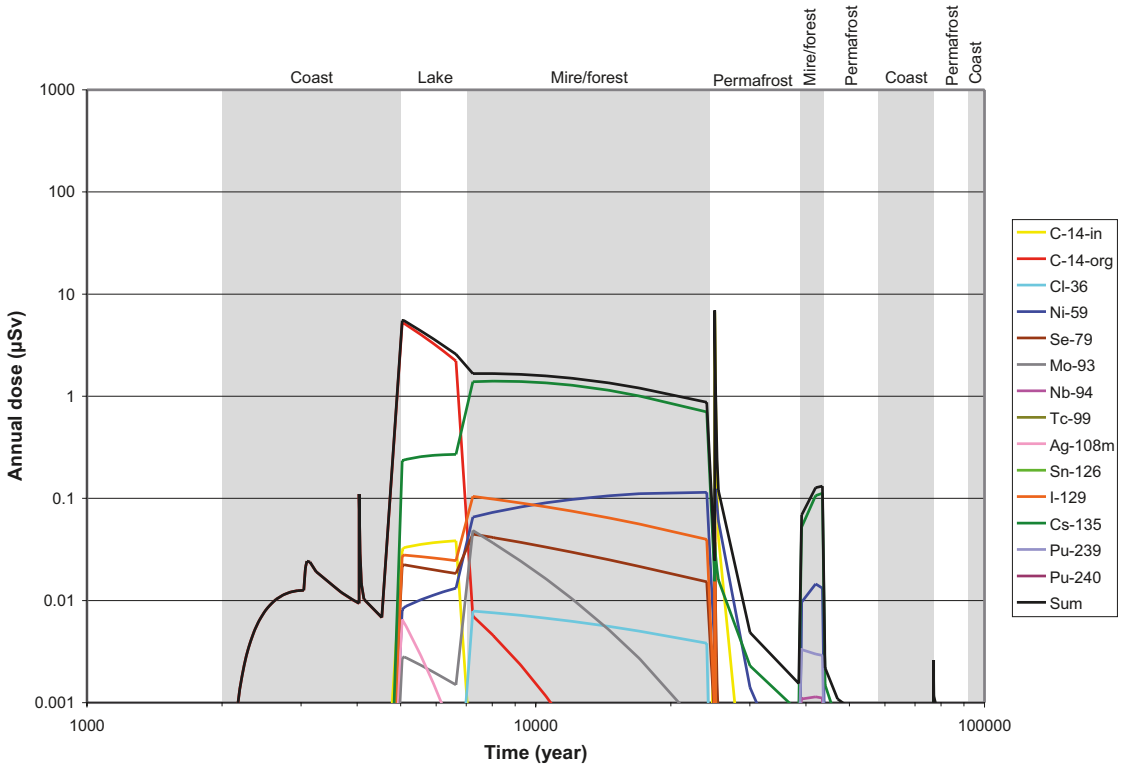

Figure 6-8. *Earlier freezing (BMA) in the Weichselian variant with talik (CC5), BMA. Mean values of the annual individual dose from radionuclide releases to the landscape. The sum corresponds to the total dose considering all released radionuclides. This calculation case considers degraded BMA barriers at year 25,000.*

Table 6-2. Peak values of the mean annual doses and time at which the peak value is obtained for releases to the landscape from the BMA in the calculation cases with earlier freezing of the repository without talik (CC4) and with talik (CC5). The value given for each calculation case is the sum of doses obtained for all released radionuclides. The radionuclides with the highest contribution to the peak doses are indicated.

Scenario	Peak annual dose µSv/year	Time of the peak years AD	Most contributing radionuclide
Without talik	11	around 39,000	I-129
With talik	6.9	around 25,000	inorganic C-14

6.3 Extreme permafrost (CC7)

The extreme permafrost calculation case (CC7) explores the consequences of an earlier permafrost period, which appears around year 10,000. The anticipated climate evolution comprises alternating periods of temperate conditions and continuous permafrost at the Forsmark site until approximately year 44,000 and thereafter a period of continuous permafrost at repository depth occurs. In this calculation case it is assumed that taliks are not formed during permafrost and groundwater is inhibited. Most other assumptions in this calculation case are the same as for the Weichselian variant (Chapter 5). However, the following differences exist.

- Degradation of the BMA is assumed to take place at 20,000 years post-closure.
- Degradation of the Silo concrete structure is assumed to take place at 20,000 years post-closure, however, the bentonite backfill remains intact throughout the assessment timescale.
- The tunnel plugs are assumed to remain intact throughout the assessment timescale.
- The geosphere changes from saline to non-saline at 1,000 years post-closure, as in CC1, and remains non-saline from here on.

6.3.1 Doses from releases to the landscape

The results of the screening study are presented in Table 6-3. The potentially important radionuclides are the same as for the Weichselian varaint. The main difference when compared to the Weichselian variant is that higher SQ values are obtained at later time points. The radionuclides with the highest SQ values are Ni-59, I-129 and Cs-135.

Time series of the mean annual doses are presented in the Figures 6-9 to 6-13. During the first 10,000 years the predicted time series are the same as for the Weichselian variant. This was expected as during this period the assumptions for the extreme permafrost calculation case are the same as for the Weichselian variant. Starting from year 10,000 differences begin to appear, with nil doses from year 10,000 to the start of the next temperate period, due to inhibition of the groundwater flow caused by the permafrost conditions. Another important difference when compared to the Weichselian variant is that higher dose values, mainly from Ni-59, I-129 and Cs-135, are obtained for the Silo and the BMA at later time points, which is due to the effect of earlier degradation of the barriers. For other repository parts this effect is not important, as their barriers are already degraded.

Table 6-3. Results of the screening study for the calculation case extreme permafrost (CC7) with releases to the landscape. The peak value of the Screening Quotient (SQ) and the time (in years AD) at which the peak SQ is observed are presented for each repository part. Values are given only for radionuclides for which SQ above 1 were obtained.

Radionuclide		Silo	BMA	BLA	1BTF	2BTF
C-14-in	Peak SQ		2		10	70
	Time		6,640		5,090	5,060
C-14-org	Peak SQ	85	67			6
	Time	5,540	5,060			5,041
Cl-36	Peak SQ	4	98			
	Time	40,040	39,050			
Ni-59	Peak SQ		339		2	4
	Time		40,040		7,240	7,240
Se-79	Peak SQ	2	190			
	Time	43,030	39,070			
Mo-93	Peak SQ		3			
	Time		39,050			
I-129	Peak SQ	32	785			
	Time	40,040	39,050			
Cs-135	Peak SQ	2	197		4	28
	Time	43,030	7,240		7,240	7,240

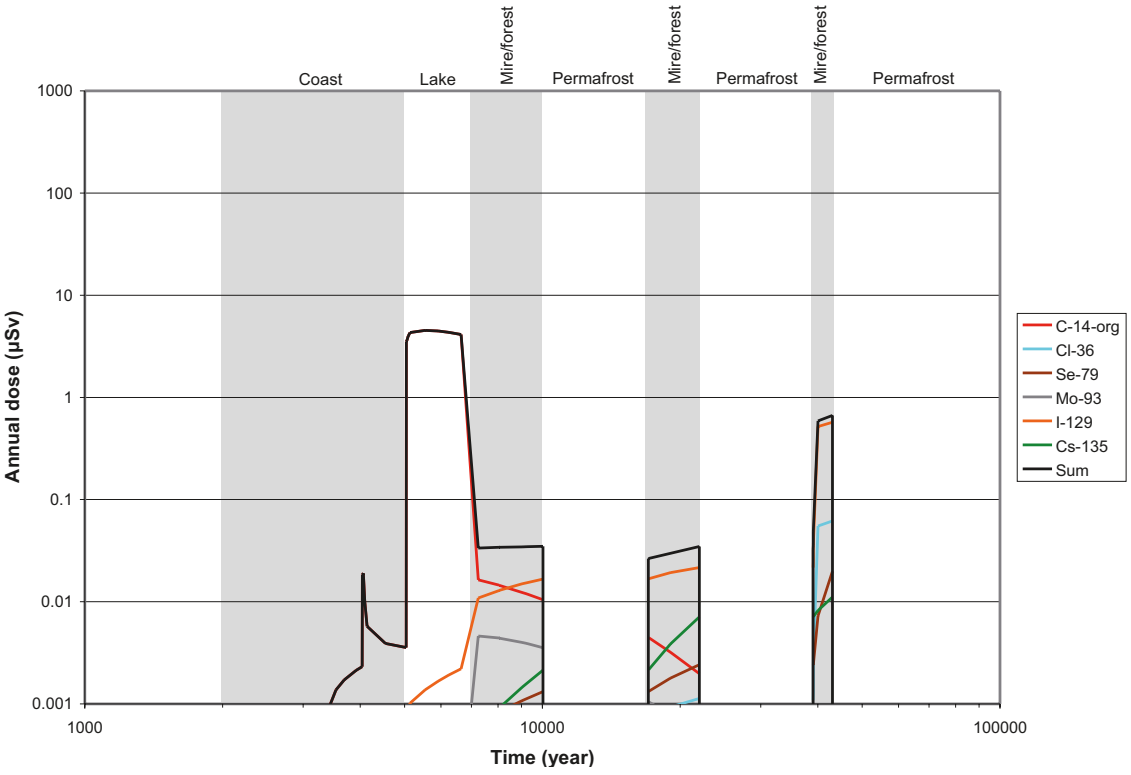

Figure 6-9. *Extreme permafrost (CC7), Silo. Mean values of the annual individual dose from radionuclide releases to the landscape from the Silo. The sum corresponds to the total dose considering all released radionuclides.*

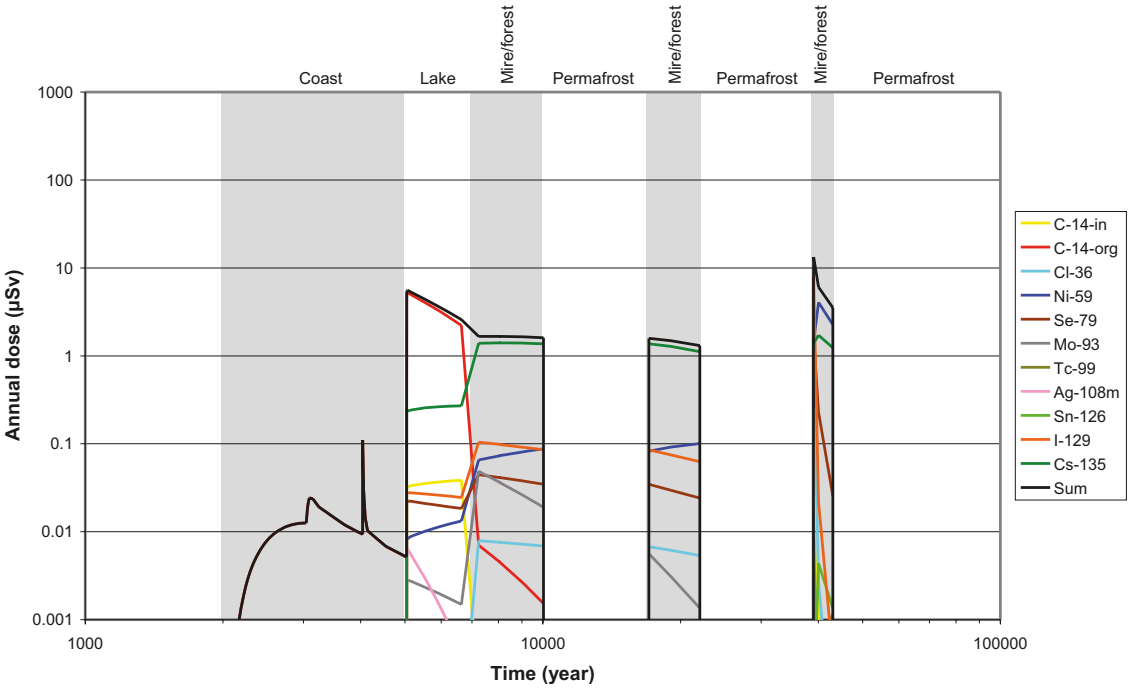

Figure 6-10. *Extreme permafrost (CC7), BMA. Mean values of the annual individual dose from radionuclide releases to the landscape from the BMA. The sum corresponds to the total dose considering all released radionuclides.*

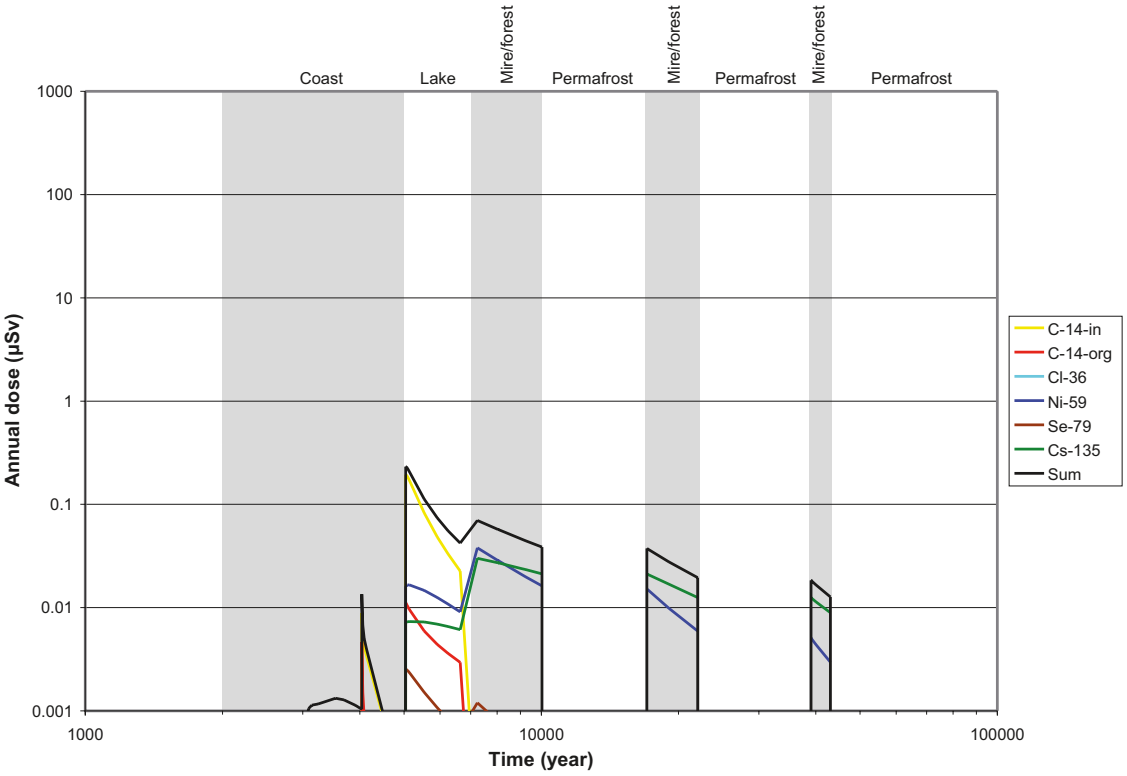

Figure 6-11. *Extreme permafrost (CC7), 1BTF. Mean values of the annual individual dose from radionuclide releases to the landscape from the 1BTF. The sum corresponds to the total dose considering all released radionuclides.*

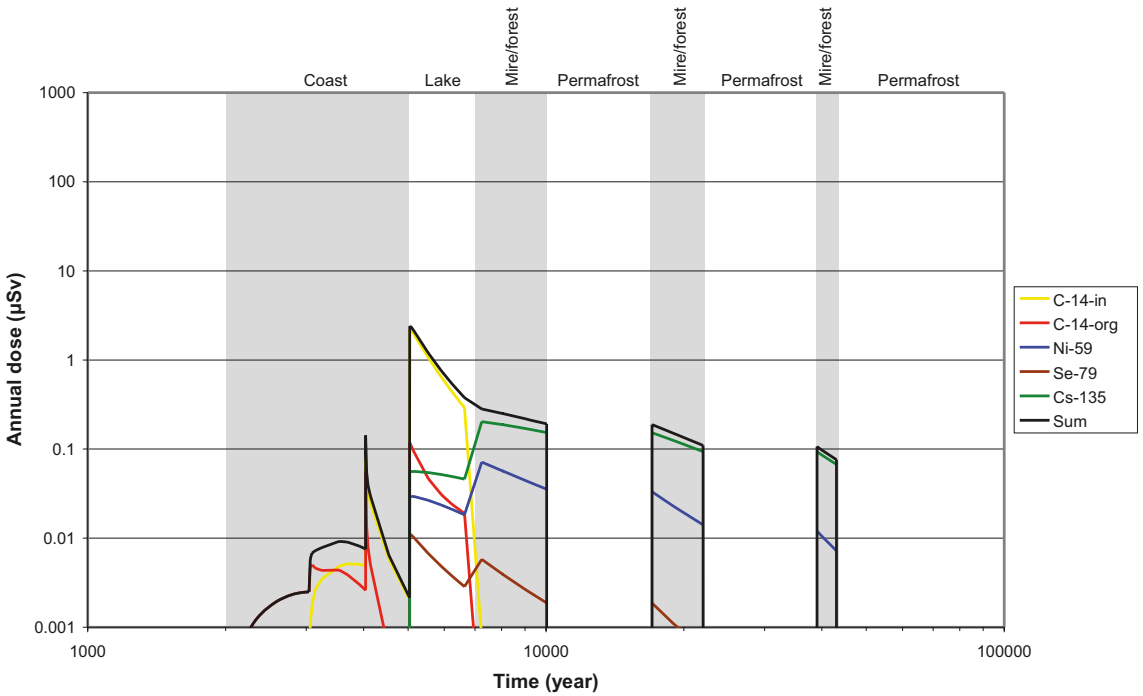

Figure 6-12. *Extreme permafrost (CC7), 2BTF. Mean values of the annual individual dose from radionuclide releases to the landscape from the. The sum corresponds to the total dose considering all released radionuclides.*

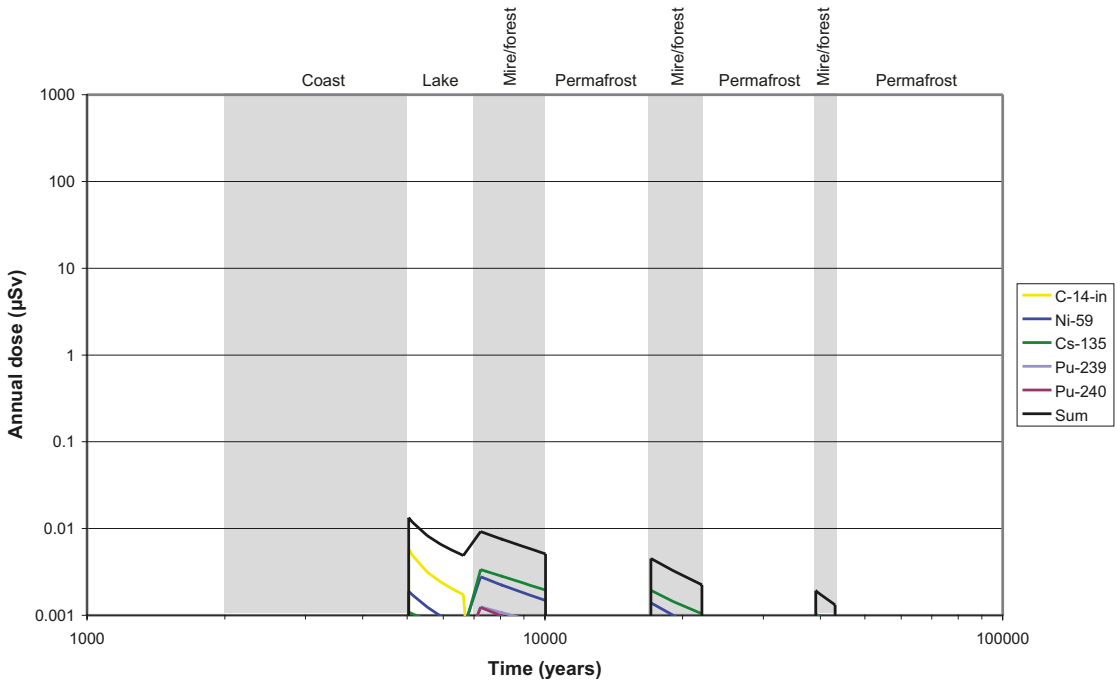

Figure 6-13. *Extreme permafrost (CC7), BLA. Mean values of the annual individual dose from radionuclide releases to the landscape from the BLA. The sum corresponds to the total dose considering all released radionuclides.*

Figure 6-14 presents the total mean annual doses from the whole repository and for each repository part taking into account all released radionuclides. As for the Weichselian variant, before the first permafrost period, the Silo and the BMA have the highest contribution to the peak dose, due to their larger inventory of C-14. These repository parts dominate the doses even for other time periods. The BLA gives the lowest contribution during the whole simulation period due to the lower radionuclide inventory and because releases from this repository part occur early in the sea period, when the dilution is higher, which leads to a lower dose per unit release rate. In contrast to the Weichselian variant, the highest peak dose is observed around year 39,000 and is dominated by I-129 releases from the BMA. The reason for this second peak is failure of the barriers, which is assumed to occur around year 22,000. Note that even though the I-129 inventory is higher in the Silo than in the BMA, the later has a higher contribution to the value of the second peak dose. This is because the bentonite backfill of the Silo, which is assumed to remain intact, reduces the releases from this repository part.

A summary of the peak values of the mean annual doses is shown in Table 6-4. The value obtained for the BMA is about two times higher than the value obtained for the Weichselian variant (see Table 5-1) for this repository part. However, the peak value from the whole SFR 1 in this calculation case is only slightly higher than the values for the Weichselian variant. This can be explained by peak values for the BMA in this calculation case being observed at later times, when the doses from other repository parts are smaller.

6.3.2 Doses from releases to a well

Times series of the mean annual doses from releases to a well are presented in Figures 6-15 to 6-19. For the 1BTF, 2BTF and BLA the predicted doses and their time variation are very close to the predictions for the Weichselian variant. For these repository parts, the peak values of the doses are observed around year 4,000. This is followed by decreasing trend of the sum of doses across the radionuclides. For the Silo and the BMA, in contrast with the results for the Weichselian variant, the peak values are observed around year 39,000. This is explained by the degradation of the barriers occurring around year 22,000. A summary of the peak values for the well doses and the most contributing radionuclides is presented in Table 6-5.

Table 6-4. Peak values of the mean annual doses and time at which the peak value is observed for releases to the landscape from each repository part and from the whole repository in the calculation case extreme permafrost (CC7). The value given for each repository part is the sum of values obtained for all released radionuclides. The radionuclides with the highest contribution to the peak doses are indicated.

Repository part	Peak annual mean dose µSv/year	Time of the peak years AD	Most contributing radionuclide
Silo	4.5	around 5,000	Organic C-14
BMA	13	around 39,000	I-129
1BTF	0.2	around 5,000	Inorganic C-14
2BTF	2.4	around 5,000	Inorganic C-14
BLA	0.01	around 5,000	Inorganic C-14
Total SFR 1	13	around 39,000	I-129

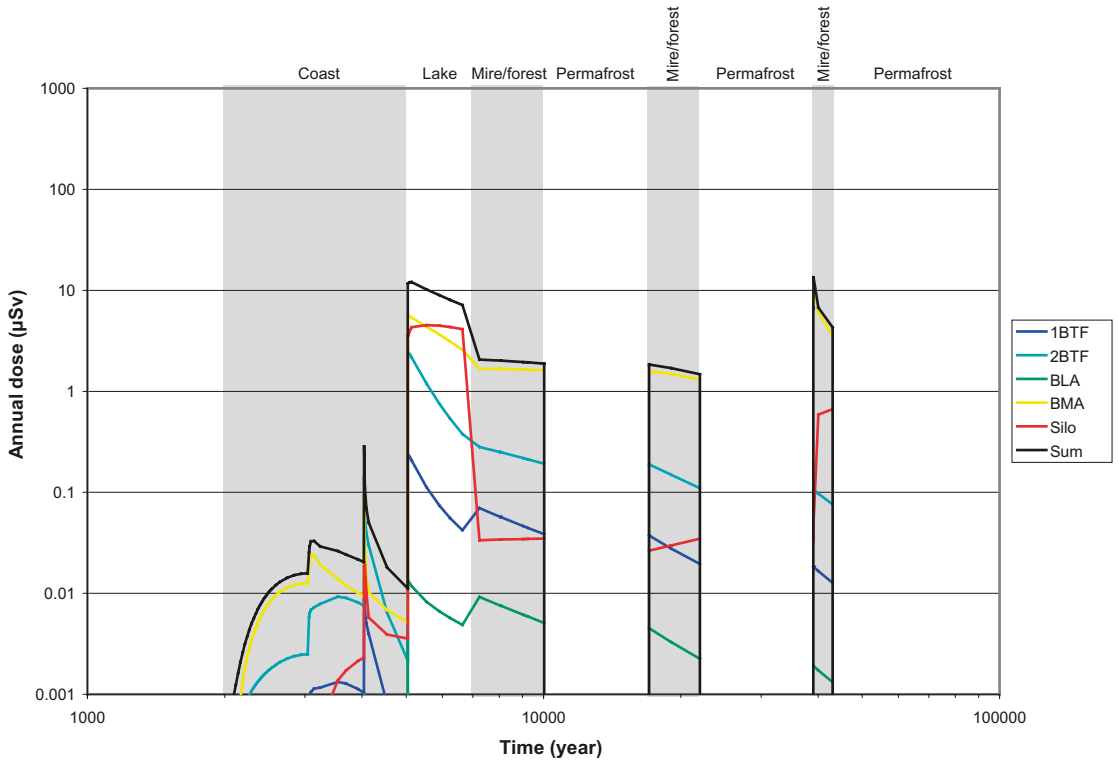

Figure 6-14. *Extreme permafrost (CC7), SFR 1. Mean values of the total annual individual dose from radionuclide releases to the landscape from each repository part and from the whole repository (Sum).*

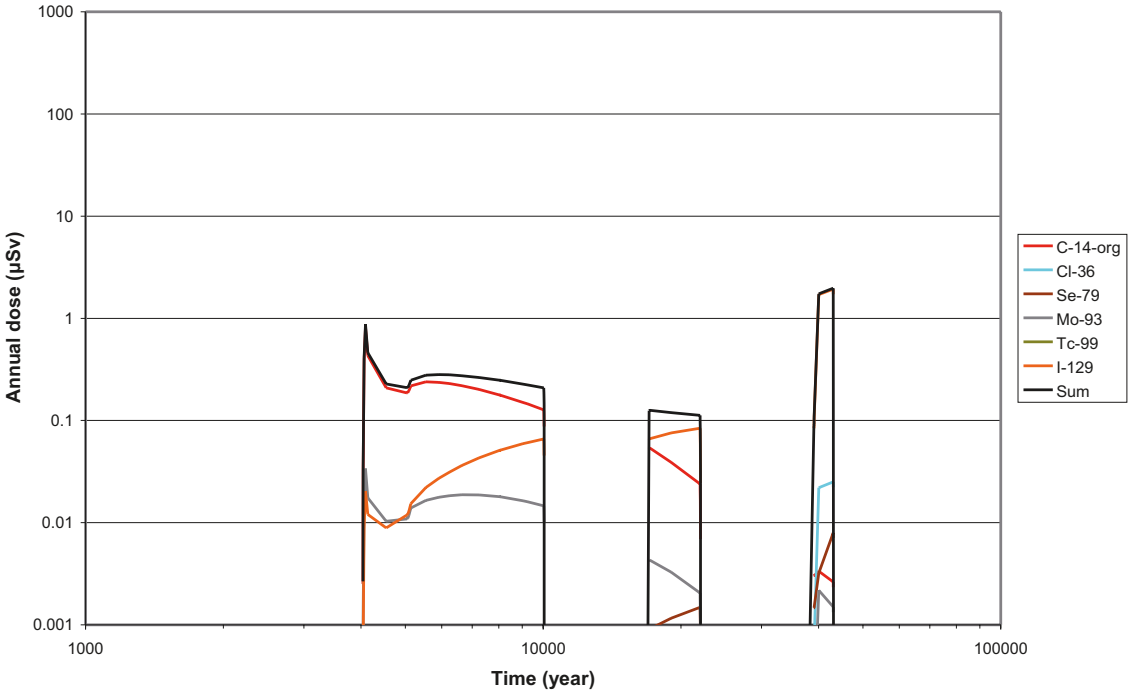

Figure 6-15. *Extreme permafrost (CC7), Silo. Moving average (50 years) of the mean annual doses from radionuclide releases to a well from the Silo. The sum corresponds to the total dose considering all released radionuclides.*

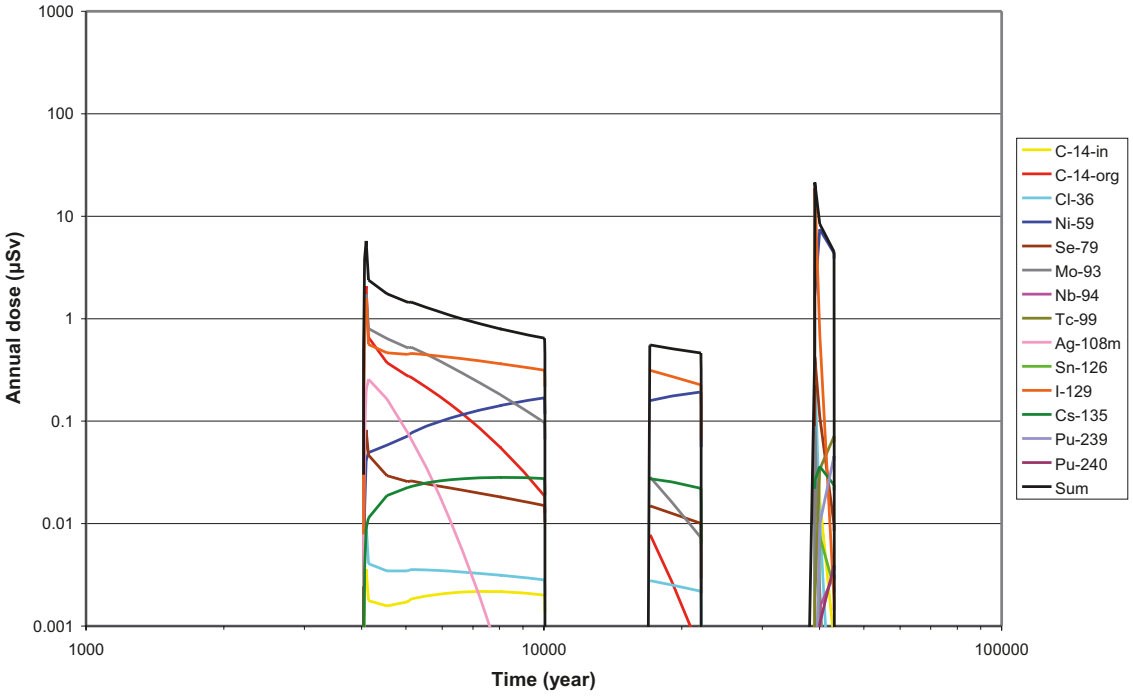

Figure 6-16. *Extreme permafrost (CC7), BMA. Moving average (50 years) of the mean annual doses from radionuclide releases to a well from the BMA. The sum corresponds to the total dose considering all released radionuclides.*

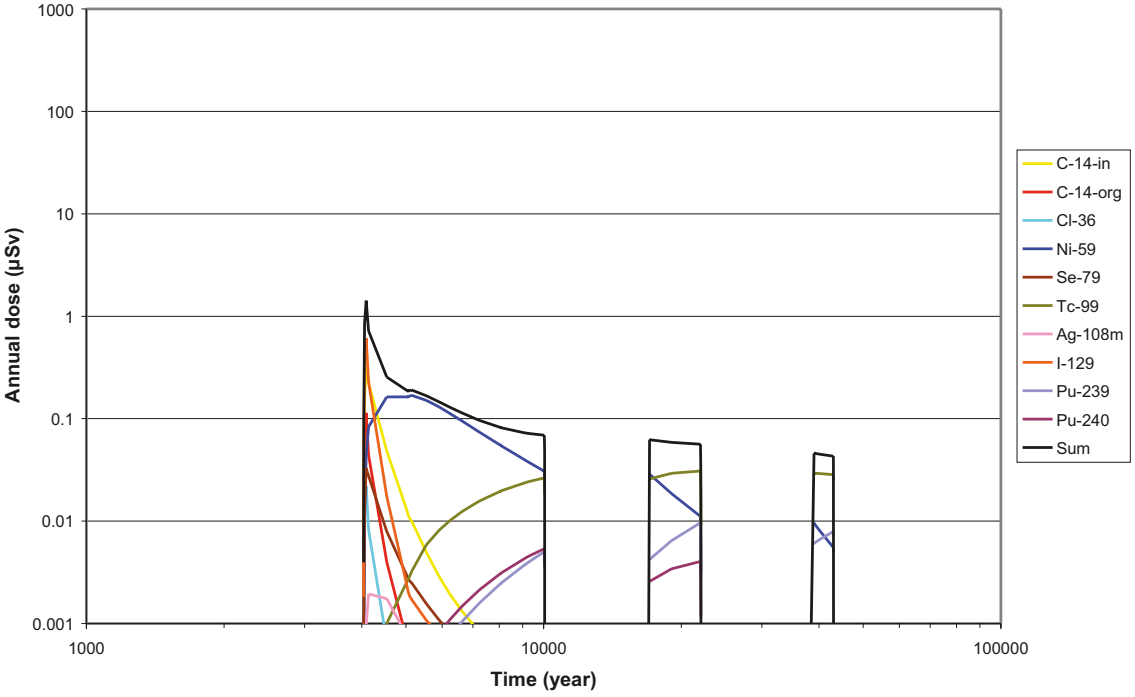

Figure 6-17. *Extreme permafrost (CC7), 1BTF. Moving average (50 years) of the mean annual doses from radionuclide releases to a well from the 1BTF. The sum corresponds to the total dose considering all released radionuclides.*

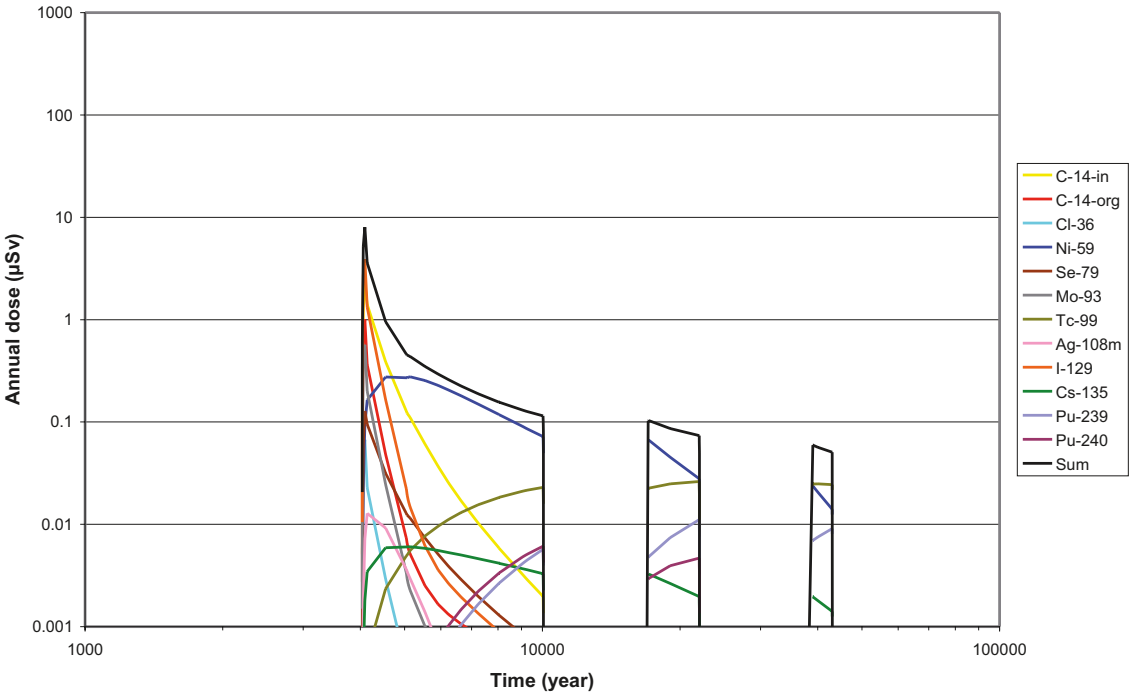

Figure 6-18. *Extreme permafrost (CC7), 2BTF. Moving average (50 years) of the mean annual doses from radionuclide releases to a well from the 2BTF. The sum corresponds to the total dose considering all released radionuclides.*

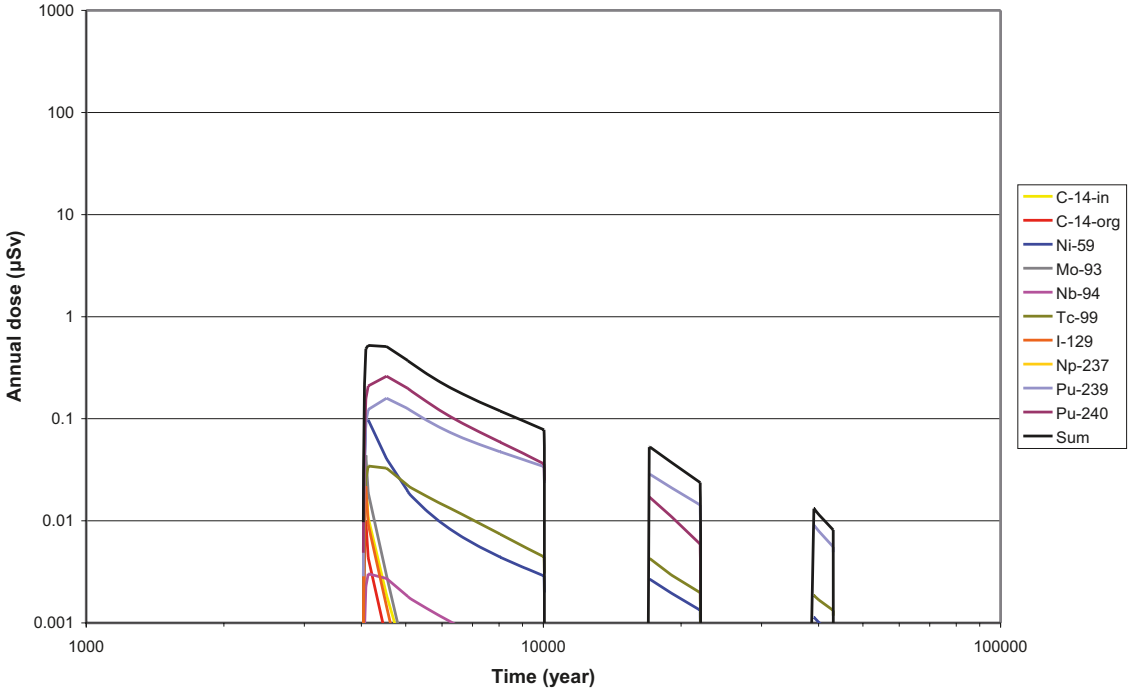

Figure 6-19. *Extreme permafrost (CC7), BLA. Moving average (50 years) of the mean annual doses from radionuclide releases to a well from the BLA. The sum corresponds to the total dose considering all released radionuclides.*

Table 6-5. Peak values of the 50-years moving average of the mean annual dose and time at which the peak value is observed for releases to a well from each repository part and summed over the vaults in the calculation case extreme permafrost (CC7). The value given for each repository part is the sum of values obtained for all released radionuclides. The radionuclides with the highest contribution to the peak doses are indicated.

Repository part	Peak annual mean dose µSv/year	Time of the peak years AD	Most contributing radionuclide
Silo	2.0	around 39,000	I-129
BMA	21	around 39,000	I-129
1BTF	1.4	around 4,000	I-129
2BTF	8.0	around 4,000	I-129
BLA	0.5	around 4,000	Pu-240
All vaults	21	around 39,000	I-129

6.4 Extreme permafrost with taliks (CC8)

Most assumptions made for this extreme permafrost calculation case (CC8) are the same that were made in calculation case 7 (Section 6.3). However, there is an important difference when compared to calculation case 7, in that it is assumed that during periods of continuous permafrost the groundwater within the repository remains un-frozen as does areas of the geosphere between the repository and the ground surface, such that a migration route to the biosphere for radionuclides is developed. In this case, releases to the biosphere during permafrost periods are assumed to be directed through taliks to larger lakes.

6.4.1 Doses from releases to the landscape

The results of the screening study for this calculation case gave nearly the same results as for the calculation case 7. The potentially important radionuclides are the same as for the Weichselian variant. The main difference when compared to the Weichselian variant is that higher SQs are obtained at later time points.

Time series of the mean annual doses are presented in the Figures 6-20 to 6-24. During the first 10,000 years the predicted time series are the same as for the calculation case extreme permafrost. This was expected as during this period the assumptions for this calculation case are the same as for the calculation case extreme permafrost. Starting from year 10,000 differences begin to appear as releases during the permafrost period are directed through a talik to a lake, whereas in the calculation case extreme permafrost no release occurs. This partially explains the observed sudden increase of the doses from C-14 at year 10,000 when the release point is changed from mire to lake.

One important difference when compared to the Weichselian variant is that higher dose values, mainly from Ni-59, I-129 and Cs-135, are obtained for the Silo and the BMA at later time points, which is due to the effect of earlier degradation of the barriers. For other repository parts this effect is less important, as their barriers are considered to fail even in the Weichselian variant. The time series at later time points is characterized by the presence of several peak values, which can be explained by sudden increases of the groundwater fluxes, and consequently of radionuclide fluxes, which occur at the same time as the release point changes between mire and lake. Note that the annual doses from unit release rate vary from one biosphere object type to another. The direction of this variation is different for different radionuclides. For example for Cs-135 releases to a mire (forest) give higher doses than releases to lake, whereas the opposite is true for C-14.

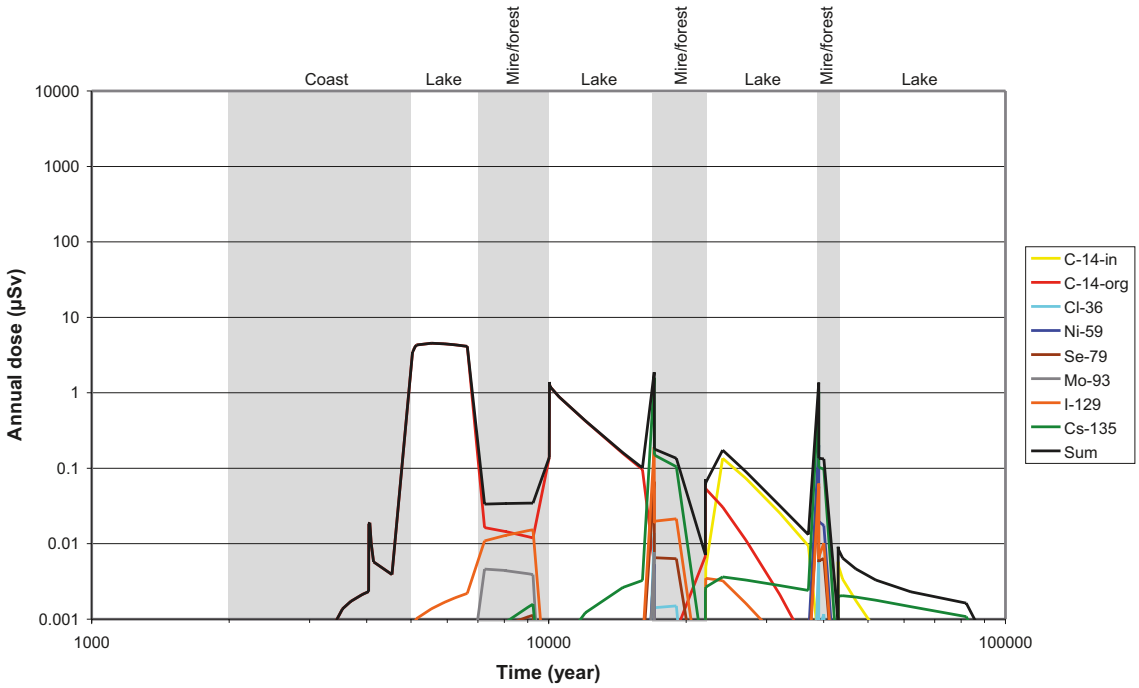

Figure 6-20. *Extreme permafrost with talik (CC8), Silo. Mean values of the annual individual dose from radionuclide releases to the landscape from the Silo. The sum corresponds to the total dose considering all released radionuclides.*

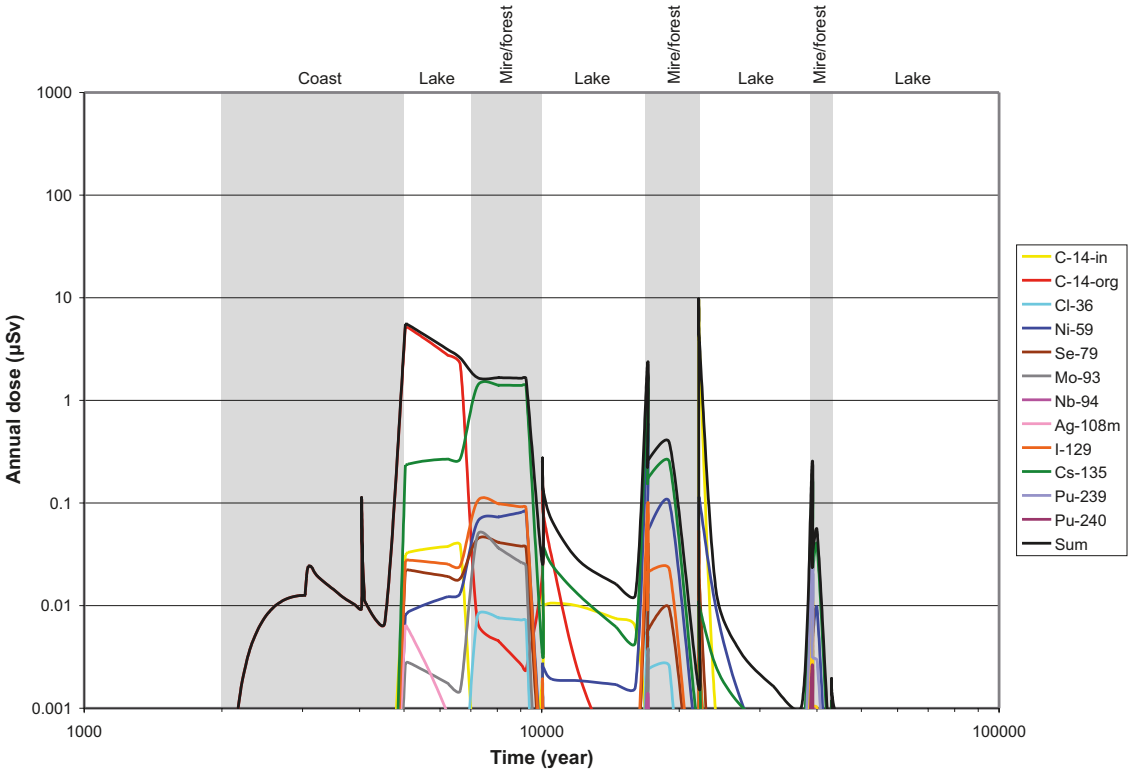

Figure 6-21. *Extreme permafrost with talik (CC8), BMA. Mean values of the annual individual dose from radionuclide releases to the landscape from the BMA. The sum corresponds to the total dose considering all released radionuclides.*

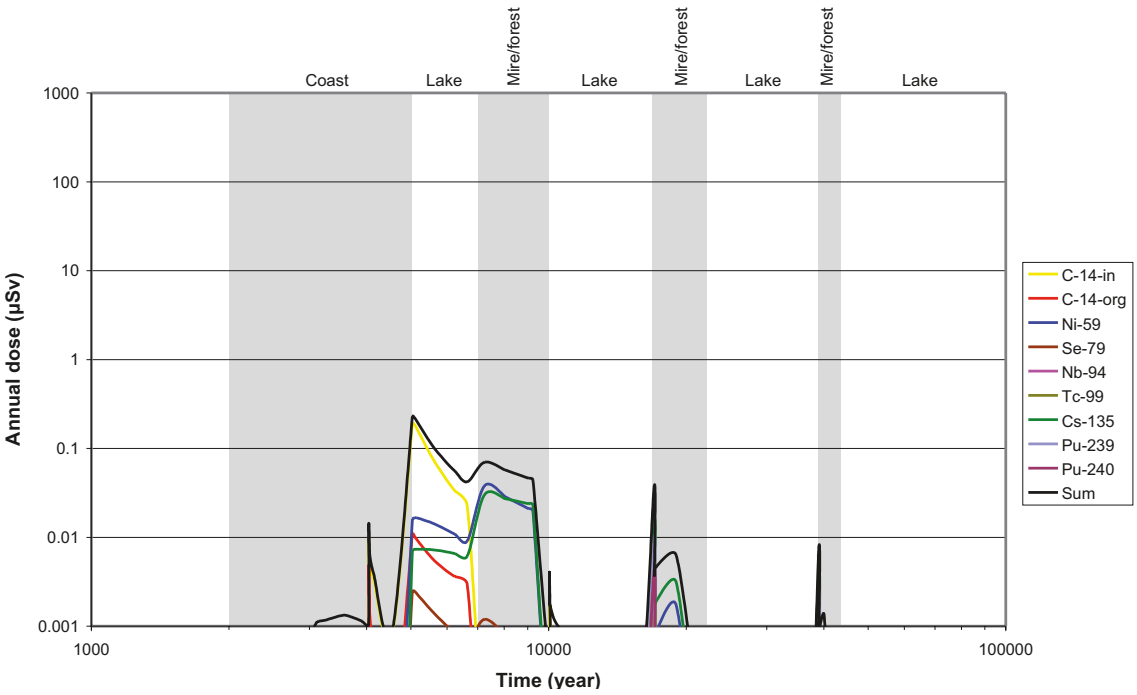

Figure 6-22. *Extreme permafrost with talik (CC8), 1BTF. Mean values of the annual individual dose from radionuclide releases to the landscape from the 1BTF. The sum corresponds to the total dose considering all released radionuclides.*

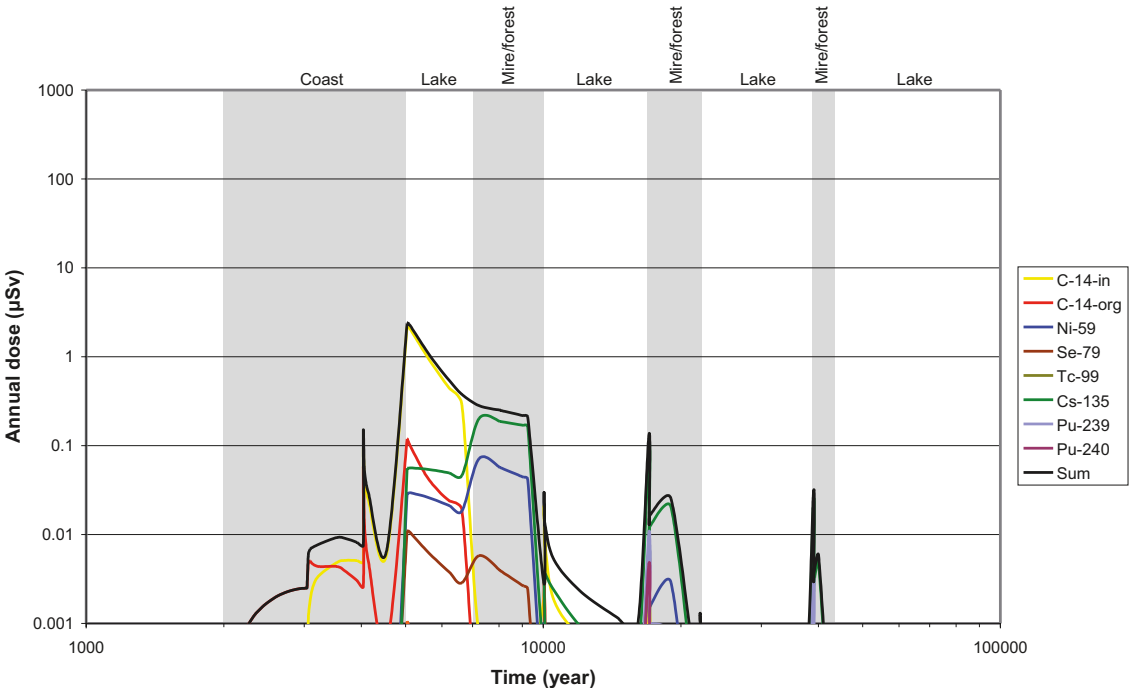

Figure 6-23. *Extreme permafrost with talik (CC8), 2BTF. Mean values of the annual individual dose from radionuclide releases to the landscape from the 2BTF. The sum corresponds to the total dose considering all released radionuclides.*

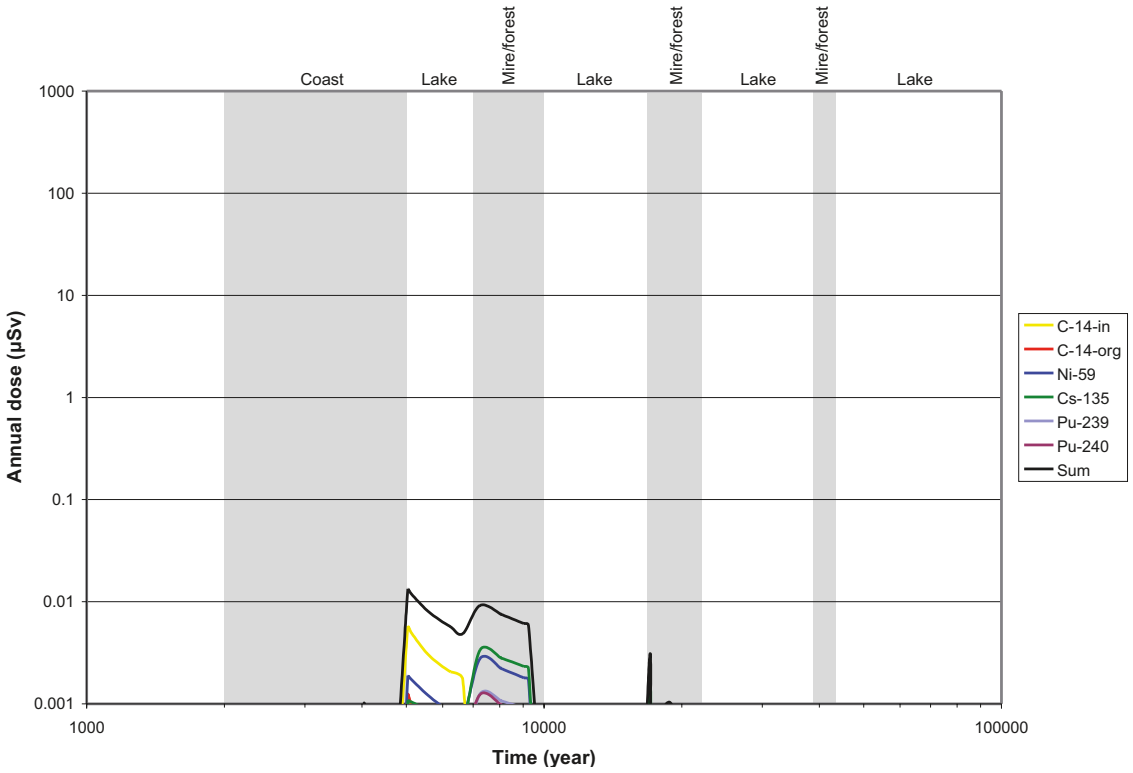

Figure 6-24. *Extreme permafrost with talik (CC8), BLA. Mean values of the annual individual dose from radionuclide releases to the landscape from the BLA. The sum corresponds to the total dose considering all released radionuclides.*

Figure 6-25 presents the total mean annual doses from the whole repository and for each repository part taking into account all released radionuclides. As for the Weichselian variant, before the first permafrost period, the Silo and the BMA have the highest contribution to the peak dose due to their larger inventory of C-14. These repository parts dominate the doses even for other time periods. The BLA gives the lowest contribution during the whole simulation period due to the lower radionuclide inventory and because releases from this repository part occur early in the sea period, when the dilution is higher, which leads to a lower dose per unit release rate. As for the Weichselian variant, the highest peak is observed around year 5,000. However, in contrast to the Weichselian variant, several other pronounced peaks are observed. The highest of these secondary peaks is associated with inorganic carbon releases from the BMA. The reason for this second peak is the failure of the barriers that is assumed to occur around year 22,000.

A summary of the peak values of the mean annual doses is shown in Table 6-6. The value obtained for the BMA is about two times higher than the value obtained for the Weichselian variant (see Table 5-1) for this repository part. However, the peak values from the whole SFR 1 in this calculation case are the same as for the Weichselian variant. This can be explained by peak values for the BMA in this calculation case being observed at later times, when the doses from other repository parts are smaller.

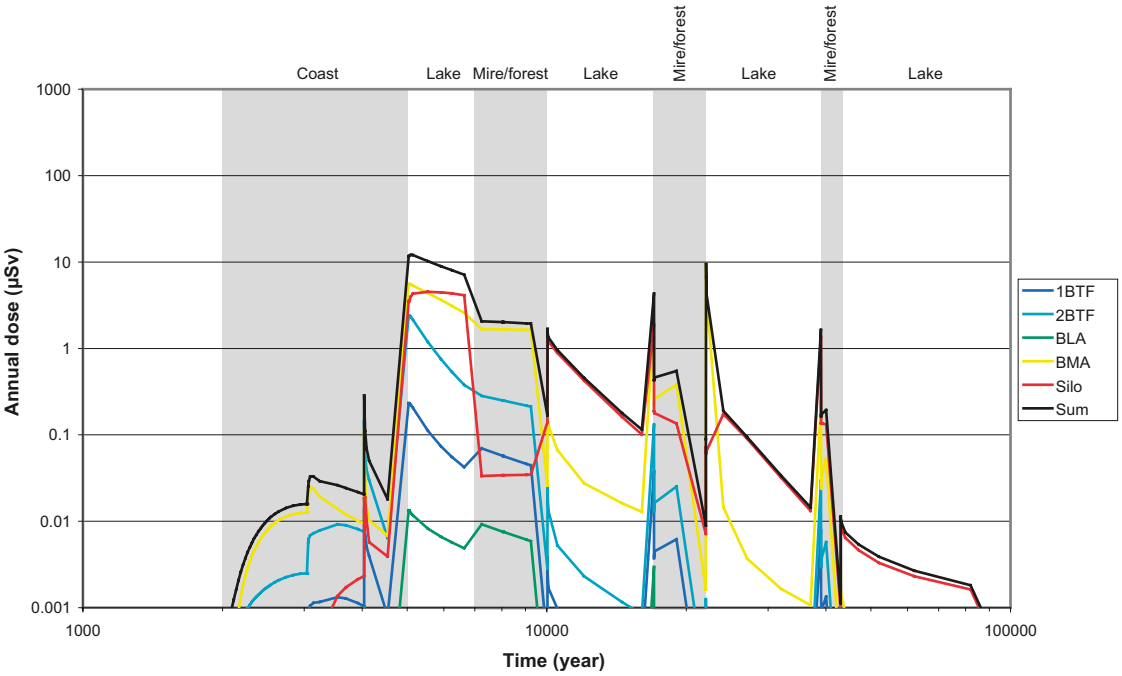

Figure 6-25. *Extreme permafrost with talik (CC8), SFR 1. Mean values of the total annual individual dose from radionuclide releases to the landscape from each repository part and from the whole repository (Sum).*

Table 6-6. Peak values of the mean annual doses and time at which the peak value is observed for releases to the landscape from each repository part and from the whole repository in the calculation case extreme permafrost with talik (CC8). The value given for each repository part is the sum of values obtained for all released radionuclides. The radionuclides with the highest contribution to the peak doses are indicated.

Repository part	Peak annual mean dose µSv/year	Time of the peak years AD	Most contributing radionuclide
Silo	4.5	around 5,000	Organic C-14
BMA	9.4	around 22,000	Inorganic C-14
1BTF	0.2	around 5,000	Inorganic C-14
2BTF	2.4	around 5,000	Inorganic C-14
BLA	0.01	around 5,000	Inorganic C-14
Total SFR 1	12	around 5,000	Inorganic C-14

6.4.2 Doses from releases to a well

Doses from release to a well have not been calculated for this calculation case. Before the first permafrost period this calculation case coincides with the calculation case extreme permafrost without talik (CC7). The results for the calculation case extreme permafrost (CC7) are shown in Figures 6-15 to 6-19. Doses from releases to a well during later temperate periods will be lower in this case compared to the calculation case extreme permafrost (CC7), since releases of radionuclides occur also during the permafrost periods through the talik which reduces the inventory.

6.5 Talik (CC2)

This calculation case (CC2) is a variant of the Weichselian variant, with the same assumptions concerning degradation of engineered barriers. In this case the situation is considered that during periods of continuous permafrost the groundwater within the repository remains un-frozen as does areas of the geosphere between the repository and the ground surface, such that a migration route for radionuclides to the biosphere is developed. During such periods the releases from the geosphere are directed through taliks to a larger lake. For the calculations it is assumed that radionuclide releases during permafrost are directed to a lake formed in this region at a future time. This lake was assumed to have the same properties, like volume, water retention times, as the last lake formed due to shore displacement in the Forsmark area /SKB 2006b/. The lake that is formed at around year 5,000 has a high probability of being transformed to a mire /Brydsten 2006/, at around year 7,000, and can therefore not be the recipient for releases through taliks during permafrost periods.

6.5.1 Doses from releases to the landscape

The results of the screening study are presented in Table 6-8. The same radionuclides, as for the Weichselian variant, are identified as potential important dose contributors.

The results until the start of the first permafrost period are the same as for the Weichselian variant. However, at later time periods higher values, than in the Weichselian variant, are observed for some radionuclides, e.g. inorganic C-14 for the BMA and I-129 for the Silo. The time dynamics of the mean annual doses are shown in Figures 6-26 to 6-30. The peak observed at around year 5,000 is caused by C-14 releases, as in the Weichselian variant. For the Silo and the BMA minor peak values of the mean annual doses are observed at later time points in connection with the formation of taliks, when the groundwater flow increases by a factor of 10 compared to the temperate conditions /Thomson et al. 2008/. This causes an increase of the releases to the biosphere of long-lived and relatively mobile radionuclides, like Ni-59, I-129 and Cs-135. For the 1BTF, the 2BTF and the BLA no notable influence of the taliks is observed. The smaller amount of activity in these repository parts together with the lack of effective barriers, result in that most of the activity has already been released at the time when the groundwater flow increases in connection with the formation of taliks.

Table 6-8. Results of the screening study for the calculation case Talik (CC2). The peak value of the Screening Quotient (SQ) and the time (in years AD) at which the peak SQ is observed are presented for each repository part. Values are given only for radionuclides for which SQ above 1 were obtained.

Radionuclide		Silo	BMA	BLA	1BTF	2BTF
C-14-in	Peak SQ		29		10	70
	Time		44,050		5,090	5,060
C-14-org	Peak SQ	85	67			6
	Time	5,540	5,060			5,039
Ni-59	Peak SQ		12		2	4
	Time		17,040		7,240	7,240
Se-79	Peak SQ		4			
	Time		7,240			
Mo-93	Peak SQ		3			
	Time		7,240			
I-129	Peak SQ	5	9			
	Time	77,040	7,240			
Cs-135	Peak SQ	17	197		4	28
	Time	39,040	7,240		7,240	7,240

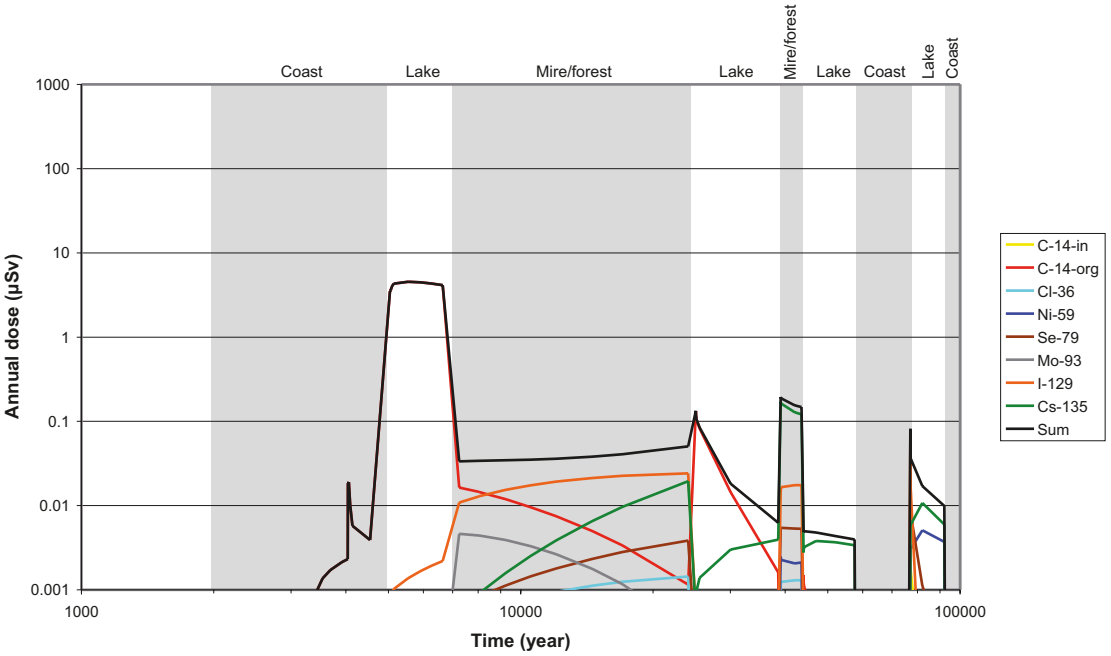

Figure 6-26. *Talik (CC2), Silo. Mean values of the annual individual dose from radionuclide releases to the landscape from the Silo. The sum corresponds to the total dose considering all released radionuclides.*

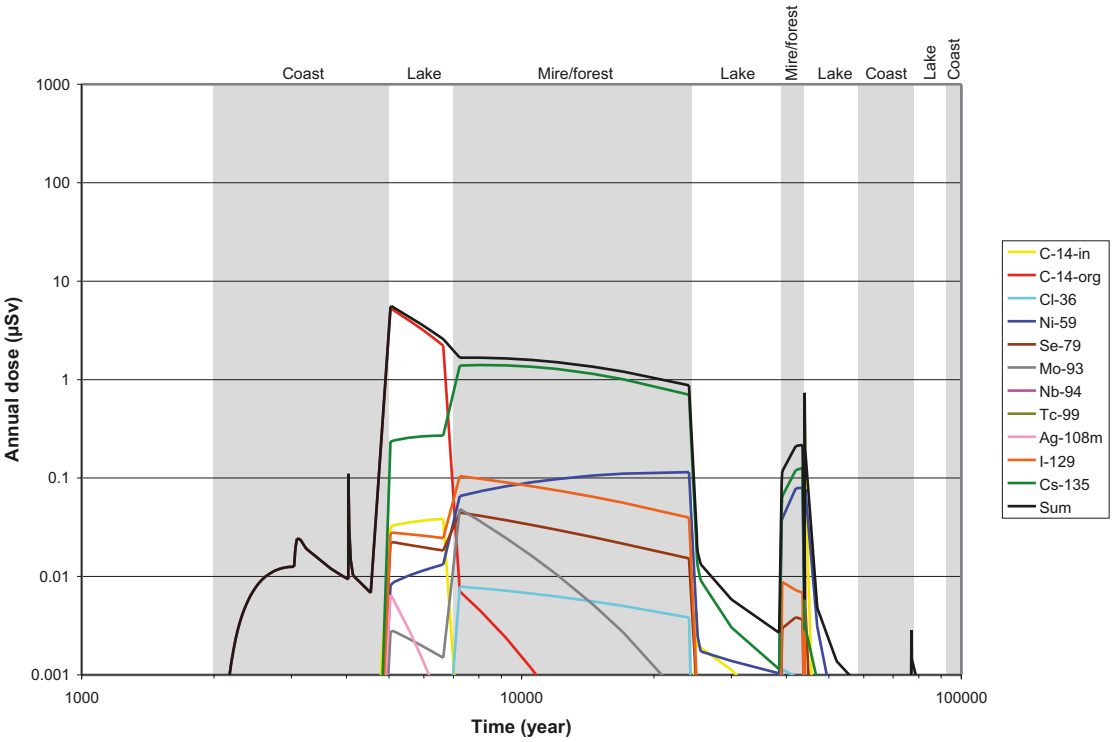

Figure 6-27. *Talik (CC2), BMA. Mean values of the annual individual dose from radionuclide releases to the landscape from the BMA. The sum corresponds to the total dose considering all released radionuclides.*

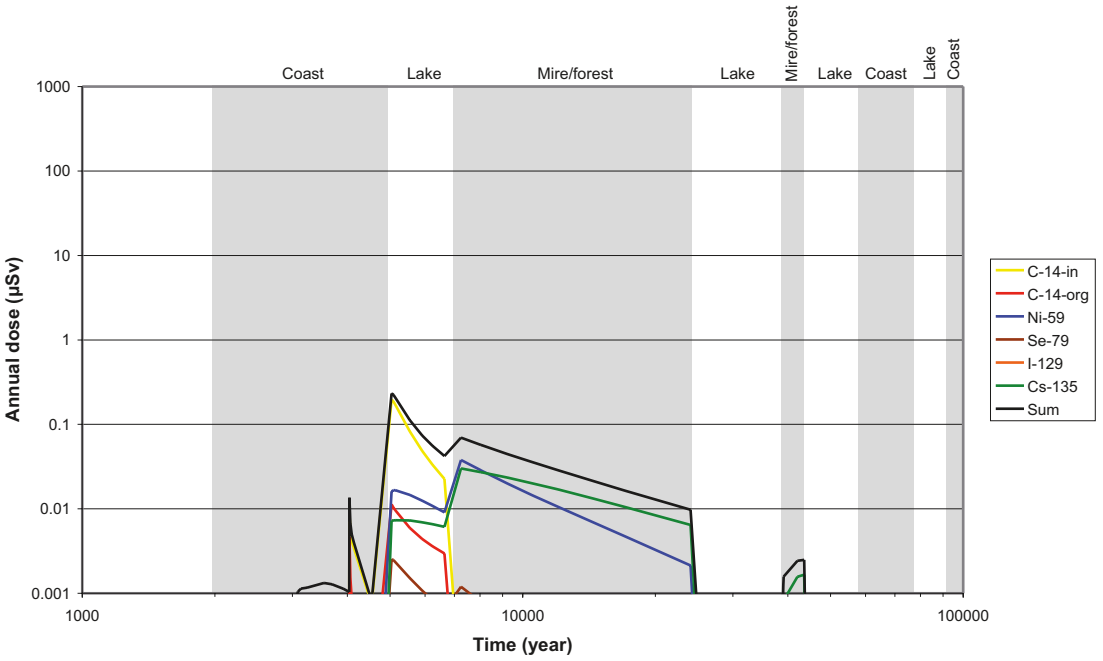

Figure 6-28. *Talik (CC2), 1BTF. Mean values of the annual individual dose from radionuclide releases to the landscape from the 1BTF. The sum corresponds to the total dose considering all released radionuclides.*

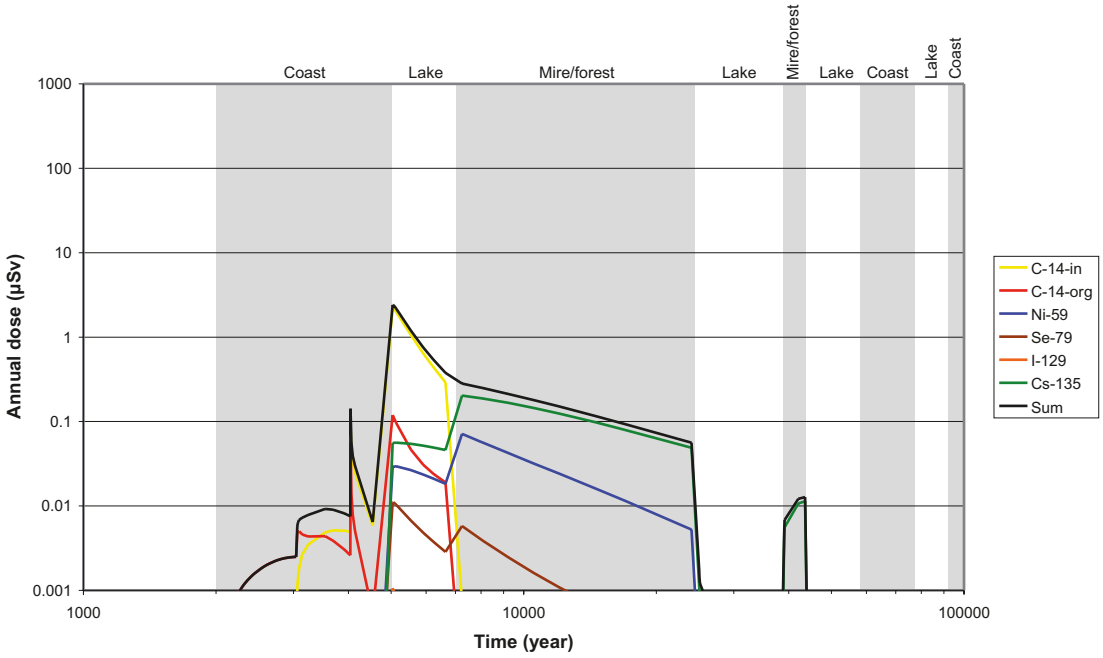

Figure 6-29. *Talik (CC2), 2BTF. Mean values of the annual individual dose from radionuclide releases to the landscape from the 2BTF. The sum corresponds to the total dose considering all released radionuclides.*

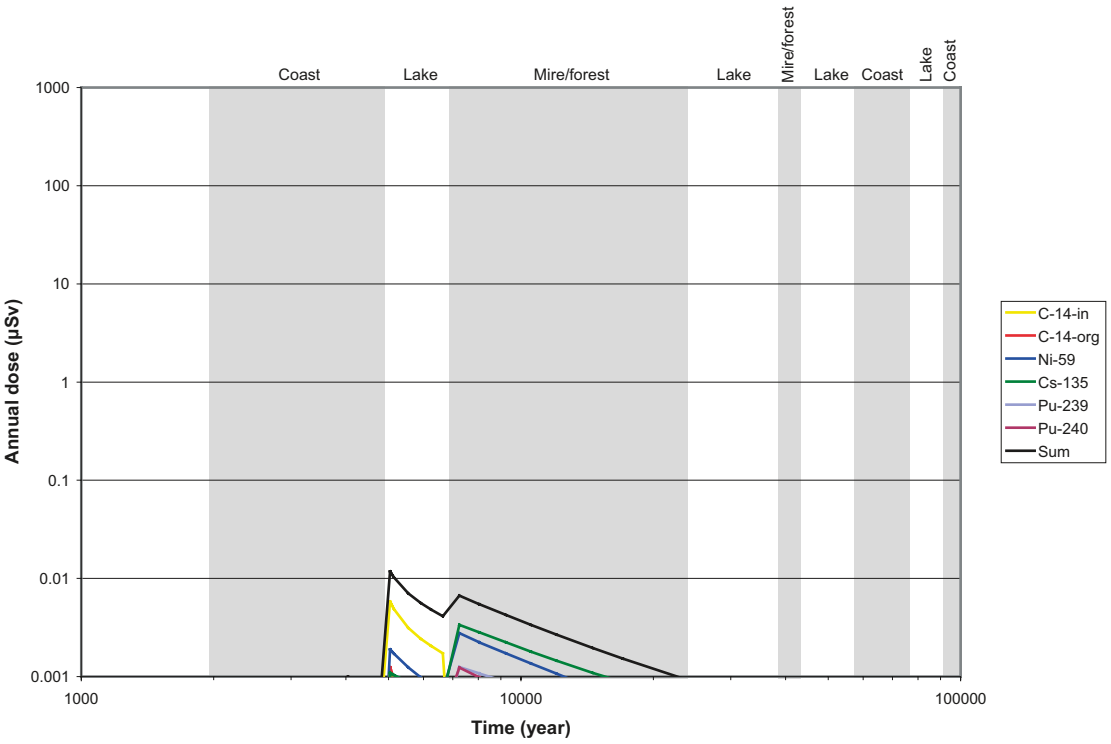

Figure 6-30. *Talik (CC2), BLA. Mean values of the annual individual dose from radionuclide releases to the landscape from the BLA. The sum corresponds to the total dose considering all released radionuclides.*

Figure 6-31 presents the total mean annual doses from the whole repository, and for each repository part, taking into account all released radionuclides. As expected, for the period until the first permafrost the time dependencies of the annual doses are the same as for the Weichselian variant. During the whole simulation period the mean annual doses are dominated by the Silo and/or the BMA. A summary of peak values of the mean annual doses for each repository part and for the whole repository is presented in Table 6-9. It can be appreciated that the peak values for this calculation case are the same that the values obtained for the Weichselian variant.

Table 6-9. Peak values of the mean annual doses and time at which the peak value is observed for releases to the landscape from each repository part and from the whole repository in the calculation case Talik (CC2). The value given for each repository part is the sum of values obtained for all released radionuclides. The radionuclides with the highest contribution to the peak doses are indicated.

Repository part	Peak annual dose µSv/year	Time of the peak years AD	Most contributing radionuclide
Silo	4.5	around 5,000	Organic C-14
BMA	5.6	around 5,000	Organic C-14
1BTF	0.2	around 5,000	Inorganic C-14
2BTF	2.4	around 5,000	Inorganic C-14
BLA	0.01	around 5,000	Inorganic C-14
Total SFR 1	12	around 5,000	Organic C-14

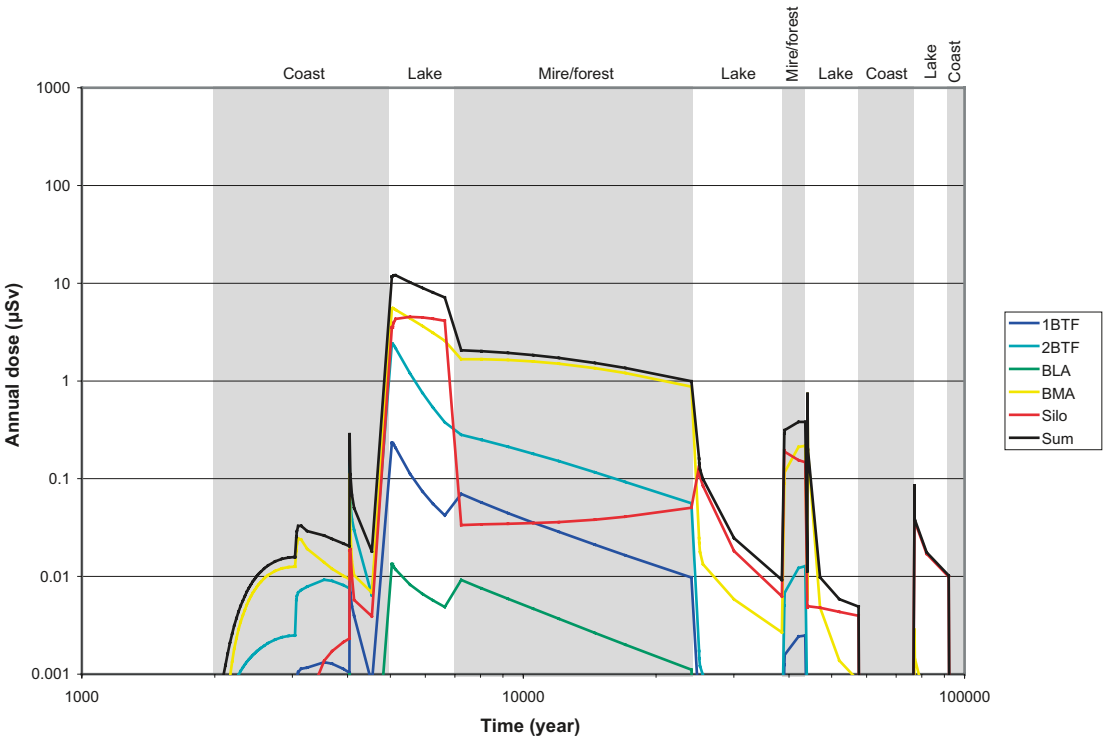

Figure 6-31. *Talik (CC2), SFR 1. Mean values of the total annual individual dose from radionuclide releases to the landscape from each repository part and from the whole repository (Sum).*

6.5.2 Doses from releases to a well

Doses from release to a well have not been calculated for this calculation case. Before the first permafrost period this calculation case coincides with the Weichselian variant. The results for the Weichselian variant are shown in Figures 5-8 to 5-12. Doses from releases to a well during later temperate periods will be lower in this case compared to the Weichselian variant, since releases of radionuclides occur also during the permafrost periods through the talik which reduces the inventory.

6.6 High concentrations of complexing agents (CC9)

This calculation case (CC9) considers the potential consequences for radionuclide releases from the repository under conditions in which the levels of complexing agents within the near-field are significantly higher than those considered in the Weichselian variant, which can lead to a reduction of the sorption in the near field for the Silo, the BMA, 1BTF and the 2BTF. For the BLA the sorption is not considered even in the Weichselian variant. All other assumptions in this calculation case are the same that for the Weichselian variant.

The calculations for this calculation case were done deterministically, using nominal values for the model parameters.

6.6.1 Doses from releases to the landscape

Time series of the annual doses to the most exposed group resulting from radionuclide releases to the landscape from the different repository parts are presented in Figures 6-32 to 6-35. Both the total dose from all radionuclides and the doses from the radionuclides with the highest contribution are presented in these figures. The time variations and levels of the total doses for the different repository parts were very close to the values obtained for the Weichselian variant. This was expected, as the radionuclides that contribute most to the total doses, C-14, Ni-59 and Cs-135, are not sensitive to changes in the concentrations of complexing agents. All other radionuclides give doses that are below 0.1 µSv/y and have a negligible contribution to the total doses. The most important effect of the higher concentrations of complexing agents is that radionuclides are released earlier to the biosphere. This has a marginal effect on the dose levels, which even are lower for the 1BTF and 2BTF than in the Weichselian variant, as the earlier releases are directed to the sea basin, where doses per unit release rate are lower. It can be observed from comparison of Figures 6-33 to 6-35 with the corresponding figures for the Weichselian variant (Chapter 5) that for the BMA, 1BTF and 2BTF the doses from actinides are higher than the values obtained for the Weichselian variant. However, the dose levels for these radionuclides are several orders of magnitude below the peak doses.

Figure 6-36 presents the total annual doses from the whole repository, and for each repository part, taking into account all released radionuclides. As for the Weichselian variant, the Silo and the BMA give the highest contribution to the peak doses due to their larger inventory of C-14. A summary of the peak values of the annual doses for each repository part and the whole repository is presented in Table 6-10. The peak values for this calculation case are nearly the same as for the Weichselian variant. Somewhat lower values were obtained for the 1BTF and 2BTF for the reasons explained above.

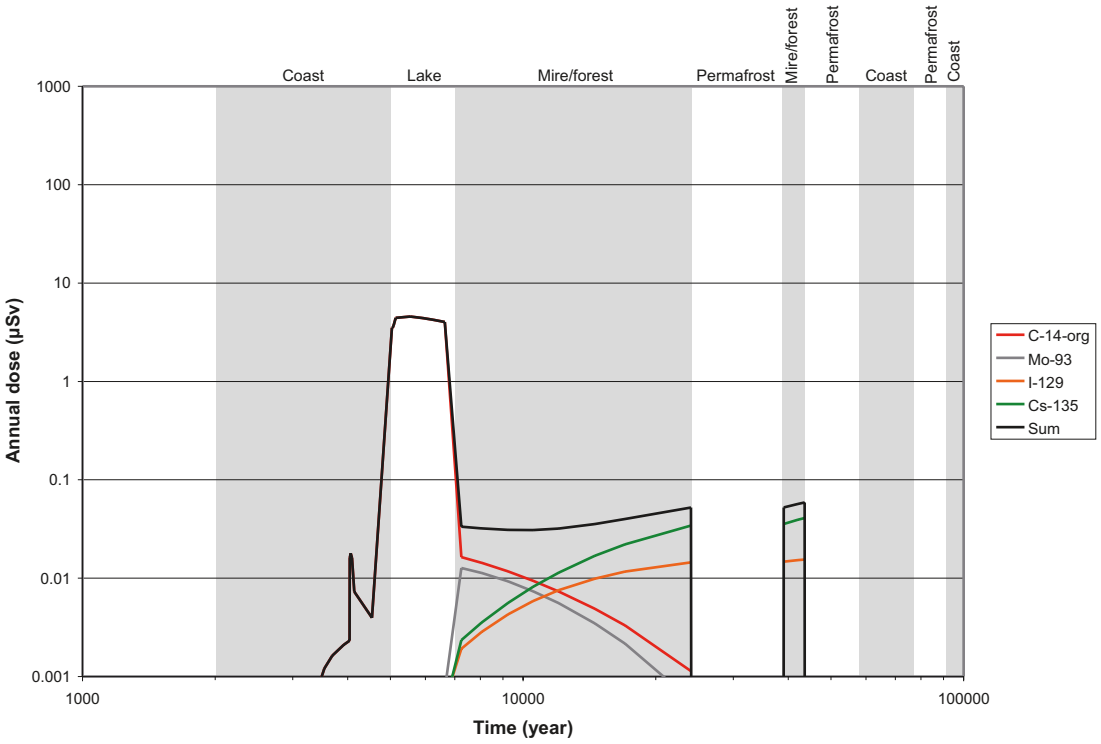

Figure 6-32. *High concentrations of complexing agents (CC9), Silo. Annual individual doses from radionuclide releases to the landscape from the Silo. The sum corresponds to the total dose considering all released radionuclides.*

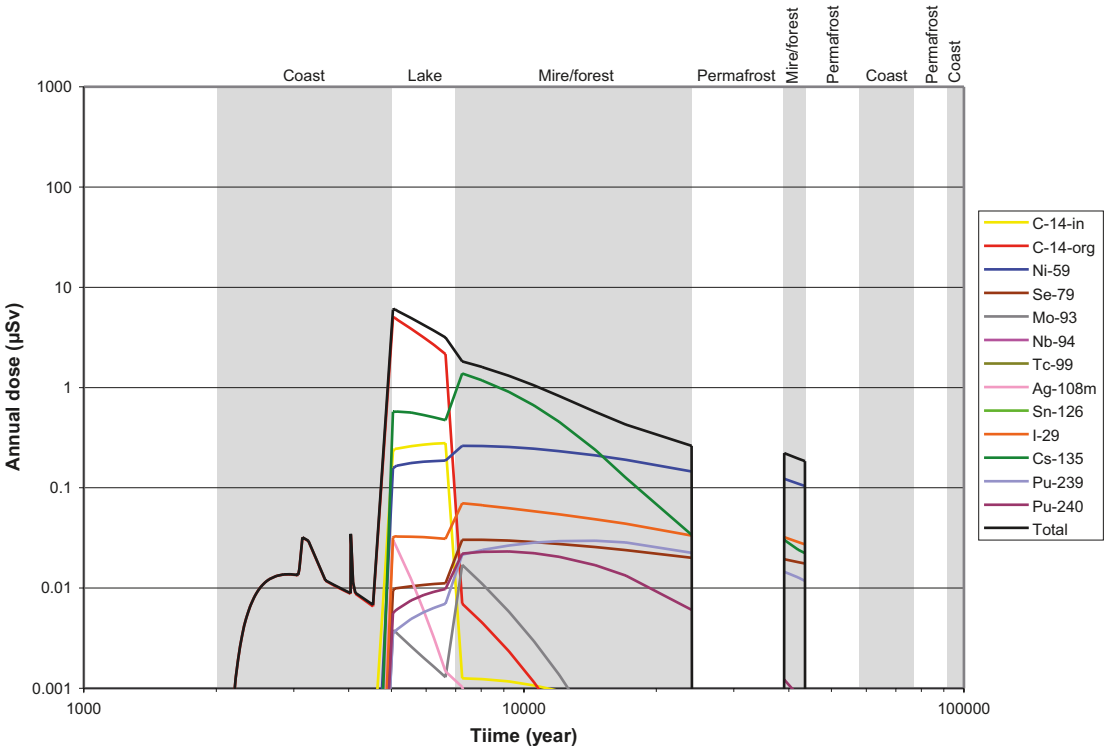

Figure 6-33. *High concentrations of complexing agents (CC9), BMA. Annual individual doses from radionuclide releases to the landscape from the BMA. The sum corresponds to the total dose considering all released radionuclides.*

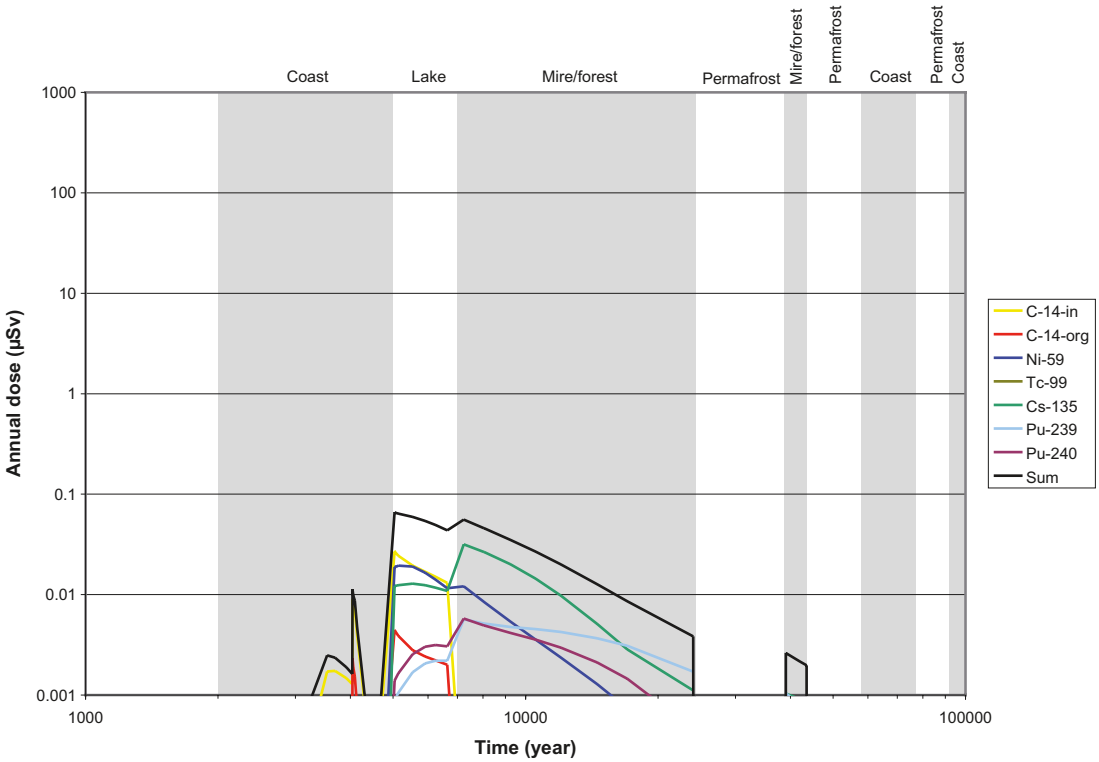

Figure 6-34. *High concentrations of complexing agents (CC9), 1BTF. Annual individual doses from radionuclide releases to the landscape from the 1BTF. The sum corresponds to the total dose considering all released radionuclides.*

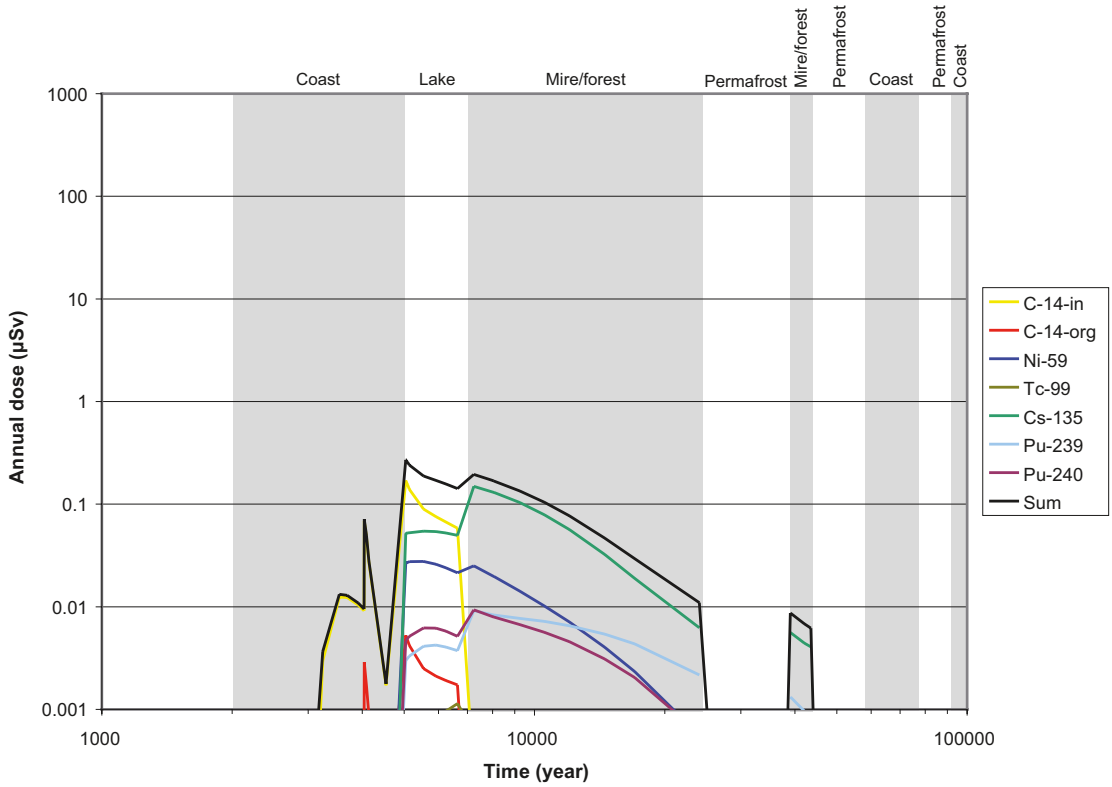

Figure 6-35. *High concentrations of complexing agents (CC9), 2BTF. Annual individual doses from radionuclide releases to the landscape from the 2BTF. The sum corresponds to the total dose considering all released radionuclides.*

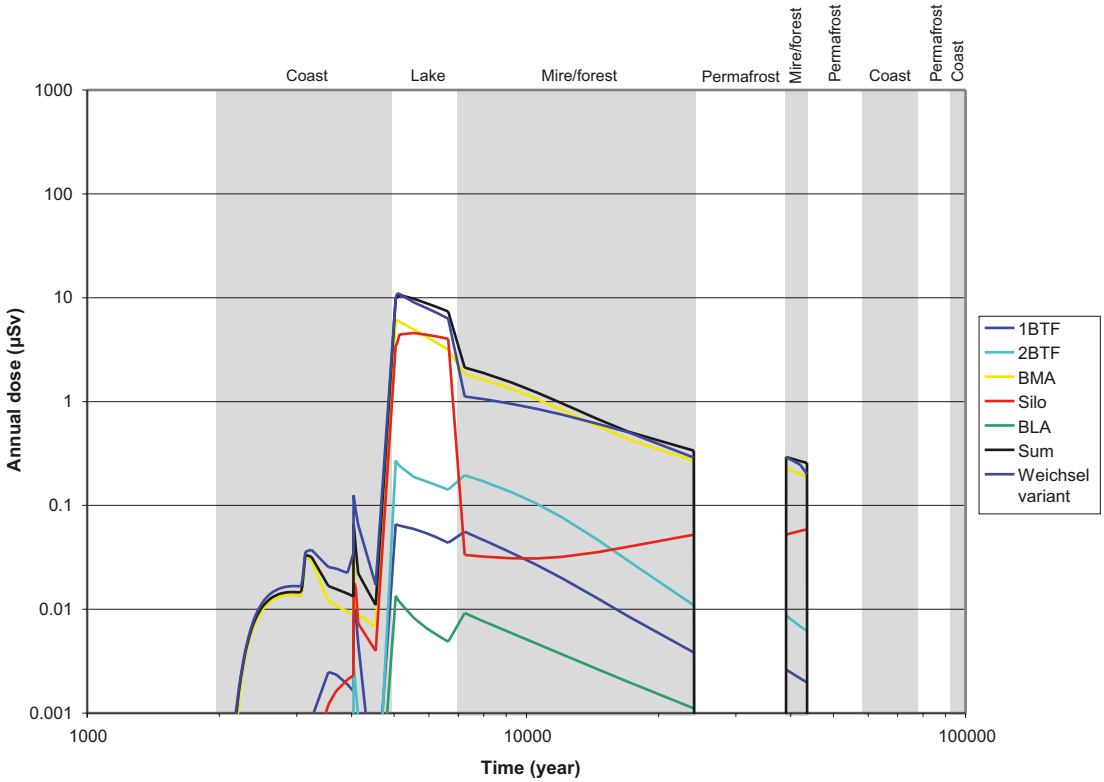

Figure 6-36. *High concentrations of complexing agents (CC9), SFR 1. Total annual individual dose from radionuclide releases to the landscape from each repository part and from the whole repository (Sum).*

Table 6-10. Peak values of the annual doses and time at which the peak value is observed for releases to the landscape from each repository part and from the whole repository in the calculation case high concentrations of complexing agents (CC9). The value given for each repository part is the sum of values obtained for all released radionuclides. The radionuclides with the highest contribution to the peak doses are indicated.

Repository part	Peak annual dose µSv/year	Time of the peak years AD	Most contributing radionuclide
Silo	4.6	around 5,000	Organic C-14
BMA	6.1	around 5,000	Organic C-14
1BTF	0.07	around 5,000	Inorganic C-14
2BTF	0.3	around 5,000	Inorganic C-14
BLA	0.01	around 5,000	Inorganic C-14
Total SFR 1	11	around 5,000	Organic C-14

6.6.2 Doses from releases to a well

Time series of the mean annual doses from releases to a well are presented in Figures 6-37 to 6-40. The most important difference when compared to the Weichselian variant is that the doses are dominated by the actinides Pu-239 and Pu-240. This is explained by higher release rates of these radionuclides, as compared to the Weichselian variant, caused by reduction of their sorption in the near field due to the presence of higher concentration of complexing agents. The increase in the release rate of the actinides produces a higher increase in the doses from a well than in the doses from releases to the landscape. The reason for this is that these radionuclides usually have lower uptake in biota. Hence, they give low doses from food ingestion if released to soil or water compartments of landscape objects, like lakes and mires. However, when released to a well, and the well water is used for irrigation, these radionuclides can directly contaminate the vegetables via interception of the irrigation water by the above parts of the plant.

A summary of the peak values of the annual doses for each repository parts and the whole repository is presented in Table 6-11. The peak values are around a factor of two higher than the values for the Weichselian variant. However, the difference between these two calculation cases would have considerably lower if 50-years moving averages would have been taken even for the calculation case with high concentrations of complexing agents.

Table 6-11. Peak values of the annual dose and time at which the peak value is observed for releases to a well from each repository part and from the whole repository (all vaults) in the calculation case high concentrations of complexing agents (CC9). The value given for each repository part is the sum of values obtained for all released radionuclides. The radionuclides with the highest contribution to the peak doses are indicated.

Repository part	Peak annual dose µSv/year	Time of the peak years AD	Most contributing radionuclide
Silo	2.7	around 4,000	Organic C-14
BMA	10	around 4,000	Mo-93
1BTF	2.2	around 4,000	Inorganic C-14
2BTF	6.4	around 4,000	Inorganic C-14
BLA	0.5	around 4,000	Inorganic C-14
All vaults	19	around 4,000	Mo-93

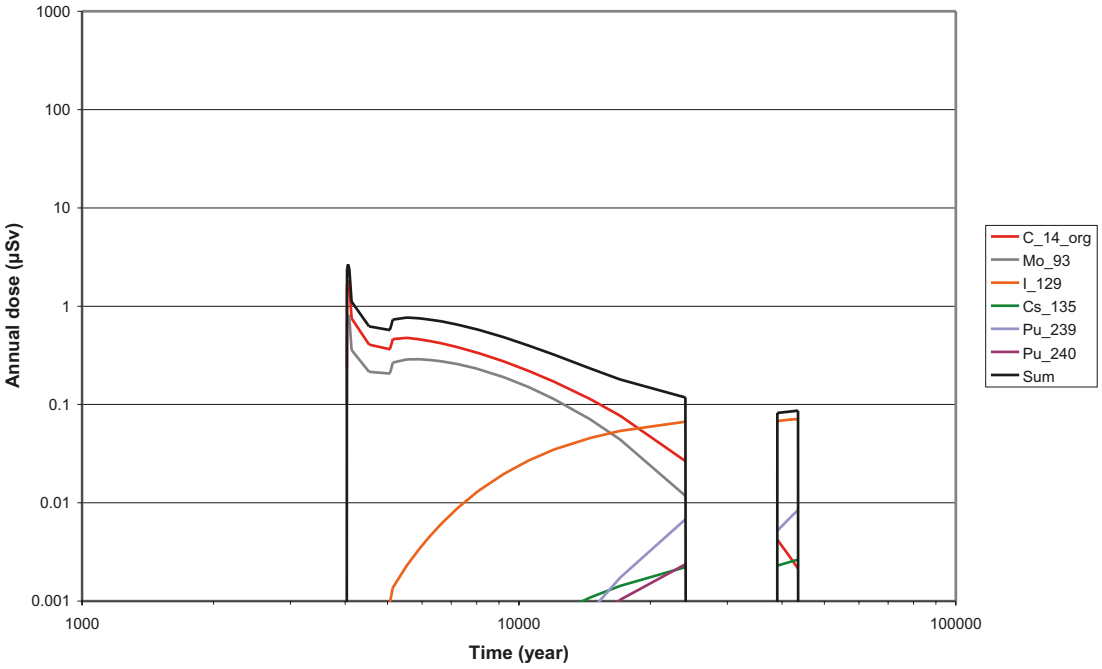

Figure 6-37. *High concentrations of complexing agents (CC9), Silo. Annual doses from radionuclide releases to a well from the Silo. The sum corresponds to the total dose considering all released radionuclides.*

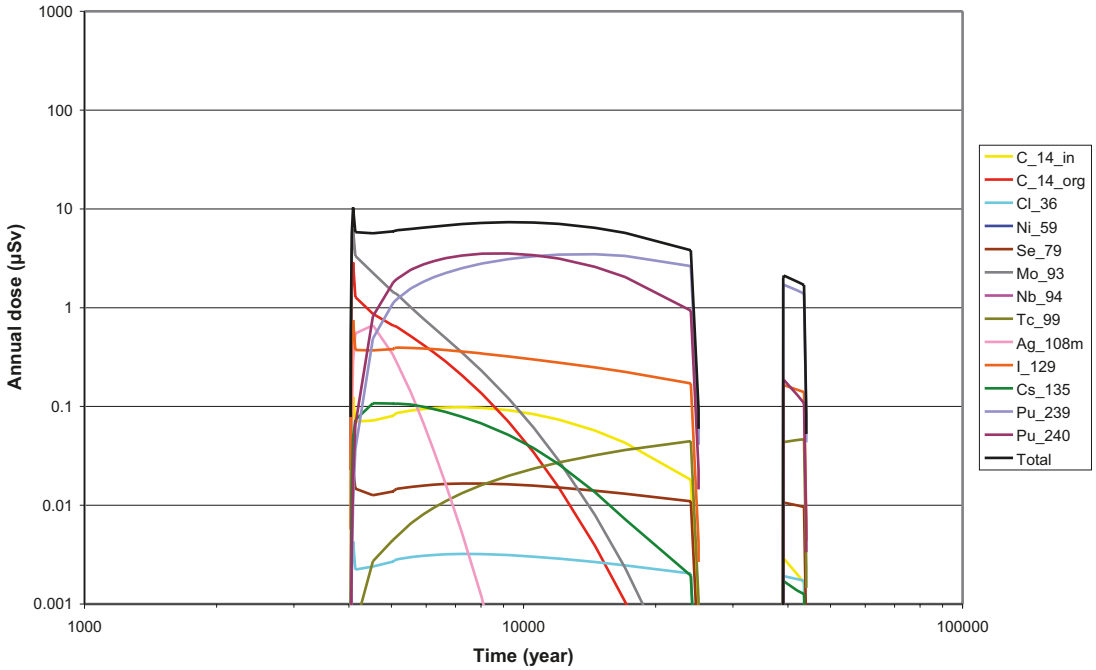

Figure 6-38. *High concentrations of complexing agents (CC9), BMA. Annual doses from radionuclide releases to a well from the BMA. The sum corresponds to the total dose considering all released radionuclides.*

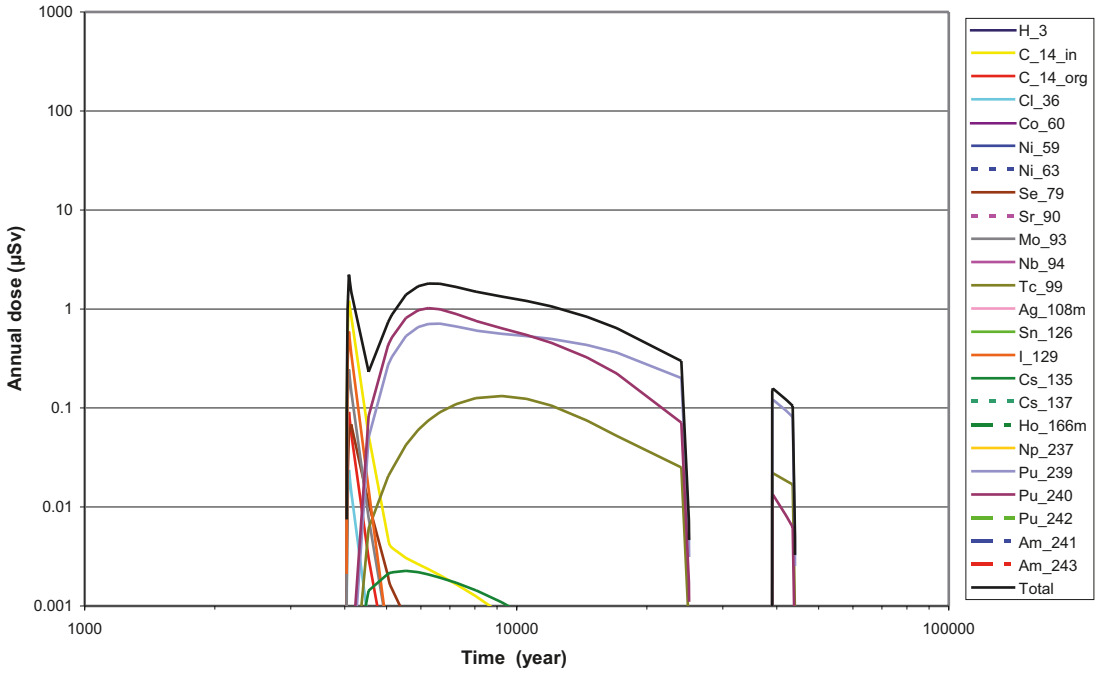

Figure 6-39. *High concentrations of complexing agents (CC9), 1BTF. Annual doses from radionuclide releases to a well from the 1BTF. The sum corresponds to the total dose considering all released radionuclides.*

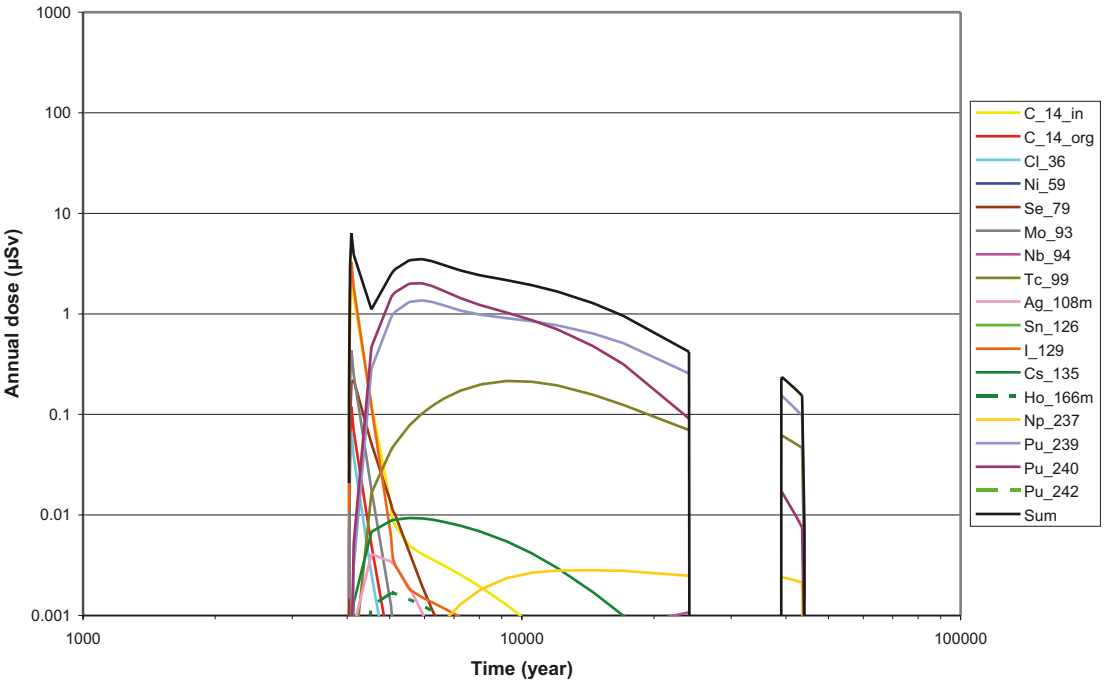

Figure 6-40. *High concentrations of complexing agents (CC9), 2BTF. Annual doses from radionuclide releases to a well from the 2BTF. The sum corresponds to the total dose considering all released radionuclides.*

6.7 Gas generated advection (CC10)

This calculation case (CC10) considers the potential consequences for radionuclide releases from the Silo when the impact of bulk gas generation is taken into account. This causes an increased initial radionuclide transport and increased releases to the biosphere. All other assumptions are likewise the Weichselian variant (CC1).

6.7.1 Doses from releases to the landscape

Time series of the mean values of the annual doses to the most exposed group resulting from radionuclide releases to the landscape from the Silo are presented in Figure 6-41. A comparison of this figure with the equivalent figure for the Weichselian variant (Figure 5-1) shows that the time dynamic and the dose levels are practically the same in both calculation cases. So, early releases, by gas driven advection, do not affect the peak values of doses to the most exposed group. The reason is that these releases are directed to a sea basin where the dilution is higher and the residence time of the water is shorter. This results in lower annual doses per unit release rate, than when releases are directed to a lake or a mire at later time periods.

6.7.2 Doses from releases to a well

Doses from releases to a well were not considered for this calculation case. The main effect of this calculation case occurs at very early stages after the repository closure, when drilling of a well is not a relevant option as the rock above the repository will be covered with water.

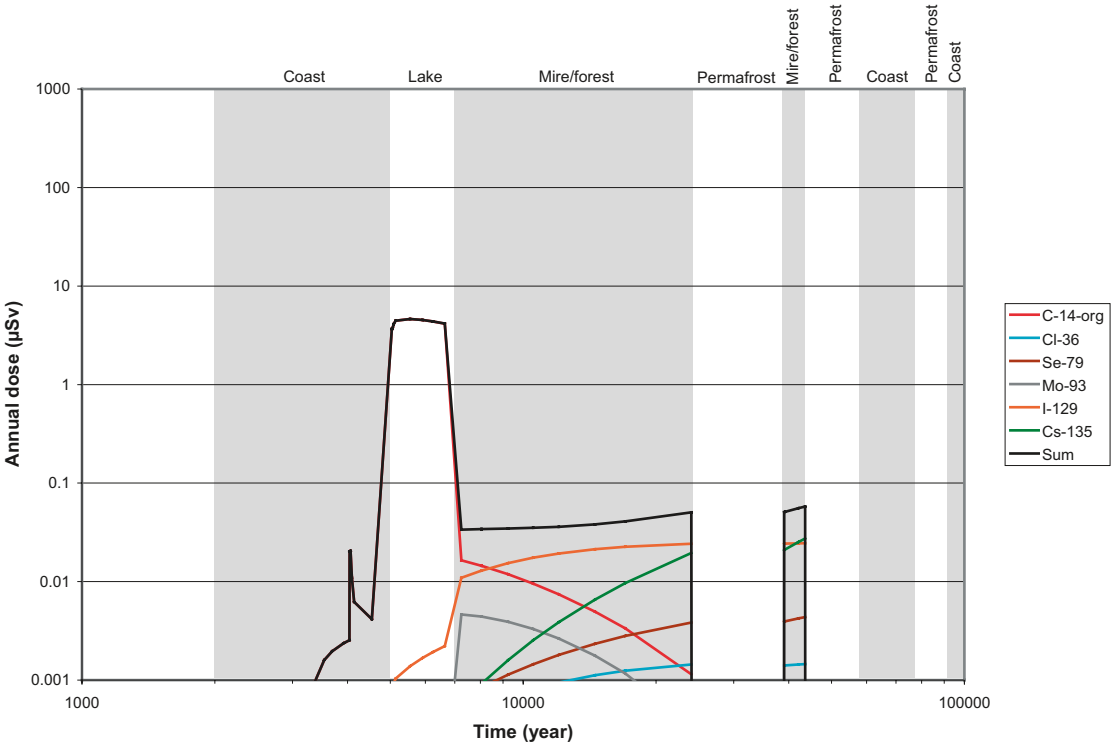

Figure 6-41. *Gas generated advection (CC10), Silo. Mean values of the annual individual dose from radionuclide releases to the landscape from the Silo.*

6.8 Intrusion well (CC11)

The calculation case intrusion well (CC11) considers the potential dose consequences from inadvertent intrusion in the repository due to drilling of wells. Consequences are calculated for an annual intake of water from the gravel surrounding the Silo or a vault.

In this scenario two variants of calculations were carried out: i) one with assumptions as in the Weichselian variant (CC1) and ii) one with assumptions as in the calculation case with high concentrations of complexing agents (CC9).

The dose calculations were carried out deterministically, using nominal values for the model parameters.

6.8.1 Intrusion well with assumptions as in the Weichselian variant

Doses from consumption of water in the gravel surrounding the Silo or a vault are shown in Figures 6-42 to 6-46, respectively. These concentrations are obtained from the calculations of the release rates of radionuclides from the repository in the Weichselian variant. Highest dose rates occur immediately around year 3,000, the first time point when wells could be drilled, as the shore level has passed the area above the repository.

The dominant radionuclide for the Silo is organic C-14, as this radionuclide is not delayed by sorption in the barriers and its inventory is high in the Silo. The dose from I-129 increases with time, as this radionuclide sorbs slightly in the technical barriers. All other radionuclides are effectively retained by the barriers causing doses below 1 µSv per year and in most cases below 0.01 µSv per year. The total dose decreases continuously during the whole simulation period.

Results for BMA are shown in Figure 6-43. Organic C-14 and I-129 give the highest dose rate, 73 µSv per year, around year 3,000. The dose rates decrease considerably after this peak-value to values below 1 µSv per year. Similarly to the Silo, there is a limited amount of radionuclides which give a substantial contribution to the total dose.

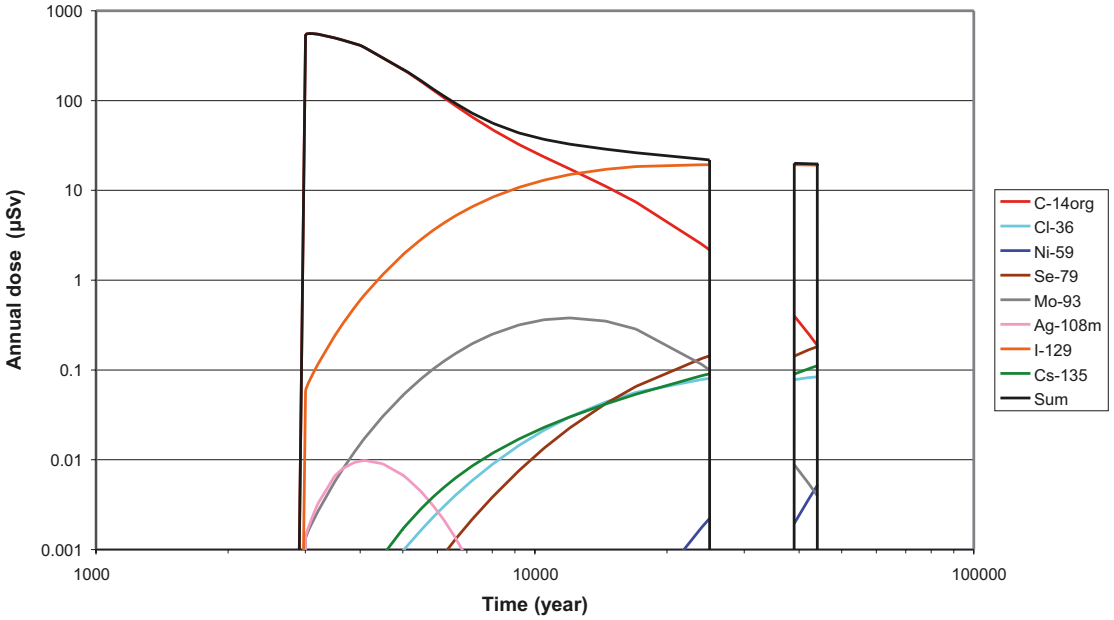

Figure 6-42. *Intrusion well with assumptions as in the Weichselian variant (CC11), Silo. Annual individual dose per radionuclide and sum from the Silo. Permafrost conditions prevail from year 25,000 to year 39,000 and no intrusion wells are expected during that time period. No wells are expected after year 44,000 due to either permafrost conditions or because the area above the repository is either covered by ice or below sea water.*

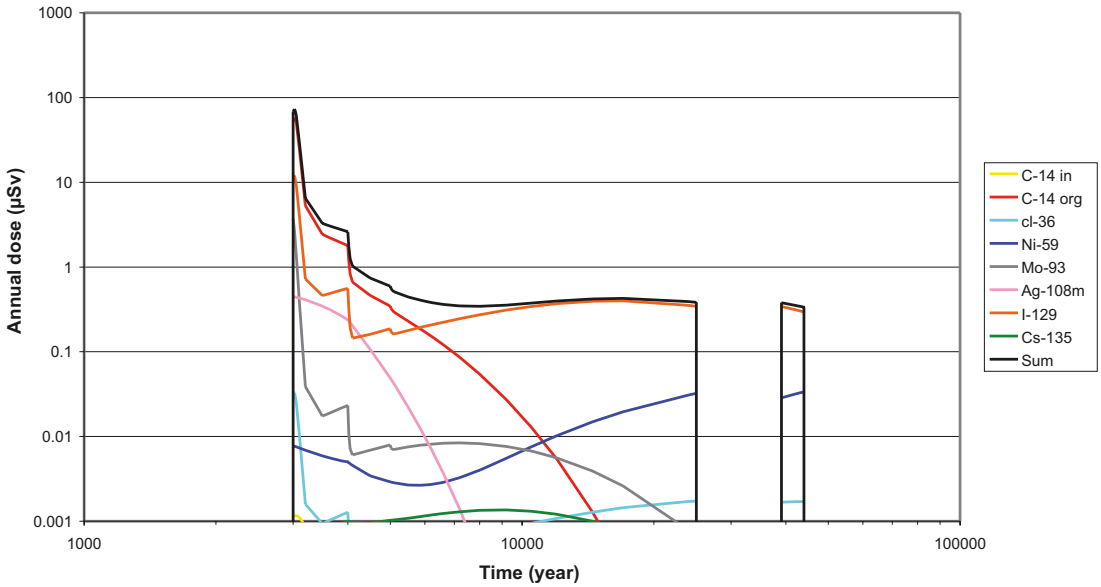

Figure 6-43. *Intrusion well with assumptions as in the Weichselian variant (CC11), BMA. Annual individual dose per radionuclide and sum from the BMA. Permafrost conditions prevail from year 25,000 to year 39,000 and no intrusion wells are expected during that time period. No wells are expected after year 44,000 due to either permafrost conditions or because the area above the repository is either covered by ice or below sea water.*

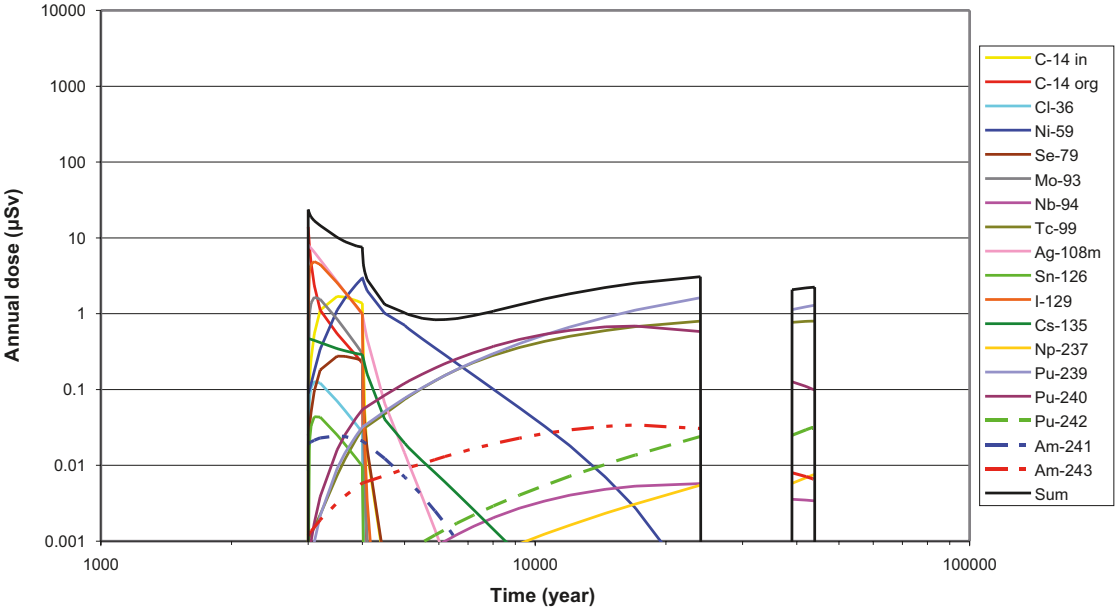

Figure 6-44. *Intrusion well with assumptions as in the Weichselian variant (CC11), 1BTF. Annual individual dose per radionuclide and sum from the 1BTF. Permafrost conditions prevail from year 25,000 to year 39,000 and no intrusion wells are expected during that time period. No wells are expected after year 44,000 due to either permafrost conditions or because the area above the repository is either covered by ice or below sea water.*

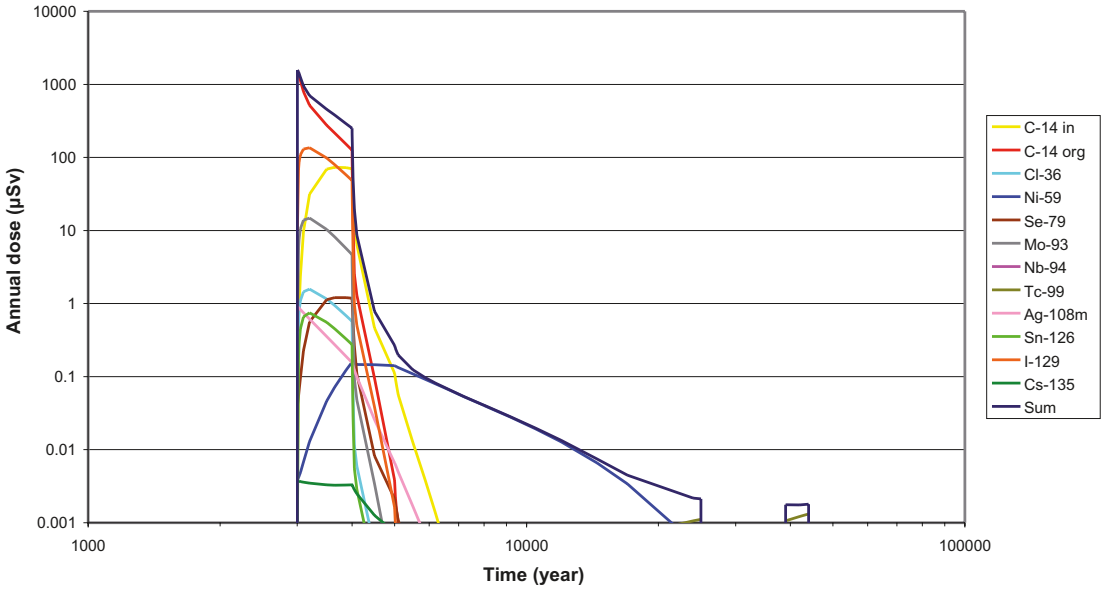

Figure 6-45. *Intrusion well with assumptions as in the Weichselian variant (CC11), 2BTF. Annual individual dose per radionuclide and sum from the 2BTF. Permafrost conditions prevail from year 25,000 to year 39,000 and no intrusion wells are expected during that time period. No wells are expected after year 44,000 due to either permafrost conditions or because the area above the repository is either covered by ice or below sea water.*

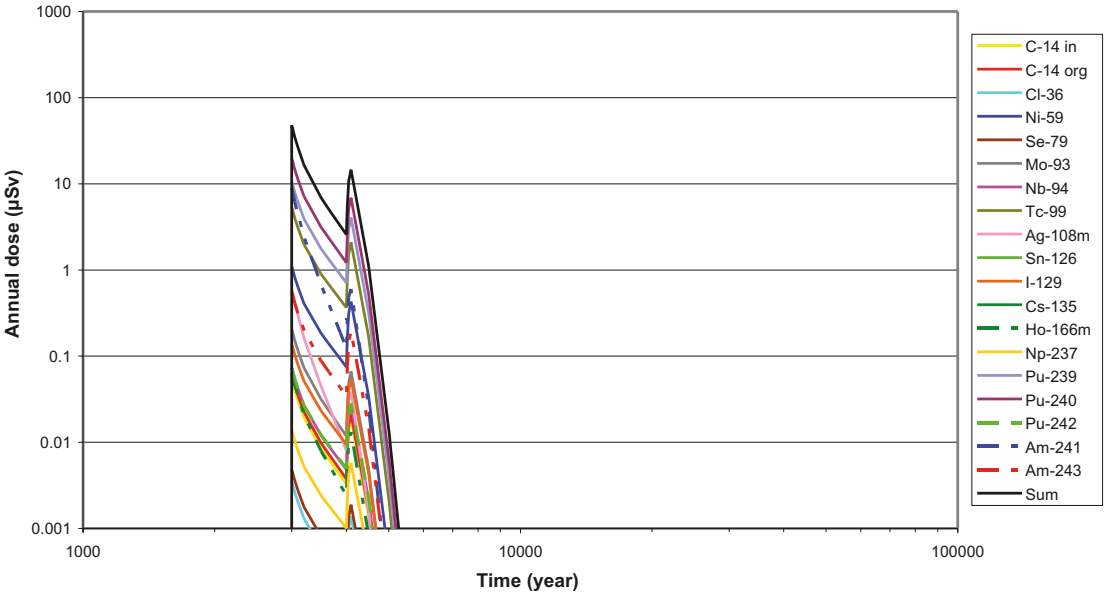

Figure 6-46. *Intrusion well with assumptions as in the Weichselian variant (CC11), BLA. Annual individual dose per radionuclide and sum from the BLA. Permafrost conditions prevail from year 25,000 to year 39,000 and no intrusion wells are expected during that time period. No wells are expected after year 44,000 due to either permafrost conditions or because the area above the repository is either covered by ice or below sea water.*

Results for 1BTF and 2BTF are shown in Figure 6-44 and 6-45, respectively. There are more radionuclides giving doses above 0,001 µSv per year for the 1BTF and the 2BTF compared to the Silo and the BMA. The radionuclide with the highest dose contribution is however still organic C-14, especially for the 2BTF, for which the highest dose is clearly dominated by organic C-14 and reaches about 1,600 µSv per year. The highest dose for the 1BTF is considerably lower, 24 µSv per year. For the 1BTF, on the other hand, actinides like Pu-239, Pu-240, Pu-242 and Am-243 give notable contributions to the dose at later time points. For the 2BTF there is no dose contribution from the actinides, due to different composition of the waste, and therefore doses decrease rapidly after the peak-value. The doses have decreased four orders of magnitude after 3,000 years.

The results for the BLA are presented in Figure 6-46. The actinides Pu-239, Pu-240 and Am-243 cause the highest exposure, as there is no sorption in the BLA and drinking water is an important exposure pathway for the α-decaying radionuclides. The lack of sorption is visible, as a second but lower peak in the dose rate occurs around year 4,000 when the groundwater flow is stepwise increased. However, the dose rates decrease substantially with time, and directly after year 5,000 the dose rates are below 0.001 µSv per year.

6.8.2 Intrusion well with assumptions as in calculation case high concentrations of complexing agents

Doses from consumption of water from the gravel surrounding the Silo and each vault are shown in Figures 6-47 to 6-50. These concentrations are obtained from the calculations of release rates of radionuclides from the repository in the calculation case high concentrations of complexing agents. No results are presented for the BLA as no sorption is considered for the BLA and increased levels of complexing agents do not affect the results.

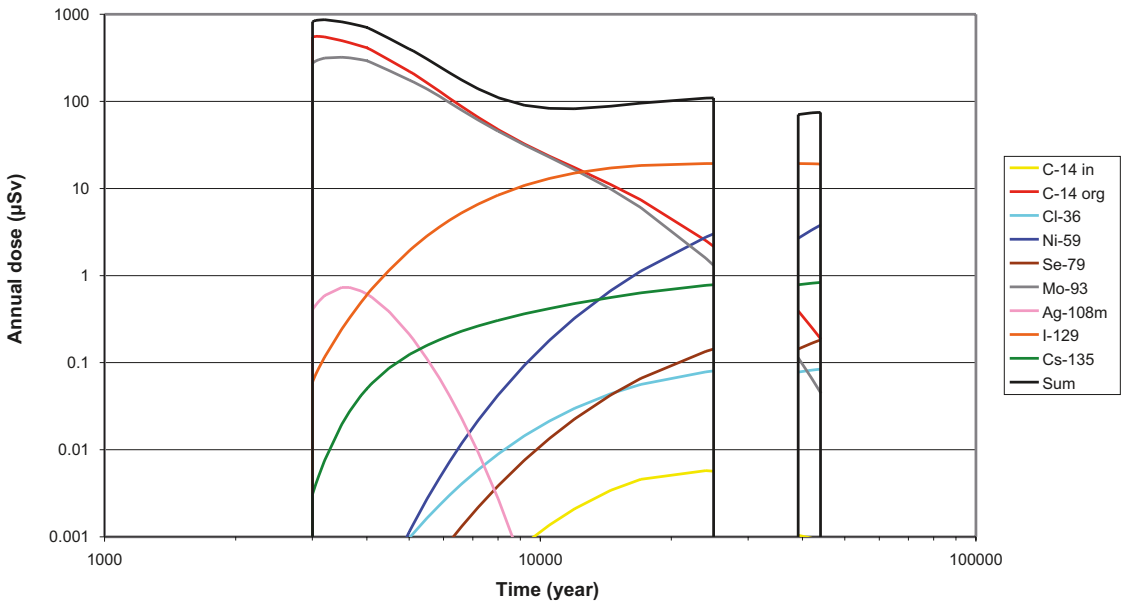

Figure 6-47. *Intrusion well with assumptions as in the calculation case high concentrations of complexing agents (CC11), Silo. Annual individual dose per radionuclide and sum from the Silo. Permafrost conditions prevail from year 25,000 to year 39,000 and no intrusion wells are expected during that time period. No wells are expected after year 44,000 due to either permafrost conditions or because the area above the repository is either covered by ice or below sea water.*

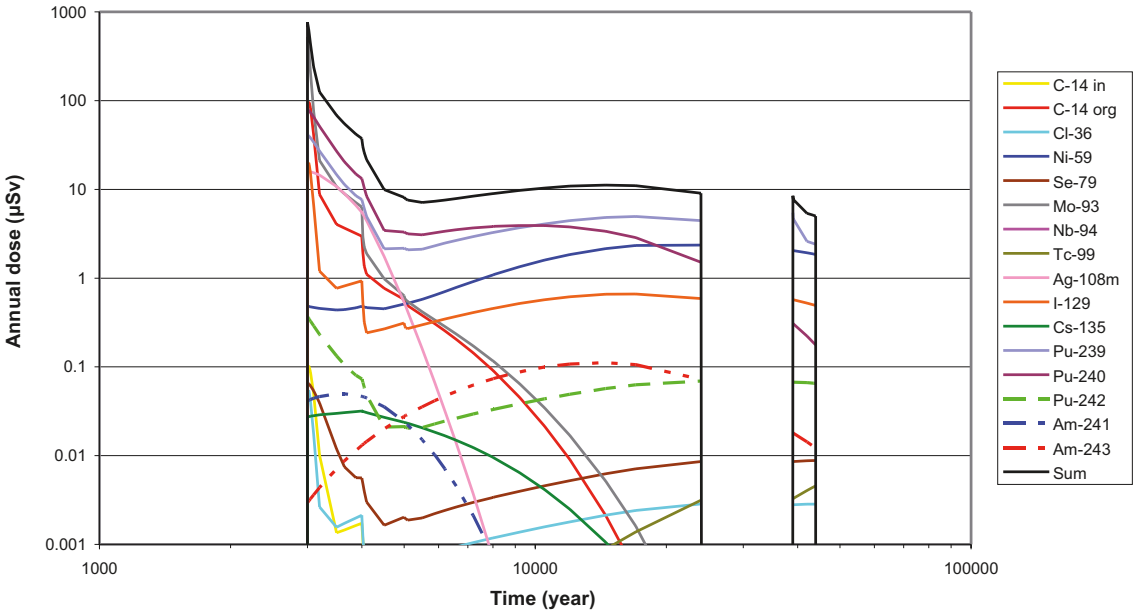

Figure 6-48. *Intrusion well with assumptions as in the calculation case high concentrations of complexing agents (CC11), BMA. Annual individual dose per radionuclide and sum from the BMA. Permafrost conditions prevail from year 25,000 to year 39,000 and no intrusion wells are expected during that time period. No wells are expected after year 44,000 due to either permafrost conditions or because the area above the repository is either covered by ice or below sea water.*

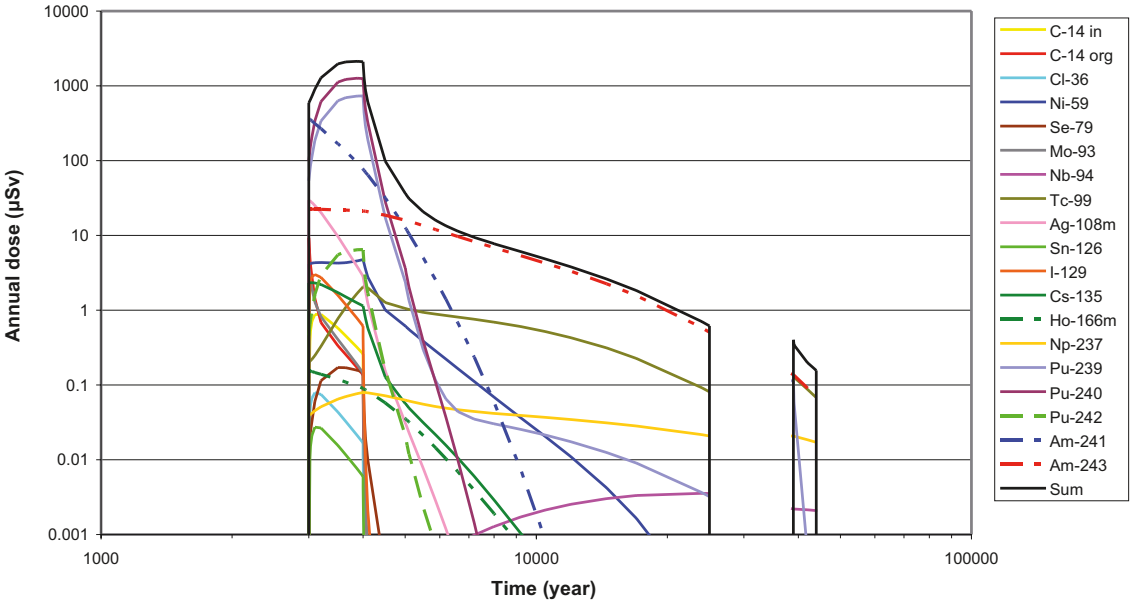

Figure 6-49. *Intrusion well with assumptions as in the calculation case high concentrations of complexing agents (CC11), 1BTF. Annual individual dose per radionuclide and sum from the 1BTF. Permafrost conditions prevail from year 25,000 to year 39,000 and no intrusion wells are expected during that time period. No wells are expected after year 44,000 due to either permafrost conditions or because the area above the repository is either covered by ice or below sea water.*

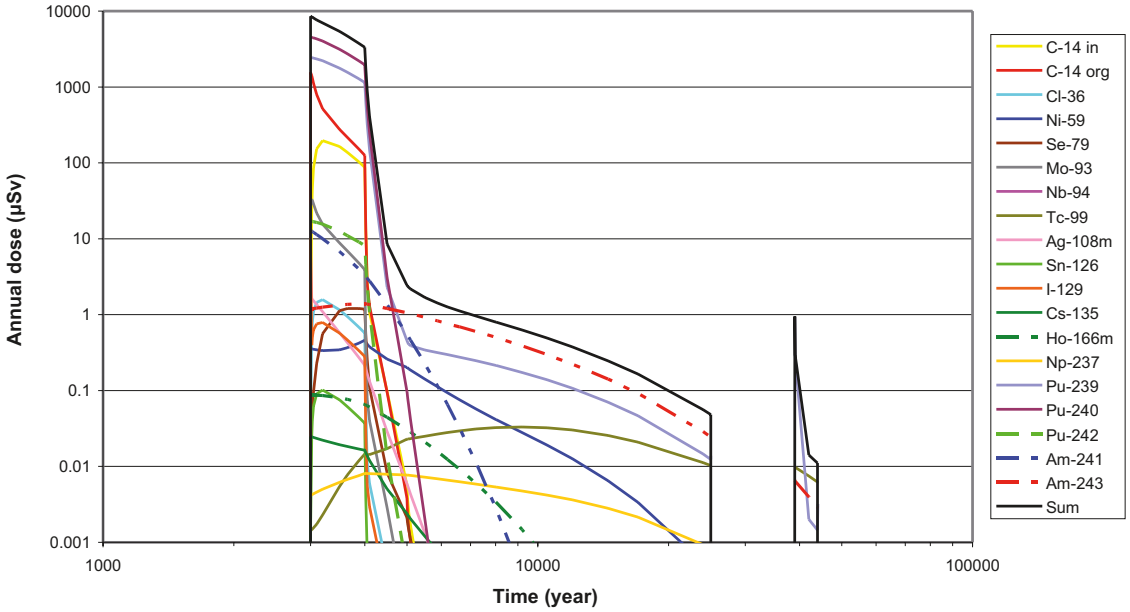

Figure 6-50. *Intrusion well with assumptions as in calculation case high concentrations of complexing agents (CC11), 2BTF. Annual individual dose per radionuclide and sum from the 2BTF. Permafrost conditions prevail from year 25,000 to year 39,000 and no intrusion wells are expected during that time period. No wells are expected after year 44,000 due to either permafrost conditions or because the area above the repository is either covered by ice or below sea water.*

Annual individual doses for the Silo are shown in Figure 6-47. The highest dose, 820 µSv per year, is due to organic C-14 and Mo-93 and occurs immediately when a well can be drilled. The increased level of complexing agents causes a higher mobility of the radionuclides and consequently there are more radionuclides contributing to dose for this case, as compared to the case of an intrusion with assumptions as in the Weichselian variant.

The results for BMA are presented in Figure 6-48. The highest dose, 460 µSv per year, is dominated by the contribution from Mo-93. Thereafter, organic C-14 gives the highest contribution. The dose rates decline quickly to a steady value below 10 µSv per year, lasting until permafrost conditions appear.

The results for the 1BTF and the 2BTF are presented in Figure 6-49 and 6-50, respectively. The highest dose for the 1BTF is 2,100 µSv per year. The 2BTF gives the highest dose rate, 8,500 µSv per year, across all vaults and the Silo due to increased release rates of the actinides Pu-239 and Pu-240. These immobile radionuclides are strongly affected by the higher concentration of complexing agents, causing higher release rates from the waste.

7 Results for calculation cases representing residual scenarios

This chapter presents the dose calculation results for calculation cases representing residual scenarios:

- A calculation case where the radionuclide inventory disposed of in SFR 1 is considered to be the maximum allowable under license conditions (CC3).
- A calculation case which considers the contribution of the near-field barrier system in retarding the release rates of radionuclides (CC12).
- A calculation case which considers the contribution of the geosphere to act as part of the barrier system and retard the release rates of radionuclides (CC13).
- A calculation case which considers the impact of the Silo and BMA barrier system in retarding the release rates of radionuclides at early times (CC14).

A more detailed description of the calculation cases are given in Table 2-5.

Residual scenarios should be seen as "what if scenarios" that aim at investigating the maximal possible impact of uncertainties on the dose predictions. Consequently, dose estimates obtained for these calculations should not be used for risk estimations, or in the summation of risk, for demonstrating compliance with the regulatory requirements.

The results are presented in the same way, explained in the introduction to Chapter 5.

7.1 Alternative inventory

This calculation case considers the consequences if the SFR 1 repository is filled with activity up to the authorised activity content of $1 \cdot 10^{16}$ Bq. The dose calculations in this calculation case have been performed by scaling up the inventories with a factor of approximately seven. All other assumptions are the same as in the Weichselian variant (CC1). Hence, the mean annual doses from releases to the landscape and a well will have the same time dependency as in the Weichselian variant, but at a higher level. A summary of the peak values of the mean annual doses for each repository part and the whole repository for releases to the landscape is presented in Table 7-1.

Table 7-1. Peak values of the mean annual doses and time at which the peak value is observed for releases to the landscape from each repository part and from the whole repository in the calculation case alternative inventory (CC3). The value given for each repository part is the sum of values obtained for all released radionuclides. The radionuclides with the highest contribution to the peak doses are indicated.

Repository part	Peak annual dose µSv/year	Time of the peak years AD	Most contributing radionuclide
Silo	32	around 5,000	Organic C-14
BMA	37	around 5,000	Organic C-14
1BTF	1.6	around 5,000	Inorganic C-14
2BTF	17	around 5,000	Inorganic C-14
BLA	0.1	around 5,000	Inorganic C-14
Total SFR 1	82	around 5,000	Organic C-14

7.2 No sorption in the near field

This calculation case (CC12) considers the consequences of neglecting sorption of any radionuclide in the near-field barriers. Sorption in the geosphere during transport with groundwater is taken into account. All other assumptions coincide with the assumptions made for the Weichselian variant (CC1).

7.2.1 Doses from releases to the landscape

Time series of the mean values of the annual doses to the most exposed group resulting from radionuclides releases from the different repository parts are presented in Figures 7-1 to 7-4. The peak dose for the Silo (Figure 7-1) appears around year 5,000 due to releases of primarily inorganic C-14. The organic C-14 is not affected by sorption and gives the same dose rate as for the Weichselian variant. The lack of sorption in near-field barriers affects release rates of inorganic C-14 considerably. It also affects the number of dose contributing radionuclides. After the peak dose, Ni-59 dominates initially the dose rates when releases are to a terrestrial area, i.e. a mire used for forestry. The contribution of Cs-135 to the dose increases with time.

For the BMA the lack of sorption in near-field material implies, in similarity to the Silo, increased dose rates. Inorganic C-14 dominates the maximum dose rate and causes also a dominating contribution to the peak dose. Organic C-14 contributes also considerably to the peak dose rate. The doses decline faster for the BMA than for the Silo, as the latter has more effective barriers than the BMA. In similarity to the Silo, almost all radionuclides contained in BMA give dose contributions above 0.001 µSv per year. It is also worth pointing out that neglecting sorption in the near-field barriers increases the contribution of actinides considerably.

The maximum dose rate due to releases from 1BTF decreases with a factor of two compared to the Weichselian variant, when sorption in the near-field is neglected. This is because a higher amount of the inorganic C-14 is released earlier to the sea basin, where the doses per unit release rates are lower.

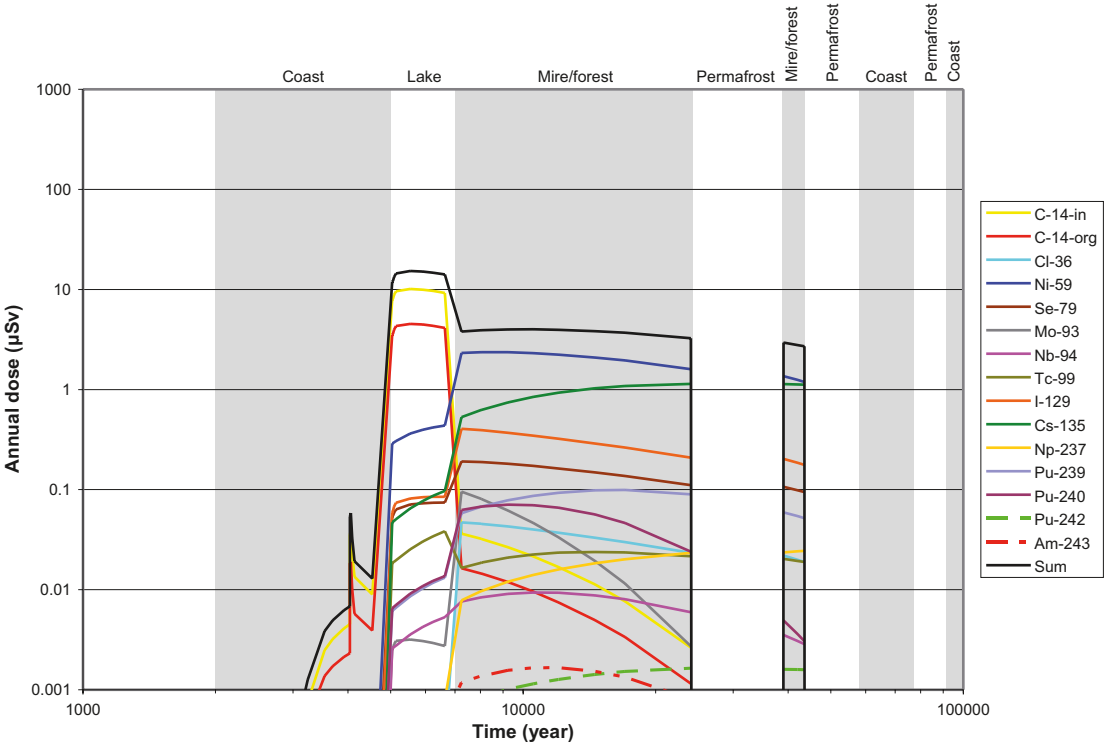

Figure 7-1. *No sorption in the near-field (CC12), Silo. Mean values of the annual individual dose from radionuclide releases to the landscape from the Silo. The sum corresponds to the total dose considering all released radionuclides.*

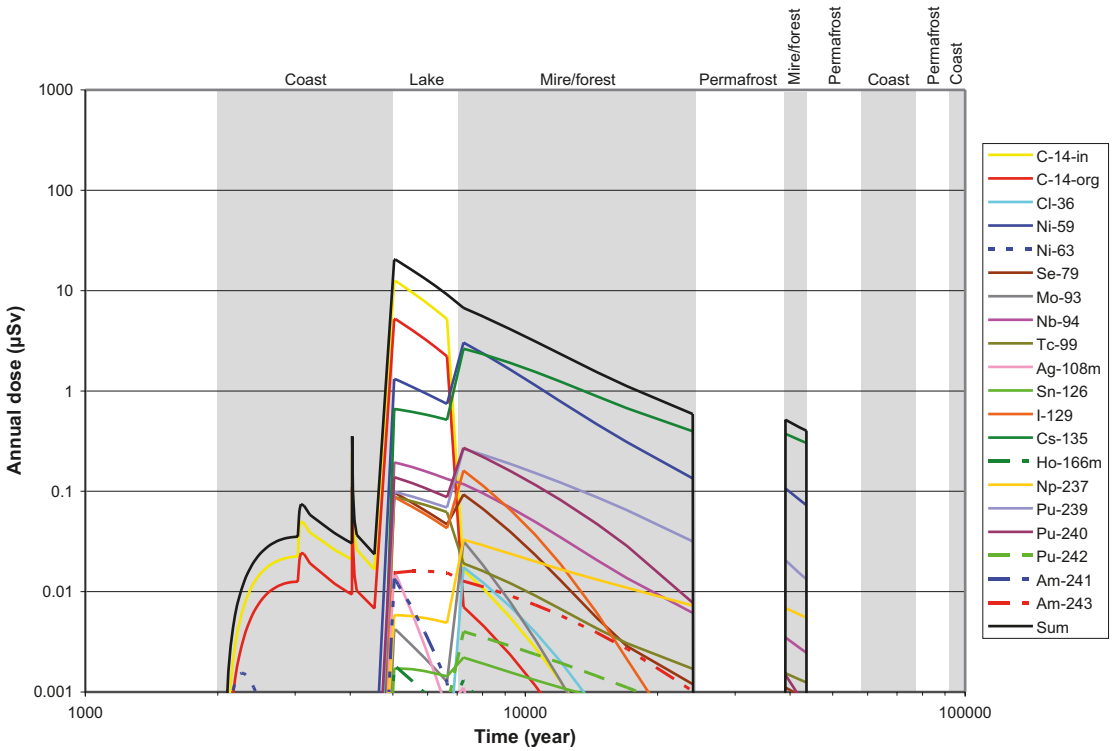

Figure 7-2. *No sorption in the near-field (CC12), BMA. Mean values of the annual individual dose from radionuclide releases to the landscape from the BMA. The sum corresponds to the total dose considering all released radionuclides.*

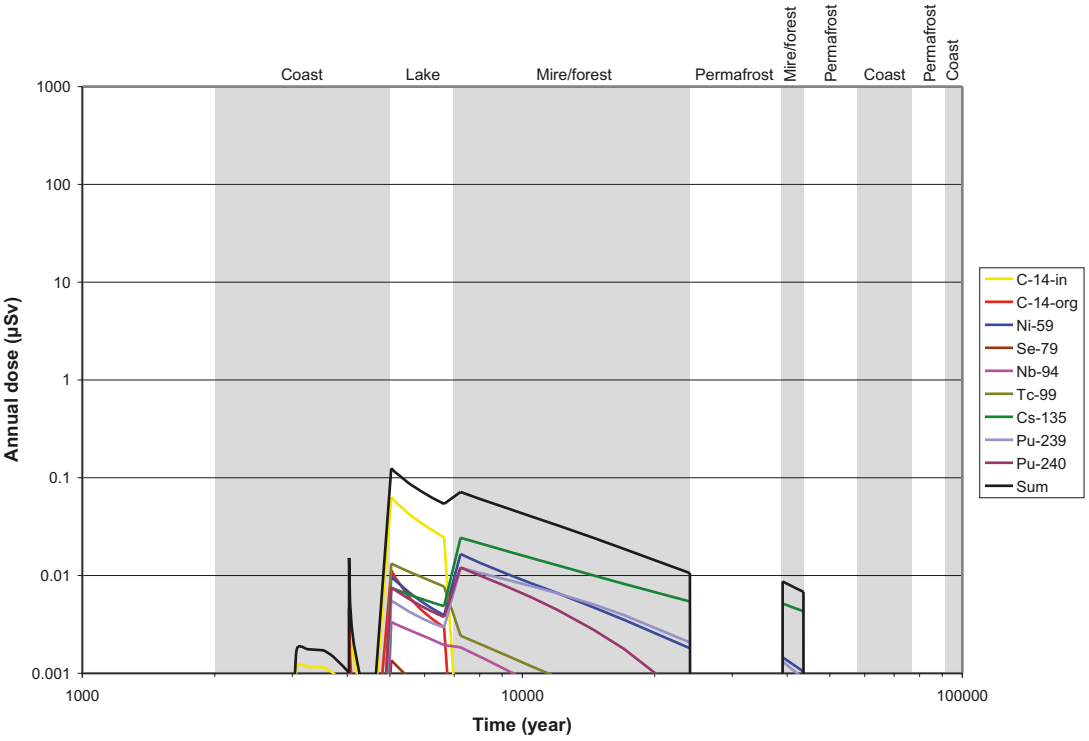

Figure 7-3. *No sorption in the near-field (CC12), 1BTF. Mean values of the annual individual dose from radionuclide releases to the landscape from the 1BTF. The sum corresponds to the total dose considering all released radionuclides.*

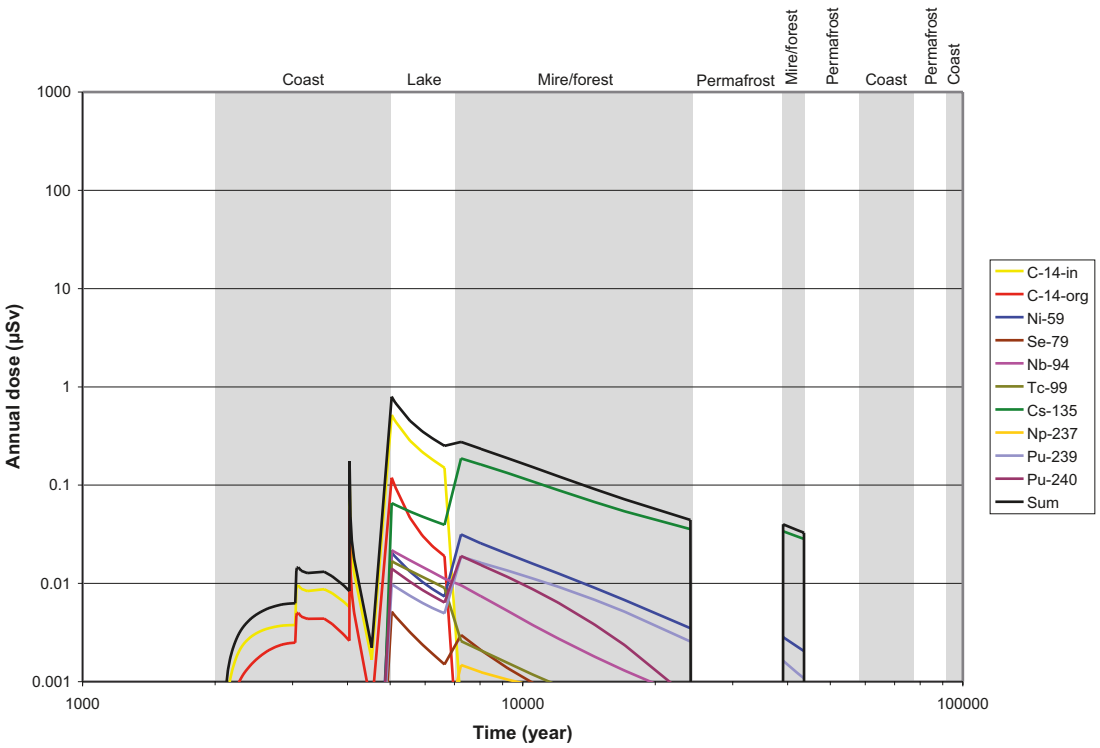

Figure 7-4. *No sorption in the near-field (CC12), 2BTF. Mean values of the annual individual dose from radionuclide releases to the landscape from the 2BTF. The sum corresponds to the total dose considering all released radionuclides.*

For the 2BTF the maximum dose rate occurs at year 5,000 due to inflow of inorganic C-14 to a lake ecosystem. The maximum dose rate has decreased, in similarity to the result for 1BTF with a factor of three. The lack of sorption has caused an earlier outflow of inorganic C-14, which thus reached the coastal area instead of the freshwater lake.

Figure 7-5 presents the total mean annual doses from the whole repository and for each repository part, taking into account all released radionuclides. As in the Weichselian variant, the Silo and the BMA have the highest contribution to the peak doses. Neglecting sorption in the near-field increases doses from the Silo and the BMA, but decreases the doses from the 1BTF and the 2BTF.

A summary of the peak values of the mean annual doses for each repository part and the whole repository is presented in Table 7-2.

Table 7-2. Peak values of the mean annual doses and time at which the peak value is observed for releases to the landscape from each repository part and from the whole repository in the calculation case with no sorption in the near field (CC12). The value given for each repository part is the sum of values obtained for all released radionuclides. The radionuclides with the highest contribution to the peak doses are indicated.

Repository part	Peak annual dose µSv/year	Time of the peak years AD	Most contributing radionuclide
Silo	15	around 5,000	Inorganic C-14
BMA	20	around 5,000	Inorganic C-14
1BTF	0.12	around 5,000	Inorganic C-14
2BTF	0.8	around 5,000	Inorganic C-14
BLA	0.01	around 5,000	Inorganic C-14
Total SFR 1	35	around 5,000	Inorganic C-14

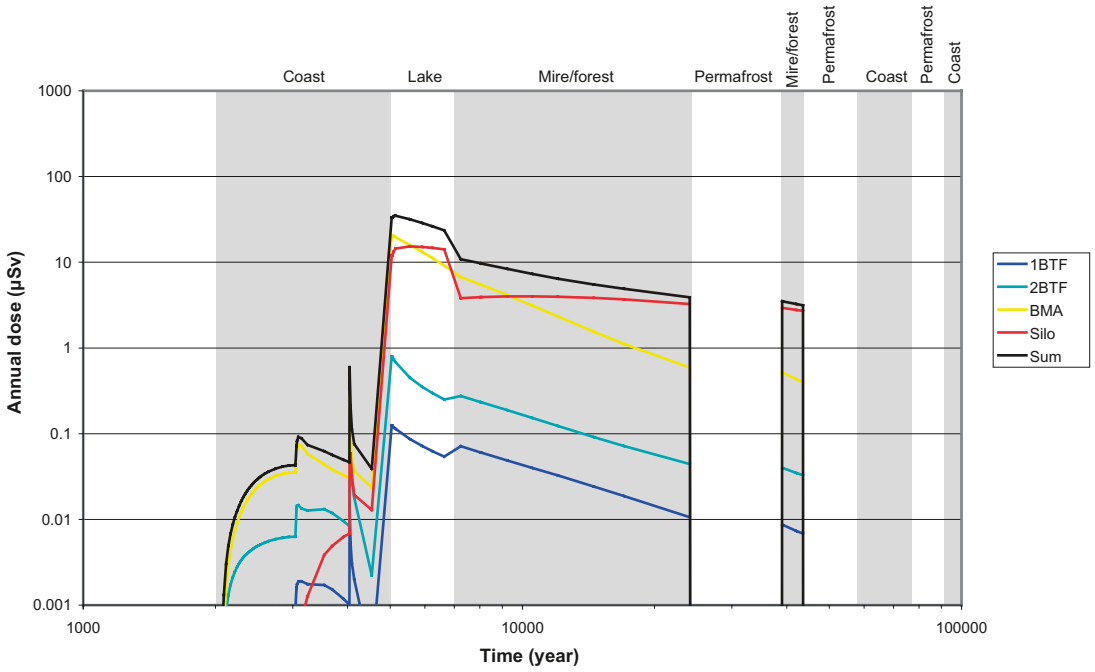

Figure 7-5. *No sorption in the near-field (CC12), SFR 1. Mean values of the total annual individual dose from radionuclide releases to the landscape from each repository part and from the whole repository (Sum).*

7.2.2 Doses from releases to a well

Time series of the mean annual doses from releases to a well are presented in Figures 7-6 to 7-9. The doses for the Silo are slightly increased from about 10 µSv per year in the Weichselian variant, to 16 µSv per year around year 10,000. Ni-59, Pu-239 and Pu-240 dominate the doses. For the BMA the peak dose is 89 µSv per year and is caused by Ni-59, Pu-239 and Pu-240. The loss of sorption in the near-field implies a much higher mobility for those radionuclides and thus higher doses. The doses for the 1BTF and the 2BTF are dominated by the actinides.

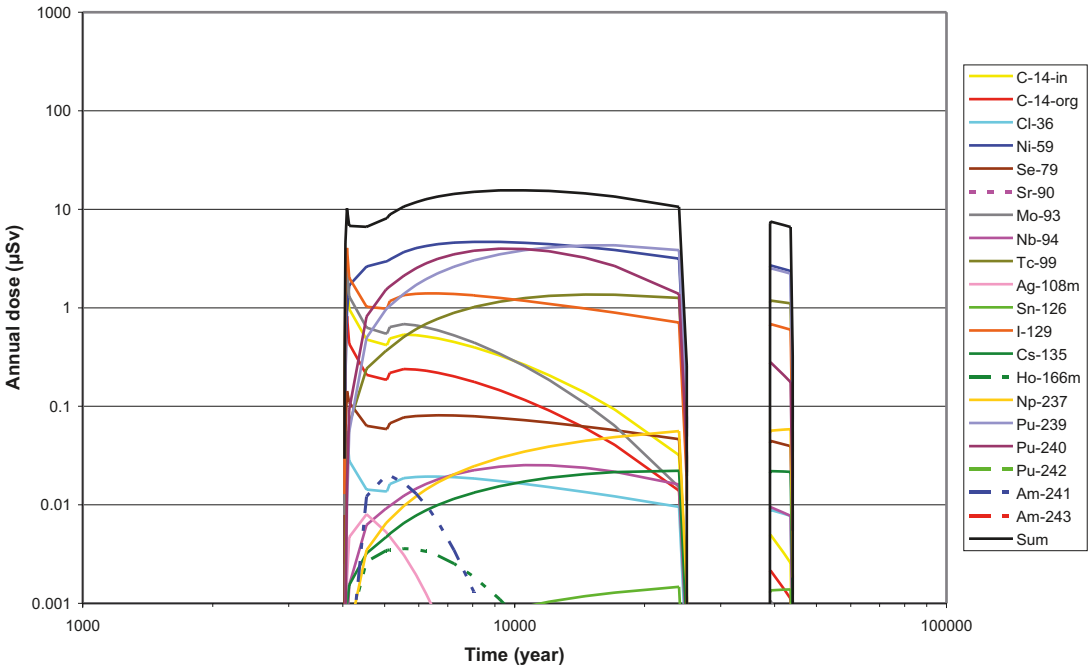

Figure 7-6. *No sorption in the near-field (CC12), Silo. Mean annual doses from radionuclide releases to a well from the Silo. The sum corresponds to the total dose considering all released radionuclides.*

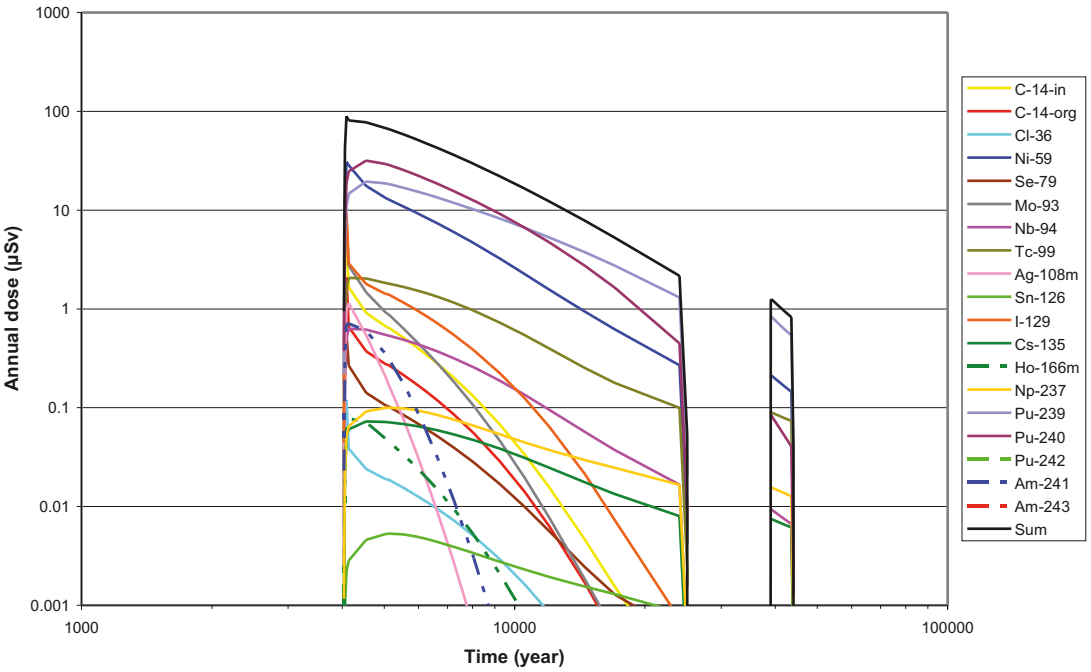

Figure 7-7. *No sorption in the near-feld (CC12), BMA. Mean annual doses from radionuclide releases to a well from the BMA. The sum corresponds to the total dose considering all released radionuclides.*

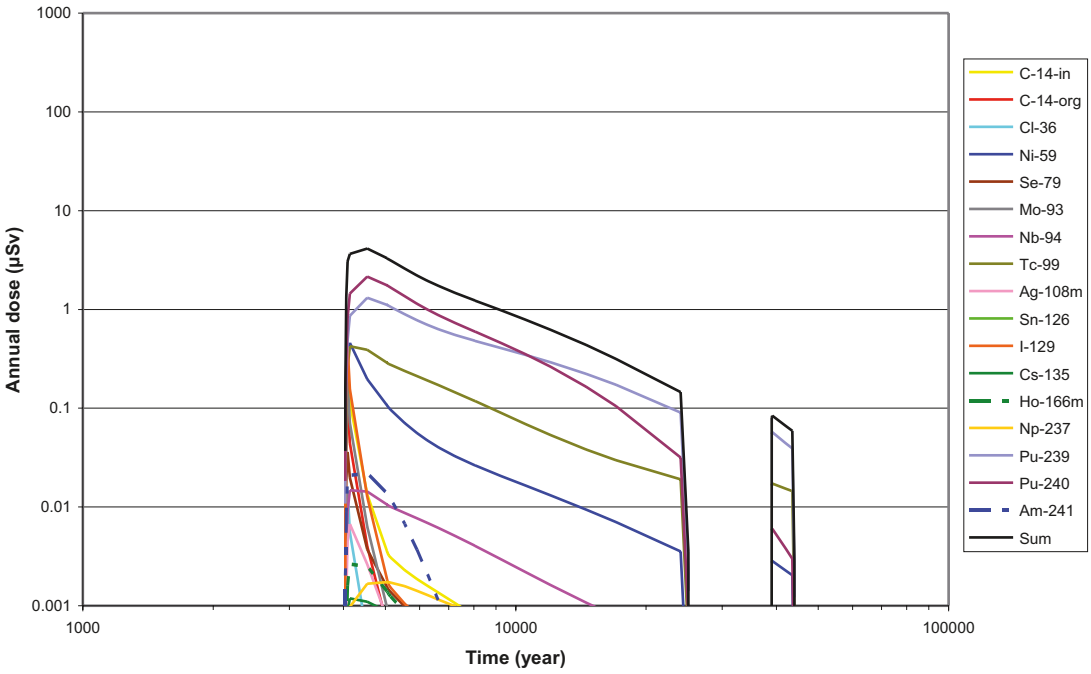

Figure 7-8. *No sorption in the near-field (CC12), 1BTF. Mean annual doses from radionuclide releases to a well from the 1BTF. The sum corresponds to the total dose considering all released radionuclides.*

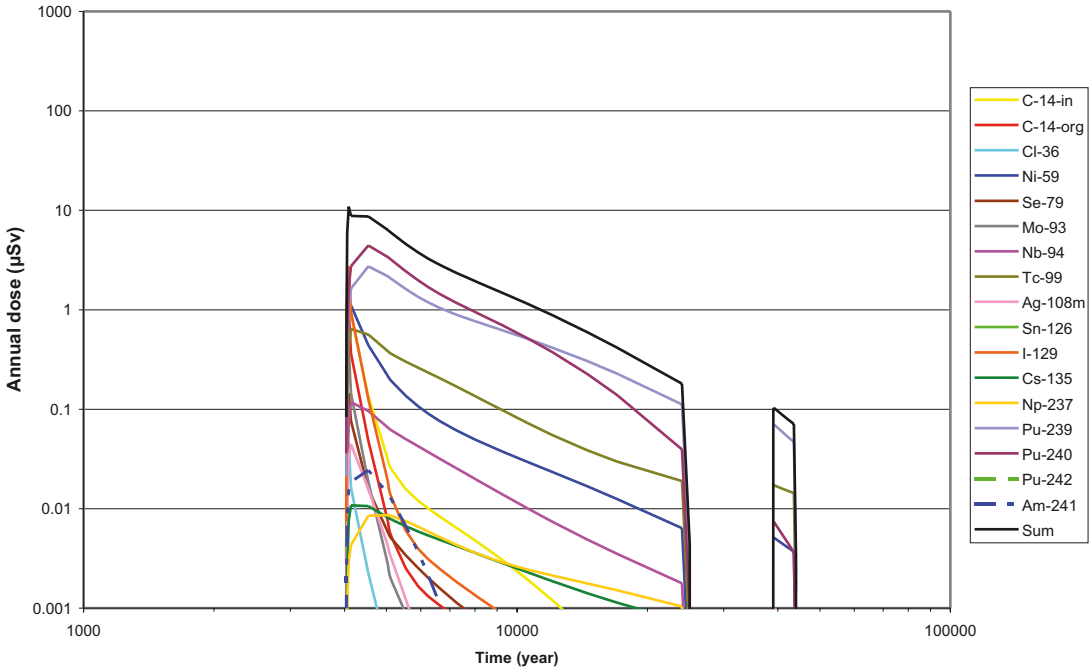

Figure 7-9. *No sorption in the near-field (CC12), 2BTF. Mean annual doses from radionuclide releases to a well from the 2BTF. The sum corresponds to the total dose considering all released radionuclides.*

7.3 Early degradation of technical barriers (CC14)

This calculation case (CC14) considers the consequences of an early sudden brake of the barriers of the Silo and the BMA. It is assumed that already at year 5,000, i.e. 3,000 years after the repository closure the barriers fail, thus causing increased inflow rates of radionuclides to the landscape, as compared to Weichselian variant. All other assumptions are the same as in the Weichselian variant (CC1).

7.3.1 Doses from releases to the landscape

Time series of the mean values of the annual doses to the most exposed group resulting from radionuclides releases from the different repository parts are presented in Figures 7-10 to 7-11. The importance of the near field barriers is notable as maximum dose rates increase considerably compared to the Weichselian variant. For the Silo a peak dose of 31 µSv per year appears at around year 6,000 due to the inflow of organic and inorganic C-14 to the lake. Dose contributions from C-14 decreases quickly as a combined effect of lower release rates and lower exposure when the biosphere object that receives the direct releases has changed from a lake to a mire. The dose rates for other mobile long-lived radionuclides also decline considerably with time, except for Ni-59 and Cs-135. However, at around year 40,000 maximum dose rates have also been reached for those radionuclides.

For the BMA a peak value of 176 µSv per year occurs, as a combined effect of releases of organic and inorganic C-14 to a lake ecosystem, at around year 5,000 when the technical barriers have completely lost their retarding function. A next, however lower peak dose is due to Ni-59 and Cs-135 when reaching a terrestrial ecosystem. The lack of barriers is visible as the actinides give low, but visible contributions to the total dose rate. As can be seen from the Figure 7-11, two groups of radionuclides can be distinguished. One group consists of radionuclides that have low dose contributions, like the actinides. Another group, with higher contribution, consists of mobile long-lived radionuclides, like Ni-59 and Cs-135. In contrast to the Silo, I-129 has, due to its limited amount, already left BMA, why it does not contribute to the long-term exposure.

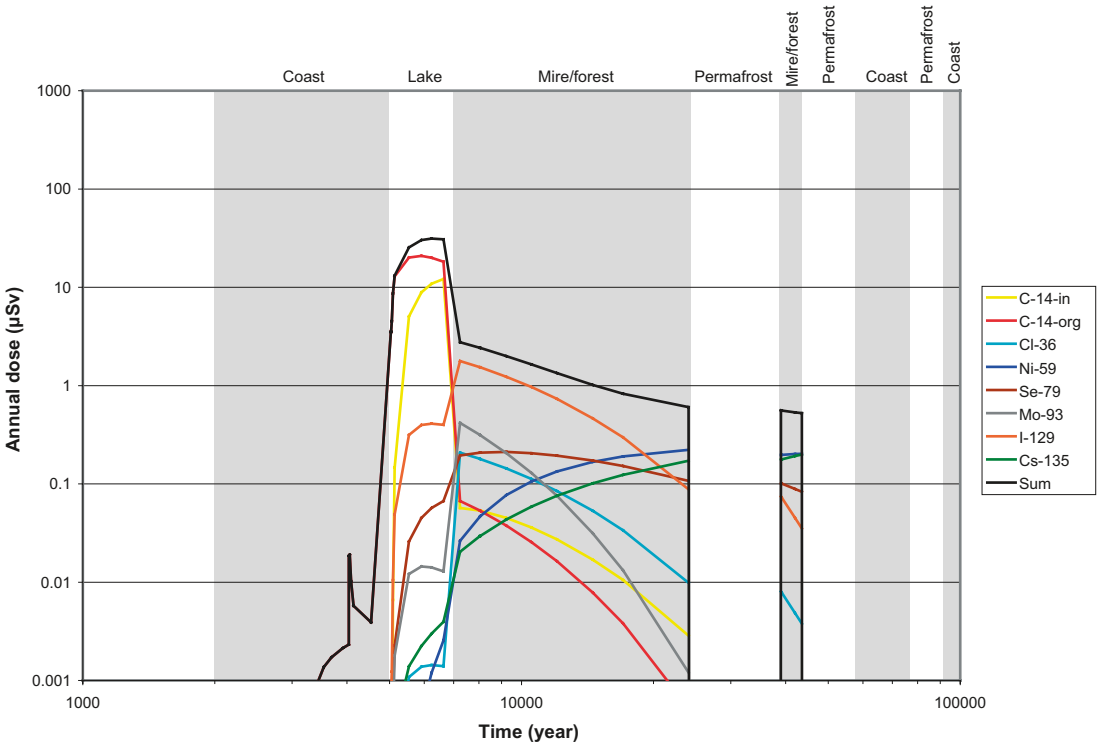

Figure 7-10. *Early degradation of technical barriers (CC14), Silo. Mean values of the annual individual dose from radionuclide releases to the landscape from the Silo. The sum corresponds to the total dose considering all released radionuclides.*

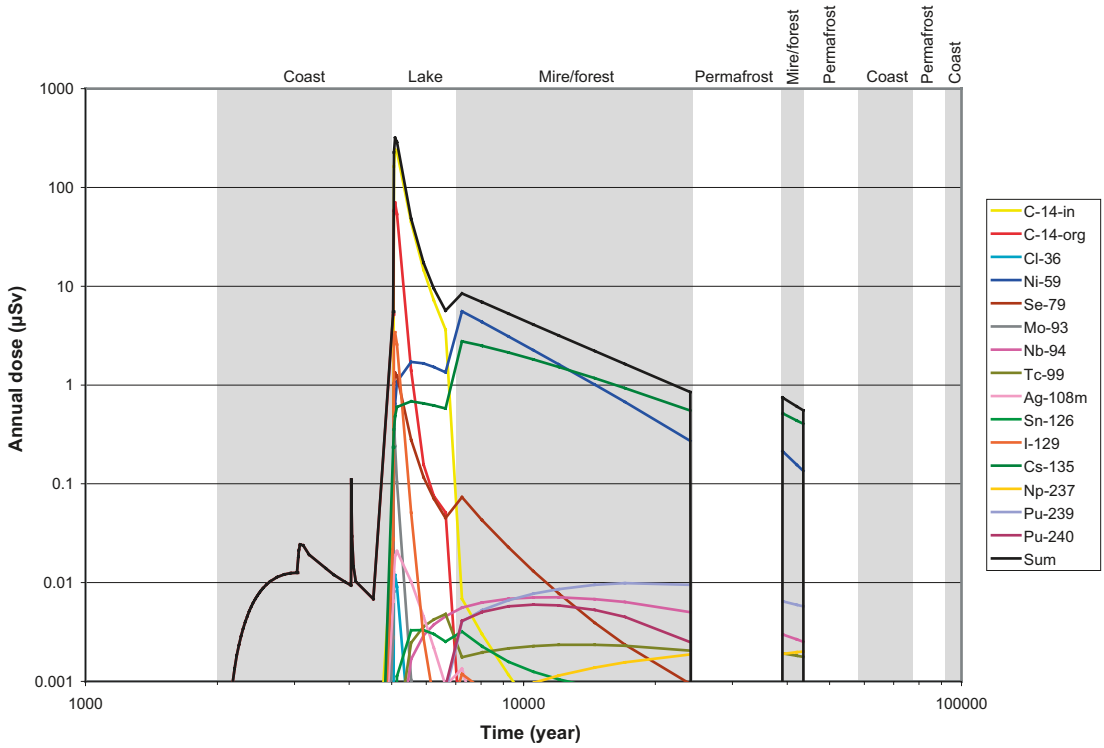

Figure 7-11. *Early degradation of technical barriers (CC14), BMA. Mean values of the annual individual dose from radionuclide releases to the landscape from the BMA. The sum corresponds to the total dose considering all released radionuclides.*

Figure 7-12 presents the total mean annual doses from the whole repository and from the Silo and the BMA, taking into account all released radionuclides. A summary of the peak values is presented in Table 7-3. This calculation case gives the highest dose rates among all calculation cases considered. It is the inorganic C-14 from the BMA, which causes the highest exposure. Organic C-14 is the second most contributing radionuclide. In a long time perspective Ni-59 and Cs-135 dominate the doses. I-129 released from the Silo has also an important contribution to the total dose rate.

Table 7-3. Peak values of the mean annual doses and time at which the peak value is observed for releases to the landscape from the Silo, the BMA and from the whole repository in the calculation case early degradation of technical barriers (CC14). The value given for each repository part is the sum of values obtained for all released radionuclides. The radionuclides with the highest contribution to the peak doses are indicated.

Repository part	Peak annual dose µSv/year	Time of the peak years AD	Most contributing radionuclide
Silo	31	around 6,000	Organic C-14
BMA	320	around 5,000	Inorganic C-14
1BTF	0.2	around 5,000	Inorganic C-14
2BTF	2.4	around 5,000	Inorganic C-14
BLA	0.01	around 5,000	Inorganic C-14
Total SFR 1	330	around 5,000	Inorganic C-14

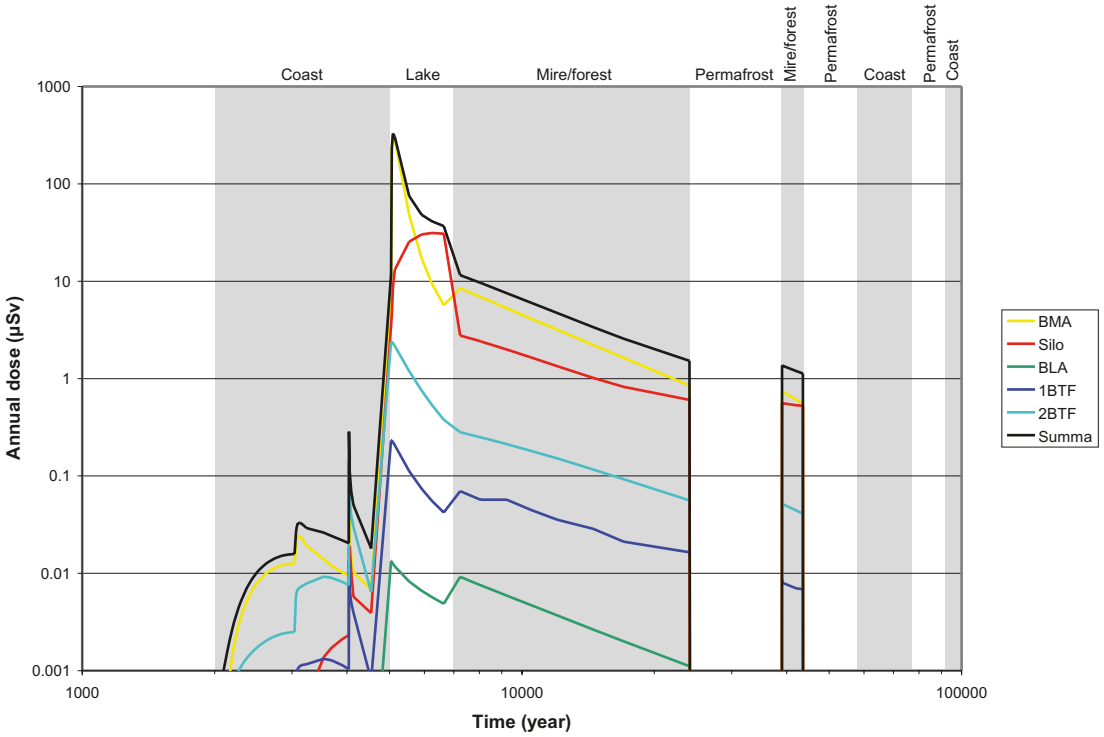

Figure 7-12. *Early degradation of technical barriers (CC14), Silo and BMA. Mean values of the total annual individual dose from radionuclide releases to the landscape from the Silo, the BMA and from the whole repository (Sum).*

7.3.2 Doses from releases to a well

Time series of the mean annual doses from releases to a well are presented in Figures 7-13 to 7-14. For the Silo the peak dose occurs when the technical barriers have degraded, at around year 5,000. At this time, I-129 dominates the exposure.

For the BMA the peak dose also occurs when the technical barriers have degraded, at around year 5,000 and reaches 120 µSv per year. At this time I-129 and Mo-93 dominate the exposure, but due to lack of barrier sorption the whole inventory of I-129 and Mo-93 is released effectively. Thereafter, Ni-59 dominates the exposures.

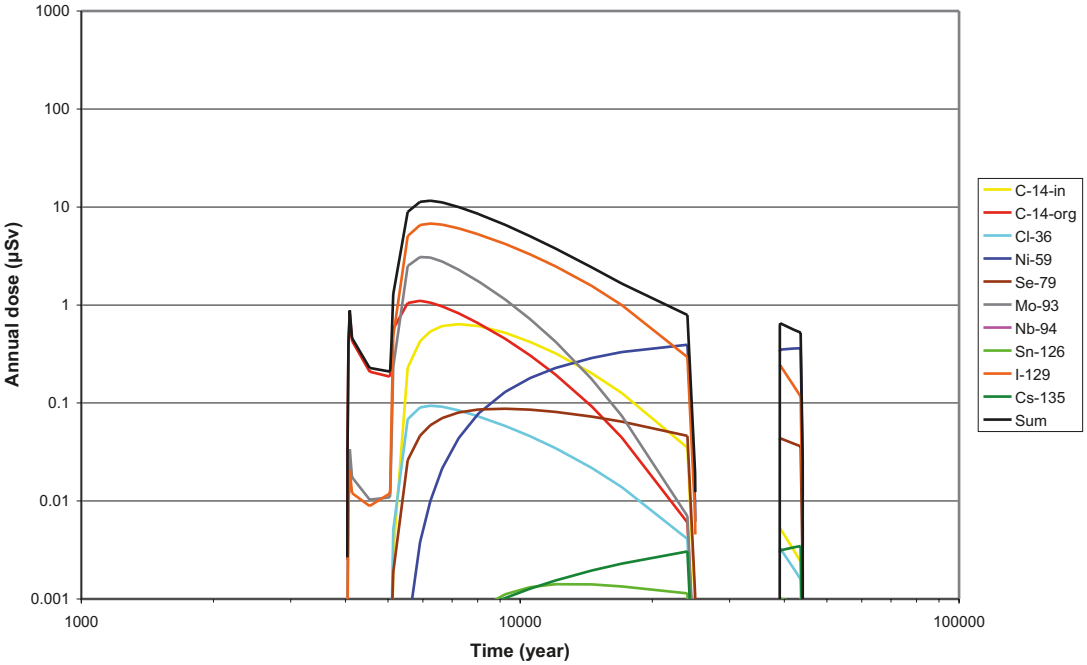

Figure 7-13. *Early degradation of technical barriers (CC14), Silo. Mean annual doses from radionuclide releases to a well from the Silo. The sum corresponds to the total dose considering all released radionuclides.*

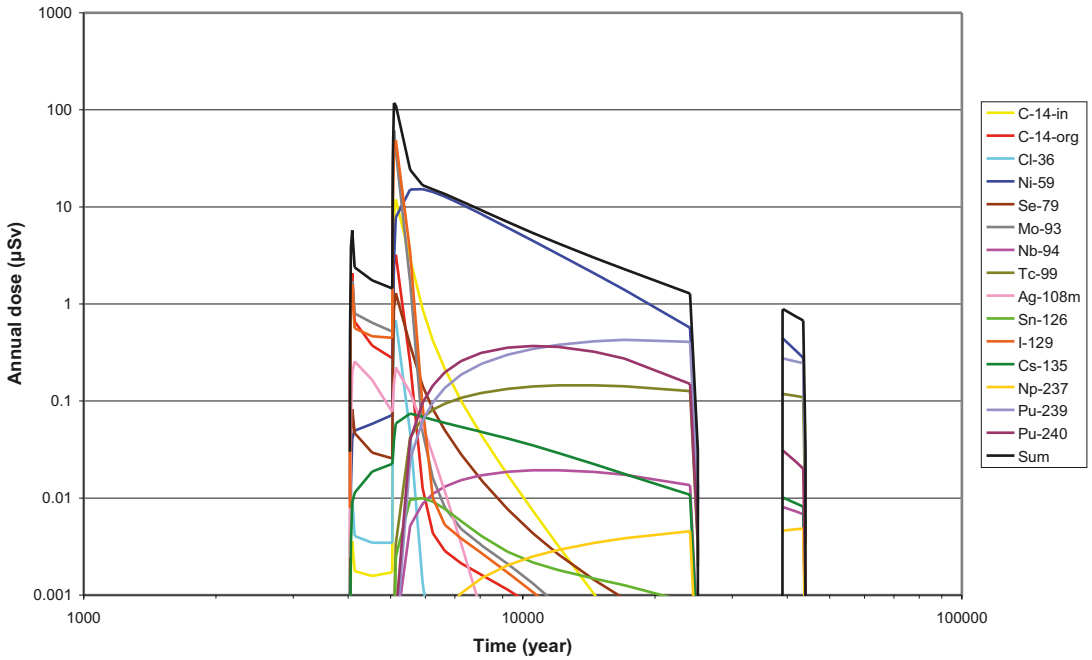

Figure 7-14. *Early degradation of technical barriers (CC14), BMA. Mean annual doses from radionuclide releases to a well from the BMA. The sum corresponds to the total dose considering all released radionuclides.*

7.4 No barrier function in the far-field

This calculation case (CC13) addresses the consequences of neglecting delay of radionuclides in the geosphere. All other assumptions are the same as in the Weichselian variant (CC1).

7.4.1 Doses from releases to the landscape

Time series of the mean values of the annual doses to the most exposed group resulting from radionuclides releases from the different repository parts are presented in Figures 7-10 to 7-11. For the Silo there are insignificant changes in dose consequences when disregarding delay in the geosphere. The results show that constructed barriers and the sand/bentonite layer surrounding the Silo are, as expected, of much more importance for retardation of radionuclides than the delay in the geosphere.

The doses from releases from the BMA are either not substantially influenced by lack of delay of radionuclides in the geosphere. The maximum dose rate increases from 5.6 µSv per year in the Weichselian variant to 6.5 µSv per year, due to somewhat higher fluxes of Cs-135. Immobile radionuclides are effectively absorbed already in the near field barriers and therefore releases rates to the biosphere are low even when neglecting delay in the geosphere.

For the 1BTF the maximum dose is 0.2 µSv per year, which is very close to the values obtained for the Weichselian variant. Pu-239 causes a very low contribution to the dose, just above 0.001 µSv per year. In general, the doses from the 1BTF decrease somewhat, when disregarding delay in the geosphere, but from an already very low level.

The dose rates for the BTF are slightly lower than when delay in the geosphere is considered. The maximum dose rate occurs at year 5,000 due to a pronounced peak inflow of inorganic C-14 to a lake ecosystem. The dose rates decrease rapidly and are low.

The absence of delay of radionuclides in the geosphere leads to an immediate inflow of radionuclides from the BLA to the surface ecosystem, which is a marine ecosystem during the first three thousands year after closure, when dose rates per unit release rates are low.

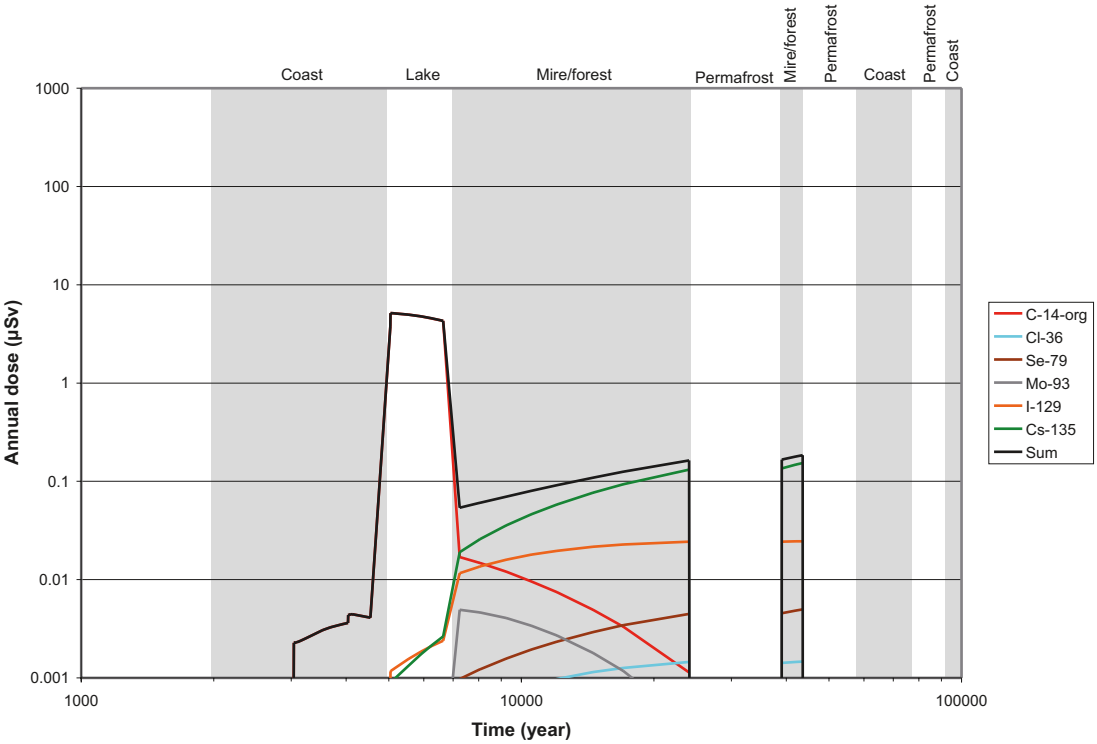

Figure 7-15. *No barrier function in the far-field (CC13), Silo. Mean values of the annual individual dose from radionuclide releases to the landscape from the Silo. The sum corresponds to the total dose considering all released radionuclides.*

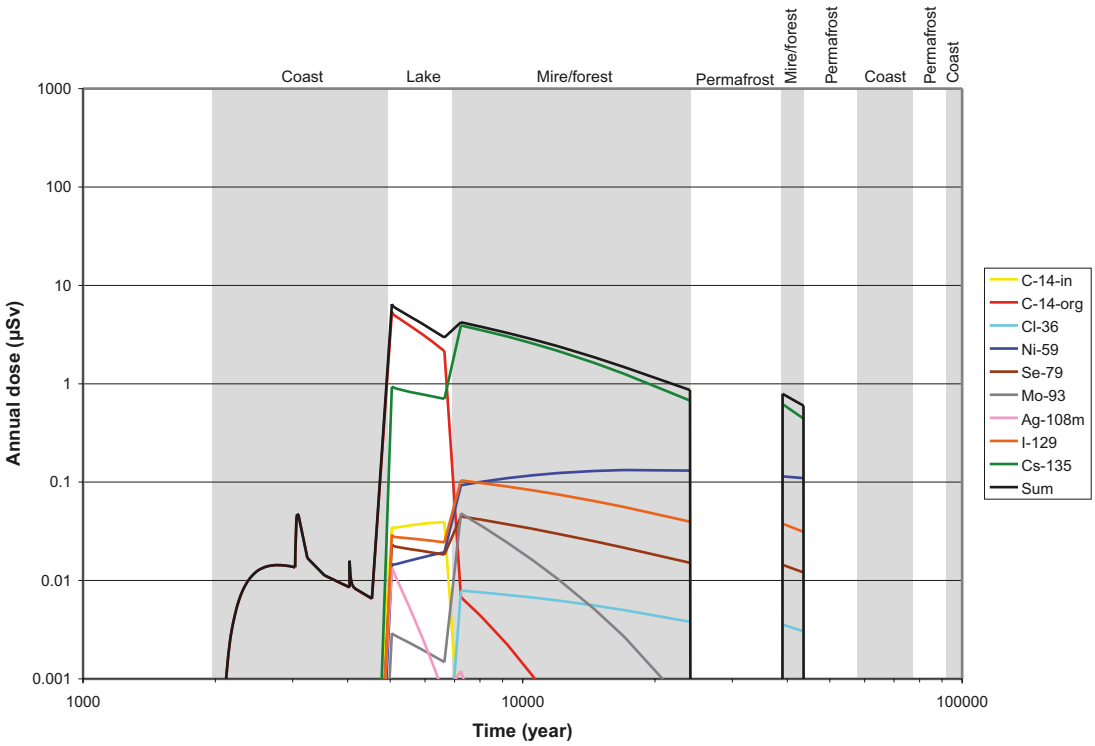

Figure 7-16. *No barrier function in the far-field (CC13), BMA. Mean values of the annual individual dose from radionuclide releases to the landscape from the BMA. The sum corresponds to the total dose considering all released radionuclides.*

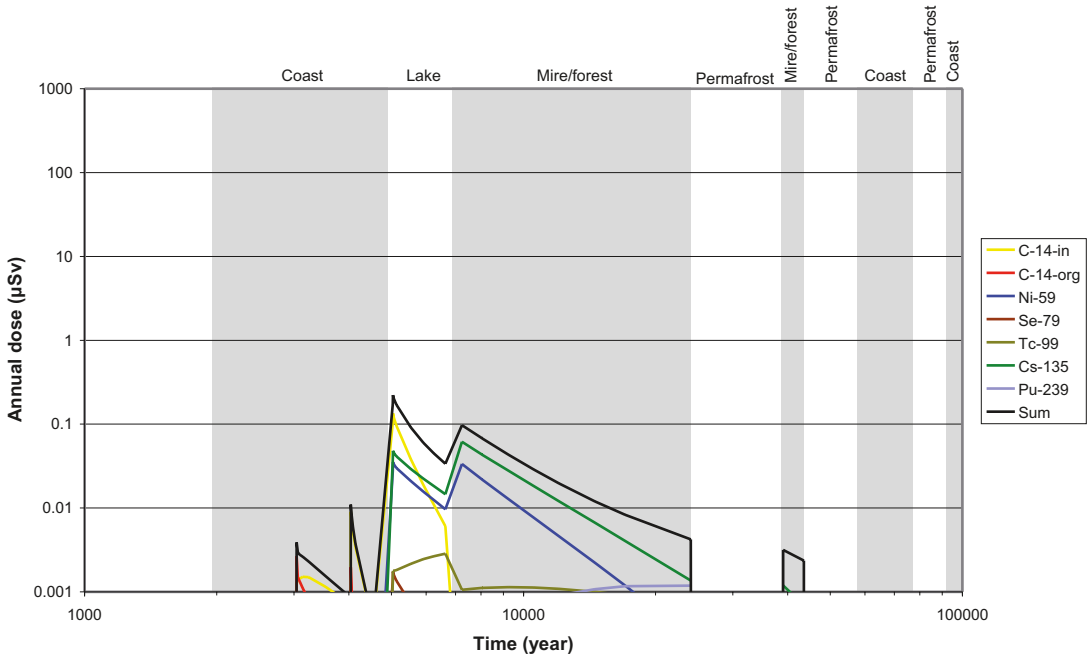

Figure 7-17. *No barrier function in the far-field (CC13), 1BTF. Mean values of the annual individual dose from radionuclide releases to the landscape from the 1BTF. The sum corresponds to the total dose considering all released radionuclides.*

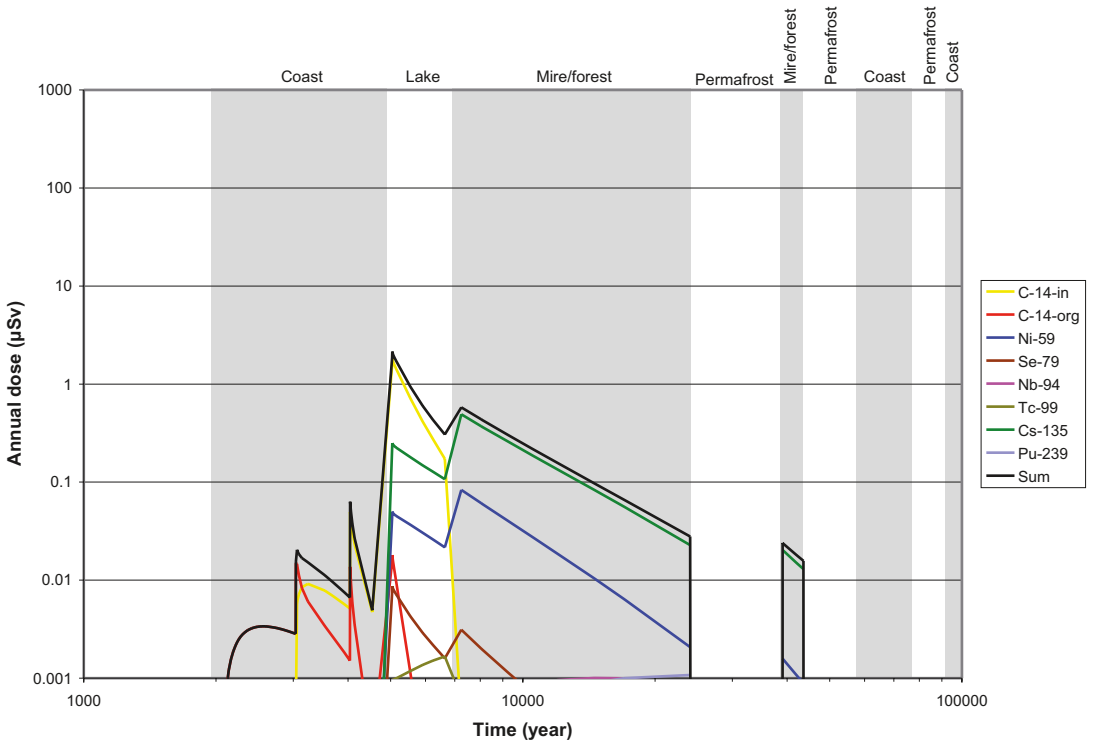

Figure 7-18. *No barrier function in the far-field (CC13), 2BTF. Mean values of the annual individual dose from radionuclide releases to the landscape from the 2BTF. The sum corresponds to the total dose considering all released radionuclides.*

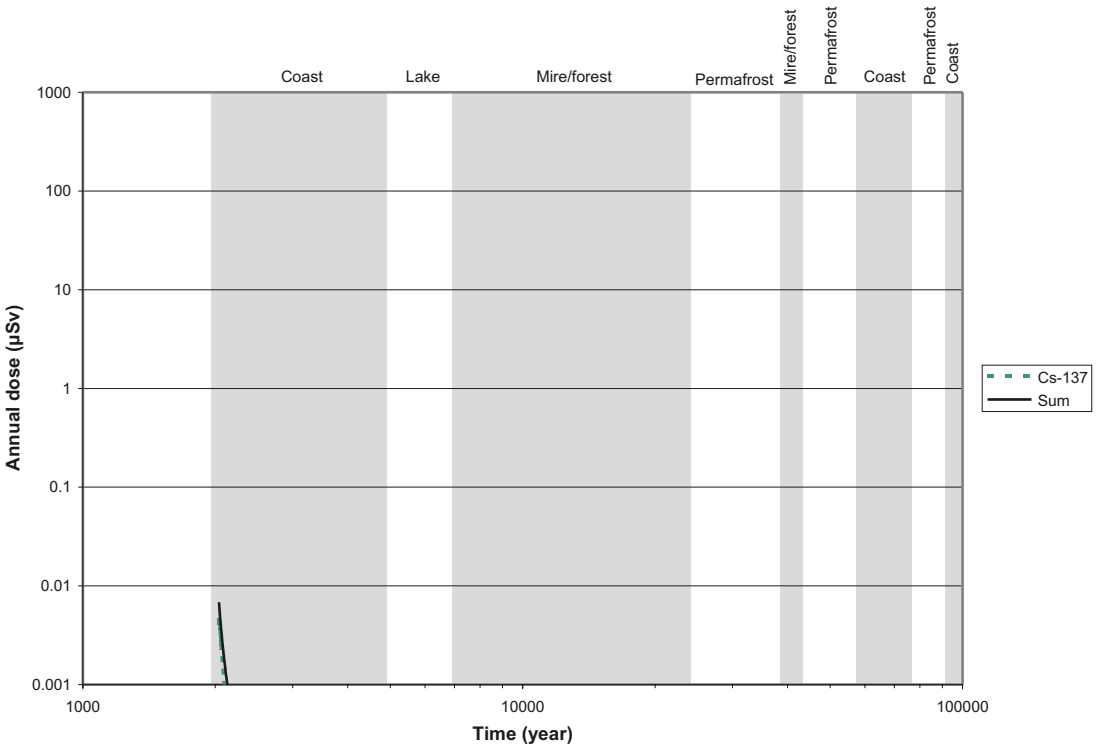

Figure 7-19. *No barrier function in the far-field (CC13), BLA. Mean values of the annual individual dose from radionuclide releases to the landscape from the BLA. The sum corresponds to the total dose considering all released radionuclides.*

Figure 7-20 presents the total mean annual doses from the whole repository and for the different repository parts, taking into account all released radionuclides. A summary of the peak values is presented in Table 7-4.

Table 7-4. Peak values of the mean annual doses and time at which the peak value is observed for releases to the landscape from each repository part and from the whole repository in the calculation case no barrier function in the far-field (CC13). The value given for each repository part is the sum of values obtained for all released radionuclides. The radionuclides with the highest contribution to the peak doses are indicated.

Repository part	Peak annual dose µSv/year	Time of the peak years AD	Most contributing radionuclide
Silo	5.2	around 5,000	Organic C-14
BMA	6.5	around 5,000	Organic C-14
1BTF	0.2	around 5,000	Inorganic C-14
2BTF	2.1	around 5,000	Inorganic C-14
BLA	0.007	around 2,050	Cs-137
Total SFR 1	14	around 5,000	Organic C-14

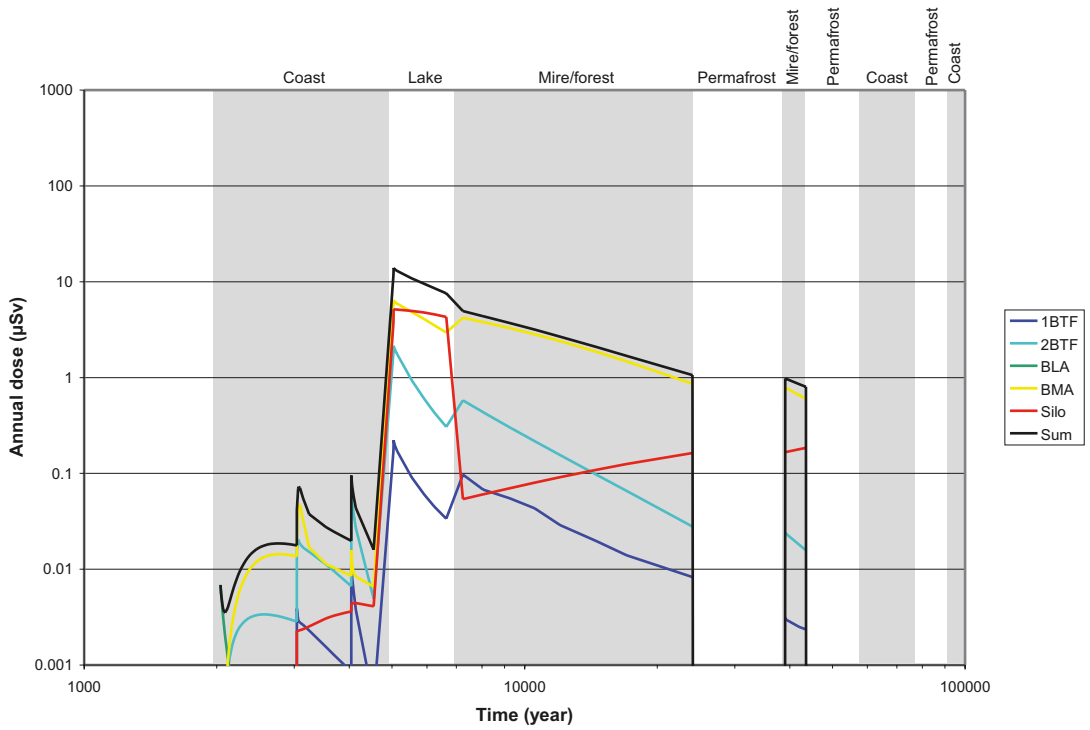

Figure 7-20. *No barrier function in the far-field (CC13), SFR 1. Mean values of the total annual individual dose from radionuclide releases to the landscape from each repository part and from the whole repository (Sum).*

8 Collective dose commitment

Using the approach described in Section 4.5, a complete (integrated over 50,000 years) collective dose commitment of about 10.9 manSv was obtained. This value was based on a release of C-14 of about $1 \cdot 10^{11}$ Bq in the main scenario during the first thousands years after closure /Thomson et al. 2008/. The incomplete, i.e. integrated over 10,000 years, collective dose commitment is then about 8 manSv. It should be noted that this value is conditioned to the assumptions that the future world population increases to 10^{10} people and stabilises at that level and that the global inventory of stable carbon does not increase from its present value /UNSCEAR 2000/.

9 Impact on non-human biota

The maximum values of concentrations in environmental media, the corresponding Environmental Media Concentration Limits (EMCL) and the calculated Risk Quotients (RQs) are presented in Tables 9-1, 9-2 and 9-3 for marine water, fresh water and soil (air) respectively. Note that the concentrations and EMCL-value of C-14 in terrestrial ecosystems are given in units of Bq/m^3 in air, and not in Bq/kg DW in soil, as it is the case for other radionuclides. As it was mentioned in Section 4.6, the EMCL-values for marine water were used to calculate RQs for brackish water. The EMCL-values for marine water are generally lower than those for fresh water, except for Cl-36 and Cs-137.

The results show that all RQs are well below one, both for each individual radionuclide and for the sum across all radionuclides. Hence, following the ERICA methodology /Erica 2008, Beresford et al. 2007/, it can be concluded that the potential impacts on non-human biota are negligible and there is no need for performing more realistic assessments. It should be noted that in the ERICA methodology, EMCL-values are not provided for some of the radionuclides of interest: Mo-93, Ag-108m, Sn-126, Ho-166m, Pu-242 and Am-243, and were therefore not evaluated.

Table 9-1. Predicted maximum radionuclide concentration in marine water, EMCL-values and the Risk Quotients (RQs).

Nuclide	Concentration Bq/m^3	EMCL Bq/m^3	Risk Quotient (RQ)
Co-60	$5.07 \cdot 10^{-4}$	7.87	$6.44 \cdot 10^{-5}$
C-14-org	$1.21 \cdot 10^{-1}$	$6.49 \cdot 10^{3}$	$1.87 \cdot 10^{-5}$
C-14-in	$5.83 \cdot 10^{-2}$	$6.49 \cdot 10^{3}$	$8.98 \cdot 10^{-6}$
Ni-59	$5.79 \cdot 10^{-2}$	$5.88 \cdot 10^{4}$	$9.85 \cdot 10^{-7}$
Ni-63	$3.58 \cdot 10^{-2}$	$4.41 \cdot 10^{4}$	$8.12 \cdot 10^{-7}$
Pu-240	$5.62 \cdot 10^{-7}$	$9.35 \cdot 10^{-1}$	$6.01 \cdot 10^{-7}$
Pu-239	$3.77 \cdot 10^{-7}$	$9.35 \cdot 10^{-1}$	$4.04 \cdot 10^{-7}$
Cs-137	$4.85 \cdot 10^{-4}$	$2.54 \cdot 10^{3}$	$1.91 \cdot 10^{-7}$
Nb-94	$8.88 \cdot 10^{-7}$	4.67	$1.90 \cdot 10^{-7}$
Am-241	$9.43 \cdot 10^{-8}$	$5.38 \cdot 10^{-1}$	$1.75 \cdot 10^{-7}$
Tc-99	$7.42 \cdot 10^{-5}$	$1.96 \cdot 10^{3}$	$3.79 \cdot 10^{-8}$
Sr-90	$2.41 \cdot 10^{-4}$	$1.54 \cdot 10^{4}$	$1.57 \cdot 10^{-8}$
I-129	$6.62 \cdot 10^{-5}$	$1.34 \cdot 10^{4}$	$4.93 \cdot 10^{-9}$
Se-79	$2.92 \cdot 10^{-5}$	$1.24 \cdot 10^{4}$	$2.36 \cdot 10^{-9}$
Cs-135	$1.54 \cdot 10^{-5}$	$1.74 \cdot 10^{5}$	$8.86 \cdot 10^{-11}$
Np-237	$4.06 \cdot 10^{-9}$	$1.20 \cdot 10^{2}$	$3.39 \cdot 10^{-11}$
Cl-36	$1.04 \cdot 10^{-4}$	$2.36 \cdot 10^{7}$	$4.39 \cdot 10^{-12}$
H-3	$1.24 \cdot 10^{-6}$	$3.55 \cdot 10^{8}$	$3.51 \cdot 10^{-15}$
Sum			$9.54 \cdot 10^{-5}$

Table 9-2. Predicted maximum radionuclide concentration in fresh water, EMCL-values and the Risk Quotients (RQs).

Nuclide	Concentration Bq/m^3	EMCL Bq/m^3	Risk Quotient (RQ)
C-14-org	$4.0 \cdot 10^{2}$	$1.6 \cdot 10^{4}$	$2.6 \cdot 10^{-2}$
C-14-in	$1.9 \cdot 10^{2}$	$1.6 \cdot 10^{4}$	$1.2 \cdot 10^{-2}$
Ni-59	$4.0 \cdot 10^{2}$	$5.7 \cdot 10^{4}$	$7.0 \cdot 10^{-3}$
Nb-94	$6.0 \cdot 10^{-3}$	4.4	$1.4 \cdot 10^{-3}$
Am-241	$6.3 \cdot 10^{-4}$	2.6	$2.4 \cdot 10^{-4}$
Pu-240	$2.5 \cdot 10^{-3}$	$2.3 \cdot 10^{1}$	$1.1 \cdot 10^{-4}$
Pu-239	$1.8 \cdot 10^{-3}$	$2.3 \cdot 10^{1}$	$7.7 \cdot 10^{-5}$
Cs-135	$1.0 \cdot 10^{-1}$	$5.5 \cdot 10^{3}$	$1.9 \cdot 10^{-5}$
I-129	$5.0 \cdot 10^{-1}$	$2.8 \cdot 10^{4}$	$1.8 \cdot 10^{-5}$
Se-79	$2.1 \cdot 10^{-1}$	$1.5 \cdot 10^{4}$	$1.4 \cdot 10^{-5}$
Tc-99	$5.7 \cdot 10^{-1}$	$5.1 \cdot 10^{4}$	$1.1 \cdot 10^{-5}$
Np-237	$2.7 \cdot 10^{-5}$	3.0	$8.9 \cdot 10^{-6}$
Cl-36	$8.0 \cdot 10^{-1}$	$1.1 \cdot 10^{5}$	$7.5 \cdot 10^{-6}$
Sum			$4.7 \cdot 10^{-2}$

Table 9-3. Predicted maximum radionuclide concentration in soil, EMCL-values and the Risk Quotients (RQs).

Nuclide	Concentration* Bq/kg DW	EMCL* Bq/kg DW	Risk Quotient (RQ)
I-129	$6.5 \cdot 10^{-1}$	$4.3 \cdot 10^{2}$	$1.5 \cdot 10^{-3}$
Ni-59	$1.8 \cdot 10^{3}$	$1.4 \cdot 10^{6}$	$1.3 \cdot 10^{-3}$
C-14-org	$2.4 \cdot 10^{-2}$	$8.3 \cdot 10^{1}$	$2.9 \cdot 10^{-4}$
C-14-in	$1.2 \cdot 10^{-2}$	$8.3 \cdot 10^{1}$	$1.4 \cdot 10^{-4}$
Cl-36	$2.0 \cdot 10^{-1}$	$1.5 \cdot 10^{3}$	$1.3 \cdot 10^{-4}$
Se-79	$1.8 \cdot 10^{-1}$	$5.0 \cdot 10^{3}$	$3.7 \cdot 10^{-5}$
Pu-239	$3.1 \cdot 10^{-2}$	$1.1 \cdot 10^{3}$	$2.9 \cdot 10^{-5}$
Pu-240	$2.8 \cdot 10^{-2}$	$1.1 \cdot 10^{3}$	$2.6 \cdot 10^{-5}$
Cs-135	$5.0 \cdot 10^{-1}$	$1.9 \cdot 10^{4}$	$2.6 \cdot 10^{-5}$
Tc-99	$1.3 \cdot 10^{-2}$	$2.1 \cdot 10^{3}$	$6.0 \cdot 10^{-6}$
Nb-94	$4.3 \cdot 10^{-2}$	$1.1 \cdot 10^{4}$	$3.9 \cdot 10^{-6}$
Np-237	$4.2 \cdot 10^{-4}$	$3.8 \cdot 10^{2}$	$1.1 \cdot 10^{-6}$
Am-241	$5.0 \cdot 10^{-4}$	$6.3 \cdot 10^{2}$	$8.1 \cdot 10^{-7}$
Sum			$3.5 \cdot 10^{-3}$

* For C-14 the concentrations and EMCL are given in Bq/m^3 in air.

10 Sensitivity and uncertainty analyses

In this chapter results from sensitivity and uncertainty analyses carried out for the main Weichselian variant (CC1) are presented. The analyses were carried out by performing probabilistic simulations using Latin Hypercube sampling. The contribution to the variance of the peak doses from uncertainties in the dose factors and release rates to the biosphere /Thomson et al. 2008/ was estimated using the method described in /Vose 1996/. Further, sensitivity analyses were carried out to estimate which model parameters contribute the most to the uncertainties in the dose factors and the release rates. The sensitivity studied for the release rates was carried out for the Silo and the BMA, which have the highest contribution to the total release rates to the biosphere (see Section 5). The Spearman Rank Correlation Coefficients (SRCCs) were used as sensitivity measure, which is appropriate for models with monotonic relationships between parameters and outputs, as it is the case for most cases studied here. No geosphere related parameters were included in the sensitivity analysis. However, as shown by the calculation case where retardation in the geosphere is neglected (CC13), the retardation in the geosphere has a marginal effect on the doses.

10.1 Uncertainty of the dose estimations

Figure 10-1 presents results of probabilistic and deterministic dose estimations for releases to the landscape in the Weichselian variant (CC1). This figure shows the uncertainty in dose estimates, due to parameter uncertainties. It is shown in this figure that the parameter uncertainties in the peak doses are rather low, but become much larger for smaller dose values observed before, and especially after, the peak doses. The relatively low parameter uncertainty of the peak doses can be explained by the dominant contribution of C-14, for which the dose factors and the biosphere release rates have low uncertainty. For the dose values near the peak dose, the mean, the median and the deterministic value are very close to each other. At the same time, for dose before and after the peak doses the mean is always much higher than the median and the deterministic value.

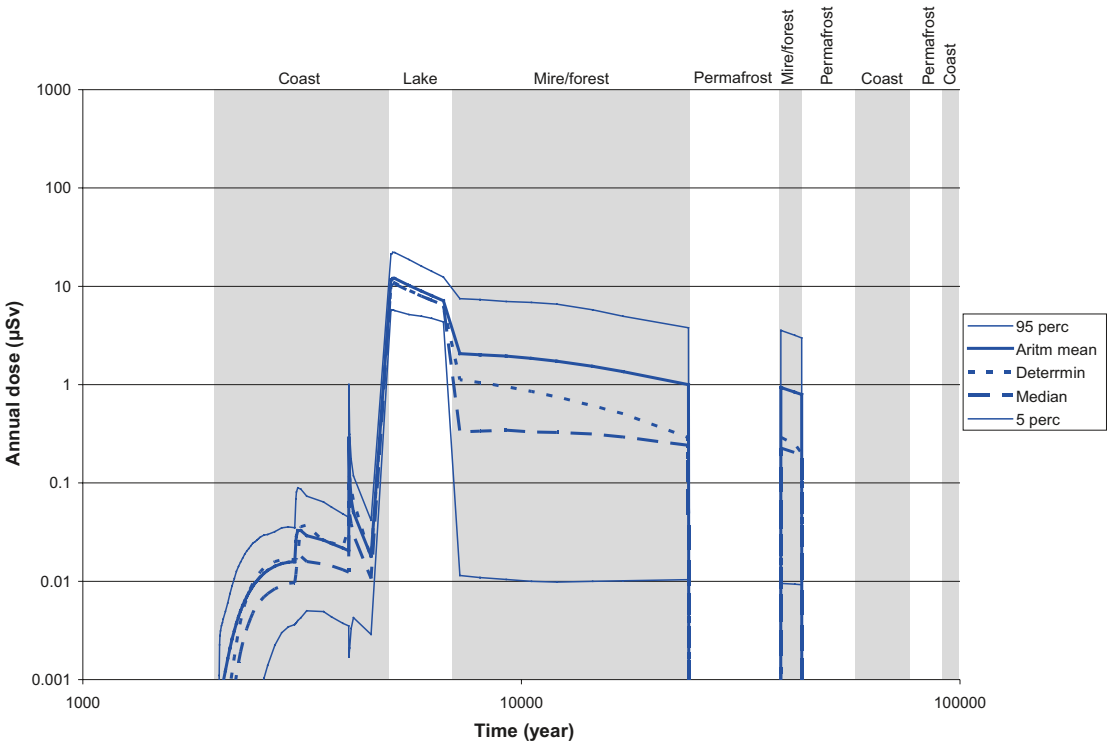

Figure 10-1. *Arithmetic mean, median, 5-th and 95-th percentiles of the annual individual dose for releases to the landscape from SFR 1 obtained for the Weichselian variant (CC1). Deterministically calculated annual rates are also shown.*

10.1.1 Releases to the landscape

Table 10-1 summarizes statistics of the peak values of annual doses obtained from probabilistic simulations for the case of releases to the landscape. The ratio between the 95 and 5 percentiles ranges from 1.5 for the BMA to 36 for the 2BTF. For the total peak doses, which are dominated by the Silo, this ratio is about 4.

Table 10-2 presents the contribution to the variance in peak dose values from uncertainty in the dose factors (DF) and releases to the biosphere (R). The uncertainty in the peak doses is mostly determined by uncertainties in predictions for C-14. This is because of the high contribution of this radionuclide to the doses. The uncertainty in the release rates has the highest contribution for all repository parts, except for the BMA for which the uncertainty of the release rates is very low.

10.1.2 Releases to a well

Table 10-3 summarizes statistics of the peak values of annual doses obtained from probabilistic simulations for the case of releases to a well. In this case, the ratios between the 95 and 5 percentiles show a much larger variation, of several orders of magnitude, than for the case with releases to the landscape (Section 10.1.1). This is partially explained by a higher uncertainty in the dose factors for the well, but also by a larger uncertainty in the release rate at year 4,000, due to transient changes in the groundwater fluxes occurring at this time. It should be noted that the dose values shown in Table 10-3 are values obtained during the simulations, i.e. a moving average of the values was not taken, as it was the case with the values reported in Chapters 5 and 6.

Table 10-4 presents estimates of the contribution to the variance of the peak dose values from uncertainty in the dose factors (DF) and release to the biosphere (R). For the Silo the uncertainty in the peak doses is mostly determined by the uncertainties for C-14, but for other repository parts other radionuclides, like Mo-93 for the BMA, I-129 for the BMA, 1BTF and 2BTF, as well as Pu-239 and Pu-240 for the BLA, have also an important contribution. The uncertainty in the release rates and in the dose factors has a similar contribution for the different repository parts.

Table 10-1. Statistics of the peak values of the annual doses (in μSv/y) obtained for releases to the landscape in the main scenario with base variant climate evolution.

	5%	50%	95%	Mean	STD	Time peak
Silo	1.9	4.4	7.1	4.5	1.5	Around 5,000
BMA	4.4	5.3	6.5	5.3	$6.8 \cdot 10^{-1}$	Around 5,000
BLA	$1.3 \cdot 10^{-3}$	$9.8 \cdot 10^{-3}$	$3.2 \cdot 10^{-2}$	$1.2 \cdot 10^{-2}$	$1.1 \cdot 10^{-2}$	Around 5,000
1BTF	$2.4 \cdot 10^{-2}$	$1.1 \cdot 10^{-1}$	$8.3 \cdot 10^{-1}$	$2.3 \cdot 10^{-1}$	$2.7 \cdot 10^{-1}$	Around 5,000
2BTF	$1.7 \cdot 10^{-1}$	1.6	6.2	2.4	2.1	Around 5,000

Table 10-2. Percentage contribution from uncertainty in the dose factors (DF) and release to the biosphere (R) to the variance in the peak values of the annual doses, obtained for releases to the landscape in the Weichselian variant.

Radionuclide	Silo		BMA		1BTF		2BTF		BLA	
	DF	R	DF	R	DF	R	DF	R	DF	R
C-14 org	10.1	89.9	73.5	2.8		0.4		0.7		7.8
C-14 inorg				0.7	0.5	98.5	1.1	98	0.5	76.8
Ni-59					0.3	0.1			3.9	1.9
Nb-94									1.1	0.2
Tc-99									1.1	0.6
C-135			7.4	15.3		0.1		0.1	1.4	1.2
Pu-239									0.6	0.3
Pu-240									1.7	0.8
Total	10.1	89.9	81	19	0.8	99.2	1.2	98.8	10.2	89.8

Table 10-3. Statistics of the peak values of the annual doses (in μSv/y) obtained for releases to a well in the Weichselian variant.

	5%	50%	95%	Mean	STD	Time peak
Silo	$5.4 \cdot 10^{-3}$	$2.9 \cdot 10^{-1}$	4.1	$9.5 \cdot 10^{-1}$	1.6	Around 4,000
BMA	$1.3 \cdot 10^{-2}$	$6.8 \cdot 10^{-1}$	$2.4 \cdot 10^{1}$	5.6	$1.8 \cdot 10^{1}$	Around 4,000
BLA	$8.1 \cdot 10^{-6}$	$3.9 \cdot 10^{-2}$	1.3	$2.6 \cdot 10^{-1}$	$7.6 \cdot 10^{-1}$	Around 4,000
1BTF	$7.1 \cdot 10^{-4}$	$1.5 \cdot 10^{-1}$	6.1	1.4	4.7	Around 4,000
2BTF	$6.3 \cdot 10^{-3}$	$8.9 \cdot 10^{-1}$	$5.4 \cdot 10^{1}$	$1.1 \cdot 10^{1}$	$3.4 \cdot 10^{1}$	Around 4,000

Table 10-4. Percentage contribution of the uncertainty in the dose factors (DF) and release to the biosphere (R) to the variance of the peak values of the annual doses obtained for releases to a well in the main scenario with base variant climate evolution.

Radionuclide	Silo		BMA		1BTF		2BTF		BLA	
	DF	R	DF	R	DF	R	DF	R	DF	R
C-14 org	67.4	30.2	11.1	9.1	0.7	1.3	1.2	2.7		
C-14 inorg					2.7	5.9	3.2	8.6		
Ni-59									0.8	0.2
Mo-93			20.2	37	5.7	7.1	0.5	0.8		
Tc-99									0.7	0.2
Ag-108m			0.4	1.4						
I-129			9.0	11.6	31.2	45.3	28.9	53.9		
C-135										
Pu-239									14.4	11
Pu-240									41	31.5
Total	67.6	32.4	40.7	59.3	40.3	59.7	33.9	66.1	57	43

10.2 Sensitivity analyses

10.2.1 Releases from the Silo

In the radionuclide transport calculations performed within the SAR-08 assessment project /Thomson et al. 2008/ a number of parameters related to the Silo were treated probabilistically using Latin Hypercube sampling. More information on how the different parameters were implemented and justification of the number of realisations are given in the radionuclide calculation report /Thomson et al. 2008/. The parameters considered in the sensitivity analysis are presented in Table 10-5, together with the names used to represent the parameters in the graphs in the remaining parts of this section.

Table 10-5. Parameters considered in the sensitivity analysis for the Silo.

Parameter	Represents
Kd_{concem}	Distribution coefficient for construction cement.
$Kd_{gravel/sand}$	Distribution coefficient for a mixture of gravel and sand.
$Kd_{sand/bentonite}$	Distribution coefficient for a mixture of sand ad bentonite.
$Kd_{bentonite}$	Distribution coefficient for the bentonite surrounding the Silo.
Uf_{2000}	Uncertainty factor that is introduced for scaling the flow for the time period between year 2,000 and 4,000 /Thomson et al. 2008/.
Uf_{4000}	Uncertainty factor that is introduced for scaling the flow for the time period from year 4,000 /Thomson et al. 2008/.

In the following subsections, results of the sensitivity analysis for the Silo are given for C-14, Ni-59, Cs-135 and Pu-239.

Organic C-14

One of the most important risk contributing radionuclides in SAR-08 is C-14, which may appear either in organic or inorganic form. Due to its comparatively short half-life and its chemical properties, C-14 is of main importance in the early part of the assessment time-period. Hence, the maximum release rate of organic C-14 was used in the sensitivity analysis together with probabilistic input data for the 960 realisations. As organic C-14 is treated as non-sorbing, only the flow uncertainty factors (Uf_{2000} and Uf_{4000}) are relevant for the result. Figure 10-2 shows Spearman Rank Correlation Coefficients for the maximum release rate of organic C-14.

The maximum release rate of organic C-14 occurs approximately at year 3,000. In Figure 10-2 it may be observed that an increase in the uncertainty factor (within the uncertainty interval considered) results in an increased flow from the Silo, which is in agreement with the understanding of the system. The fact that the flow uncertainty factor for later times, Uf_{4000}, shows to be significant in the analysis, although the analysis were carried out for the maximum flow at a time much earlier, is attributed to the fact that these two parameters are correlated, which is further shown in Figure 10-3.

Inorganic C-14

As mentioned above, one of the most important risk contributing radionuclides in SAR-08 is C-14, which may appear either in organic or inorganic form. Due to its comparatively short half-life and its chemical properties, C-14 is of main importance in the early part of the assessment time-period. Hence, the maximum release rate of inorganic C-14, which occurs around year 4,000, was used as input for the sensitivity analysis together with probabilistic input data for the 960 realisations. Inorganic C-14 is, as opposed to organic C-14, assumed to have a small sorption capability /Thomson et al. 2008/, which influence the results.

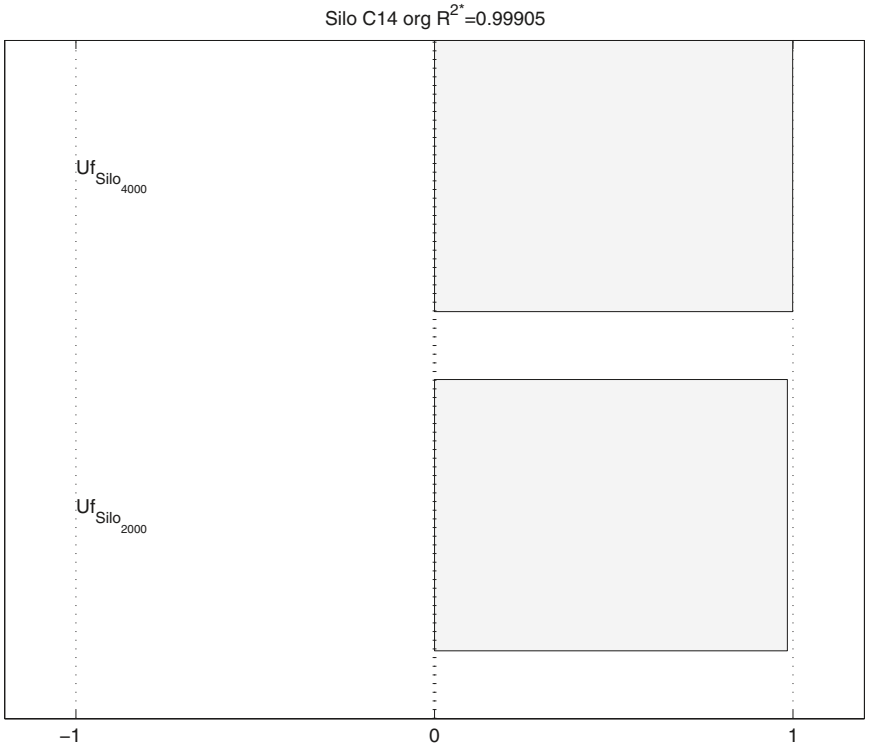

Figure 10-2. *Spearman Rank Correlation Coefficients for the maximum near field release rate of organic C-14. The parameters studied are flow uncertainty factors, Uf_{2000} and Uf_{4000}.*

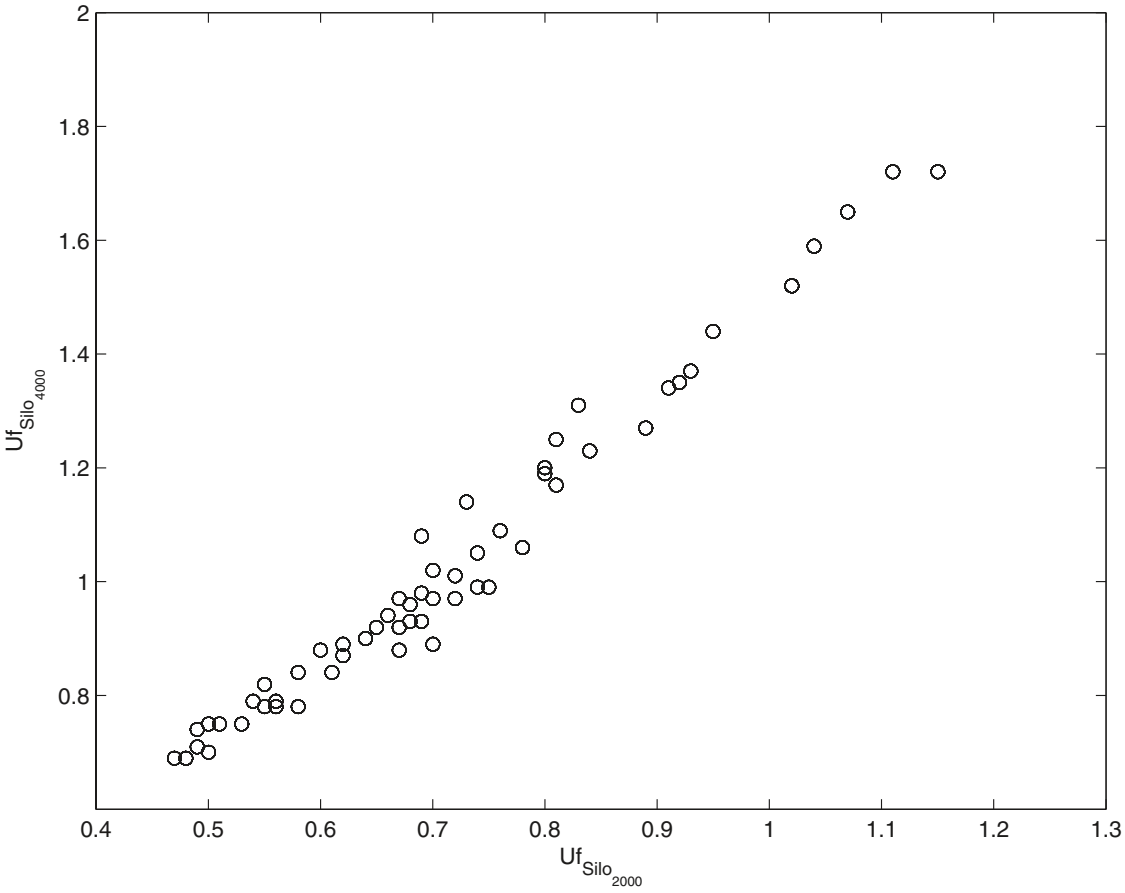

Figure 10-3. *Scatter plot of the flow uncertainty factors Uf_{4000} (y-axis) versus the flow uncertainty factors Uf_{2000} (x-axis).*

Figure 10-4 shows SRCCs for the maximum release rate of organic C-14. It can be seen that the solely most important uncertainty contributor is the distribution coefficient for construction cement. Less important contributors to the uncertainty are the flow uncertainty factors, *Uf*. The fact that both flow uncertainty factors appear in the analysis is attributed to the fact that both flow uncertainty factors are correlated. The way the uncertainties affect the result is in agreement with the understanding of the system, a decreased distribution coefficient (lower *Kd*) as well as an increased flow (higher *Uf*) through the system, results in higher release rates.

Ni-59

Nickel-59 is one of the important radionuclides in the later part of the assessment time-period and has an intermediate sorption capacity. As the half-life of Ni-59 is relatively long ($7.60 \cdot 10^4$ years), the inventory of Ni-59 will be substantial throughout the assessment period. Hence, the release rate at the time-step prior to the start of the permafrost period at year 25,000 was chosen as the dependent variable for the sensitivity analysis.

Figure 10-5 shows SRCCs for Ni-59. The predominant uncertainty contributor is the distribution coefficient of the construction cement, Kd_{concem}, followed by uncertainties in the distribution coefficient of sand/bentonite and the flow uncertainty factors (also for Ni-59 these two are correlated and have hence the corresponding importance). All results are in agreement with the understanding of the system, a decreased distribution coefficient (lower *Kd*), as well an increased flow (higher U_f) through the system, result in higher release rates.

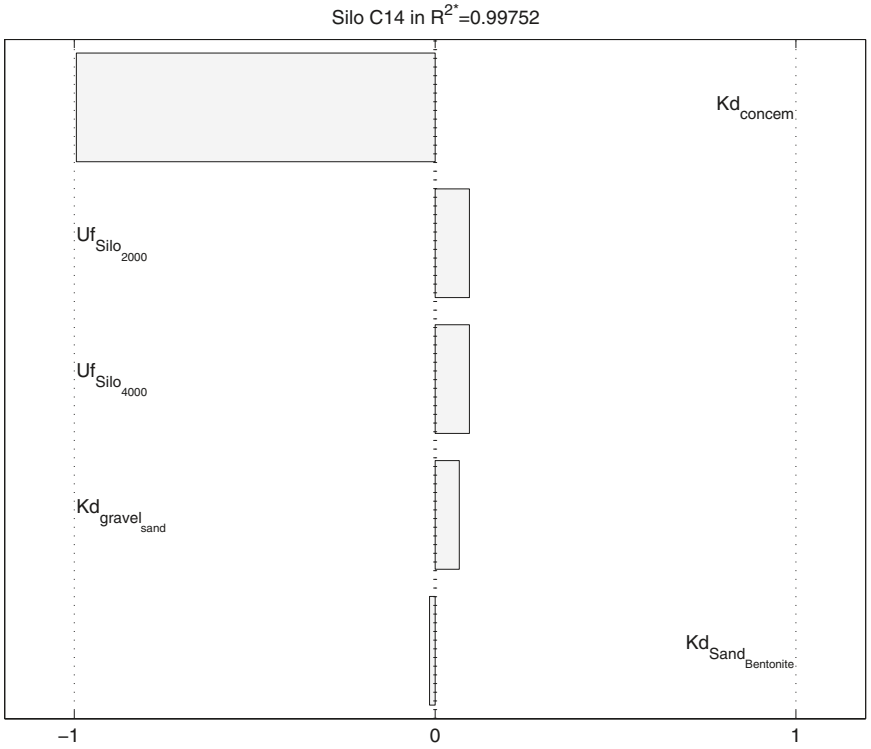

Figure 10-4. *Spearman Rank Correlation Coefficients for the maximum near field release rate of inorganic C-14. The parameters studied are the distribution coefficient of the construction cement, the gravel/sand and the sand/bentonite (Kd_{concem}, $Kd_{gravelsand}$ and $Kd_{sandbentonite}$, respectively) and the flow uncertainty factors, Uf_{2000} and Uf_{4000}.*

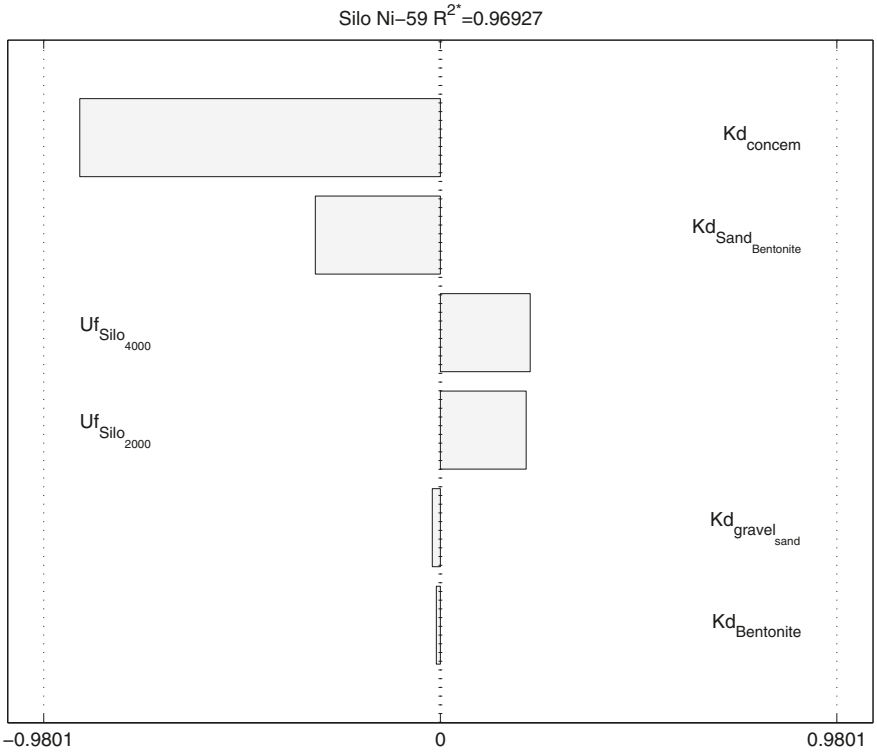

Figure 10-5. *Spearman Rank Correlation Coefficients for maximum the near field release rate of Ni-59. The parameters studied are the distribution coefficient in the construction cement, the gravel/sand, the sand/bentonite and the bentonite (Kd_{concem}, $Kd_{gravelsand}$, $Kd_{sandbentonite}$ and $Kd_{bentonite}$, respectively) and the flow uncertainty factors, Uf_{2000} and Uf_{4000}.*

Cs-135

Caesium-135 is one of the important radionuclides in the later part of the assessment time-period and has an intermediate sorption capacity. As the half-life of Cs-135 is relatively long ($2.30 \cdot 10^6$ years), the inventory of Cs-135 will be substantial throughout the assessment time-period. Hence, the release rate at the time-step prior to the start of the permafrost at year 25,000 was chosen as the dependent variable for the sensitivity analysis.

Figure 10-6 shows the SRCCs for Cs-135. The predominant uncertainty contributor is the distribution coefficient of construction cement Kd_{concem}, followed by uncertainties in the distribution coefficient for sand/bentonite and the flow uncertainty factors (also for Cs-135 these two are correlated and have hence the corresponding importance). All results are in agreement with the understanding of the system, a decreased distribution coefficient (lower *Kd*) as well an increased flow (higher U_f) through the system, result in higher release rates.

Pu-239

Plutonium-239 is, compared with the radionuclides reported above, of less importance for the SAR-08 results. It is however relevant to perform a sensitivity analysis for the release rate of Pu-239, as it is a strongly sorbing radionuclide and a somewhat different behaviour is to be expected. The half-life of Pu-239 is in the intermediate range, but long enough ($2.41 \cdot 10^4$ years) for Pu-239 to be important throughout the whole assessment period. Hence, the release rate at the time-step prior to the start of the permafrost period at year 25,000 was chosen as the dependent variable for the sensitivity analysis.

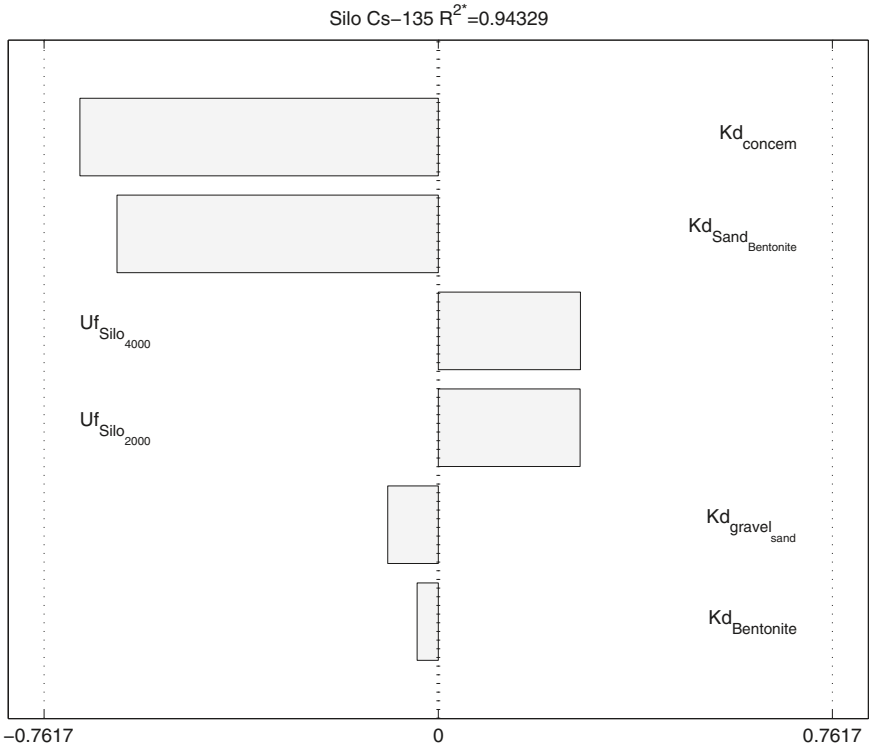

Figure 10-6. *Spearman Rank Correlation Coefficients for the maximum near field release rate of Cs-135. The parameters studied are the distribution coefficient in the construction cement, the gravel/sand, the sand/bentonite and the bentonite (Kd_{concem}, $Kd_{gravelsand}$, $Kd_{sandbentonite}$ and $Kd_{bentonite}$, respectively) and the flow uncertainty factors, Uf_{2000} and Uf_{4000}.*

Figure 10-7 shows the SRRCs for Pu-239. The predominant uncertainty contributor is the distribution coefficient of construction cement, followed by the distribution coefficient of sand/bentonite and the flow uncertainty factors (also for Pu-239 these two are correlated and have hence the corresponding importance). All results are in agreement with the understanding of the system, a decreased distribution coefficient (lower *Kd*), as well an increased flow (higher U_f) through the system, result in higher release rates.

It must however be noted, that the coefficient of determination (R^{2*}) for the SRCCs is low, suggesting that there might be other important parameters, that are not included in the sensitivity analysis and/or that the dependencies between the parameters and the release rates are non-monotonic.

10.2.2 Releases from the BMA

In the radionuclide transport calculations performed within the SAR-08 assessment project /Thomson et al. 2008/ a number of parameters related to the BMA were treated probabilistically using Latin Hypercube sampling. More information on how the different parameters were implemented and justification of the number of realisations is given in the radionuclide release calculation report /Thomson et al. 2008/. The parameters considered in the sensitivity analysis are presented in Table 10-6, together with the names used to represent the parameters in the graphs in the remaining parts of this chapter.

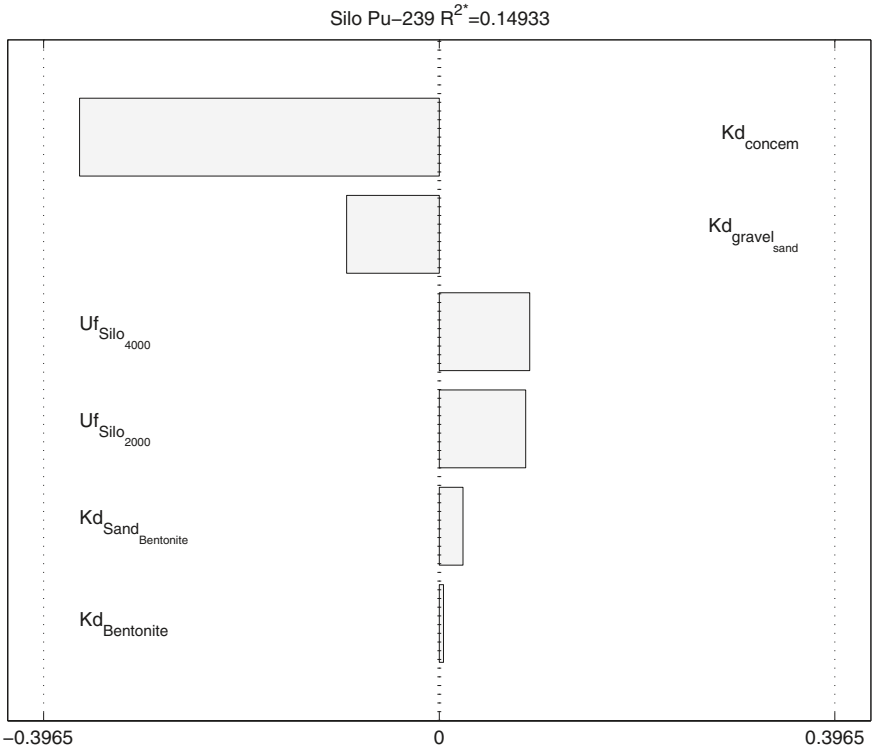

Figure 10-7. *Spearman Rank Correlation coefficients for the maximum near field release rate of Pu-239. The parameters studied are the distribution coefficient in the construction cement, the gravel/sand, the sand/bentonite and the bentonite (Kd_{concem}, $Kd_{gravelsand}$, $Kd_{sandbentonite}$ and $Kd_{bentonite}$, respectively) and the flow uncertainty factors, Uf_{2000} and Uf_{4000}. Note, however, the low R^{2*} value further discussed in the text.*

Table 10-6. Parameters included in the sensitivity analysis for the BMA.

Parameter	Represents
Kd_{concem}	Distribution coefficient for construction cement.
$Kd_{gravel/sand}$	Distribution coefficient for a mixture of gravel and sand.
Uf_{2000}	Uncertainty factor that is introduced for scaling the flow for the time period between year 2,000 and 4,000 /Thomson et al. 2008/.
Uf_{4000}	Uncertainty factor that is introduced for scaling the flow for the time period from year 4,000 /Thomson et al. 2008/.

In the following subsections, results of the sensitivity analysis for the BMA are given for C-14, Ni-59, Cs-135 and Pu-239.

Organic C-14

One of the most important risk contributing radionuclides in SAR-08 is C-14, which may appear either in organic or inorganic form. Due to its comparatively short half-life and its chemical properties, C-14 is of main importance in the early part of the assessment time-period. Hence, the maximum release rate of organic C-14 was used in the sensitivity analysis, together with probabilistic input data for the 960 realisations. As organic C-14 is treated as non-sorbing only the flow uncertainty factors (Uf_{2000} and Uf_{4000}) are relevant for the results. Figure 10-8 shows SRCCs for the maximum release rate of organic C-14.

The maximum release rate of organic C-14 occurs approximately at year 3,000. In Figure 10-8 it may be observed that an increase in the uncertainty factor (within the uncertainty interval considered) results in an increased flow from the BMA, which is in agreement with the understanding of the system. The fact that the flow uncertainty factor for later times, Uf_{4000}, shows to be significant, although the analysis were carried out for the maximum flow at a time much earlier, is attributed to the fact that these two parameters are correlated which is further shown in Figure 10-3.

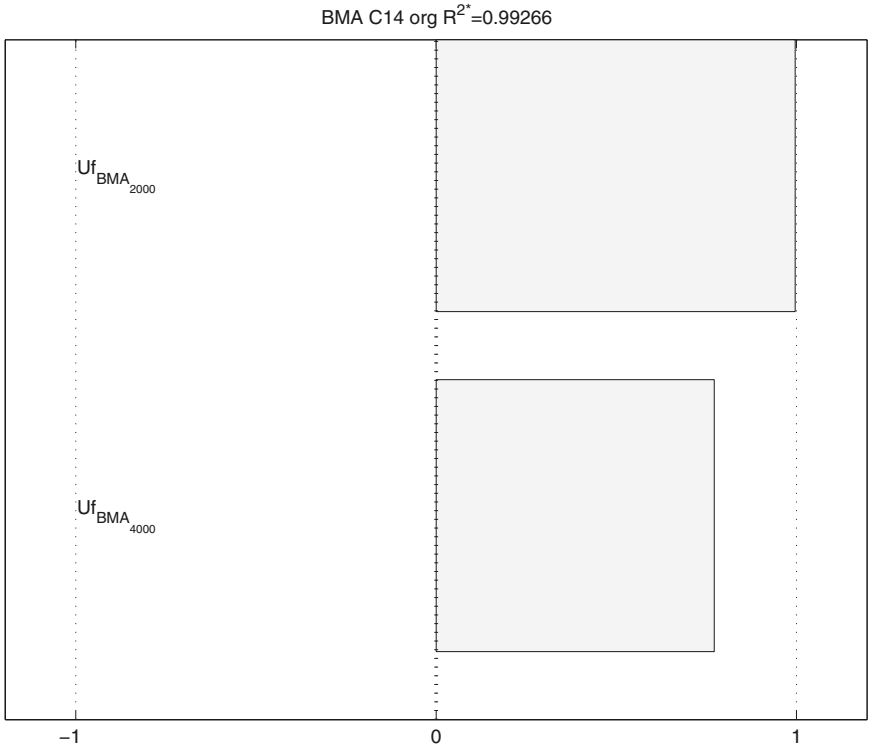

Figure 10-8. *Spearman Rank Correlation Coefficients for the maximum near field release rate of organic C-14. The parameters studied are flow uncertainty factors, Uf_{2000} and Uf_{4000}.*

Inorganic C-14

As mentioned above, one of the most important risk contributing radionuclides in SAR-08 is C-14, which may appear either in organic or inorganic form. Due to its comparatively short half-life and its chemical properties, C-14 is of main importance in the early part of the assessment time-period. Hence, the maximum release rate of inorganic C-14, which occurs around year 4,000, was used as input for the sensitivity analysis together with probabilistic input data for the 960 realisations. Inorganic C-14 is, as opposed to organic C-14, assumed to have a small sorption capability /Thomson et al. 2008/ which influence the results.

Figure 10-9 shows SRCCs for the maximum release rate of inorganic C-14. The solely most important uncertainty contributor is the distribution coefficient of construction cement. Less important (insignificant) uncertainties have the distribution coefficient of sand/gravel and the flow uncertainty factors, U_f. The reason why both flow uncertainty factors show a contribution to the uncertainty is that both flow uncertainty factors are correlated. The way the uncertainties affect the result is in agreement with the understanding of the system, a decreased distribution coefficient (lower *Kd*), as well as an increased flow (higher U_f) through the system, result in higher release rates.

Ni-59

Nickel-59 is one of the important radionuclides in the later part of the assessment time-period and has an intermediate sorption capacity. As the half-life of Ni-59 is relatively long ($7.60 \cdot 10^4$ years), the inventory of Ni-59 will be substantial throughout the assessment period. Hence, the release rate at the time-step prior to the start of the permafrost period at year 25,000 was chosen as the dependent variable for the sensitivity analysis.

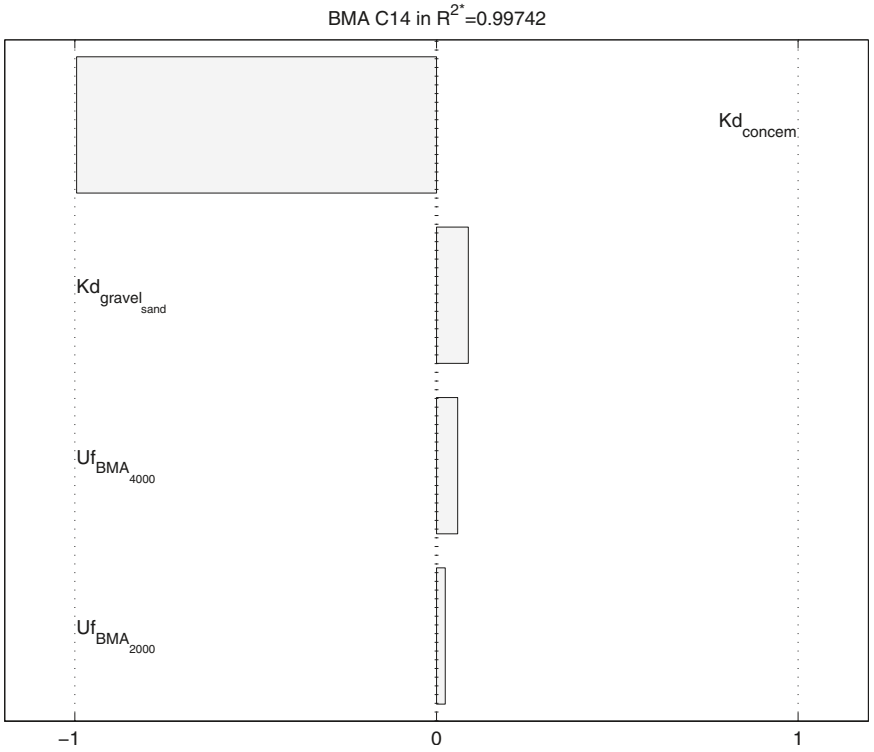

Figure 10-9. *Spearman Rank Correlation Coefficients for the maximum near field release rate of inorganic C-14. The parameters studied are the distribution coefficient of the construction cement and the gravel/sand (Kd_{concem}, and $Kd_{gravelsand}$, respectively) and the flow uncertainty factors, Uf_{2000} and Uf_{4000}.*

Figure 10-10 shows the SRCCs for Ni-59. The predominant uncertainty contributor is the distribution coefficient of construction cement, Kd_{concem}, followed by uncertainties in the distribution coefficients of sand/bentonite and the flow uncertainty factors (also for Ni-59 these two are correlated and have hence the corresponding importance). All results are in agreement with the understanding of the system, a decreased distribution coefficient (lower *Kd*), as well an increased flow (higher U_f) through the system, result in higher release rates.

Cs-135

Caesium-135 is one of the important radionuclides in the later part of the assessment time-period and has an intermediate sorption capacity. As the half-life of Cs-135 is relatively long ($2.30 \cdot 10^6$ years), the inventory of Cs-135 will be substantial throughout the assessment time-period. Hence, the release rate at the time-step prior to the start of the permafrost period at year 25,000 was chosen as the dependent variable for the sensitivity analysis.

While the used linear sensitivity model showed to be adequate for the radionuclides reported earlier in the current chapter, the analysis yields both small R^{2*}-values and unrealistic results. The reason for this can be seen in Figure 10-11 and Figure 10-12 where the distribution coefficients of the construction cement and the sand/gravel mixture are presented together with the flux from the near field. It may be seen, especially in Figure 10-11, that the response is not monotonic, but there are additional contributing factors.

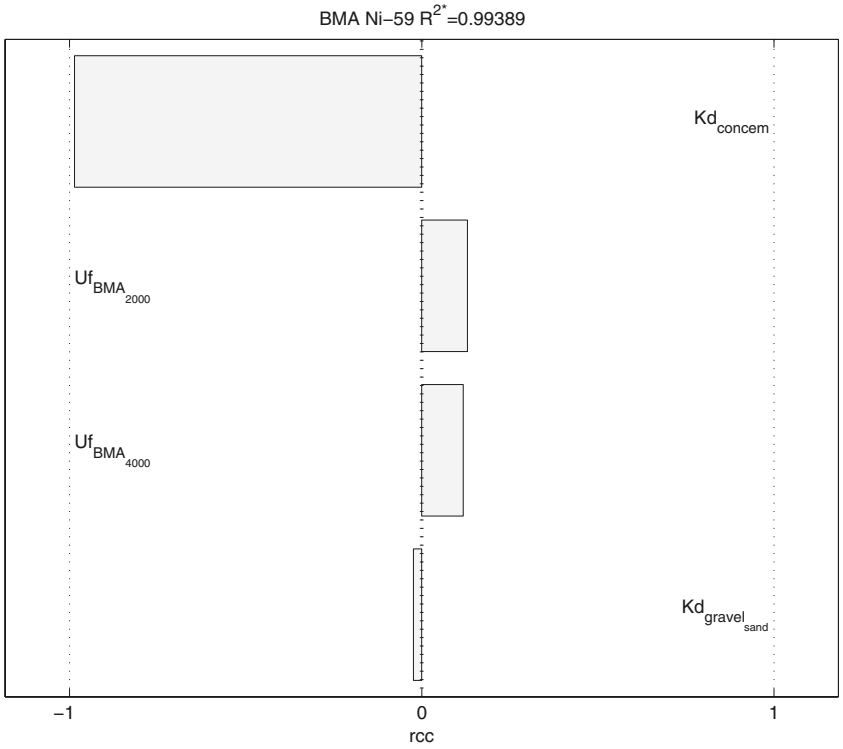

Figure 10-10. *Spearman Rank Correlation Coefficients for the maximum near field release rate of Ni-59. The parameters studied are the distribution coefficient of the construction cement and the gravel/sand (Kd_{concem}, and $Kd_{gravelsand}$, respectively) and the flow uncertainty factors, Uf_{2000} and Uf_{4000}.*

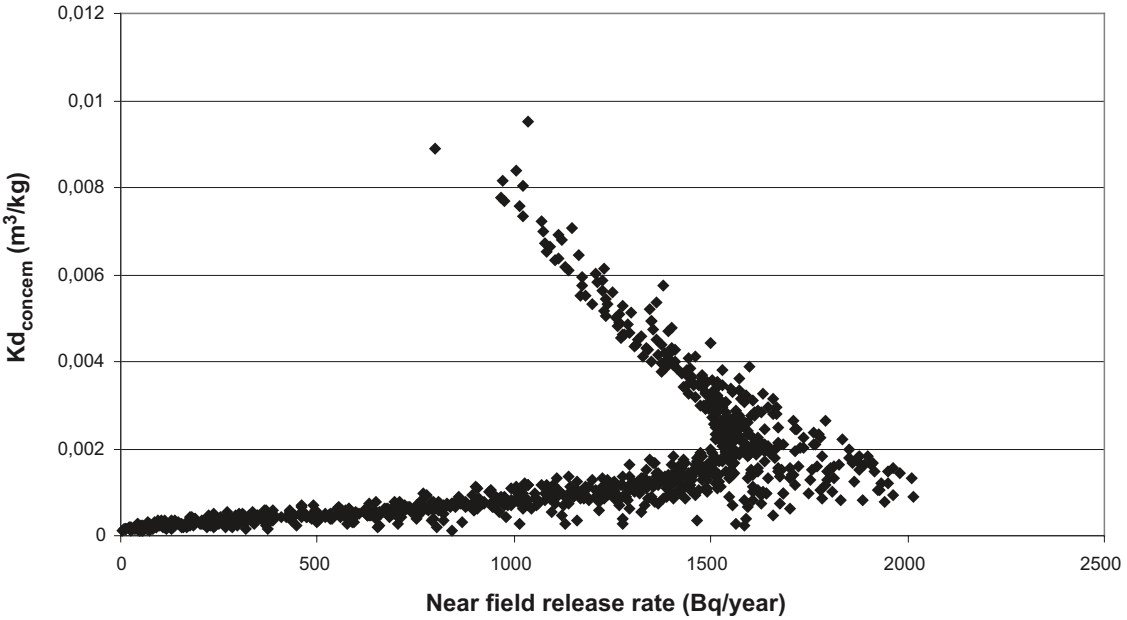

Figure 10-11. *Scatter plot of the distribution coefficient of the construction cement, Kd_{concem} versus the near field release rates and for Cs-135.*

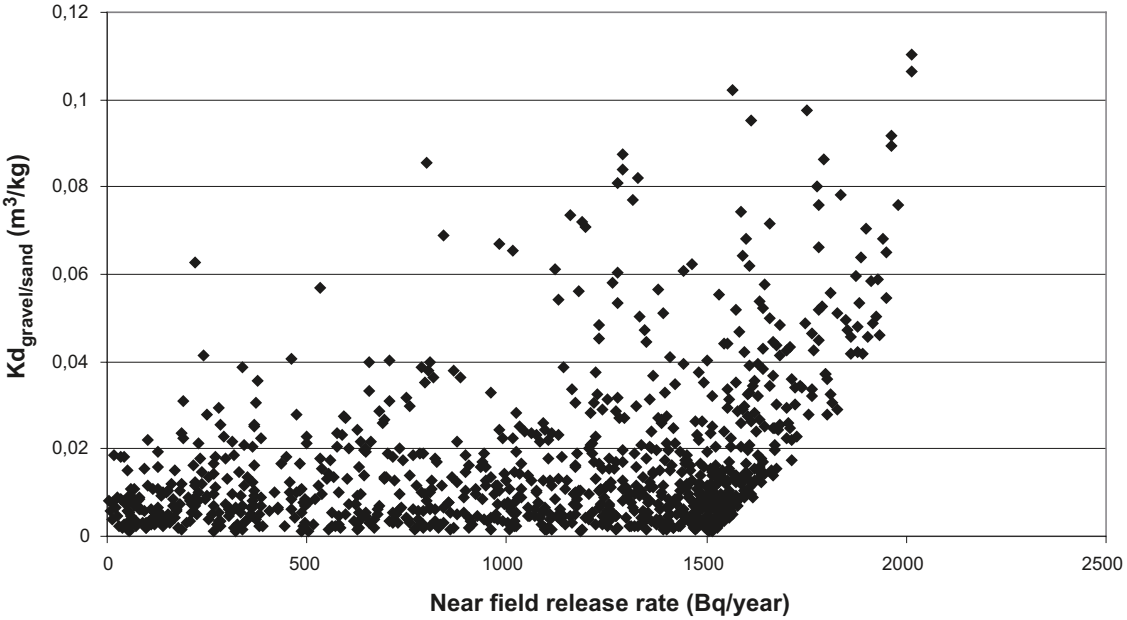

Figure 10-12. *Scatter plot of the distribution coefficient of the gravel/sand mixture cement, $Kd_{gravel/sand}$ versus the near field release rates for Cs-135.*

Pu-239

Plutonium-239 is, compared to the radionuclides reported in the earlier subsections, of less importance for the SAR-08 results. It is however still relevant to perform a sensitivity analysis of the release rate of Pu-239, as it is a strongly sorbing radionuclide. The half-life of Pu-239 is in the intermediate range, but is long enough ($2.41 \cdot 10^4$ years) for Pu-239 to be important throughout the assessment period. The release rate at the time-step prior to the start of the permafrost period at year 25,000 was chosen as the dependent variable for the sensitivity analysis.

Figure 10-13 shows the SRCCs for Pu-239. The predominant uncertainty contributor is the distribution coefficient of the construction cement, with the gravel/sand distribution coefficients at second place, followed by the flow uncertainty factors (also for Pu-239 these two are correlated and have hence the corresponding importance). All results are in agreement with the understanding of the system, a decreased distribution coefficient (lower *Kd*) results in higher release rates, as well as an increased flow (higher U_f) through the system.

It must however be noted that the R^{2*} value for the ranked correlation coefficient is low, suggesting that there might be other important parameters that are not included in the analysis.

10.2.3 Dose Factors for releases to the landscape

The results of the sensitivity analyses for the dose factors for releases to the landscape are presented in Figure 10-14 and 10-15 for C-14 and Cs-135, respectively. These radionuclides were selected for the analysis, as they have the highest contribution to the uncertainty of the dose estimates (see Section 10.1.1). The results are presented for landscape configuration where the receptor of releases is a lake, as the peak doses are associated to this case.

For C-14, the parameters with the highest effect on the uncertainty of the dose factors are the Dissolved Inorganic Carbon (DIC) content and the Net Primary Production (NPP). In the case of Cs-135 the bioaccumulation factor for fish have a dominant effect on the uncertainty of the dose factors.

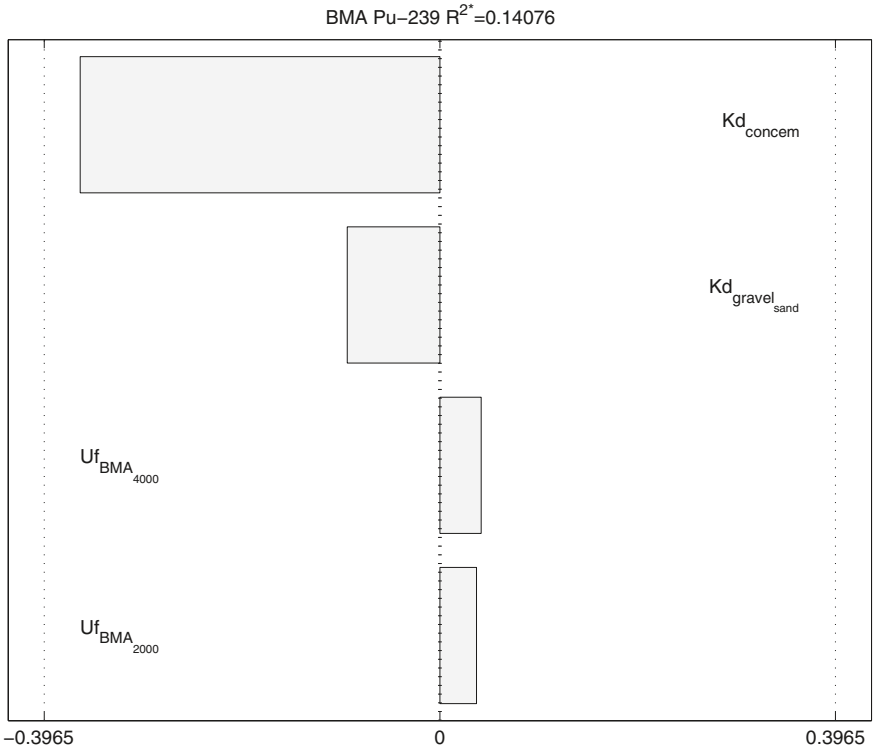

Figure 10-13. *Spearman Rank Correlation Coefficients for the maximum near field release rate of Pu-239. The parameters studied are the distribution coefficient of the construction cement and the gravel/sand (Kd_{concem}, and $Kd_{gravelsand}$, respectively) and the flow uncertainty factors, Uf_{2000} and Uf_{4000}.*

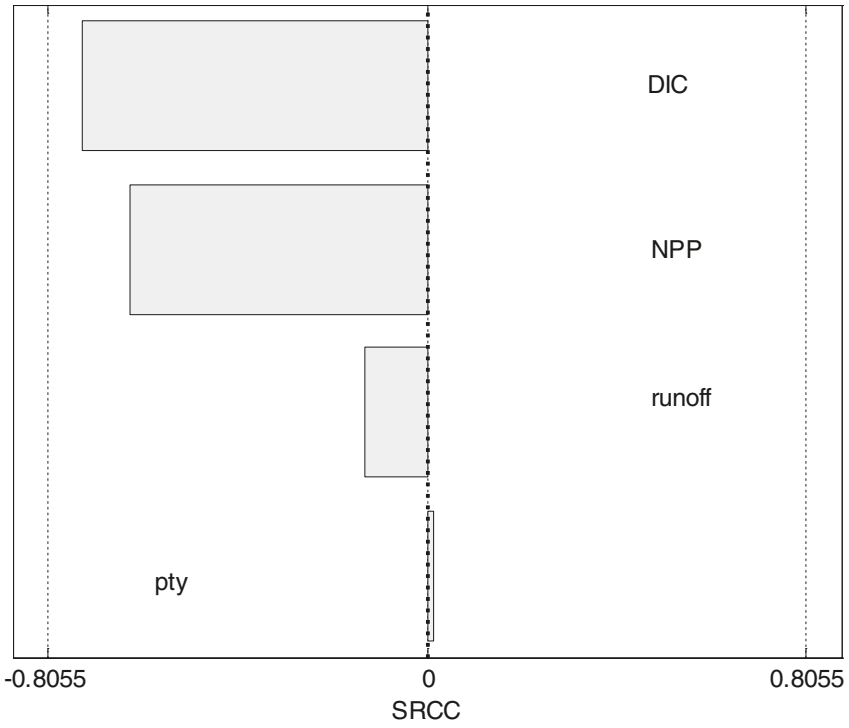

Figure 10-14. *Spearman Rank Correlation Coefficients of the total annual doses per unit release rate of C-14 obtained for the case of releases to a lake. The parameters shown are: DIC – dissolved inorganic carbon, NPP – net primary production, runoff – average runoff in the area, pty – food production in the lake.*

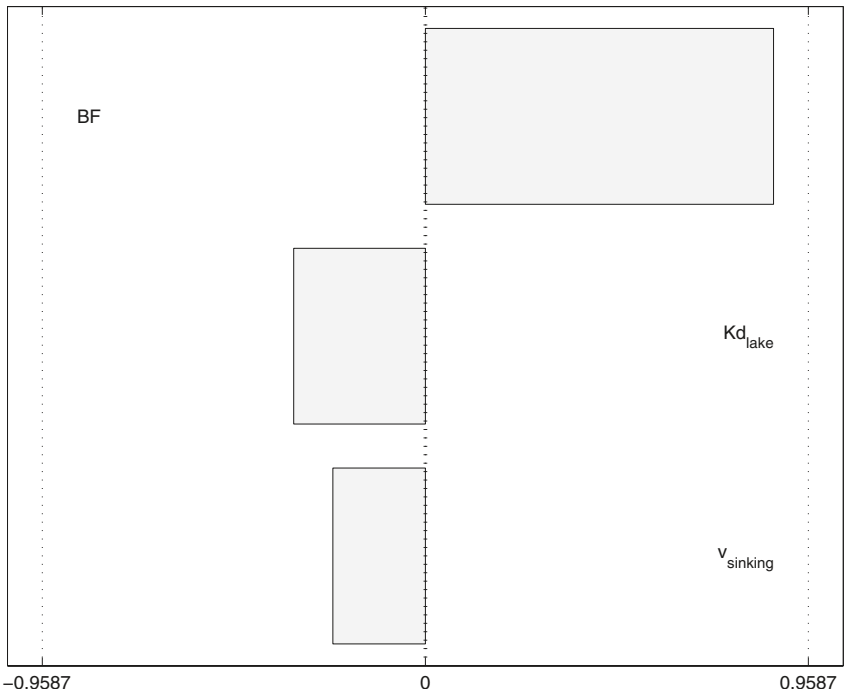

Figure 10-15. *Spearman Rank Correlation Coefficients of the total annual doses per unit release rate of Cs-135 obtained for the case of releases to a lake. The parameters shown are: BF – bioaccumulation factor, Kd_lake – distribution coefficient in lakes, v_sinking – sedimentation velocity.*

10.2.4 Dose Factors for releases to a well

The results of the sensitivity analyses carried out for the dose factors for releases to a well are presented in Figures 10-16, 10-17 and 10-18 for C-14, I-129 and Pu-239 respectively. These radionuclides were selected for the analysis as they have the highest contribution to the uncertainty of the dose estimates (see Section 10.1.2).

For the three studied radionuclides the uncertainty of the well capacity has a dominant effect on the uncertainty of the dose factors.

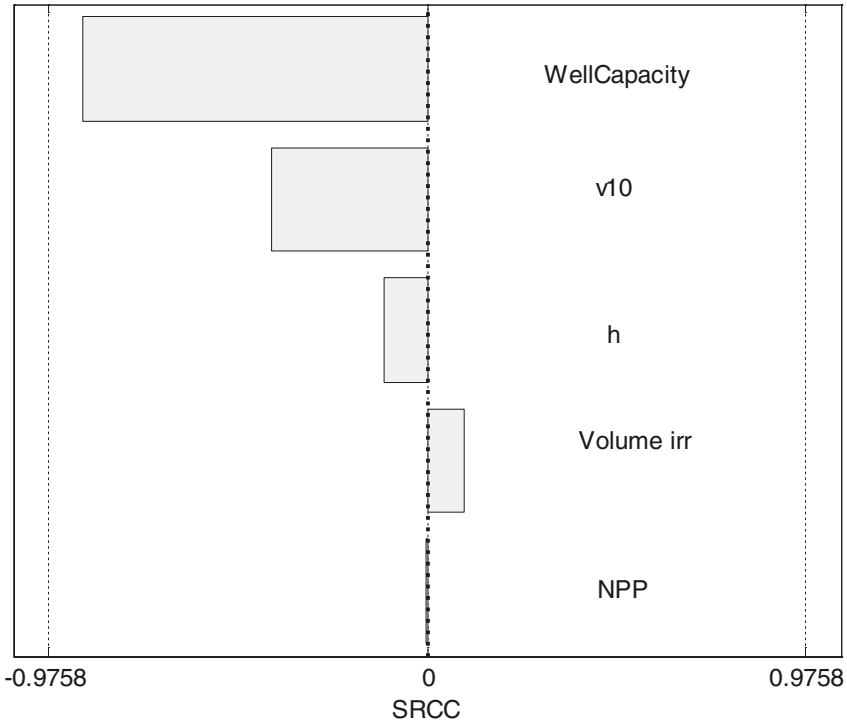

Figure 10-16. *Spearman Rank Correlation Coefficients of the total annual doses per unit release rate of C-14 obtained for the case of releases to a well. The parameters shown are: well capacity, v10 – wind speed at 10 m, h – mixing height, Volume irr – irrigation volume, NPP- net primary production.*

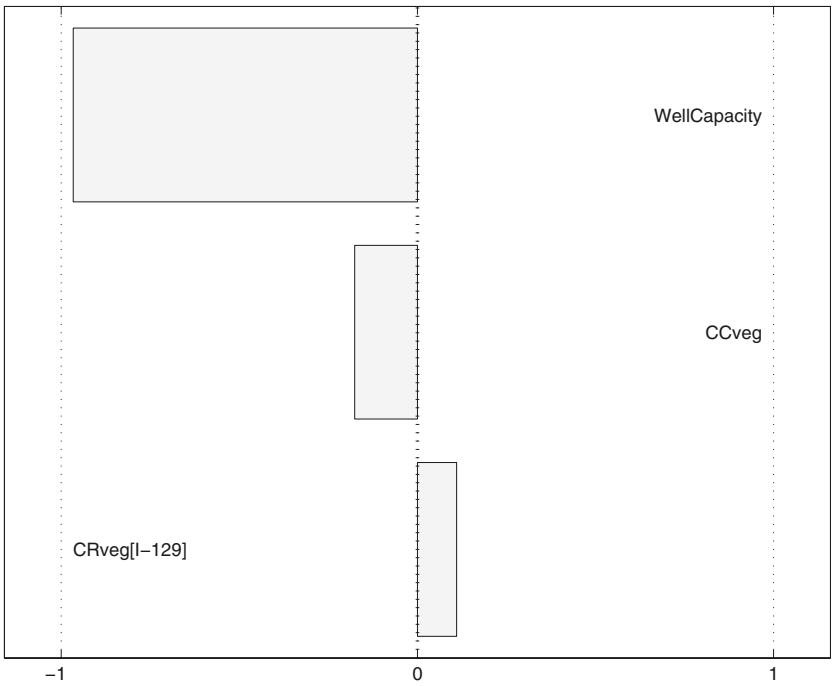

Figure 10-17. *Spearman Rank Correlation Coefficients of the total annual doses per unit release rate of I-129 obtained for the case of releases to a well. The parameters shown are: well capacity, CCveg – carbon content of vegetables, CRveg[I-129] concentration ratio of I-129 from soil to vegetables.*

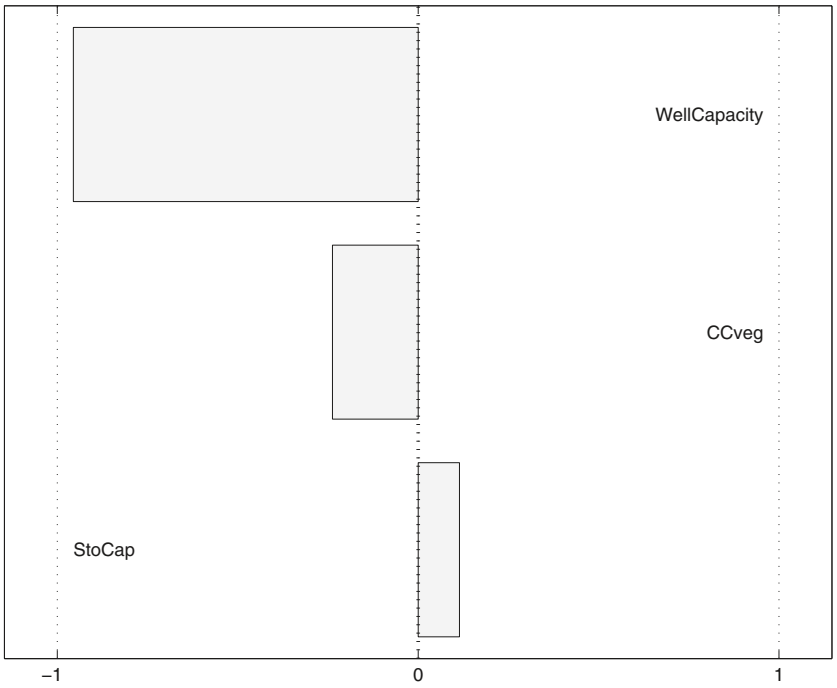

Figure 10-18. *Spearman Rank Correlation Coefficients of the total annual doses per unit release rate of Pu-239 obtained for the case of releases to a well. The parameters shown are: well capacity, CCveg – carbon content of vegetables, StoCap – water storage capacity of vegetables.*

11 Conclusions

This report presents estimations of annual doses to the most exposed groups from potential radionuclide releases from the SFR 1 repository for a number of calculation cases, selected using a systematic approach for identifying relevant scenarios for the safety analysis. The dose estimates can be used for demonstrating that the long term safety of the repository is in compliance with the regulatory requirements. In particular, the mean values of the annual doses can be used to estimate the expected risks to the most exposed individuals, which can then be compared with the regulatory risk criteria. In doing this, other aspects need to be considered, such as the probability of the different scenarios. Also, it is important to take into consideration that the doses have been calculated for the potentially most exposed group, consisting of only a few people that make maximal use of the potentially affected area of the landscape. It is assumed that the members of the most exposed group spend all time in the most affected area and that all food and water that they consume comes from this area.

The dose calculations were carried out for a period of 100,000 years, which was sufficient to observe peak doses in all scenarios considered. Releases to the landscape and to a well were considered. The peaks of the mean annual doses from releases to the landscape are associated with C-14 releases to a future lake around year 5,000 AD. In the case of releases to a well, the peak annual doses were obtained around year 4,000 AD, when an increase of groundwater discharges occurs in connection with the ongoing shoreline displacement. The peaks for the well are also dominated by C-14, although a few other radionuclides also contribute. This pattern of the peak doses was observed for calculation cases of the main scenario and less probable scenarios. Moreover, the predicted doses, including peak dose values, for calculation cases of the less probable scenarios were very close to the predictions for calculation cases of the main scenario.

Predicted doses during the first 1,000 years after the repository closure did not exceed 0.05 μSv/y. Low release rates are predicted for this period, when the recipient for the releases is the sea, and doses per unit release rate are low, as compare to the case with releases to a lake or a mire. Doses from short-lived radionuclides were very low, as these can only be released during the sea period, when doses per unit release rate are lower due to larger dilution. The doses for actinides were also low, due to effective retention in the engineered barriers and their low inventory. In general, total mean annual individual doses were low during the whole simulation period, with values below 14 μSv/y for the main and less probable scenarios. The collective incomplete dose commitment from releases during the first 1,000 years after repository closure was estimated at 8 manSv.

The assessment of the impact on non-human biota showed that the potential impact is negligible for all radionuclides and ecosystems of relevance.

Uncertainty analyses were carried out using probabilistic methods. These analyses showed that the parameter uncertainty in the peak doses from releases to the landscape are low due to the dominant role of C-14, for which the dose factors and the biosphere release rates have low uncertainty. The uncertainty in the release rates to the biosphere has the highest contribution to the overall uncertainty of the peak dose estimates. This is true for all repository parts, except for the BMA for which the uncertainty of the release rates is very low. The uncertainty of the peak dose estimates for releases to a well was higher, which can be explained by a higher uncertainty in the dose factors for the well and in the release rates to the biosphere at year 4,000 AD, when the peak doses to releases to a well are observed. The higher uncertainty of the release rates at year 4,000 AD can be explained by transient changes in the groundwater fluxes occurring at this time.

Sensitivity studies were carried out to identify the near field and biosphere parameters that have the highest contribution to the uncertainty of the peak dose estimates. Geopshere parameters were not included in the sensitivity studies. However, a calculation case where retardation in the geosphere was neglected showed that retardation in the geosphere has a marginal effect on the doses. The parameters with the highest contribution to the uncertainties in estimates of release rates from the near field are the flow uncertainty factors for non-sorbing radionuclides and the distribution coefficients in the construction cement for sorbing radionuclides. The biosphere parameters with the highest effect on the uncertainty of the peak dose estimates for releases to the landscape are the dissolved inorganic carbon content and the net primary production in lakes. In the case of releases to a well, the biosphere parameter with the highest and dominant effect on the uncertainty of dose estimates is the well capacity.

12 References

Almkvist L, Gordon A, 2007. Low and intermediate level waste in SFR 1. Reference waste inventory 2007. SKB R-07-17, Svensk Kärnbränslehantering AB.

Altman P L, Ditmer D S, 1964. Biology Data Book (Federation of American Societiesfor Experimental Biology, Washington DC.

Andersson E, Kumblad L, 2006. A carbon budget for an oligotrophic clearwater lake in mid-Sweden. Aquatic Sciences, Vol 68, pp 52–64.

Avila R, 2006a. The ecosystem models used for dose assessments in SR-Can. SKB R-06-81, Svensk Kärnbränslehantering AB.

Avila R, 2006b. Model of the long-term transfer of radionuclides in forests SKB TR-06-08 Svensk Kärnbränslehantering AB.

Avila R, Bergström U, 2006. Methodology for calculation of doses to man and implementation in Pandora. SKB R-06-68, Svensk Kärnbränslehantering AB.

Avila R, Ekström P A, Kautsky U, 2006. Development of Landscape dose conversion factors for dose-assessments in SR-Can. SKB TR-06-15, Svensk Kärnbränslehantering AB.

Avila R, Pröhl G, 2008. Models used in the SFR 1 SAR-08 and KBS-3H safety assessments for calculation of ^{14}C doses. SKB R-08-16, Svensk Kärnbränslehantering AB.

Banse K,Mosher S, 1980. Adult Body Mass and Annual Production/Biomass Relationships of Field Populations. Ecological Monographs, Vol 50 (3), pp 355–379.

Beresford N A, Brown J, Copplestone D, Garnier-Laplace J, Howard B, Larsson C M, Oughton D, Pröhl G, Zinger I (ed), 2007. An integrated approach to the assessment and management of environmental risks from ionising radiation. Description of purpose, methodology and application. EC project contract N° FI6R-CT-2004-508847.

Berglund B, 2005. »Orättvis« effekt av fysisk aktivitet – Otränade måste träna längre tid för att nå uppsatta mål om prevention. Läkartidningen, Vol 102 (46), pp 3456–3462.

Bergström U, Barkefors C, 2004. Irrigation in dose assessments models. SKB R-04-26, Svensk Kärnbränslehantering AB.

Bergström U, Puigdomenech I, 1987. Radiological consequences to man due to leakage from a final repository for reactor waste (SFR). SKB Progress report, SFR 87-12, Svensk Kärnbränslehantering AB.

Blomqvist P, Nilsson E, Brunberg A-K, 2002. Habitat distribution, water chemistry, and biomass and production of pelagic and benthic microbiota in Lake Eckarfjärden, Forsmark. SKB R-02-41, Svensk Kärnbränslehantering AB.

Boresjö Bronge L, Wester K, 2002. Vegetation mapping with satellite data of the Forsmark and Tierp region. SKB R-02-06, Svensk Kärnbränslehantering AB.

Borgiel M, 2004. Sampling of freshwater fish. Forsmark site investigation. SKB P-04-06, Svensk Kärnbränslehantering AB.

Bourquin A, 2008. Man and Mollusc's Data Base of Edible Molluscs. http://www.manandmollusc.net/molluscan_food_files/molluscan_food_terrestrial.html [Accessed 2008-03-31].

Bosson E, Berglund S, 2006. Near-surface hydrogeological model of Forsmark. Open repository and solute transport applications – Forsmark 1.2. SKB R-06-52, Svensk Kärnbränslehantering AB.

Brunberg A-K, Carlsson T, Blomqvist P, Brydsten L, Strömgren M, 2004. Identification of catchments, lake-related drainage parameters and lake habitats. Forsmark site investigation. SKB P-04-25, Svensk Kärnbränslehantering AB, Stockholm.

Brunberg A-K, Blomqvist P, 2000. Post-glacial, land rise-induced formation and development of lakes in the Forsmark area, central Sweden. SKB TR-00-02, Svensk Kärnbränslehantering AB.

Brydsten L, 1999. Shore line displacement in Öregrundsgrepen. SKB TR-99-16, Svensk Kärnbränslehantering AB.

Brydsten L, 2006. A model for landscape development in terms of shoreline displacement, sediment dynamics, lake formation, and lake choke-up processes. SKB TR-06-40, Svensk Kärnbränslehantering AB.

Bäckblom G, Munier R, 2002. Effects of earthquakes on the deep repository for spent fuel in Sweden based on case studies and preliminary model results. SKB TR-02-24, Svensk Kärnbränslehantering AB.

Böðvarsson R, Lund B, Roberts R, Slunga R, 2006. Earthquake activity in Sweden. Study in connection with a proposed nuclear waste repository in Forsmark or Oskarshamn. SKB R-06-67, Svensk Kärnbränslehantering AB.

Cantrell K J, Serne R J, Last G V, 2003. Hanford Contaminant Distribution Coefficient Database and Users Guide. PNNL-13895 Rev 1.

Coughtrey P J, Thorne M C, 1983. Radionuclide distribution and transport in terrestrial and aquatic Ecosystems – A critical review of data. Volume 1. A.A. Balkema, Rotterdam. (EUR-8115-III) ISBN 90-6191-280-6.

Degerman E, Nyberg P, Näslund I, Jonasson D, 1998. Ekologisk fiskevård. Sportfiskarna, Sveriges sportfiske- och Fiskevårdsförbund, Jönköping, Sweden.

Downing I A, Plante C, 1993. Production of fish populations in lakes. Can. J. Fish. Aquat. Sci., Vol 50, pp 110–120.

Dyson R D, 1978. Cell biology. Allyn & Bacon, Boston, 616 pp.

Ekman M, 1996. A consistent map of the postglacial uplift of Fennoscandia. Terra-Nova Vol 8 (2), pp 158–165.

Ekström P-A, Broed R, 2006. Sensitivity analysis methods and a biosphere test case implemented in EIKOS. Posiva Working Report 2006-31.

Elhammar A, Sandkvist Å 2005. Detailed marine geological survey of the sea bottom outside Forsmark. SKB P-03-101, Svensk Kärnbränslehantering AB, Stockholm.

Engqvist A, Andrejev O, 1999. Water exchange of Öregrundsgrepen. A baroclinic 3D-model study. SKB TR-99-11, Svensk Kärnbränslehantering AB.

Erica, 2008. http://www.erica-project.org/ downloaded 2008-04-14.

Eriksson S, Sellei C, Wallström K, 1977. The structure of the plankton community of the Öresundsgrepen. (southwest Bothnian Sea). Helgoländer wiss, Meeresunters, Vol 30, pp 582–597.

EUR, 1996. Directive from the council 96/29/Euratom of the 13th of May 1996. In Swedish: Rådets direktiv 96/29/Euratom av den 13 maj 1996. EU Official Journal L 159, 29 June 1996.

Firestone, R B, Baglin C M, Frank, Chu Chu, S Y, 1999. Table of isotopes. Eight edition, ISBN 0-471-35633-6.

Fiskeriverket, 2003. Kräftfiskevård. Hot, möjligheter och bestämmelser. Fiskeriverket f-FAKTA 15, Fiskeriverket, Göteborg, Sweden.

FREDERICA, 2005. ERICA Deliverable 1: Progress on the production of the web-based effects database: FREDERICA (April 2005).

Gentzschein B, Levén J, Follin S, 2006. A comparison between well yield data from the site investigation in Forsmark and domestic wells in northern Uppland. SKB P-06-53, Svensk Kärnbränslehantering AB.

Grip H, Rodhe A, 1985. Vattnets väg från regn till bäck, Forskningsrådets förlagstjänst, Karlshamn, Sweden. ISBN 91-86344-17-X (in Swedish).

Gustafsson B, 2004. Sensitivity of the Baltic Sea salinity to large perturbations in climate. Climate research, Vol 27, pp 237–251.

Hedenström A, Risberg J, 2003. Shore line displacement in northern Uppland during the last 6500 calendar years. SKB TR-03-17, Svensk Kärnbränslehantering AB.

Holmén J, Stigsson M, 2001. Modelling of future hydrogeological conditions at SFR. SKB R-01-02, Svensk Kärnbränslehantering AB.

IAEA, 2001. Generic Models for Use in Assessing the Impact of Discharges of Radioactive Substances to the Environment Safety. IAEA Safety Report Series No 19.

IAEA, 2005. Derivation of activity concentration values for the purposes of exclusion, exemption and clearance. Safety Report Series 44, Vienna.

ICRP, 1975. ICRP Publication 23: Report of the task group on reference man, ICRP23. Pergamon Press, Oxford.

ICRP, 2003. ICRP Publication 89: Basic anatomical and physiological data for use in radiological protection: Reference values. Annals of the ICRP, 3-4. Pergamon, Oxford (UK), 265 pp.

Johansson Karl-Johan 2000. Iodine in soil. SKB TR-00-21, Svensk Kärnbränslehantering AB.

Johansson P-O, Werner K, Bosson E, Berglund S, Juston J, 2005. Description of climate, surface hydrology, and near-surface hydrogeology. Forsmark 1.2. SKB R-05-06, Svensk Kärnbränslehantering AB.

Jordbruksverket, 2007. Statistik från Jordbruksverket Statistikrapport 2007:2 Konsumtionen av livsmedel och dess näringsinnehåll.

Karlsson S, Bergström U, Meili M, 2001. Models for dose assessments – Models adapted to the SFR-area, Sweden. SKB TR-01-04, Svensk Kärnbränslehantering AB.

Kautsky U, 1995. Ecosystem processes in coastal areas of the Baltic Sea. Ph. D. thesis, Dept. Zoology, Stockholm Univ., 124 pp.

Kautsky H, Plantman P, Borgiel M, 1999. Quantitative distribution of aquatic plant and animal communities in the Forsmark-area. SKB R-99-69, Svensk Kärnbränslehantering AB.

Kautsky U (editor), 2001. The biosphere today and tomorrow in the SFR area. A summary of knowledge for the SAFE-project. SKB R-01-27, Svensk Kärnbränslehantering AB.

Kiljunen M, Vanhatalo M, Mäntyniemi S, Peltonen H, Kuikka S, Kiviranta H, Parmanne R, Tuomisto J T, Vuorinen P J, Hallikainen A, Verta M, Jönni J, Jones R I, Karjalainen J, 2007. Human Dietary Intake of Organochlorines from Baltic Herring: Implications of Individual Fish Variability and Fisheries Management. AMBIO, Vol 36 (2), pp 257–264.

Lindborg T (ed), 2005. Description of surface systems. Preliminary site description Forsmark area – version 1.2. SKB R-05-03, Svensk Kärnbränslehantering AB.

Lindgren M, Pettersson M, Karlsson S, Moreno L, 2001. Project SAFE – Radionuclide release and dose from the the SFR repository. SKB R-01-18, Svensk Kärnbränslehantering AB.

Livsmedelsverket, 2005. http://www.slv.se, Database: Livsmedelsdatabasen ”Sök i Näringsinnehåll i mat” downloaded October 2005.

Ludvigson J-E, 2002. Brunnsinventering i Forsmark. SKB R-02-17, Svensk Kärnbränslehantering AB.

Lundberg S, Proschwitz T V, 2007. Mälarens stormusselfauna – Resultat från inventeringar längs Mälarens stränder. PM från Naturhistoriska riksmuseet 2007:2, Stockholm, Sweden.

Miliander S, Punakivi M, Kyläkorpi L, Rydgren B, 2004. Human population and activities in Forsmark. Site description. SKB R-04-10, Svensk Kärnbränslehantering AB.

Mo K, Smith S, 1988. Mjukbottenfaunan i Öregrundsgrepen 1978–1986. Naturvårdsverket Rapport 3467, 43 p. (in Swedish).

Negus C L, 1966. A Quantitative Study of Growth and Production of Unionid Mussels in the River Thames at Reading. The Journal of Animal Ecology, Vol 35 (3), pp 513–532.

Neuman E, 1982. Species composition and seasonal migrations of the coastal fish fauna in the southern Bothnian Sea, in Coastal research in the Gulf of Bothnia. Müller K, Editor. Dr. W Junk Publishers.

Nilsson A-C, Karlsson S, Borgiel M, 2003. Forsmark site investigations. Sampling and analyses of surface waters. Results from sampling in the Forsmark area, March 2002 to March 2003. SKB P-03-27, Svensk Kärnbränslehantering AB.

Persson J, Wallin M Wallström K, 1993. Kustvatten i Uppsala län 1993. Vol 2, Upplands-stiftelsen, Uppsala, 246 pp.

Randall R G, Minns C K, 2000. Use of fish production per unit biomass ratios for measuring the productive capacity of fish habitats. Can. J. Fish. Aquat. Sci. Vol 57, pp 1657–1667.

Rouwenhorst R J, Johannes F J, Scheffers W A, Van Dijken J P, 1991. Determination of protein concentration by total organic carbon analysis. Biochemical Methods Vol 22 (2), pp 119–28.

SGU, 2008. Brunnsarkivet, www.sgu.se.

Sheppard S C, Ciffroy P, Siclet F, Damois C, Sheppard M I, Stephenson M, 2006. Conceptual approaches for the development of dynamic specific activity models of ^{14}C transfer from surface water to humans, J. Environ. Radioactivity, Vol 87, pp 32–51.

Sigurdsson T, 1987. Bottenundersökning av ett område ovanför SFR, Forsmark. SFR 87-07, Svensk Kärnbränslehantering AB (in Swedish).

SKB, 2001. SFR 1 Slutförvar för radioaktivt driftavfall, Slutlig säkerhetsrapport. Version 1.0, Svensk Kärnbränslehantering AB (in Swedish).

SKB, 2004. Interim main report of the safety assessment SR-Can. SKB-R-04-11, Svensk Kärnbränslehantering AB.

SKB, 2005. Database: svn.sth-proper.skb.se/project/SR-Can Bio/Forsmark/Syntes/LandscapeparametersFM.xls, Revison: 256, 2005-06-22.

SKB, 2006a. Long-term safety for KBS-3 repositories at Forsmark and Laxemar – a first evaluation. Main report of the SR-Can project. SKB TR-06-09, Svensk Kärnbränslehantering AB.

SKB, 2006b. The biosphere at Forsmark. Data assumptions and models used in the SR-Can assessment. SKB R-06-82, Svensk Kärnbränslehantering AB.

SKB, 2006c. Climate and climate related conditions – report for the safety assessment SR-Can. SKB TR-06-23, Svensk Kärnbränslehantering AB.

SKB, 2008a. Säkerhetsredovisning SFR 1, Allmän del 2 – Långsiktig säkerhet. Svensk Kärnbränslehantering AB (in Swedish).

SKB, 2008b. Säkerhetsredovisning SFR 1, Allmän del 1 – Anläggningsutformning och drift. Svensk Kärnbränslehantering AB (in Swedish).

Snoeijs P, 1985. Microphytobenthic biomass and environmental data in and around the Forsmark Biotest Basin, 1983–1985. 1985:2, Växtbiologiska Instutionen, Uppsala.

Snoeijs P, 1986. Primary production of microphytobenthos on rocky substrates in the Forsmark biotest basin, 1984. National Swedish environmental protection board report, Vol 3216, pp 1–24.

Snoeijs P, Mo K, 1987. Macrofauna on rocky substrates in the Forsmark biotest basin (March 1984 – March 1985). Report 3397, National Swedish Environmental Protection Board.

SSI FS 1998:1. The Swedish Radiation Protection Institute's Regulations on the Protection of Human Health and the Environment in connection with the Final Management of Spent Nuclear Fuel and Nuclear Waste. Statens strålskyddsinstitut.

SSI FS 2005:5. The Swedish Radiation Protection Institute's guidelines on the application of the regulations (SSI FS 1998:1) concerning protection of human health and the environment in connection with the final management of spent nuclear fuel and nuclear waste. Statens strålskyddsinstitut.

Thomson G, Miller A. Smith G., 2008. Radionuclide release calculations for SAR-08. SKB R-08-14, Svensk Kärnbränslehantering AB.

UNSCEAR, 2000. Sources and effects of ionizing radiation, Vol. I, Sources, United Nations Scientific Committee on the Effects of Atomic Radiation UNSCEAR 2000 Report to the General Assembly with scientific annexes.

Vidstrand P, Näslund J-O, Hartikainen J, Svensson U, 2007. Hydrogeological flux scenarios at Forsmark —Generic numerical flow simulations and compilation of climatic information for use in the safety analysis SFR 1 SAR-08. SKB R-07-63, Svensk Kärnbränslehantering AB.

Vose D, 1996. Quantitative risk analysis: A guide to Monte Carlo simulation modelling. John Wiley & Sons Ltd., Chichester.

Åstrand P-G, Jones J, Broed R, Avila R, 2005. Pandora technical description and user guide. Posiva Working Report 2005-64.

Appendix A

Model descriptions

Aquatic model

Transfer of radionuclides between aquatic objects

Fluxes between coastal objects

The following expressions are used for calculating the fluxes of radionuclides between water compartments of coastal objects.

The water and suspended matter from objects 11 (SAFE-basin), 2 and 4 to object 3 (Öregrundsgrepen) and from object 3 to object 1 (Baltic sea) are described by water retention times according to

$$TC_i = \frac{1}{RETTIME_i} \quad \text{(A.1)}$$

$RETTIME_i$ = Water retention time in the compartments 11, 2, 4 and 3 [year]
(i = Object number)

The water flow to the objects 11, 2 and 4 from object 3 and from object 1 to object 3 is related to the volume ratio of the two compartments as follows:

$$TC_I = \frac{A_{MI} \cdot D_{MI}}{A_3 \cdot D_3} \cdot \frac{1}{RETTIME_{MI}} \quad \text{(A.2)}$$

where

A_{MI} = Area of Object I [m^2]

A_3 = Area of Object 3 [m^2]

D_{MI} = Mean water depth in the Object I [m]

D_3 = Mean water depth in Object 3 [m]

$RETTIME_{MI}$ = Water retention time in the Object I [years]

Fluxes of water and suspended matter from a lake

The outflows of water from lakes are determined by the annual rate of runoff, size of the catchment area and lake volume according to the following expression:

$$TC = \frac{Catchm \cdot Runoff}{Lakearea \cdot MeanD} \quad \text{(A.3)}$$

where

Catchm = Catchment area [m^2]

Runoff = Annual runoff [$m^3/(m^2$, year)]

Lake area = Area of lake [m^2]

MeanD = Mean depth of lake [m]

The suspended matter follows the water and therefore the same transfer coefficients are used. Particulate matter as a whole may have a longer turnover time because of settling and resuspension, which is accounted for by the exchange of material between suspended and surficial sediments.

Transfer of radionuclides within aquatic objects

The conceptual model for turnover of radionuclides in the aquatic objects is shown in Figure A-1 /SKB 2004/.

Transfer of radionuclides from water in surface sediment (5) to lake water (1)

$$TC_{5,1} = \frac{\ln(2)}{\frac{DS}{V_{adv}}} \qquad \text{(A.4)}$$

where

DS = Depth of upper sediment

V_{adv} = Velocity of water flow from upper sediment to the water body [m/year]

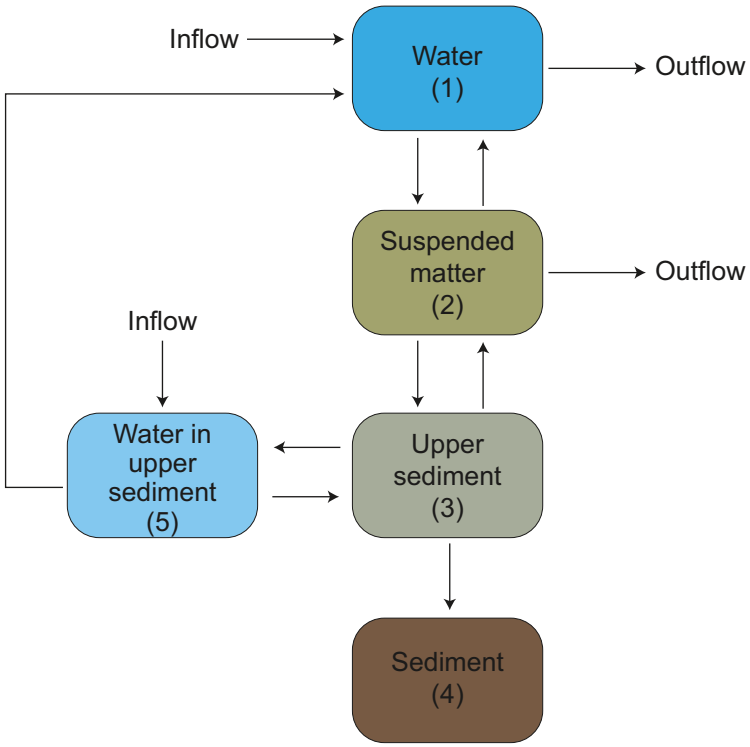

Figure A-1. *Structure of the model system for the aquatics objects*

Interaction of elements between pore water (5) and upper sediment (3)

Interaction of elements between pore water and upper sediment is a time-dependent process. A parameter is therefore introduced described as the half-time to reach sorption equilibrium (here called T_k).

From pore water to the solid phase:

$$TC_{5,3} = \frac{\ell n(2) \cdot K_d \cdot \rho}{T_k \cdot \varepsilon} \quad \text{(A.5)}$$

and from solid phase to pore water:

$$TC_{3,5} = \frac{\ell n(2)}{T_k} \quad \text{(A.6)}$$

where

K_d = Distribution coefficient, ratio of element concentrations in the solid and the dissolved phase [m^3/kg], see Table in Appendix B

P = Bulk density of sediment [kg/m^3]

ε = Porosity of sediment [–]

T_k = Half-time to reach sorption equilibrium [year]

Interaction of elements between water(1) and suspended matter (2)

The interaction of elements between water and suspended matter is based on that a steady-state condition is reached, but not instantaneous between the radionuclides dissolved in water and the fraction sorbed to the particulate matter. Therefore, the transfer from water to suspended matter is described by a transfer rate of sorption that is proportional to the concentration of suspended matter and the nuclide sorption affinity, described by a distribution coefficient. The process is time-dependent and therefore a parameter for the half-time to reach sorption equilibrium (here called T_k) has been used:

$$TC_{1,2} = \frac{\ell n(2)}{T_k} \cdot Susp_i \cdot K_d \quad \text{(A.7)}$$

and a simple rate of desorption from suspended matter to water:

$$TC_{2,1} = \frac{\ell n2}{T_k} \quad \text{(A.8)}$$

where

T_k = Half-time to reach sorption equilibrium [year]

$Susp_i$ = Suspended matter in object i [kg/m^3]

K_d = Distribution coefficient, ratio of element concentrations in the solid and the dissolved phase [m^3/kg], see Table in Appendix B

Sedimentation and resuspension processes

A fraction of the suspended matter is assumed to reach the upper sediment through sedimentation (gross sedimentation). This transfer rate is described by the ratio of the mean settling velocity and the mean water depth:

$$TC_{2,3} = \frac{V_{SINK}}{D_i} \quad \text{(A.9)}$$

where

V_{SINK} = Particle settling velocity [m/year]

D_i = Mean water depth [m] in object t i

Part of uppers sediment is resuspended, described by the following expression:

$$TC_{3,2} = \frac{GR}{DS} \cdot (1 - Frac) \quad \text{(A.10)}$$

or transferred to deeper sediment :

$$TC_{3,4} = \frac{GR}{DS} \cdot Frac \quad \text{(A.11)}$$

where

GR = Annual sedimentation rate [m/year]

DS = Depth of upper sediment [m]

Frac = Fraction of accumulation bottom [–]

Mire model

The mire is described by two compartment, see Figure A-2 /Karlsson et al. 2001/

The turnover of radionuclides in the system is described by the following expression.

From dissolved to particulate form:

$$TC = \frac{K_d \cdot \ln(2)}{T_k} \cdot \frac{D_p \cdot \rho_p}{\varepsilon_p \cdot D_p} = \frac{K_d \cdot \ln(2)}{T_k} \cdot \frac{\rho_p}{\varepsilon_p} \quad \text{(A.12)}$$

and from particulate to dissolved fraction by:

$$TC = \frac{\ln(2)}{T_k} \quad \text{(A.13)}$$

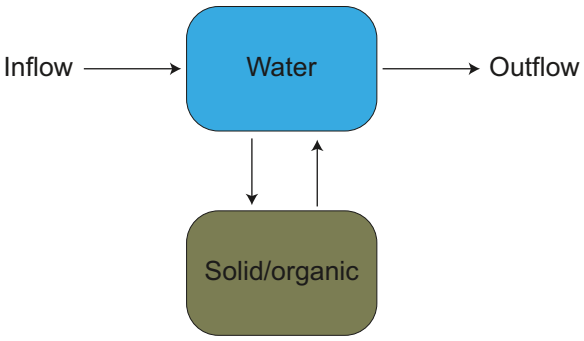

Figure A-2. *Structure of the model for the mire objects.*

where

K_d = Diswtribution coefficient, ratio of element concentrations in the solid and the dissolved phase [m^3/kg], see Table in Appendix B

D_p = Depth of peat in mire [m]

ε_p = Porosity of peat [m^3/m^3]

T_k = Half-time to reach sorption equilibrium [year]

ρ_p = Density of the peat [kg/m^3]

The transfer coefficient for the horizontal flow is based on water balance and becomes:

$$TC = \frac{R \cdot Catchm}{\varepsilon_p \cdot D_p \cdot Marea} \quad \text{(A.14)}$$

where

R = Runoff [$m^3/(m^2 \cdot year)$]

Catchm = Catchment area [m^2]

Marea = Area of mire [m^2]

D_p = Depth of peat in mire [m]

ε_p = Porosity of peat [m^3/m^3]

Irrigation model

Water from wells located in the drainage area of the repository was also used for irrigation of vegetables, in addition to the water consumption. Radionuclides transferred to soil by irrigation water will build concentrations, at levels determined by element properties and environmental conditions /Karlsson et al. 2001, Avila 2006a/.

The transfer rate describing the loss of radionuclide from upper soil is obtained by /Karlsson et al. 2001/:

$$TC = \frac{R}{\varepsilon_t \cdot D_{ts} \cdot RET} + \frac{BioT}{D_{ts}(1-\varepsilon_t) \cdot \rho_p} \quad \text{(A.15)}$$

where

$$RET = 1 + K_d \cdot \rho_p \cdot \frac{(1-\varepsilon_t)}{\varepsilon} \quad \text{(A.16)}$$

and

R = Runoff [$m^3/(m^2$ year)]

ε_t = Porosity of topsoil [–]

D_{ts} = Depth of topsoil [m]

BioT = Transport due to bioturbation [$kg/(m^2$ year)]

ρ_p = Density of soil particles [kg/m^3]

K_d = Distribution factor, concentration of an element on solids relative to dissolved [m^3/kg]

Retention of radionuclides on surfaces of vegetation was expresses as /Bergström and Barkefors 2004/:

$$C_{sv} = \frac{TIRR \cdot LAI \cdot StoCap \cdot Kret_i}{N \cdot Yield} \cdot C_{fw} \qquad \text{(A.17)}$$

where

C_{sv} = Concentration of radionuclide in surfaces of vegetation [Bq//kg FW]

TIRR = Annual total irrigation rate per area [m/(m^2, year)]

LAI = Leaf area index [m^2/m^2]

StoCap = Water storage on vegetation surface per LAI [m^3/m^2]

$Kret_i$ = Element dependent retention factor on surfaces of vegetation [–]

N = Number of irrigation occasions per year

Yield = Yield values of vegetables [kg FW/m^2]

C_{fw} = Concentration of radionuclide (i) in well water [Bq/m^3]

Appendix B

Nuclide and element specific data

Table B-1. Nuclide specific parameters; half-lives /Firestone et al. 1999/, dose coefficients for adults (ingestion and inhalation from /EUR 1996/ and external exposure coefficients from /Avila and Bergström 2006/.

Nuclide	Type of dominating decay	Half-life Year	External exposure (Sv/h)/(Bq/m^3)	Ingestion Sv/Bq	Inhalation Sv/Bq
H-3	β	12		1.8E–11	2.6E–10
C-14	β	5,730	1.9E–17	5.8E–10	5.8E–9
				2.9E–11*	
Cl-36	β	301,000	2.1E–19	9.3E–10	7.3E–9
Co-60	β, γ	5.3	–	3.4E–9	3.1E–8
Ni-59	β	76,000	3.0E–13	6.3E–11	4.4E–10
Ni-63	β	100.1	–	1.5E–10	1.3E–9
Se-79	β	1,130,000	–	2.9E–9	6.8E–9
Sr-90	β	29	2.9E–19	2.8E–8	1.6E–7
Zr-93	β	1,530,000	1.2E–17	1.1E–9	2.5E–8
Nb-94	β, γ	20,000	1.8E–13	1.7E–9	4.9E–8
Mo-93	EC	4,000	8.0E–18	3.1E–9	2.3E–9
Tc-99	β	211,000	2.1E–18	6.4E–10	1.3E–8
Ag-108m	γ	418	1.8E–16	2.3E–9	3.7E–8
Sn-126	β, γ	100,000	6.2E–19	4.7E–9	2.8E–8
I-129	β	15,700,000	1.6E–17	1.1E–7	3.6E–8
Cs-135	β	2,300,000	1.3E–13	2.0E–9	8.6E–9
Cs-137	β, γ	30	1.4E–13	1.3E–8	3.9E–8
Ho-166m	γ	1,200	5.6E–16	2.0E–9	1.2E–7
Np-237	α	2,144,000	1.8E–15	1.1E–7	5.0E–5
Pu-238	α	88	2.2E–18	2.3E–7	1.1E–4
Pu-239	α	24,110	5.1E–18	2.5E–7	1.2E–4
Pu-240	α	6,563	2.2E–18	2.5E–7	1.2E–4
Pu-242	α	372,300	1.9E–18	2.4E–7	1.1E–4
Am-241	α	432	2.8E–17	2.0E–7	9.6E–5
Am-243	α	7,370	2.9E–15	2.0E–7	9.6E–5

* Used for exposure from drinking water.

Table B-2. Values of bioaccumulation factors for elements in brackish water expressed in Bq per kg carbon in fish relative to Bq per m^3 water[1)], nominal values and ranges used in the probabilistic calculations. The distribution is also given (T = triangular, LT = logtriangular) /Karlsson et al 2002/.

Element	Distribution	Min	Nominal value	Max
H	T	3.65E–03	7.25E–03	1.45E–02
Cl	LT	7.25E–04	7.25E–03	7.25E–02
Co	LT	2.17E–01	2.17E+00	3.60E+00
Ni	LT	2.17E–01	2.17E+00	3.60E+00
Se	T	1.45E+01	2.90E+01	5.80E+01
Sr	LT	7.20E–03	2.17E–01	7.16E+00
Mo	LT	7.25E–03	7.25E–02	3.63E–01
Zr	LT	7.25E–02	7.25E–01	1.50E+00
Nb	LT	7.25E–03	7.25E–01	3.63E+00
Tc	LT	7.25E–03	2.17E–01	6.50E–01
Ag	T	7.24E–01	3.62E+00	7.24E+00
Sn	LT	7.25E–01	7.25E+00	7.25E+01
I	T	7.23E–02	2.17E–01	6.53E–01
Cs	T	7.50E–01	1.45E+00	3.63E+00
Ho	LT	2.17E–02	2.17E–01	2.17E+00
Np[2)]	LT	7.24E–02	3.62E–01	2.17E+02**
Pu	LT	3.61E–02	2.17E–01	3.62E–01
Am	LT	4.20E–02	4.20E–01	8.40E–01

[1)] Calculated from fresh weight by assuming a carbon content of 0.13%, based on an average value in fish according to /Jordbruksverket 2007/.

[2)] Increased range compared to /Karlsson et al. 2002/.

Table B-3. Element specific distribution coefficients Kd [m^3/kg] for suspended matter in coastal water, nominal values and ranges used in the probabilistic calculations. The distribution is also given (T = triangular, LT = logtriangular) /Karlsson et al. 2001/.

Element	Distribution	Min	Nominal value	Max
H	LT	1E–04	1E–03	1E–02
Cl	LT	1E–04	1E–03	1E–02
Co	LT	1E+01	1E+02	1E+03
Ni	LT	1E+00	1E+01	1E+02
Se	LT	5E–01	5E+00	5E+01
Sr	LT	1E–02	1E–01	1E+00
Mo	LT	1E–04	1E–03	1E–02
Zr	LT	5E+00	5E+01	5E+02
Nb	LT	1E+00	1E+01	1E+02
Tc	LT	1E–02	1E–01	1E+00
Ag	LT	1E–01	1E+00	1E+01
Sb	LT	1E–01	1E+00	1E+01
Sn	LT	5E+00	5E+01	5E+02
I[1)]	LT	3E–02	3E–01	3E+00
Cs	LT	1E+00	1E+01	1E+02
Ho	LT	1E–02	1E–01	1E+00
Np	LT	1E+00	1E+01	1E+02
Pu	LT	1E+01	1E+02	1E+03
Am	LT	1E+00	1E+01	1E+02

[1)] Ranges used correspond to a factor of 10 up and down from the nominal value and not the range given in /Karlsson et al. 2002/.

Table B-4. Values of distribution coefficients [m³/kg] for elements in peat soil (also used for elements in sediments), nominal values and ranges used in the probabilistic calculations. The distribution is also given (LT = logtriangular, LN = lognormal).

Element	Distribution	Min	Nominal value	Max
H	LT	1E–04	1E–03	1E–02
Cl[1)]	LN	1E–03	1E–01	1E+00
Co	LT	1E–01	1E +00	1E +01
Ni	LT	1E–01	1E+00	1E+01
Se[2)]	LT	2E–02	2E–01	2E+00
Sr	LT	2E–02	2E–01	2E+00
Mo	LT	1E–02	1E–01	1E+00
Zr	LT	7E–01	7E+00	7E+01
Nb	LT	2E–01	2E+00	2E+01
Tc	LT	5E–04	5E–03	5E–02
Ag	LT	2E+00	2E+01	2E+02
Sb	LT	1E–01	1E+00	1E+01
Sn	LT	2E–01	2E+00	2E+01
I[3)]	LT	3E–02	3E–01	3E+00
Cs[4)]	LT	1E–01	1E+00	1E+01
Ho	LT	3E–01	3E+00	3E+01
Np	LT	5E–01	5E+00	5E+01
Pu	LT	5E–01	5E+00	5E+01
Am	LT	5E–01	5E+00	5E+01

[1)] Standard deviation = 10.

[2)] Value for Se was decreased with a factor of 10 from /Karlsson et al 2002/ according to the information in /Cantrell et al. 2003/.

[3)] Values for I was increased with a factor of 10 from /Karlsson et al. 2002/ to reflect /Johansson 2000/ that I is effectively sorbed in organic soils.

[4)] Values for soil was used, because the values for organic soil in Karlsson et al. 2002 were lower than for general soil.

Table B-5. Values of distribution coefficients [m³/kg] for elements in suspended matter in fresh-water, nominal values and ranges used in the probabilistic calculations. The distribution is also given (LT = logtriangular) /Karlsson et al. 2002/.

Element	Distribution	Min	Nominal value	Max
Cl[1)]	LT	1E–04	1E–03	1E–02
Ni	LT	1E+00	1E+01	1E+02
Se	LT	5E–01	5E+00	5E+01
Mo	LT	1E–04	1E–03	1E–02
Zr[1)]	LT	5E+00	5E+01	5E+02
Nb	LT	1E+00	1E+01	1E+02
Tc	LT	1E–02	1E–01	1E+00
Ag	LT	2E–01	2E+00	2E+01
Sn	LT	5E+00	5E+01	5E+02
I[2)]	LT	3E–02	3E–01	3E+00
Cs	LT	1E+00	1E+01	1E+02
Ho	LT	3E–02	3E–01	3E+00
Np	LT	1E+00	1E+01	1E+02
Pu	LT	1E+01	1E+02	1E+03
Am[1)]	LT	1E+00	1E+01	1E+02

[1)] Values for brackish water /Karlsson et al. 2002/. For Zr lower values for fresh water than for brackish water was given in /Karlsson et al. 2002/ why the brackish water value was selected.

[2)] Increased range compared to /Karlsson et al. 2002/.

Table B-6. Values of bioaccumulation factors for elements in fresh water expressed in Bq per kg carbon in fish relative to Bq per m^3 water, nominal value and ranges used in the probabilistic calculations. The distribution is also given (LT = logtriangular).

Elements	Distribution	Min	Nominal value	Max
Cl	LT	7.3E–02	3.6E–01	7.20E–01
Ni	LT	2.2E–01	2.20E+00	2.20E+01
Se	LT	7.3E+00	2.90E+01	7.30E+01
Mo	LT	7.3E–03	7.3E–02	7.3E–01
Zr	LT	2.2E–02	1.4E+00	2.2E+00
Nb	LT	7.2E–01	2.2E+00	2.2E+02
Tc	LT	2.0E–01	2.0E–01	8.7E+00
Ag	LT	7.2E–01	3.6E+00	7.2E+01
Sn	LT	2.2E+00	2.2E+01	2.2E+02
I	LT	7.3E–02	1.40E+0	3.6E+00
Cs	LT	3.6E+01	7.2E+01	1.5E+03
Ho	LT	2.2E–02	2.2E–01	2.2E+00
Np	LT	7.30E–02	3.6E–01	2.2E+01
Pu	LT	2.9E–02	2.0E–01	2.2E+00
Am	LT	2.5E–01	7.0E–01	7.30E+00

Table B-7. Values of aggregated transfer factor from agricultural production expressed in Bq per kg carbon per Bq per kg dry soil, nominal value, mean value and ranges used in the probabilistic calculations. The distribution is also given (LN = Lognormal).

Element	Distribution	Nominal value	Mean value	Standard deviation
Cl	LN	7.14E+01	1.45E+02	1.71E+02
Ni	LN	3.43E–01	7.14E–01	1.77E+00
Se	LN	3.70E+01	2.90E+01	4.51E+01
Mo	LN	1.45E+00	3.38E+00	7.73E+00
Zr	LN	1.60E–03	3.70E–03	8.92E–03
Nb	LN	7.80E–03	1.67E–02	3.65E–02
Tc	LN	8.65E+00	1.25E+01	5.30E+01
Ag	LN	1.32E+00	2.65E+00	6.78E+00
Sn	LN	6.44E–01	1.91E+00	6.68E+00
I	LN	4.32E–01	1.10E+00	2.39E+00
Cs	LN	2.47E–01	5.56E–01	1.36E+00
Ho	LN	1.45E–02	4.72E–02	1.96E–01
Np	LN	2.50E–02	7.17E–02	2.34E–01
Pu	LN	2.00E–04	5.30E–04	1.85E–03
Am	LN	4.50E–04	5.30E–04	1.85E–03

Table B-8. Values of aggregated transfer factor* from forestry products expressed in Bq per kg carbon per Bq per kg dry soil, nominal value, mean value and ranges used in the probabilistic calculations. The distribution is also given (LN = Lognormal).

Element	Distribution	Nominal value	Mean value	Standard deviation
Cl	LN	5.13E+02	7.70E+02	6.62E+02
Ni	LN	2.53E+00	7.33E+00	8.86E+00
Se	LN	3.64E+02	2.65E+02	1.84E+02
Mo	LN	1.46E+01	3.02E+01	2.99E+01
Zr	LN	1.80E–02	3.76E–02	3.60E–02
Nb	LN	9.00E–02	1.89E–01	1.85E–01
Tc	LN	1.83E+01	5.27E+01	4.70E+01
Ag	LN	9.10E+00	1.68E+01	1.52E+01
Sn	LN	1.82E+00	5.54E+00	6.03E+00
I	LN	1.13E+01	1.02E+01	1.19E+01
Cs	LN	1.96E+02	6.38E+02	1.60E+03
Ho	LN	1.80E–02	3.77E–02	3.74E–02
Np	LN	1.28E+00	1.37E+00	1.62E+00
Pu	LN	3.64E–02	7.94E–02	1.00E–01
Am	LN	2.36E–02	2.27E–01	7.40E–01

Table B-9. Values of distribution coefficients [m^3/kg] for elements in soil, nominal value and ranges. The distribution is also given (LT = logtriangular).

Element	Distribution	Min	Nominal value	Max
Cl-	LT	0.0001	0.0010	0.01
Ni	LT	0.05	0.5	5
Se	LT	0.001	0.01	0.1
Zr	LT	0.1	1	10
Nb	LT	0.05	0.5	5
Mo	LT	0.01	0.1	1
Tc	LT	0.0005	0.0050	0.05
Ag	LT	0.01	0.1	1
Sn	LT	0.01	0.1	1
I	LT	0.03	0.3	3
Cs	LT	0.1	1	10
Ho	LT	0.1	1	10
Np	LT	0.01	0.1	1
Pu	LT	0.5	5	50
Am	LT	0.2	2	20

Table B-10. Values of root-uptake factors for vegetables [Bq/kg FW per Bq/kg dry soil] for elements in soil, nominal value and ranges. The distribution is also given (T = triangular, LT = logtriangular).

Element	Distribution	Min	Nominal value	Max
Cl	T	1.0	3.0	10
Ni	LT	0.002	0.02	0.2
Se	LT	0.1	2.0	3
Zr	LT	1.0E–5	1.0E–4	1.0E–3
Nb	LT	5.0E–5	5.0E–4	5.0E–3
Mo	LT	0.008	0.08	0.8
Tc	LT	0.01	2.0	8.0
Ag	LT	0.01	0.1	1.0
Sn	LT	0.005	0.05	0.5
I	LT	0.003	0.03	0.3
Cs	LT	0.002	0.02	0.2
Ho	LT	0.0003	0.0030	0.03
Np	LT	0.0004	0.0040	0.04
Pu-	LT	2.0E–6	2.0E–5	2.0E–4
Am	LT	7.0E–6	7.0E–5	7.0E–4

Table B-11 Retention factors [–] for element sorbing on surfaces of vegetation, nominal value and ranges. The distribution is also given (T = triangular).

Elements	Distribution	Nominal value	Ranges
Anions (Cl, I)	T	0.5	0.3–0.7
(Cs)	T	1	0.5–1.5
Cations (Ni, Se, Zr, Nb, Mo, Tc, Ag, Sn, Ho, Np, U, Pu, Am)	T	2	1.5–2.5

Appendix C

Derivation of aggregated transfer factors for forests

This appendix describes the method applied for derivation of the aggregated transfer factors for forests, which is an update of the method applied in SR-Can /Avila 2006a/.

The aggregated transfer factors that were used in SR-Can /Avila 2006a/ for forests considered only the consumption of roe deer and moose. The derivation of an aggregated transfer factor that accounts for all forest products requires knowledge of the fractional contribution of different forest products to the yearly carbon intake. This parameter is unknown and it is difficult to estimate, special for exposures in the future. Hence, an alternative approach was here applied, where it is assumed that all food products that are produced in the forest are consumed. The average radionuclide intake rate by an individual of the group consuming forest food products can be then obtained as:

$$Intake^{j} = IR_C * C^{j}_{media} * \sum_k \frac{p_k}{P} * TF_k^{j} \qquad \text{(C.1)}$$

where,

IR_C is the annual intake of carbon by an individual [kgC/yr],

C^{j}_{media} is the *j-th* radionuclide concentration in soil [Bq/kg DW],

$TF_k{}^{j}$ is the transfer factor from soil to the forest food product "*k*" [Bq/kgC per Bq/kg DW],

p_k is the yearly production of the forest food product "*k*" [kgC/m^2/yr],

P is the total production of food in the forest [kgC/m^2/yr].

The sum in Equation C.1 is the Aggregated Transfer Factor (TF_{agg}) for forests, which is the ratio between the radionuclide concentration in the diet and the radionuclide concentration in the environmental media (soil). Hence, the TF_{agg} for forests is defined as the sum of the TFs of the different forest food products weighted with their fractional contribution to the total food production in the forest. The TFs for roe deer and moose were obtained with the Equations C.2 and C.3. Other forest food products included in the calculation were berries and mushrooms. Their transfer factors were obtained by dividing the concentration ratios reported in /Avila 2006b/ by the carbon content given in Table C-1. The carbon content is given in units of kg C/kg FW, whereas the CRs for mushrooms and berries in /Avila 2006b/ are given in units of Bq/kg DW per Bq/kg DW. Hence, the TFs for berries and mushrooms should be corrected by dividing by a factor equal to ratio of the fresh weight (FW) and dry weight (DW) of mushrooms and berries, respectively. In the calculation of TFagg values given in Appendix B this correction factor was set to 1. As the moisture content of mushrooms and berries can be rather high (up-to 90%), the values of TFagg for forests given in Appendix B are overestimated, around a factor of 10.

Probability density functions of the TF_{agg} for forests were obtained by performing probabilistic simulations and are presented in Appendix B. The values of the productivity of the different forest products used in the calculations are presented in Table 3.5 /SKB 2006b/.

The TFs for roe deer and moose (in Bq/kg C per Bq/kg DW) were calculated with the following equations /Avila 2006a/:

$$TF^{j}_{roedeer} = (f^{roedeer}_{mush} * CR^{j}_{mush} + f^{roedeer}_{und} * CR^{j}_{und} + f^{roedeer}_{leaves} * CR^{j}_{leaves} + f^{roedeer}_{wood} * CR^{j}_{wood}) * \frac{f^{j}_{gut} * F^{j}_{soft} * a^{j} * W^{b^{j}}_{roedeer}}{CC_{meat}} \quad \text{(C.2)}$$

$$TF^{j}_{moose} = (f^{moose}_{mush} * CR^{j}_{mush} + f^{moose}_{und} * CR^{j}_{und} + f^{moose}_{leaves} * CR^{j}_{leaves} + f^{moose}_{wood} * CR^{j}_{wood}) * \frac{f^{j}_{gut} * F^{j}_{soft} * a^{j} * W^{b^{j}}_{moose}}{CC_{meat}} \quad \text{(C.3)}$$

where,

$f^{roedeer}_{mush}, f^{roedeer}_{und}, f^{roedeer}_{leaves}, f^{roedeer}_{wood}$ are the fractions of mushrooms, understorey plants, tree leaves and tree wood, respectively, in the roe deer diet [dimensionless],

$f^{moose}_{mush}, f^{rmoose}_{und}, f^{rmoose}_{leaves}, f^{moose}_{wood}$ are the fractions of mushrooms, understorey plants, tree leaves and tree wood, respectively, in the roe deer diet [dimensionless],

CR^{j}_{mush}, CR^{j}_{und}, CR^{j}_{leaves}, CR^{j}_{wood} are *j-th* radionuclide concentration ratios from soil to mushrooms, understorey plants, tree leaves and tree wood respectively [Bq/kg DW per Bq/kg DW],

f^{j}_{gut} is the gut uptake fraction of the ***j-th*** radionuclide [unitless],

a^{j} is the multiplier in the allometric relationship for the ***j-th*** radionuclide [in appropriate units],

b^{j} is the exponent in the allometric relationship for the ***j-th*** radionuclide [unitless],

F^{j}_{soft} is the *j-th* radionuclide fraction in the animal soft tissues [unitless].

The values of the parameters in Equations C.2 and C.3 were taken from /Avila 2006b/ with the exception of the fraction of radionuclides in soft-tissues, which were taken from /Coughtrey and Thorne 1983/. The carbon content in a forest product (Table C-1) was estimated using the following equation, relating the protein, carbohydrates and fat content with the carbon content in food /Altman and Ditmer 1964, Dyson 1978, Rouwenhorst et al. 1991/:

$$CC_k = 0.53 \cdot Proteins_k + 0.44 \cdot Carbohydrates_k + 0.66 \cdot Lipids_k \quad \text{(C.4)}$$

where,

CC_k is the carbon content in the food product "*k*" [kgC/kg FW],

$Proteins_k$ is the protein content in the food product "*k*" [kg /kg FW],

$Carbohydrates_k$ is the carbohydrate content in the food product "*k*" [kg /kg FW],

$Lipids_k$ is the lipid content in the food product "*k*" [kg /kg FW].

The coefficients in Equation C.4 are the carbon content (in kg C/kg) of proteins, carbohydrates and lipids, respectively. The values of the content of proteins, carbohydrates and lipid in forest products were taken from the database of the Swedish Food Administration /Livsmedelsverket 2005/**.**

Table C-1. Carbon content (kg C/kg FW) in different forest product calculated with Equation C.4.

Forest product	Carbon content (kg C per kg FW)
Meat	0.165
Berries	0.053
Mushrooms	0.013

Appendix D

Dose Factors

This Appendix presents the Dose Factors that were calculated as described in Section 4.1, 4.2 and 4.3.

Table D-1. Dose Factors (Sv/y per Bq/y) for the coast ecosystem. Mean value, standard deviation and percentiles are presented.

Nuclide	Mean	Std	5%	50%	95%
H-3	5.51E–22	1.82E–22	3.03E–22	5.24E–22	8.96E–22
C-14	1.72E–16	5.00E–16	4.89E–17	1.05E–16	3.58E–16
Cl-36	3.77E–20	3.83E–20	5.13E–21	2.51E–20	1.21E–19
Co-60	1.71E–17	9.73E–18	4.44E–18	1.57E–17	3.58E–17
Ni-59	3.27E–19	1.86E–19	8.27E–20	2.95E–19	6.65E–19
Ni-63	7.74E–19	4.38E–19	2.06E–19	7.03E–19	1.60E–18
Se-79	3.62E–16	1.20E–16	1.98E–16	3.46E–16	5.91E–16
Sr-90	5.76E–17	9.30E–17	1.97E–18	2.23E–17	2.51E–16
Mo-93	8.94E–19	7.51E–19	1.55E–19	6.81E–19	2.43E–18
Nb-94	3.31E–18	3.66E–18	1.36E–19	1.94E–18	1.13E–17
Tc-99	3.53E–19	3.05E–19	4.01E–20	2.65E–19	9.76E–19
Ag-108m	3.27E–17	1.29E–17	1.36E–17	3.17E–17	5.52E–17
Sb-125	5.99E–18	6.09E–18	8.07E–19	3.87E–18	1.82E–17
Sn-126	1.92E–16	1.95E–16	2.51E–17	1.22E–16	6.11E–16
I-129	1.27E–16	5.45E–17	5.22E–17	1.20E–16	2.25E–16
Cs-135	1.43E–17	5.21E–18	7.33E–18	1.37E–17	2.36E–17
Cs-137	9.20E–17	3.37E–17	4.72E–17	8.73E–17	1.55E–16
Ho-166m	2.45E–18	2.52E–18	3.30E–19	1.59E–18	7.94E–18
Np-237	3.38E–15	7.85E–15	6.23E–17	5.26E–16	1.83E–14
Pu-239	1.46E–16	7.17E–17	4.91E–17	1.36E–16	2.72E–16
Pu-240	1.45E–16	7.13E–17	5.05E–17	1.36E–16	2.76E–16
Pu-242	1.38E–16	6.57E–17	4.78E–17	1.29E–16	2.60E–16
Am-241	2.17E–16	1.31E–16	5.41E–17	1.91E–16	4.56E–16
Am-242m	2.07E–16	1.25E–16	5.06E–17	1.80E–16	4.40E–16
Zr-93	2.10E–18	1.28E–18	5.04E–19	1.84E–18	4.46E–18
Am-243	2.17E–16	1.30E–16	5.39E–17	1.94E–16	4.66E–16

Table D-2. Dose Factors (Sv/y per Bq/y) for the lake existing between year 5,000 and 7,000. Mean value, standard deviation and percentiles are presented.

Nuclide	Mean	Std	5%	50%	95%
C-14	1.74E–13	2.17E–14	1.43E–13	1.72E–13	2.12E–13
Cl-36	9.16E–15	4.15E–15	3.43E–15	8.68E–15	1.71E–14
Ni-59	4.64E–15	4.99E–15	5.29E–16	2.88E–15	1.55E–14
Se-79	2.88E–12	1.23E–12	1.09E–12	2.75E–12	5.04E–12
Mo-93	1.17E–14	1.11E–14	2.07E–15	7.93E–15	3.66E–14
Nb-94	5.80E–13	1.01E–12	3.32E–14	2.13E–13	2.54E–12
Tc-99	2.34E–14	2.51E–14	5.08E–15	1.34E–14	7.56E–14
Ag-108m	1.91E–13	9.47E–14	6.60E–14	1.78E–13	3.70E–13
I-129	3.45E–12	2.47E–12	5.66E–13	2.86E–12	8.25E–12
Cs-135	9.97E–12	1.08E–11	1.58E–12	5.73E–12	3.29E–11
Np-237	4.23E–12	7.06E–12	2.71E–13	1.72E–12	1.76E–11
Pu-239	7.56E–13	1.00E–12	4.44E–14	3.87E–13	2.74E–12
Pu-240	7.49E–13	1.06E–12	4.09E–14	3.99E–13	2.74E–12
Pu-242	7.27E–13	9.93E–13	4.84E–14	3.81E–13	2.76E–12
Am-241	6.08E–12	5.81E–12	1.07E–12	4.00E–12	1.86E–11
Zr-93	8.52E–15	9.76E–15	4.33E–16	4.89E–15	2.99E–14
Sn-126	1.38E–12	2.32E–12	2.71E–14	5.51E–13	5.77E–12
Ho-166m	8.48E–14	1.53E–13	3.59E–15	2.58E–14	3.92E–13
Am-243	6.09E–12	5.42E–12	1.14E–12	4.27E–12	1.78E–11

Table D-3. Dose Factors (Sv/y per Bq/y) for lakes existing during periods with talik. Mean value, standard deviation and percentiles are presented.

Nuclide	Mean	Std	5%	50%	95%
C-14	1.02E–14	9.29E–15	4.46E–15	7.67E–15	2.19E–14
Cl-36	8.85E–17	4.01E–17	3.31E–17	8.38E–17	1.65E–16
Ni-59	6.43E–17	6.29E–17	8.91E–18	4.36E–17	1.99E–16
Se-79	3.28E–14	1.27E–14	1.40E–14	3.14E–14	5.59E–14
Mo-93	1.13E–16	1.08E–16	2.00E–17	7.66E–17	3.54E–16
Nb-94	8.29E–15	1.32E–14	6.58E–16	3.01E–15	3.67E–14
Tc-99	2.26E–16	2.43E–16	4.91E–17	1.29E–16	7.30E–16
Ag-108m	2.15E–15	9.94E–16	7.96E–16	2.03E–15	3.97E–15
I-129	3.38E–14	2.43E–14	5.57E–15	2.80E–14	8.39E–14
Cs-135	1.36E–13	1.31E–13	3.21E–14	8.45E–14	4.35E–13
Np-237	6.01E–14	9.04E–14	4.89E–15	2.47E–14	2.41E–13
Pu-239	2.49E–14	2.35E–14	4.33E–15	1.66E–14	7.50E–14
Pu-240	2.51E–14	2.42E–14	4.22E–15	1.68E–14	7.83E–14
Pu-242	2.41E–14	2.31E–14	3.94E–15	1.57E–14	7.20E–14
Am-241	8.77E–14	7.02E–14	2.39E–14	6.34E–14	2.47E–13
Zr-93	2.06E–16	1.68E–16	2.10E–17	1.55E–16	5.27E–16
Sn-126	3.22E–14	4.26E–14	1.06E–15	1.57E–14	1.23E–13
Ho-166m	8.37E–16	1.51E–15	3.49E–17	2.54E–16	3.80E–15
Am-243	8.77E–14	7.01E–14	2.37E–14	6.33E–14	2.42E–13

Table D-4. Dose Factors (Sv/y per Bq/y) for the forest ecosystem. Mean value, standard deviation and percentiles are presented.

Nuclide	Mean	Std	5%	50%	95%
C-14	7.62E–16	1.14E–15	1.99E–16	4.85E–16	2.04E–15
Cl-36	1.46E–12	3.49E–12	3.65E–14	3.45E–13	6.16E–12
Ni-59	2.32E–14	4.34E–14	1.05E–15	9.63E–15	8.52E–14
Se-79	7.46E–12	9.25E–12	6.22E–13	4.14E–12	2.37E–11
Mo-93	4.54E–13	7.50E–13	2.45E–14	2.12E–13	1.74E–12
Nb-94	6.36E–13	5.33E–13	9.87E–14	4.64E–13	1.78E–12
Tc-99	8.50E–15	1.16E–14	8.16E–16	4.72E–15	3.01E–14
Ag-108m	1.02E–12	9.17E–13	3.21E–13	7.82E–13	2.38E–12
I-129	1.67E–11	3.00E–11	8.58E–13	6.65E–12	6.91E–11
Cs-135	5.81E–11	1.43E–10	9.37E–13	1.56E–11	2.39E–10
Np-237	2.98E–11	4.69E–11	1.90E–12	1.48E–11	1.06E–10
Pu-239	3.58E–12	5.03E–12	3.07E–13	1.98E–12	1.28E–11
Pu-240	2.65E–12	3.65E–12	2.59E–13	1.47E–12	8.89E–12
Pu-242	4.10E–12	6.77E–12	2.98E–13	2.05E–12	1.33E–11
Am-241	9.71E–13	3.09E–12	4.46E–14	2.91E–13	3.48E–12
Zr-93	1.02E–14	1.39E–14	9.05E–16	6.21E–15	3.05E–14
Sn-126	2.48E–12	4.25E–12	1.19E–13	1.11E–12	9.00E–12
Ho-166m	3.00E–13	1.09E–13	1.16E–13	3.04E–13	4.69E–13
Am-243	5.70E–12	1.94E–11	2.03E–13	1.59E–12	2.23E–11

Table D-5. Dose Factors (Sv/y per Bq/y) for an agricultural ecosystem. Mean value, standard deviation and percentiles are presented.

Nuclide	Mean	Std	5%	50%	95%
C-14	6.22E–16	9.76E–16	1.57E–16	3.96E–16	1.62E–15
Cl-36	3.11E–13	1.15E–12	5.15E–15	5.78E–14	1.27E–12
Ni-59	2.23E–15	6.76E–15	3.42E–17	5.10E–16	9.09E–15
Se-79	8.21E–13	1.76E–12	3.03E–14	2.92E–13	3.38E–12
Mo-93	5.45E–14	1.89E–13	8.51E–16	1.32E–14	2.02E–13
Nb-94	6.12E–13	5.12E–13	9.47E–14	4.46E–13	1.72E–12
Tc-99	2.03E–15	9.25E–15	1.65E–17	3.71E–16	7.72E–15
Ag-108m	2.90E–13	3.71E–13	1.41E–13	2.08E–13	6.72E–13
I-129	1.61E–12	4.06E–12	3.49E–14	4.70E–13	6.88E–12
Cs-135	6.19E–14	2.02E–13	7.64E–16	1.37E–14	2.50E–13
Np-237	1.77E–12	5.95E–12	6.49E–14	5.07E–13	6.49E–12
Pu-239	3.07E–13	2.38E–13	4.97E–14	2.44E–13	8.02E–13
Pu-240	2.21E–13	1.50E–13	4.61E–14	1.82E–13	5.04E–13
Pu-242	3.36E–13	3.26E–13	4.57E–14	2.50E–13	8.90E–13
Am-241	3.36E–14	2.13E–14	1.40E–14	3.05E–14	5.87E–14
Zr-93	1.03E–15	1.97E–15	4.72E–17	4.00E–16	3.64E–15
Sn-126	7.92E–13	2.78E–12	1.02E–14	1.63E–13	3.03E–12
Ho-166m	3.00E–13	1.09E–13	1.17E–13	3.04E–13	4.70E–13
Am-243	2.17E–13	2.27E–13	4.50E–14	1.76E–13	5.18E–13

Table D-6. Dose Factors (Sv/y per Bq/y) for a well used for drinking and irrigation. Mean value, standard deviation and percentiles are presented.

Nuclide	Mean	Std	5%	50%	95%
C-14	9.14E–15	1.08E–14	3.46E–16	4.29E–15	3.48E–14
Cl-36	5.94E–13	8.39E–13	1.86E–14	2.54E–13	2.29E–12
Ni-59	4.53E–14	6.67E–14	1.42E–15	1.88E–14	1.61E–13
Se-79	3.10E–12	5.43E–12	8.03E–14	1.12E–12	1.15E–11
Zr-93	6.85E–13	9.56E–13	2.33E–14	2.95E–13	2.50E–12
Nb-94	1.70E–12	2.24E–12	5.16E–14	7.50E–13	6.59E–12
Mo-93	2.50E–12	3.54E–12	7.74E–14	1.03E–12	9.32E–12
Tc-99	5.06E–13	7.97E–13	1.51E–14	2.07E–13	1.82E–12
Ag-108m	2.27E–12	3.35E–12	7.33E–14	9.72E–13	8.47E–12
Sn-126	4.27E–12	7.32E–12	1.22E–13	1.63E–12	1.57E–11
I-129	5.64E–11	7.67E–11	1.91E–12	2.52E–11	2.00E–10
Cs-135	1.16E–12	1.67E–12	3.72E–14	4.97E–13	4.18E–12
Ho-166m	2.10E–12	2.68E–12	7.27E–14	9.46E–13	7.74E–12
U-238	2.81E–11	3.87E–11	9.65E–13	1.21E–11	1.06E–10
Np-237	6.99E–11	9.81E–11	2.35E–12	2.89E–11	2.58E–10
Pu-239	1.56E–10	2.16E–10	5.37E–12	6.69E–11	5.73E–10
Pu-240	1.55E–10	2.12E–10	5.37E–12	6.54E–11	5.70E–10
Am-241	1.25E–10	1.75E–10	4.15E–12	5.36E–11	4.64E–10

Table D-7. Dose Factors (Sv/y per Bq/y) obtained for the case of unit releases to the landscape during 2,500 years – used for calculations of annual doses due to released from the Silo caused by earthquakes.

Radionuclide	Ecosystem			
	Coast	Small lake	Agricultural land	Large lake
Ag-108m	2.5E–17	2.7E–13	2.2E–13	2.8E–15
Am-241	2.6E–16	3.9E–12	2.8E–14	4.8E–14
Am-243	2.6E–16	4.1E–12	9.5E–14	4.8E–14
C-14	9.1E–17	1.7E–13	3.1E–16	8.3E–15
Cl-36	2.1E–20	1.2E–14	2.4E–14	1.1E–16
Co-60	2.2E–17	0.0E+00	0.0E+00	0.0E+00
Cs-135	8.9E–18	4.1E–12	1.6E–14	4.8E–14
Cs-137	5.7E–17	0.0E+00	0.0E+00	0.0E+00
H-3	3.9E–22	0.0E+00	0.0E+00	0.0E+00
Ho-166m	1.3E–18	1.5E–14	2.9E–13	1.5E–16
I-129	7.3E–17	5.5E–12	4.9E–13	5.3E–14
Mo-93	6.9E–19	8.3E–15	1.5E–14	8.1E–17
Nb-94	3.8E–18	1.0E–13	3.7E–13	1.2E–15
Ni-59	4.2E–19	3.9E–15	6.9E–16	4.6E–17
Ni-63	9.9E–19	0.0E+00	0.0E+00	0.0E+00
Np-237	1.2E–16	1.1E–12	2.5E–13	1.3E–14
Pu-239	1.6E–16	5.9E–13	1.2E–13	1.8E–14
Pu-240	1.6E–16	5.8E–13	1.1E–13	1.8E–14
Pu-242	1.6E–16	5.7E–13	1.1E–13	1.7E–14
Se-79	2.6E–16	2.7E–12	7.4E–13	2.8E–14
Sn-126	1.0E–16	1.7E–12	1.6E–13	3.3E–14
Sr-90	1.8E–17	0.0E+00	0.0E+00	0.0E+00
Tc-99	4.2E–19	4.9E–15	1.1E–15	4.8E–17

Table D-8. Dose Factors (Sv/y per Bq/y) obtained for the case of unit releases to the landscape during 300 years – used for calculations of annual doses due to released from the BMA caused by earthquakes.

Radionuclide	Ecosystem			
	Coast	Small lake	Agricultural land	Large lake
Ag-108m	2.5E–17	2.7E–13	8.9E–14	2.8E–15
Am-241	2.6E–16	3.9E–12	1.2E–14	4.8E–14
Am-243	2.6E–16	4.0E–12	1.6E–14	4.8E–14
C-14	9.1E–17	1.7E–13	3.1E–16	8.3E–15
Cl-36	2.1E–20	1.2E–14	2.4E–14	1.1E–16
Co-60	2.2E–17	0.0E+00	0.0E+00	0.0E+00
Cs-135	8.9E–18	4.0E–12	4.8E–15	4.8E–14
Cs-137	5.7E–17	0.0E+00	0.0E+00	0.0E+00
H-3	3.9E–22	0.0E+00	0.0E+00	0.0E+00
Ho-166m	1.3E–18	1.5E–14	7.8E–14	1.5E–16
I-129	7.3E–17	5.5E–12	3.3E–13	5.3E–14
Mo-93	6.9E–19	8.3E–15	1.5E–14	8.1E–17
Nb-94	3.8E–18	1.0E–13	7.7E–14	1.2E–15
Ni-59	4.2E–19	3.8E–15	2.1E–16	4.6E–17
Ni-63	9.9E–19	0.0E+00	0.0E+00	0.0E+00
Np-237	1.2E–16	1.1E–12	3.8E–14	1.3E–14
Pu-239	1.6E–16	5.3E–13	1.8E–14	1.8E–14
Pu-240	1.6E–16	5.3E–13	1.8E–14	1.8E–14
Pu-242	1.6E–16	5.1E–13	1.6E–14	1.7E–14
Se-79	2.6E–16	2.7E–12	6.0E–13	2.8E–14
Sn-126	1.0E–16	1.5E–12	3.3E–14	3.3E–14
Sr-90	1.8E–17	0.0E+00	0.0E+00	0.0E+00
Tc-99	4.2E–19	4.9E–15	1.1E–15	4.8E–17

Appendix E

Supporting studies for the dose assessments

This appendix describes three studies that were carried out in support to the dose assessment approaches that were applied in the SAR08 safety assessment:

1. Comparison of the exposure from different landscape objects.
2. Comparison between releases to water and sediments in aquatic objects.
3. Comparison of the accumulation of radionuclides in lakes and mires.

The first study was carried out for all relevant radionuclides. The second and third studies were carried out for a selection of radionuclides with contrasting sorption properties.

E1 Comparison of the exposure from different landscape objects

For each landscape configuration, described in Chapter 3, a study was carried out to identify in which landscape object the highest concentrations and doses are obtained. Probabilistic simulations were carried out with each of the landscape models with a constant release rate of 1 Bq/y during 20,000 years. The mean values of the concentrations in the environmental media, obtained for the different landscape objects were compared. The environmental media that were used in the comparisons were:

- Sea water for the landscape configuration in the first 3,000 years after closure, when all landscape objects are sea basins (Table E1-1).
- Fresh water for the landscape configuration that prevails from 3,000 years to 5,000 years after closure, when objects 11 and 4 are lakes and other objects are sea basins (Table E1-2).
- Soil for the landscape configuration that prevails starting from 7,000 years after closure, when objects 11, 4 and 2 are mires and other objects are sea basins (Table E1-3).

The results (see Tables E1-1, E1-2 and E1-3) indicate that the highest concentrations, and doses, in all studied cases are obtained for object 11, which receives all direct releases from the geosphere during the whole simulation period.

Table E1-1. Radionuclide concentrations in sea water (in Bq/m³) at the end of the simulation period (20,000 years) in each of the landscape objects. The values were obtained from simulations with the landscape model used in the first 3,000 years after closure, when all landscape objects are sea basins. A constant input rate of 1 Bq/y during 20,000 years was used.

Radionuclide	Object 11	Object 4	Object 2	Object 3	Object 1
H-3	2,7E–11	1,1E–11	1,1E–11	1,1E–11	4,6E–13
Cl-36	2,8E–11	1,2E–11	1,2E–11	1,2E–11	1,0E–12
Co-60	2,7E–11	1,1E–11	1,1E–11	1,1E–11	2,3E–13
Ni-59	2,8E–11	1,2E–11	1,2E–11	1,2E–11	1,0E–12
Ni-63	2,8E–11	1,2E–11	1,2E–11	1,2E–11	8,8E–13
Se-79	2,8E–11	1,2E–11	1,2E–11	1,2E–11	1,0E–12
Sr-90	2,7E–11	1,2E–11	1,2E–11	1,2E–11	6,8E–13
Mo-93	2,8E–11	1,2E–11	1,2E–11	1,2E–11	1,0E–12
Nb-94	2,8E–11	1,2E–11	1,2E–11	1,2E–11	1,0E–12
Tc-99	2,8E–11	1,2E–11	1,2E–11	1,2E–11	1,0E–12
Ag-108m	2,8E–11	1,2E–11	1,2E–11	1,2E–11	1,0E–12
Sb-125	2,7E–11	1,1E–11	1,1E–11	1,1E–11	1,6E–13
Sn-126	2,8E–11	1,2E–11	1,2E–11	1,2E–11	9,5E–13
I-129	2,8E–11	1,2E–11	1,2E–11	1,2E–11	1,0E–12
Cs-135	2,8E–11	1,2E–11	1,2E–11	1,2E–11	1,0E–12
Cs-137	2,7E–11	1,2E–11	1,2E–11	1,2E–11	6,7E–13
Ho-166m	2,8E–11	1,2E–11	1,2E–11	1,2E–11	1,0E–12
Np-237	2,8E–11	1,2E–11	1,2E–11	1,2E–11	1,0E–12
Pu-239	2,8E–11	1,2E–11	1,2E–11	1,2E–11	8,7E–13
Pu-240	2,8E–11	1,2E–11	1,2E–11	1,2E–11	8,7E–13
Pu-242	2,8E–11	1,2E–11	1,2E–11	1,2E–11	8,7E–13
Am-241	2,8E–11	1,2E–11	1,2E–11	1,2E–11	9,9E–13
Am-242m	2,8E–11	1,2E–11	1,2E–11	1,2E–11	9,2E–13
Zr-93	2,8E–11	1,2E–11	1,2E–11	1,2E–11	9,5E–13

Table E1-2. Radionuclide concentrations in lake water (in Bq/m³) at the end of the simulation period (20,000 years) in lake objects 11 and 4. The values were obtained from simulations with the landscape model used from 2,000 years to 4,000 years after closure when objects 11 and 4 are lakes and other objects are sea basins. A constant input rate of 1 Bq/y during 20,000 years was used.

Radionuclide	Object 11	Object 4
Cl-36	1,6E–07	3,4E–08
Ni-59	1,1E–07	2,1E–08
Se-79	1,3E–07	2,7E–08
Mo-93	1,6E–07	3,4E–08
Nb-94	1,0E–07	2,0E–08
Tc-99	1,6E–07	3,4E–08
Ag-108m	1,3E–07	2,8E–08
I-129	1,5E–07	3,3E–08
Cs-135	1,1E–07	2,0E–08
Np-237	1,0E–07	2,0E–08
Pu-239	4,2E–08	5,5E–09
Pu-240	4,1E–08	5,5E–09
Pu-242	4,2E–08	5,6E–09
Am-241	1,0E–07	1,9E–08
Zr-93	5,9E–08	9,0E–09
Sn-126	5,9E–08	8,9E–09
Ho-166m	1,5E–07	3,3E–08
Am-243	1,0E–07	1,9E–08

Table E1-3. Radionuclide concentrations in soil (in Bq/kg DW) at the end of the simulation period (20,000 years) in mire objects 11, 4 and 2. The values were obtained from simulations with the landscape model used from 7,000 years after closure when object s 11, 4 and 2 are mires and other objects are sea basins. A constant input rate of 1 Bq/y during 20,000 years was used.

Radionuclide	Object 11	Object 4	Object 2
Cl-36	1,8E–08	4,0E–09	3,0E–09
Ni-59	4,4E–07	9,5E–08	7,1E–08
Se-79	9,0E–08	2,0E–08	1,5E–08
Mo-93	4,3E–08	9,4E–09	7,0E–09
Nb-94	7,6E–07	1,6E–07	1,2E–07
Tc-99	2,4E–09	5,3E–10	3,9E–10
Ag-108m	2,0E–07	1,0E–08	5,7E–09
I-129	1,4E–07	2,9E–08	2,2E–08
Cs-135	4,5E–07	9,7E–08	7,3E–08
Np-237	1,8E–06	3,8E–07	2,8E–07
Pu-239	1,5E–06	3,1E–07	2,3E–07
Pu-240	1,1E–06	2,1E–07	1,5E–07
Pu-242	1,8E–06	3,7E–07	2,8E–07
Am-241	1,8E–07	2,0E–08	1,3E–08
Zr-93	2,3E–06	4,7E–07	3,5E–07
Sn-126	8,4E–07	1,8E–07	1,3E–07
Ho-166m	3,5E–07	5,8E–08	4,1E–08
Am-243	1,1E–06	2,2E–07	1,6E–07

E2 Comparison between releases to water and sediments

In this study a comparison of predicted radionuclide concentrations in lake water was made between two cases:

- In the first case a constant release rate of 1Bq/y was directed to the water of a lake with properties like object 11, during 20,000 years,
- In the second case a constant release rate of 1 Bq/y was directed to the water in the top sediment of the same lake during 20,000 years.

Values of the radionuclide concentrations in the lake water at the end of the simulation period (20,000 years) for the two studied cases are presented in Table E2-1. The highest values of the concentrations in water of all studied radionuclides are obtained for the first study case with direct releases to the lake water.

Table E2-1. Radionuclide concentration in the lake water (Bq/m^3) for the two cases considered in the study. The Kd peat and Kd lake are the distribution coefficients for the sediments and suspended matter, respectively.

Nuclide	Kd peat	Kd lake	Release to water	Release to top sediment
I-129	0,3	0,3	2,03E–07	1,19E–07
Ni-59	1	10	1,96E–07	7,50E–08
Se-79	0,2	5	2,03E–07	1,35E–07
Cl-36	0,01	0,001	2,03E–07	1,98E–07
Mo-93	0,1	0,001	2,03E–07	1,60E–07
Cs-135	1	10	1,97E–07	7,11E–08
Am-241	5	10	1,90E–07	3,30E–08
Pu-239	5	100	1,31E–07	3,29E–08
Tc-99	0,005	0,1	2,03E–07	2,00E–07
Nb-94	2	10	1,94E–07	5,79E–08

E3 Comparison of the accumulation in lakes and mires

In this study, the retention of radionuclides in mires and in lake sediments was compared for two cases:

- In the first case a constant release of 1 Bq/y was directed to a mire, with properties like object 11, during 20,000 years,
- In the second case a constant release of 1 Bq/y was directed to the water in the top sediment of a lake during 2,000 years and to a mire during the following 18,000 years. The properties of the lake and the mire were taken as for object 11.

Table E3-1 presents values of the radionuclide inventory in the mire at the end of the whole simulation period (20,000 years). The results are presented for a selection of radionuclides with contrasting Kd values. It can be seen from this table, that for all studied radionuclides, the inventories were higher in the second case than in the first. This indicates that there is a higher retention in the lake sediments than in the mire, from 1.4 to 9.2 times higher. At the same time, the difference between the retention in lake sediments and mires increases as the distribution coefficient (Kd) decreases and is highest for Tc-99 which has a very low Kd value (0.005 m^3/kg). This is explained by differences in the conceptual models used for the lake and the mire (see Appendix A). In the lake model the sediment growth is taken into account, whereas is the mire model the growth of the mire is not considered. A radionuclide that is retained in the top sediment of the lake can be transferred to the deep sediment, where it is retained (see Figure A-1 in Appendix A). This is not the case for the mire, where there is transfer in both directions between the water and the solid/organic compartments (Figure A-2 in Appendix A).

For all studied radionuclides equilibrium in the radionuclide inventories in the mire was observed within the simulation period of 20,000 years (see Figure E3-1). This means that if inventories at the end of the simulation period are used for calculating the concentrations and the doses, this will not lead to underestimations of the doses.

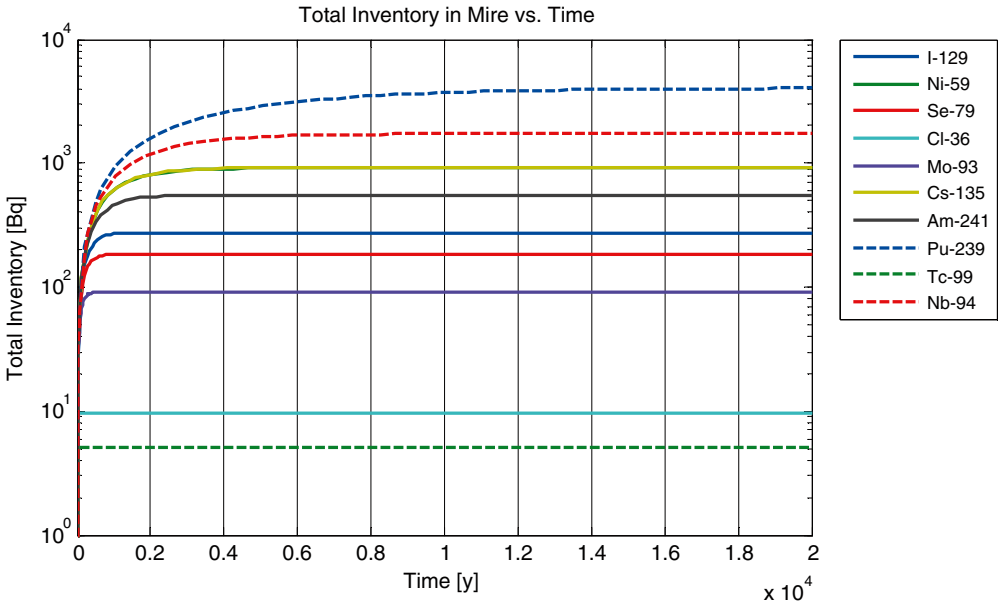

Figure E3-1. *Total inventory in the mire as a function of time resulting from a constant releases rate of 1 Bq/y during 20,000 years.*

Table E3-1. Radionuclide inventories at the end of the simulation period (20,000 years) for the two studied cases: Case 1 with a constant release rate of 1 Bq/y during 20,000 years to a mire and Case 2 with a constant releases rate of 1 Bq/y during 2,000 years to a lake and during 18,000 years to a mire.

Nuclide	Kd	Case 1 Mire	Case 2 Lake – Mire	Ratio Case 2/Case 1
I-129	0,3	2,8E+02	1,1E+03	3,9
Ni-59	1	9,1E+02	2,1E+03	2,3
Se-79	0,2	1,8E+02	9,0E+02	4,9
Cl-36	0,01	9,7E+00	8,4E+01	8,6
Mo-93	0,1	9,1E+01	4,8E+02	5,3
Cs-135	1	9,2E+02	2,1E+03	2,3
Am-241	5	5,5E+02	9,9E+02	1,8
Pu-239	5	4,0E+03	5,6E+03	1,4
Tc-99	0,005	5,1E+00	4,7E+01	9,2
Nb-94	2	1,7E+03	2,9E+03	1,7

Appendix F

Detailed results for the calculation case earthquake

This appendix presents detailed results of the doses and risk calculations that were carried out using the methods described in Section 4.3.

Table F-1. Peak values of the maximum annual doses (Sv/y) resulting from damages of the Silo associated with earthquakes. Values for each radionuclide and for the sum across all radionuclides are given. The approximate time (in years post closure) at which the peak dose is observed is also indicated.

Radionuclide	Time Years	Peak value Sv/y
Ag-108m	3,000	6.9E–08
Am-241	3,000	6.3E–06
Am-243	3,000	1.0E–06
C-14	3,000	2.2E–04
Cl-36	5,000	1.0E–08
Co-60	0	7.4E–07
Cs-135	3,000	6.6E–06
Cs-137	0	2.5E–06
H-3	0	5.4E–15
Ho-166m	5,000	4.5E–08
I-129	3,000	1.8E–06
Mo-93	5,000	7.4E–09
Nb-94	5,000	2.0E–06
Ni-59	3,000	1.1E–05
Ni-63	0	3.5E–07
Np-237	4,782	1.0E–07
Pu-239	3,000	1.9E–06
Pu-240	3,000	3.0E–06
Pu-242	3,000	1.8E–08
Se-79	3,000	1.1E–06
Sn-126	3,000	8.4E–08
Sr-90	0	7.9E–08
Tc-99	3,000	7.0E–07
Total	3,000	2.6E–04

Table F-2. Peak values of the maximum annual doses (Sv/y) resulting from damages of the BMA associated with earthquakes. Values for each radionuclide and for the sum across all radionuclides are given. The approximate time (in years post closure) at which the peak dose is observed is also indicated.

Radionuclide	Time Years	Peak value Sv/y
Ag-108m	3,000	2.6E–08
Am-241	3,000	7.3E–07
Am-243	3,000	2.3E–06
C-14	3,000	3.9E–05
Cl-36	5,000	1.7E–08
Co-60	0	5.1E–07
Cs-135	3,000	1.2E–05
Cs-137	0	3.9E–06
H-3	0	4.9E–15
Ho-166m	5,000	2.3E–08
I-129	3,000	3.1E–06
Mo-93	3,000	5.2E–09
Nb-94	3,000	1.1E–06
Ni-59	3,000	2.6E–05
Ni-63	0	8.5E–07
Np-237	3,465	9.8E–08
Pu-239	3,000	3.2E–06
Pu-240	3,000	5.1E–06
Pu-242	3,000	3.9E–08
Se-79	3,000	1.9E–06
Sn-126	3,000	1.4E–07
Sr-90	0	1.0E–07
Tc-99	3,000	5.6E–08
Total	3,000	9.5E–05

Table F-3. Peak values of the annual risk (1/y) resulting from damages of the Silo associated with earthquakes of magnitude 5. Values for each radionuclide and for the sum across all radionuclides are given. The time (in years post closure) at which the peak risk is observed is also indicated.

Radionuclide	Time Years	Peak value 1/y
Ag-108m	3,000	1.8E–09
Am-241	3,000	1.4E–07
Am-243	3,000	2.0E–09
C-14	3,000	4.4E–07
Cl-36	5,000	1.7E–11
Co-60	262	3.9E–12
Cs-135	3,000	1.1E–08
Cs-137	1,494	7.6E–11
H-3	614	6.7E–20
Ho-166m	5,000	1.7E–10
I-129	3,000	3.0E–09
Mo-93	5,000	1.5E–11
Nb-94	5,000	3.5E–09
Ni-59	3,000	1.9E–08
Ni-63	2,490	3.5E–11
Np-237	4,293	1.7E–10
Pu-239	3,000	3.4E–09
Pu-240	3,000	5.9E–09
Pu-242	3,000	3.0E–11
Se-79	3,000	1.9E–09
Sn-126	3,000	1.4E–10
Sr-90	1,444	2.3E–12
Tc-99	3,000	1.2E–09
Total	3,000	6.4E–07

Table F-4. Peak values of the annual risk (1/y) resulting from damages of the Silo associated with earthquakes of magnitude 6. Values for each radionuclide and for the sum across all radionuclides are given. The time (in years post closure) at which the peak risk is observed is also indicated.

Radionuclide	Time Years	Peak value 1/y
Ag-108m	3,000	2.8E–10
Am-241	3,000	2.3E–08
Am-243	3,000	3.1E–10
C-14	3,000	7.1E–08
Cl-36	5,000	2.8E–12
Co-60	265	6.2E–13
Cs-135	3,000	1.8E–09
Cs-137	1,500	1.2E–11
H-3	618	1.1E–20
Ho-166m	5,000	2.7E–11
I-129	3,000	4.8E–10
Mo-93	5,000	2.5E–12
Nb-94	5,000	5.7E–10
Ni-59	3,000	3.1E–09
Ni-63	2,490	5.5E–12
Np-237	5,000	2.8E–11
Pu-239	3,000	5.5E–10
Pu-240	3,000	9.5E–10
Pu-242	3,000	4.8E–12
Se-79	3,000	3.0E–10
Sn-126	3,000	2.3E–11
Sr-90	1,429	3.6E–13
Tc-99	3,000	1.9E–10
Total	3,000	1.0E–07

Table F-5. Peak values of the annual risk (1/y) resulting from damages of the BMA associated with earthquakes of magnitude 5. Values for each radionuclide and for the sum across all radionuclides are given. The time (in years post closure) at which the peak risk is observed is also indicated.

Radionuclide	Time Years	Peak value 1/y
Ag-108m	3,000	9.6E–12
Am-241	3,000	1.9E–10
Am-243	3,000	4.7E–10
C-14	3,000	8.3E–09
Cl-36	5,000	3.4E–12
Co-60	265	2.7E–12
Cs-135	3,000	2.5E–09
Cs-137	300	1.1E–10
H-3	300	6.0E–20
Ho-166m	5,000	5.0E–12
I-129	3,000	6.3E–10
Mo-93	3,000	1.2E–12
Nb-94	3,000	2.2E–10
Ni-59	3,000	5.2E–09
Ni-63	300	7.4E–11
Np-237	3,000	2.0E–11
Pu-239	3,000	6.5E–10
Pu-240	3,000	1.0E–09
Pu-242	3,000	7.8E–12
Se-79	3,000	3.8E–10
Sn-126	3,000	2.7E–11
Sr-90	300	2.9E–12
Tc-99	3,000	1.1E–11
Total	3,000	2.0E–08

Table F-6. Peak values of the annual risk (1/y) resulting from damages of the BMA associated with earthquakes of magnitude 6. Values for each radionuclide and for the sum across all radionuclides are given. The time (in years post closure) at which the peak risk is observed is also indicated.

Radionuclide	Time Years	Peak value 1/y
Ag-108m	3,000	1.6E–12
Am-241	3,000	3.1E–11
Am-243	3,000	7.7E–11
C-14	3,000	1.3E–09
Cl-36	5,000	5.6E–13
Co-60	262	4.2E–13
Cs-135	3,000	4.1E–10
Cs-137	300	1.8E–11
H-3	300	9.5E–21
Ho-166m	5,000	8.3E–13
I-129	3,000	1.0E–10
Mo-93	3,000	2.0E–13
Nb-94	3,000	3.6E–11
Ni-59	3,000	8.5E–10
Ni-63	300	1.2E–11
Np-237	3,000	3.2E–12
Pu-239	3,000	1.1E–10
Pu-240	3,000	1.7E–10
Pu-242	3,000	1.3E–12
Se-79	3,000	6.1E–11
Sn-126	3,000	4.4E–12
Sr-90	300	4.7E–13
Tc-99	3,000	1.8E–12
Total	3,000	3.2E–09